Chair of Fermentation Engineering
Faculty of Technology
Bielefeld University

Dissertation
in fulfillment of the requirements for the degree
Doctor of Natural Sciences (Dr. rer. nat.)

Development of methods for the production and purification of streptavidin from *Streptomyces avidinii* and heterologous hosts

---

submitted by

Jakob Michael Müller
born on the 4th of April 1986 in Sulzbach-Rosenberg

Bielefeld, April 2016

"I have yet to see any problem, however complicated, which, when you looked at it the right way, did not become still more complicated."

- Paul Alderson

The practical work of this thesis has been performed at the Chair of Fermentation Engineering at the Faculty of Technology at Bielefeld University from 2012 to 2016 under the supervision of Dr. Joe Max Risse. Parts of this work were financially supported by the Scholarship Programme of the German Environmental Foundation (Deutsche Bundesstiftung Umwelt, DBU, AZ20012/199, 6/2012-5/2015) and the Bielefelder Nachwuchsfonds (7-12/2015).

Reviewers:

Main reviewer:	Dr. Joe Max Risse Chair of Fermentation Engineering, Bielefeld University
Secondary reviewer:	Prof. Dr. Jörn Kalinowski Research group 'Microbial Genomics and Biotechnology' at the CeBiTec at Bielefeld University

Printed on non-ageing paper °° ISO 9706

Parts of this thesis have been published in:

- Müller J.M., Risse J.M., Jussen D. & Flaschel E. (2013): Development of fed-batch strategies for the production of streptavidin by *Streptomyces avidinii* based on power input and oxygen supply studies. *Journal of Biotechnology* **163**(3), 325–332, DOI: 10.1016/j.jbiotec.2012.10.021; With permission from Elsevier, Copyright 2013.
- Müller J.M., Risse J.M., Jussen D. & Flaschel E. (2016): Corrigendum to "Development of fed-batch strategies for the production of streptavidin by *Streptomyces avidinii* based on power input and oxygen supply studies." [J. Biotechnol. 163 (2013) 325-332] *Journal of Biotechnology* **226**, 76–77, DOI: 10.1016/j.jbiotec.2012.10.021; With permission from Elsevier, Copyright 2016.
- Müller J.M., Risse J.M., Friehs K. & Flaschel E. (2015): Model-based development of an assay for the rapid detection of biotin-blocked binding sites of streptavidin. *Engineering in Life Sciences* **15**, 627–639, DOI: 10.1002/elsc.201400227; Copyright Wiley-VCH Verlag GmbH & Co. KGaA. Reproduced with permission.
- Müller J.M., Wetzel D., Flaschel E., Friehs K. & Risse J.M. (2016): Constitutive production and efficient secretion of soluble full-length streptavidin by an *Escherichia coli* 'leaky mutant'. *Journal of Biotechnology* **221**, 91–100, DOI: 10.1016/j.jbiotec.2016.01.032; With permission from Elsevier, Copyright 2016.
- Müller J.M., Bruhn S., Flaschel E., Friehs K. & Risse J.M. (2016): GAP promoter-based fed-batch production of highly bioactive core streptavidin by *Pichia pastoris*. *Biotechnology Progress* **32**, 855–864, DOI: 10.1002/btpr.2283; Copyright Wiley-VCH Verlag GmbH & Co. KGaA. Reproduced with permission.
- Wetzel D., Müller J.M., Flaschel E., Friehs K. & Risse J.M. (2016): Fed-batch production and secretion of streptavidin by *Hansenula polymorpha*: evaluation of genetic factors and bioprocess development. *Journal of Biotechnology* **225**, 3–9, DOI: 10.1016/j.jbiotec.2016.03.017; With permission from Elsevier, Copyright 2016.

Lectures on excerpts of the work were held at:

- 9^{th} Congress of Chemical Engineering / 2^{nd} European Congress of Applied Biotechnology (ECCE 9/ECAB 2) 2013, The Hague, Netherlands. Title: 'Development of fed-batch strategies for the production of streptavidin by *Streptomyces avidinii*'.
- DECHEMA Himmelfahrtstagung 2015, Hamburg-Bergedorf, Germany. Title: 'Rapid monitoring of biotin-blocked binding sites of streptavidin during fermentation'.

Posters were presented at:

- 30^{th} DECHEMA Jahrestagung, 2012, Karlsruhe, Germany.
- DECHEMA Summer School 'Quantitative Biology', 2013, Berlin, Germany.
- 32^{nd} DECHEMA Jahrestagung, 2015, Aachen, Germany.

Contents

List of Figures

List of Tables

1 Abstract

The biotin-binding protein streptavidin (SAV) is applied in a large variety of methods due to its extremely high affinity to the vitamin biotin, ranging from protein purification and use as a bioinsecticide to tumor staining. However, common processes for the production and purification of the protein show a diverse range of serious deficiencies like low productivities and concentrations of product, the application of the toxic and flammable organic solvent methanol in heterologous production, and labile, expensive gel materials used for affinity chromatography of SAV. Hence, this project focused on the development of advanced strategies for the production and purification of the protein, targeting an economical and sustainable supply of SAV for common applications.

Optimization of process conditions for the natural producer *Streptomyces avidinii* led to a highly ecological bioreactor fed-batch process based on the constant feeding of glucose. Reproducibly yielding 39.2 μM of SAV in 14 days (114 nM h^{-1}), this strategy surpassed previously reported concentrations for this host by the factor 12.7. Continuous cultivation indicated that even higher productivities can be achieved at dilution rates in the range of 0.2 h^{-1}. A systematic variation of the rotary frequency of the stirrer revealed shear-sensitive properties of the streptomycete. Moreover, shake flask studies led to a selection of efficient strategies for the control of morphology.

Heterologous expression of the SAV gene was analyzed applying three hosts: the GRAM-negative bacterium *Escherichia coli* and the yeasts *Pichia pastoris* and *Hansenula polymorpha*.

For *E. coli*, broad optimization of process conditions allowed a more holistic view of the production of SAV by this biotechnological model bacterium. Application of the periplasmic 'leaky mutant' JW1667-5 (Δ*lpp-752::kan*), the constitutive β-lactamase promoter from *E. coli*, the *bglA*-leader peptide from *Bacillus amyloliquefaciens*, and addition of the non-ionic surfactant Triton™ led to the secretion of more than 90 % of SAV to the medium. Bioreactor fed-batch fermentation at 30 °C resulted in 2.6 ±0.2 μM of highly bioactive SAV in 40 h (65.2 nM h^{-1}), exceeding all reference concentrations for the soluble, secretory production of full-length SAV by *E. coli*.

For *P. pastoris*, a new strategy for the methanol-free production of a shortened form of SAV based on the constitutive GAP promoter was developed. This study demonstrates for the first time that SAV can be produced in a growth-associated manner by the biotin auxotrophic yeast, obviating the need for an induction by methanol. Productivity was greatly enhanced by successive cooling and acidification throughout the cultivation. Model-based evaluation of the optimized conditions in the bioreactor revealed that the majority of product accumulated in the late phase of fermentation at diminishing

growth rates. This is atypical for GAP promoter-based production processes, since the activity of P_{GAP} is usually known to be positively correlated to the growth rate of the host. The final fed-batch process led to 4.2±0.1 μM of SAV in 72 h (57.8 nM h^{-1}). Compared to literature, the proportion of biotin-blocked binding sites $Q_{blocked}$ was lowered from 20 % to 0±2 %.

The yeast *H. polymorpha* has not been used for the production of SAV prior to this project. Establishing this host for the production of SAV included genetic aspects, process development, and up-scaling to the bioreactor. Like observed for *E. coli*, cultivation at 30 instead of 37 °C turned out to be beneficial, resembling typical conditions for the natural producer *S. avidinii*. Application of the FMD promoter and a full-length SAV gene allowed the accumulation of SAV in the absence of methanol ('derepression'). However, production was enhanced upon induction by the organic solvent. A three-stage process, consisting of a batch phase and two phases of DO-stat feeding of glucose and methanol, respectively, yielded 11.4±0.2 μM of SAV in 216 h (52.5 nM h^{-1}). These properties resemble reference results reported for the methanol-based expression of a full-length SAV gene using *P. pastoris*. Remarkably, $Q_{blocked}$ was as low as 1.1±3.8 %.

In addition to these studies, a novel fluorometric assay was developed for the rapid detection of biotin-blocked binding sites of SAV based on the heat-based displacement of biotin from the binding pocket. Model-based evaluation of association and dissociation courses led to conditions allowing the detection of all biotin-blocked binding sites in a sample independent of the degree of biotin saturation. This new strategy facilitates analysis of the bioactivity and host toxicity of SAV during heterologous production. Furthermore, it may simplify the development of methods for the non-denaturing separation of SAV and biotin by revealing changes of the overall concentration of SAV rather than the concentration of biotin-free binding sites.

To demonstrate the latter feature, the assay was used for the development of methods for the partial recovery of biotin-blocked binding sites of SAV by hydrogen peroxide treatment and UV radiation. Incubation in the presence of hydrogen peroxide at elevated temperatures resulted in the recovery of up to 30 % of biotin-blocked binding sites of a completely biotin-saturated sample of SAV without major effects on the overall bioactivity of SAV.

Purification of SAV was studied by aqueous two-phase extraction, thermal inactivation of contaminating proteins, diafiltration, dialysis, and ammonium sulfate precipitation. The efficiency of the methods was assessed by SDS-PAGE analysis and determination of total protein. The results indicate that for many applications the direct use of crude supernatants or SAV purified by these simple and inexpensive procedures may be sufficient, whereas purification by chromatography may be necessary if high product purities are required.

2 Introduction

The protein streptavidin (SAV) was first isolated from supernatants of the filamentous soil bacteria *Streptomyces avidinii* and *S. lavendulae* in the early 1960s (Stapley *et al.*, 1963; Chaiet & Wolf, 1964). As shown in Fig. 2.1, SAV naturally occurs in a homotetrameric structure.

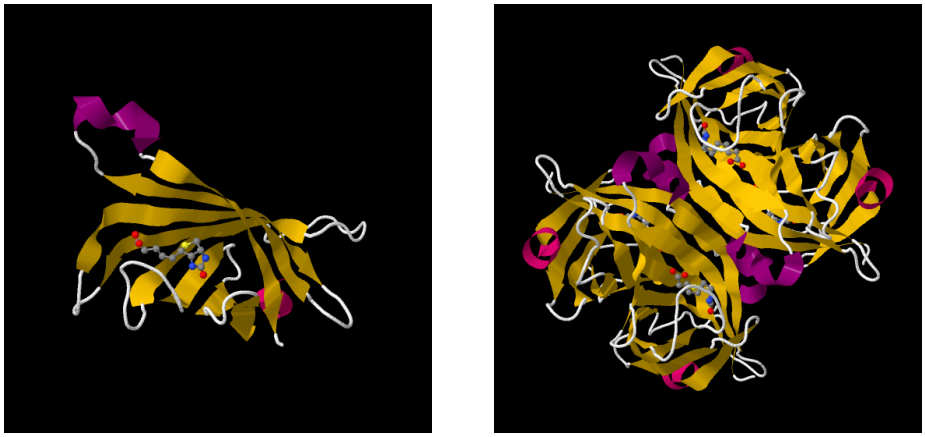

(a) monomer (b) homotetramer

Fig. 2.1: Protein backbone structure of SAV and bound biotin according to the data of Weber *et al.* (1989). Biotin is located inside of a highly stable β-barrel structure.[1]

The interaction of SAV and its binding partner biotin (vitamin H, MW: 244.3 Da) serves as a model interaction in molecular biology and is used for numerous applications in this field. SAV therefore has an extraordinary value as a biotechnological product. Naturally, SAV is part of the antibiotic complex MSD-235 (Stapley *et al.*, 1963; Chaiet & Wolf, 1964), which may be the reason for its natural occurrence (Tausig & Wolf, 1964; Bayer *et al.*, 1995). This hypothesis is supported by toxic effects observed in animal dietary studies upon feeding of raw egg white, which contains the biotin-binding protein avidin (Boas, 1924).

2.1 Binding of biotin to streptavidin (SAV)

To this date, the interaction of SAV and its binding partner biotin is one of the strongest known non-covalent interactions in biological systems, characterized by a dissociation constant K_d in the

[1] Visual representation created in Jmol (www.jmol.org).

range of 10^{-15} M (Sano *et al.*, 1996). As shown in Fig. 2.1, biotin is bound by SAV inside of a highly stable β-barrel structure, which is part of the core sequence of the protein. The interaction is subject to stabilization by hydrogen bonds and van der Waals forces (Weber *et al.*, 1989). Fig. 2.2 shows molecular interactions of biotin and the binding pocket of SAV.

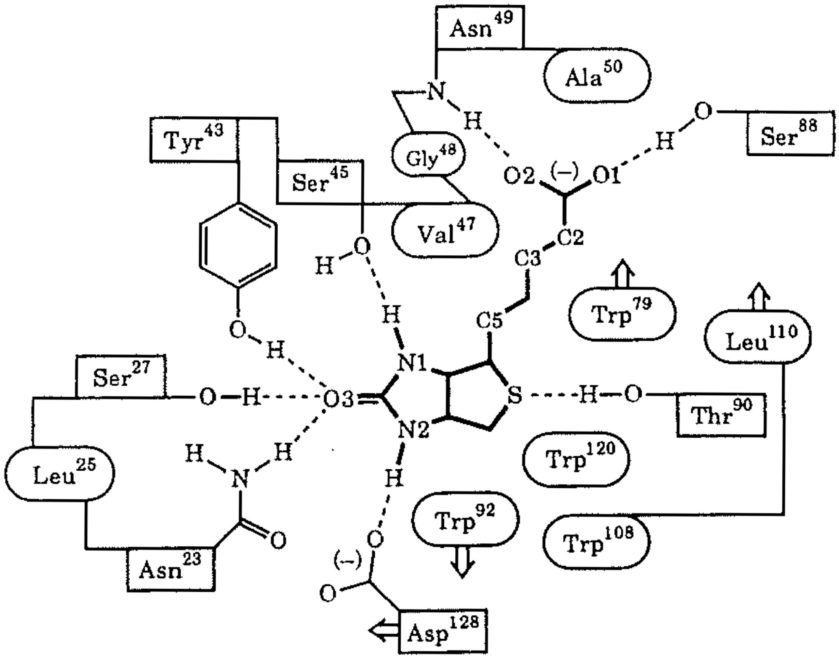

Fig. 2.2: Schematic representation of the interaction of biotin and the binding pocket of SAV according to Miyamoto & Kollman (1993). Amino acids marked by squares are involved in the formation of hydrogen bonds, whereas ellipsoids indicate van der Waals interactions. Trp^{120} belongs to the neighboring monomer of SAV in a dimer.

Generally, Fig. 2.2 indicates that the amino acids located in close proximity to the binding pocket mainly interact with the heterocycles of the headgroup as well as the terminally carboxylated hydrocarbon chain of biotin. Interestingly, the valerate group of biotin binds to a neighboring monomer of SAV (interaction with Lys-121 and Trp-120), which causes a strong dimer stabilization (Miyamoto & Kollman, 1993; Sano *et al.*, 1995, 1996).

The stabilizing effect of bound biotin on SAV has been studied in detail (Sano *et al.*, 1996; González *et al.*, 1997, 1999; Katz, 1997). From the thermodynamical perspective, the interaction of SAV and the vitamin is characterized by a total free energy of binding of 300 to 330 kJ per mol of tetrameric SAV (Miyamoto & Kollman, 1993; Green, 1990). These aspects lead to a remarkable rupture force of 250 pN for the release of SAV-bound biotin (Grubmüller *et al.*, 1996).

2.2 Properties and applications of SAV

Applications of SAV range from molecular biology and medicine to the downstream processing of various biomolecules. Searching the literature database Google Scholar[2] for articles containing the term 'streptavidin' in their title yields 35,900 results.[3] The enormous popularity of the molecular tool SAV is due to its extraordinary binding properties and its stability towards extrema of pH (Sano & Cantor, 1995), temperature (González *et al.*, 1999; Waner *et al.*, 2004), organic solvents, and denaturing agents (Sano & Cantor, 1990a; Kurzban *et al.*, 1991). Expression of the SAV gene may lead to shortened forms of the protein, termed 'core streptavidins', depending on the degree of proteolysis on SAV (Bayer *et al.*, 1989; Sano *et al.*, 1995). Chain lengths range from the 159 AA (16.5 kDa per monomer) of the full-length mature protein down to 125 (residues 14-138, 13.1 kDa, Pähler *et al.*, 1987) or even 119 AA (residues 15-133, 12.6 kDa, Sano *et al.*, 1995). An analysis of Bayer *et al.* (1989) revealed that these truncated forms of SAV are used for commercial preparations, too.

Core SAV offers advantageous properties for applications due to an enhanced structural stability and an improved accessibility of the binding site towards biotinylated macromolecules (Sano *et al.*, 1995). Furthermore, it is characterized by an increased proteolytic stability (Pähler *et al.*, 1987; Bayer *et al.*, 1989). These aspects along with the potentially lower metabolic burden for the host cell due to the shortened chain length of the protein make core SAV genes an interesting target for heterologous expression. The amino acid sequence of SAV is shown below.

```
  1 MRKIVVAAIA VSLTTVSITA SASADPSKDS KAQVSAAEAG ITGTWYNQLG
 51 STFIVTAGAD GALTGTYESA VGNAESRYVL TGRYDSAPAT DGSGTALGWT
101 VAWKNNYRNA HSATTWSGQY VGGAEARINT QWLLTSGTTE ANAWKSTLVG
151 HDTFTKVKPS AASIDAAKKA GVNNGNPLDA VQQ
```

The blue sequence corresponds to the native secretion signal peptide of 24 AA, which is cleaved off during secretion. Thus, mature, full-length SAV contains 159 of the 183 AA of the unprocessed protein (UniProt No. P22629, www.uniprot.org). The green region represents a shortened core-SAV gene (AA 13-139 of the native protein), which was applied in some of the studies of heterologous expression during this thesis.

An *in silico*-analysis of the signal peptide[4] (Bagos *et al.*, 2010) suggests with a high probability[5]

[2] scholar.google.com
[3] search performed 23rd of March, 2016
[4] http://www.compgen.org/tools/PRED-TAT/
[5] Reliability score: 0.996, see Fig. 8.1 on p. 180 in the supplements.

that the protein is secreted via the Sec pathway (unfolded secretion, see p. 18*ff.*).

Unlike the biotin-binding protein avidin from chicken egg white (Woolley & Longsworth, 1942) SAV is not glycosylated (Livnah *et al.*, 1993) and has a neutral isoelectric point, which ranges from 5 to 8 depending on the preparation (Dittmer *et al.*, 1989). This reduces unspecific binding of contaminating proteins (Wood & Warnke, 1981). The dissociation constant for the formation of the SAV-biotin complex leads to a practically irreversible binding of biotin. These combined properties therefore allow harsh washing conditions for its application (Rybak *et al.*, 2004), e.g., in ELISA-based methods.

2.2.1 Ligands of SAV and resulting applications

Applications of SAV can be divided into (*i*) methods involving SAV as a coupling agent between several biotinylated molecules and (*ii*) methods exploiting SAV itself, e.g., for the purification of other macromolecules.

However, biotin is not the only compound that can be applied for the use of SAV-based systems. Table 2.1 provides an overview of various SAV-binding molecules described in literature. Based on their chemical identity the molecules can be divided into four groups:

1. biotin and biotin derivatives
2. SAV-binding peptides
3. nucleic acid aptamers
4. chemically derived ligands

To further extend the range of potential applications of SAV, the protein has been engineered in numerous studies. Muteins[6] showing a mono- (Qureshi *et al.*, 2001; Wu & Wong, 2006; Demonte *et al.*, 2014) or dimeric (Sano *et al.*, 1997) instead of the native homotetrameric structure (Fig. 2.1b) have been designed and characterized. Variants with different biotin-binding properties, e.g. for the reversible binding of the vitamin (Qureshi *et al.*, 2001), were also in the focus of interest.

Generally, the tetrameric structure of SAV allows its use as a crosslinking agent, which is exploited in many applications, e.g., for immunochemical staining. Corresponding procedures typically involve a biotinylated antibody which binds to the target molecule. By the binding of this antibody, SAV links the target structure to a biotinylated detection marker, e.g., an enzyme catalyzing a colorimetric reaction or a fluorescent molecule. Depending on the quality of SAV used, up to three binding sites are

[6] A blend of the terms 'mutated' and 'protein'.

Tab. 2.1: Affinity constants K_d of various SAV-binding molecules.

designation	type [1]	K_d	sequence	reference [2]
biotin	B	1 fM	-	Sano *et al.* (1996)
B4F [3]	B	0.14 nM	-	Aslan *et al.* (2005)
desthiobiotin	B	0.01-2 nM	-	Green (1970)
diaminobiotin	B	0.12 μM	-	Germeroth *et al.* (2013)
iminobiotin, pH 11 [4]	B	0.035 nM	-	Fudem-Goldin & Orr (1990)
iminobiotin, pH 4 [4]	B	<1 mM	-	Fudem-Goldin & Orr (1990)
Strep-tag I [5]	P	36 μM	WSHPQFEK	IBA Lifesciences (2009)
Strep-tag II	P	72 μM	WRHPQFGG	IBA Lifesciences (2009)
Nano-tag$_9$	P	17 nM	DVEAWLGAR [6]	Lamla & Erdmann (2004)
Nano-tag$_{15}$	P	4 nM	DVEAWLGARVPLVET [6]	Lamla & Erdmann (2004)
SBP-tag [7]	P	2.5 nM	MDEKTTGWRGGHVVEGLAG ELEQLRARLEHHPQGQREP	Keefe *et al.* (2001)
glycoluril	C	2.5 μM	-	Katz *et al.* (1996)
HABA [8]	C	0.14 mM	-	Weber *et al.* (1994)
RNA aptamer	N	7 nM [9]	(113 bases)	Tahiri-Alaoui (2002)
RNA aptamer	N	70 nM	UCAUGCAAGUGCGUAAGAU AGUCGCGGGCCGGGGGCGU AU	Srisawat & Engelke (2001)
DNA aptamer	N	69 nM	(81 bases, ssDNA)	Wang *et al.* (2009)

[1] type of ligand: P = peptide ligand, B = biotin or biotin derivative, C = chemically derived ligand, N = nucleic acid ligand
[2] References refer to the given affinity constant, not the paper first describing the molecule.
[3] biotin-4-fluorescein
[4] The 2-imino residue of iminobiotin is subjected to a pH-dependent protonation/deprotonation, causing the binding of SAV at pH 11 (unprotonated) and its release at pH 4 (protonated).
[5] only for *N*-terminal fusion to the target protein
[6] The initial methionine has to be formylated for binding to SAV (Perbandt *et al.*, 2007).
[7] **S**treptavidin-**B**inding **P**eptide
[8] 2-(4-hydroxyphenylazo)benzoic acid. HABA shows a drastically (up to 165fold) increased affinity for SAV upon methylation at the 3'- and 5'-positions of the hydroxyphenyl-cycle (Weber *et al.*, 1994). However, the resulting derivatives are not commercially available.
[9] Binding data in the presence of biotin suggest that the aptamer does not directly bind to the biotin binding pocket of SAV.

available for the detection procedure, thus ideally resulting in a threefold signal amplification. In the presence of twofold biotinylated molecules, formation of complexes involving several molecules of SAV may lead to an even stronger amplification of the signal. A schematic representation of the procedure is shown in Fig. 2.3.

This detection method is nearly universally applicable, depending on the availability of biotinylated compounds or other SAV-binding ligands (see Table 2.1).

Among the most popular non biotin-related binding partners are the peptide tags Strep-tag I (Schmidt & Skerra, 1993) and II (Schmidt *et al.*, 1996), which are commonly used in the downstream processing of proteins (Schmidt & Skerra, 2007). Both tags are characterized by dissociation constants in the micromolar range (see Table 2.1, p. 7). In addition to these peptide tags, the biotin-derivative 2-iminobiotin is frequently applied for affinity chromatography of SAV due to a pH-dependent binding and release of the protein (Hofmann *et al.*, 1980).

The numerous variants of SAV and potential ligands, as well as the extraordinary stability and

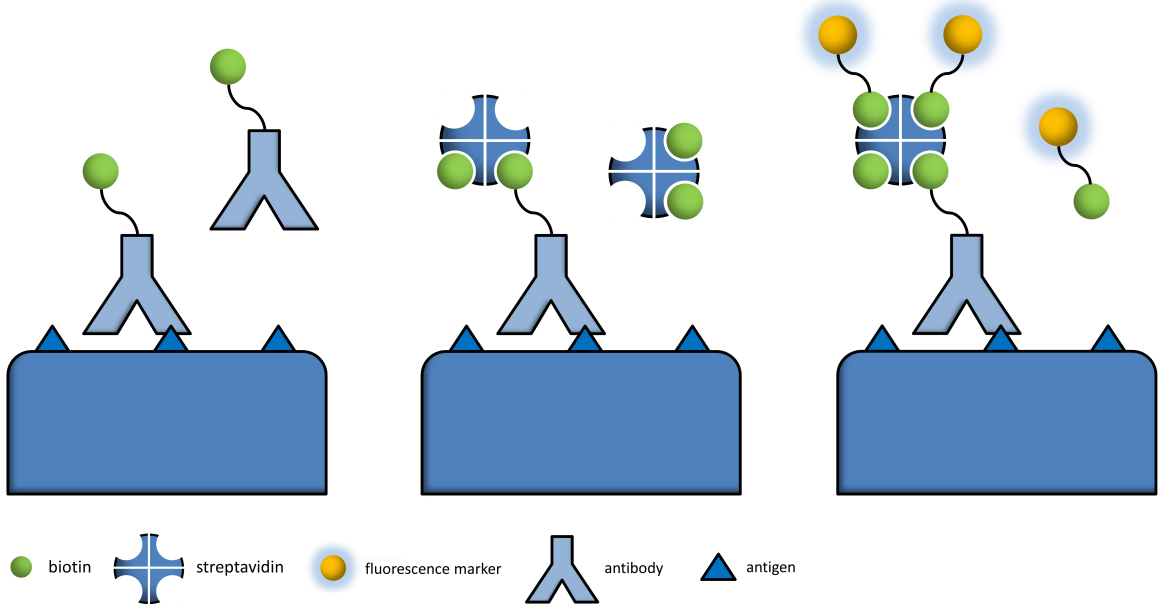

Fig. 2.3: Scheme for immunostaining of an antigen by SAV, biotinylated antibodies and detection markers. From left to right: targeting of the antigen, addition of SAV, and fluorescence labelling. Washing steps are performed between every step to remove unbound fractions of all binding partners. The SAV tetramer binding to the antibody would allow a twofold signal amplification due to one biotin-blocked binding site (see section 3.1, p. 28).[7]

specificity of SAV-based systems result in a nearly universal applicability of SAV as a molecular tool. SAV can thus be referred to as the "Swiss Army Knife" of molecular biology. To illustrate this, Table 2.2 shows a selection of the highly diverse scope of applications for SAV. Recent developments in the field of SAV-biotin technology were summed up by Dundas *et al.* (2013).

2.3 Other biotin-binding proteins

The biotin-binding ability of SAV is shared by many other proteins. The most common protein in this context is avidin, which was isolated from chicken egg white (Woolley & Longsworth, 1942). However, due to a basic isoelectric point and glycosylation, this protein is prone to unspecific binding of contaminating proteins. In respect to this disadvantage, engineering of charged groups on the protein surface yielded a neutral,[8] unglycosylated variant of avidin termed 'NeutrAvidin™' (Hiller *et al.*, 1987),

[7] Figure created in PowerPoint (see Table 2.4, p. 24).

[8] Isoelectric point: 6.3 for commercial preparations according to Invitrogen. https://tools.thermofisher.com/content/sfs/manuals/mp00887.pdf, revision 23/02/2009.

Tab. 2.2: Selected applications of SAV.

application	reference(s)
analysis of DNA-protein interactions	Wu (2006)
containment of GMOs[1]	Szafranski *et al.* (1997); Kaplan *et al.* (1999)
crosslinking of polymer nanospheres	Chen *et al.* (2005)
detection of cortisol	Patzl (1990)
detection of nucleic acids	Forster *et al.* (1985)
detection of pathogens	Blake & Weimer (1997); Call *et al.* (2003); Lee *et al.* (2004)
drug targeting	Muzykantov *et al.* (1999); Nguyen *et al.* (2013)
immobilization of antibodies	Gretch *et al.* (1987)
preparation of ssDNA[2]	Wilson (2011)
purification of proteins	Schmidt & Skerra (1993); Schmidt *et al.* (1996)
	Keefe *et al.* (2001); Lamla & Erdmann (2004)
targeted precipitation of biotinylated proteins	Navakouski *et al.* (2009)
thermoprecipitation of biotinylated biomolecules	Malmstadt *et al.* (2003)
thermoprecipitation of polymers	Fong *et al.* (1999)
tumor imaging	Kalofonos *et al.* (1990); Diaz-Moralli *et al.* (2011)
use as an insecticide	Morgan *et al.* (1993)

[1] genetically modified organisms
[2] single-stranded DNA

which shows properties comparable to those of SAV. Hertz & Sebrell (1942) demonstrated that the egg white of amphibia like the wood frog *Rana sylvatica* and the pickerel frog *R. palustris*, as well as of various bird species like duck, goose, and turkey also contains biotin-binding proteins.

More recently, a large variety of avidin-like proteins was isolated from a wide range of bacteria. Bayer *et al.* (1995) isolated two comparable proteins from supernatants of strains of *Streptomyces venezuelae*. The emerging field of whole-genome sequencing led to the discovery of biotin-binding proteins in numerous organisms. Two 'bradavidins', proteins serving the same function from the symbiotic, root nodule-inhabiting bacterium *Bradyrhizobium japonicum*, were identified (Nordlund *et al.*, 2005; Helppolainen *et al.*, 2008). All of these proteins occur in tetrameric form. Due to this feature, the discovery of a biotin-binding natural dimer isolated from *Rhizobium etli*, accordingly termed 'rhizavidin', came as a surprise (Helppolainen *et al.*, 2007).

However, the host range for biotin-binding proteins is even more diverse than expected. Lately, 'xenavidin' was isolated from the frog *Xenopus tropicalis* (Määttä *et al.*, 2009), 'zebavidin' was identified in the zebrafish *Danio rerio* (Taskinen *et al.*, 2013), and a family of 'lentiavidins', characterized by low isoelectric points, was discovered in the shiitake mushroom *Lentinula edodes* (Takakura *et al.*, 2016).

Thus, the binding of biotin is a common feature of many different proteins from a broad range of organisms, demonstrating that the properties of SAV are not as unique as previously assumed, but rather just one contribution to a large family of proteins.

2.4 Homologous and heterologous production of SAV

Production of SAV is either performed by the closely related (Ochi, 1989) natural producers *S. avidinii* and *S. lavendulae* or by heterologous expression in a variety of hosts.

2.4.1 Homologous production of SAV

Streptomycetes are GRAM-positive, GC-rich (Woese, 1987) aerobic actinobacteria showing filamentous growth. Over two thirds of all microbial antibiotics are derived from strains of the genus *Streptomyces*, emphasizing their vital importance for the production of pharmaceuticals (Bérdy, 2012). The metabolic complexity of streptomycetes and the broad variety of products is reflected by typically 20-40 gene clusters for the formation of secondary metabolites and a remarkable genome size in the range of 8-10 Mb (Nett *et al.*, 2009).

S. avidinii, one member of this genus, is commonly used for the production of SAV.

2.4.1.1 Morphology

Streptomycetes typically exhibit a complex life cycle. Grown on solid media, spores germinate and give rise to vegetative hyphae, so-called substrate mycelia, reaching deep down into the substrate. Upon substrate depletion, this step is followed by the formation of aerial hyphae growing into the air. This coincides with the start of production of many antibiotics, which typically accumulate as secondary metabolites. In the final step of this developmental cycle, aerial hyphae differentiate into spores (Flärdh & Buttner, 2009). The morphological development is visualized in Fig. 2.4a.

In liquid media, two major forms of hyphae can be observed: mycelial pellets of varying size (see Fig. 2.4b) and dispersed filamentous growth. Liquid cultures often consist of a combination of both morphologies. The morphological variety brings about numerous challenges on the level of cultivation. The effect of biomass on the viscosity of the culture broth strongly depends on the type of hyphae. Pellets typically only have a weak impact on the rheology (flow behavior) of the culture broth, whereas filaments may drastically influence this parameter (Metz *et al.*, 1979). Especially for increasing biomass concentrations, filamentous suspensions tend to be highly viscous (Metz *et al.*, 1979) and exhibit a non-Newtonian rheology, which is characterized by a shear-dependent viscosity. In the latter case, the viscosity therefore depends on the type of stirrer, the previous treatment of the broth, and the stirring frequency in the bioreactor. The rheology of filamentous suspensions can often be described as pseudoplastic[9] or shear-thinning[10] (Olsvik & Kristiansen, 1994). Thus, pellet growth may be

[9] Decreasing viscosity with increasing shear rate.
[10] Decreasing viscosity over time upon shearing.

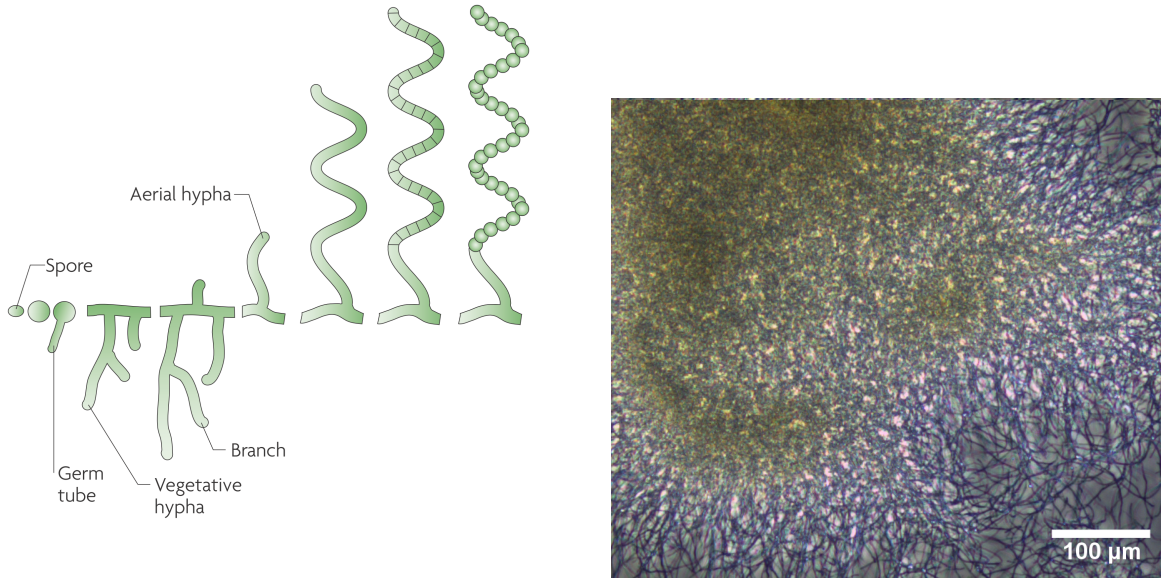

(a) Developmental cycle of streptomycetes grown on solid media (Flärdh & Buttner, 2009).

(b) Pellet formation of *Streptomyces avidinii* in submerged culture.

Fig. 2.4: Morphology of streptomycetes.

advantageous regarding the viscosity of the culture broth. Then again, this morphological appearance may bring about nutrient limitation within the pellets (Nielsen, 1996), as shown in Fig. 2.5.

From the engineering point of view, the viscous effects of high concentrations of filamentous biomass cause separation of the reactor into different zones, especially for large cultivation volumes. The regions of the reactor close to the stirrer are typically less viscous and well aerated, but tend to overheat. Contrarily, the regions bordering the reactor wall are oxygen-depleted and overcooled. Thus, it is very difficult to maintain optimal conditions for production throughout the whole fermenter (Braun & Vecht-Lifshitz, 1991). Effects of oxygen depletion for filamentous growth were, e.g., characterized by Járai *et al.* (1969) for *S. lavendulae*. High stirring frequencies may minimize these effects, but come at the cost of high power consumption and potential damage of the filaments due to increased shearing (Braun & Vecht-Lifshitz, 1991).

Product formation by filamentous organisms is strongly dependent on their morphology. Filamentous growth was found to be preferable for the production of proteases by *Aspergillus niger*, whereas pellets were beneficial for glucoamylase production by the same host (Papagianni & Moo-Young, 2002). These examples illustrate that control of the morphology is critical for optimal production.

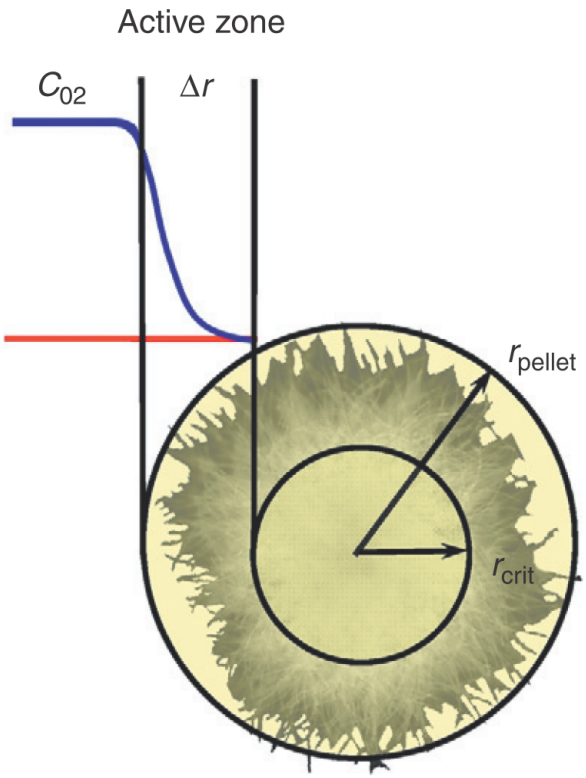

Fig. 2.5: Nutrient gradient within a pellet according to Wucherpfennig *et al.* (2010). The blue line indicates the course of the concentration of nutrients like oxygen within the pellet, whereas the red line is the limiting concentration. For pellets exceeding the critical pellet radius r_{crit}, growth of the culture is limited by the given nutrient caused by nutrient deprivation in the pellet.

2.4.1.2 Control of morphology

Pellet formation depends on a large variety of factors, including microbiological parameters like inoculum size and the growth rate, as well as physicochemical properties like shear rate, the presence of surface-active agents, pH, temperature, and the ionic strength of the medium (Metz & Kossen, 1977; Braun & Vecht-Lifshitz, 1991). Additionally, the availability of nutrients and oxygen plays a key role in morphological development (Papagianni *et al.*, 1999; Metz & Kossen, 1977). The complexity of pellet formation is illustrated in Fig. 2.6.

In addition to a targeted modification of the properties discussed in the previous paragraph, supplementation of microparticles to the cultivation medium may also contribute to a more homogeneous broth, as shown for the addition of talc- and aluminum oxide particles by Kaup *et al.* (2008). The authors were able to reduce the pellet size of *Streptomyces aureofaciens* by a factor of 5.4 by the

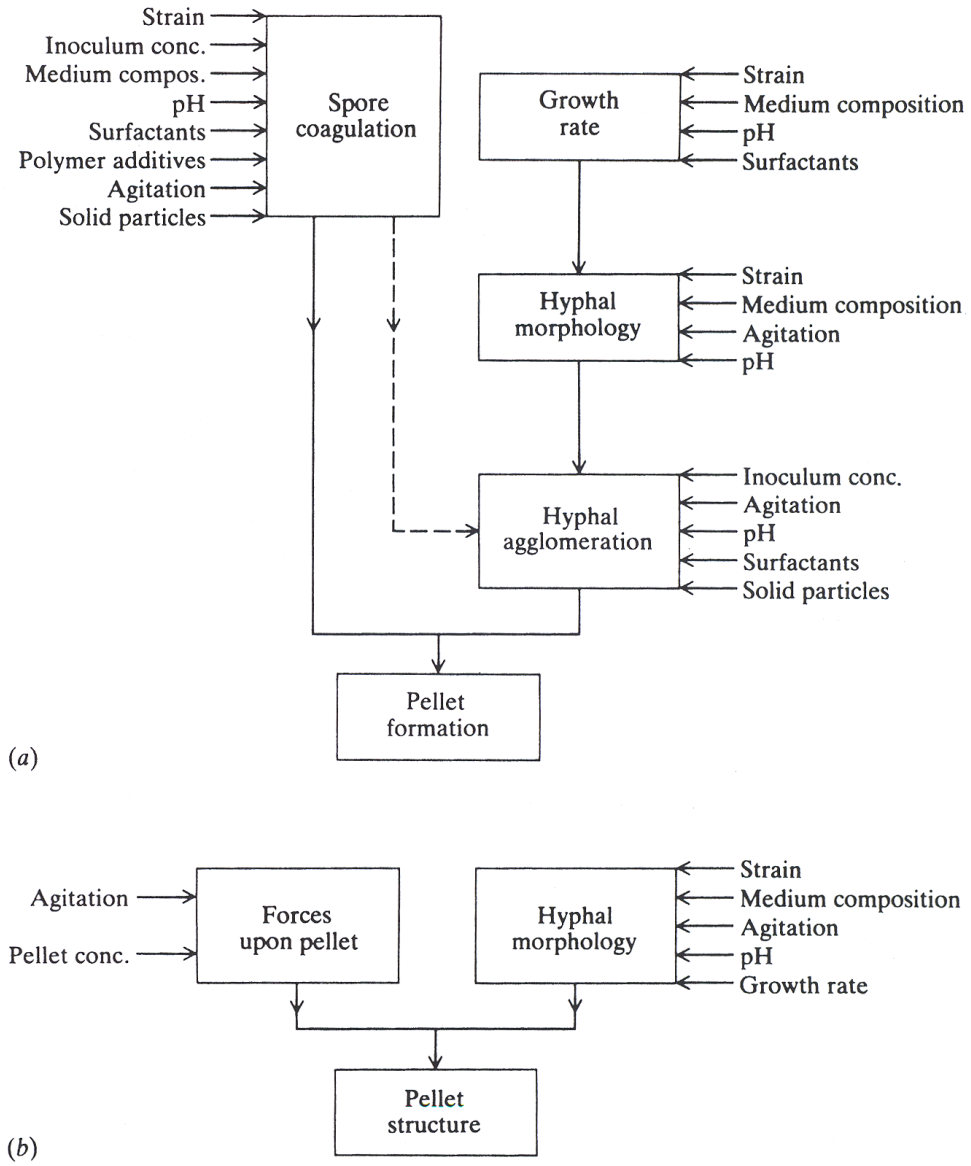

Fig. 2.6: Factors influencing the formation (a) and structure (b) of pellets. The figure was adapted from Bailey (1986), based on the data of Metz & Kossen (1977).

addition of microparticles. Kaup *et al.* (2008) demonstrated that the effect may increase the accumulation of various products. Based on this finding, they established the term 'microparticle-enhanced cultivation' (MPEC). The reduced pellet diameter was attributed to cell-particle-collisions, as well as shear stress resulting from rotating particles in shake flasks. By varying the size and concentration of the microparticles, a precise regulation of the pellet diameter is possible, which may help to avoid nutrient and oxygen depletion inside of large pellets (Nielsen, 1996). In the meantime, this effect has

been confirmed for a large variety of filamentous organisms, as reviewed by Walisko *et al.* (2012).

2.4.1.3 Production of SAV by *S. avidinii*

S. avidinii is an aerobic, mesophile (temperature optimum: 28-30 °C) and neutrophile (optimum of pH: 6.5) organism (Aldwin *et al.*, 1990). The strain has been used for the production of SAV in several batch studies in shake flasks in either complex (Aldwin *et al.*, 1990; Kolomiets & Zdor, 1998) or synthetic media (Cazin Jr. *et al.*, 1988).

However, to date no sophisticated strategies for fed-batch or continuous cultivation in the bioreactor or for the control of morphology have been reported. This is detrimental for the efficient production of SAV due to the problems arising from the morphology discussed in section 2.4.1.1, strongly limiting product concentrations and productivities reported in literature.

2.4.2 Heterologous production of SAV

SAV is a rather small protein (16.5 kDa per monomer), even for constructs based on the full-length gene. Moreover, it does not contain disulfide bonds and is not glycosylated. These advantageous properties and the numerous applications of the protein (section 2.2, p. 5*ff.*) led to a wide range of studies of heterologous expression of the SAV gene by a broad range of hosts.

Initially, heterologous expression of the SAV gene was carried out in the GRAM-positive hosts *Streptomyces lividans* (Meade & Jeffrey, 1986; Noda *et al.*, 2015) and *Bacillus subtilis* (Nagarajan *et al.*, 1993; Wu & Wong, 2002; Wu *et al.*, 2002), and the GRAM-negative model bacterium *Escherichia coli* (Sano & Cantor, 1990b; Thompson & Weber, 1993; Gallizia *et al.*, 1998; Veiko *et al.*, 1999; Wu & Wong, 2006; Miksch *et al.*, 2008; Chen *et al.*, 2014). More recently, the yeast *Pichia pastoris* was identified as a suitable host for the heterologous production of SAV (Casteluber *et al.*, 2012; Nogueira *et al.*, 2014). A study applying *Saccharomyces cerevisiae* focused on secretion of SAV to the surface of the yeast (Furukawa *et al.*, 2006), but even optimized conditions yielded diminishing concentrations of the protein using this strategy (Hong Lim *et al.*, 2012).

In summary, the vast majority of studies was performed applying unicellular organisms for which sophisticated process strategies are available. Important process parameters like the final product concentration and productivity of these publications are summarized in Table 7.4 (p. 167) in the 'Summary and Outlook'-part of this thesis.

In respect of the application as an insecticide, additional projects focused on expression of the SAV gene in tissues of tobacco (*Nicotiana tabacum*) (Murray *et al.*, 2002; Markwick *et al.*, 2003) and apple plants (*Malus domestica*) (Markwick *et al.*, 2003). However, despite allowing relatively high concentrations of SAV, these hosts are evidently not comparable to bacterial or yeast-based systems

with regard to long generation times and complicated downstream processing and are therefore not suited for industrial production processes.

The broad range of hosts successfully used for expression of the SAV gene experimentally confirmed the suitable theoretical properties for the heterologous production of SAV discussed above. However, the biotin-binding ability of the protein leads to a significant downside of corresponding processes.

2.4.3 Product toxicity for heterologous expression of the SAV gene

Understanding the function of biotin in the cellular metabolism is indispensable for the evaluation of cytotoxic effects of SAV.

2.4.3.1 Functions and metabolism of biotin

The vitamin biotin is an essential part of many biochemical pathways in pro- and eukaryotes. It serves as a cofactor in carboxyl transfer reactions (Attwood & Wallace, 2002) and is involved in pathways like fatty acid synthesis, gluconeogenesis and in the amino acid metabolism (Streit & Entcheva, 2003). Unlike humans and animals, which require biotin in their diets, microbes, plants and fungi are typically able to synthesize the vitamin by themselves (Streit & Entcheva, 2003).

Biotin metabolism and recycling leads to different cellular intermediates and side products of the vitamin. Fig. 2.7 outlines these aspects.

Biotin as well as its numerous intermediates show a diverse range of affinities for the protein SAV, leading to toxic effects during heterologous production of the protein. Generally, information on the affinity of the degradation products of biotin to SAV is sparse. Furthermore, their cellular localization is not characterized sufficiently. Therefore, the following section mainly focuses on the toxic effects associated to free biotin and biotinylated proteins.

2.4.3.2 Host toxicity of SAV

Two main types of toxic effects may occur upon expression of the SAV gene in heterologous hosts: SAV may bind free biotin, causing biotin deprivation of the host. Alternatively, complex formation of SAV and biotinylated proteins may - e.g., in the case of important enzymes - interfere with their function, leading to secondary damage to the host. Generally, the toxic impact caused by the binding of biotinylated proteins may vary depending on their host-dependent quantity (Fall *et al.*, 1975).

Host toxicity for the production of SAV by *E. coli*

The binding of biotinylated proteins is of increased importance for the expression of core SAV genes, as they improve the accessibility of the binding pocket of SAV towards biotinylated ligands (Sano

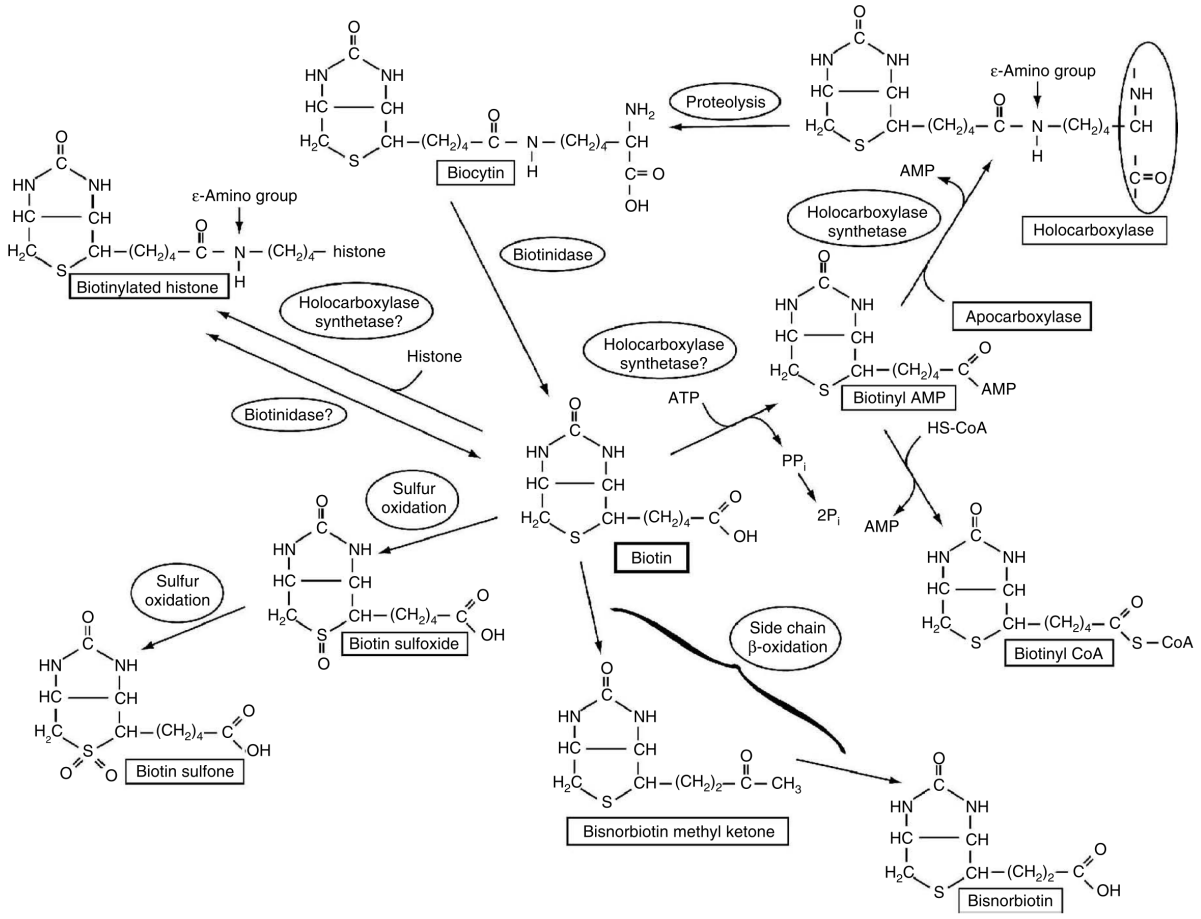

Fig. 2.7: Metabolism, recycling and degradation of biotin according to Rucker *et al.* (2007).

et al., 1995). Wang *et al.* (2005) observed a copurification of the biotin carboxyl carrier protein (BCCP) during the soluble production and periplasmic secretion of core SAV by *E. coli*. As BCCP is part of the acetyl-CoA carboxylase, an enzyme in fatty acid synthesis, toxic effects can be assumed.

These findings are supported by the data of Miksch *et al.* (2008), who analyzed soluble expression of a full-length SAV gene. Their study was based on secretion to the medium by a Sec signal peptide (see section 2.4.3.3) and release into the medium by a bacteriocin release protein. A negative correlation of the maximal optical density and maximal overall concentration of SAV can be deduced from the data, emphasizing the toxic effects of the protein.[11]

As decelerated growth was also observed for the cytoplasmic expression of SAV by Sørensen *et al.* (2003b), toxic effects in all cellular compartments are probable.

[11] OD_{600} of ∼21 for ∼0.7 μM, OD of ∼14 for ∼1.8 μM of SAV in shake flasks (Miksch *et al.*, 2008).

Host toxicity for the production of SAV by *B. subtilis*

Poor growth was also observed for the overexpression of a full-length SAV gene and secretion of the protein to the medium by *B. subtilis* (Wu & Wong, 2002; Wu *et al.*, 2002). This has been linked to the reduced availability of biotinylated enzymes and biotin deficiency (Wu & Wong, 2002). For this host, two enzymes are biotinylated and thus potentially affected, namely the pyruvate carboxylase and - like in *E. coli* - the biotin carboxyl carrier protein (Marini *et al.*, 1995). Both enzymes are involved in fatty acid synthesis.

Engineering of the producer strain to provide elevated levels of biotin was tested by (Wu & Wong, 2002) to alleviate the toxic effects. However, this strategy came at the cost of decreased bioactivity of SAV (approx. 20 % of biotin-blocked binding sites).

Reduction of host toxicity by insoluble production and other methods

Generally, toxic effects can be reduced by provoking the formation of biologically inactive inclusion bodies (IB) via overexpression in the cytoplasm, like performed by Sano & Cantor (1990b), Thompson & Weber (1993), and Chen *et al.* (2014). Similar aggregates may accumulate upon overexpression and secretion to the periplasm, as summed up by Baneyx (1999). Miroux & Walker (1996) studied this strategy for cytotoxic membrane proteins, suggesting that the choice of the host strain is of vital importance for high product concentrations. Additionally, tightly regulated promoter systems are part of the strategy of choice for many proteins as summed up by Hannig & Makrides (1998). By reducing the toxic effects to the host, these aspects may improve transformability of and plasmid stability in the producer strain (Dumon-Seignovert *et al.*, 2004).

However, as IB formation brings about the necessity of time-consuming solubilization and refolding accompanied by the loss of product, soluble expression seems to be a favorable approach.

Host toxicity for the production of SAV by yeast

Concerning biotin deprivation of the host, additional problems may arise for the application of yeast-based expression systems, since these organisms are typically biotin auxotrophic (Gasser *et al.*, 2010). In general, corresponding problems can be targeted by excessive supplementation of biotin.[12] However, this strategy results in reduced yields of bioactive SAV. To prevent this problem in the context of avidin production, Jungo *et al.* (2007b) studied the growth-promoting effects of oleic acid and aspartic acid for the cultivation of *P. pastoris* in biotin-free media, observing partial recovery from growth-limiting effects. Moreover, regarding the cultivation of yeast, studies of Zurek *et al.* (1996) using *H. poly-*

[12] See section 3.10 in the manuscript on the development of an assay for the detection of biotin-blocked binding sites of SAV, p. 30*ff.*, for an example.

morpha indicate that biotin-free complex media may be a suitable alternative to biotin-supplemented synthetic media for an improved bioactivity of SAV.

Generally, secretory pathways are a key factor for the soluble expression of SAV, since most of the toxic effects are likely to be due to intracellular complex formation.

2.4.3.3 Secretory pathways

The toxic effects resulting from the production of SAV depend on the cellular localization of SAV and biotinylated proteins as discussed in the previous section. However, the type of secretion system is also relevant for the efficient transport of SAV to the periplasm or medium.

Bacterial secretion

The two most commonly used pathways for the secretion of proteins are the twin-arginine translocation (Tat) and the general secretory (Sec) pathway. These pathways are widespread, existing in bacteria, archaea, and eukarya alike. Secretion depends on *N*-terminal signal peptides, consisting of a positively charged, polar 'n-region', an uncharged, hydrophobic 'h-region', and a second polar 'c-region'. The signal peptide is recognized by the secretory machinery and cleaved off during secretion (Natale *et al.*, 2008). Both pathways are visualized in Fig. 2.8b.

Drawbacks and benefits of secretion via Sec and Tat were summed up by Natale *et al.* (2008). Generally, the Sec pathway is based on the secretion of unfolded proteins, whereas Tat translocates folded proteins. In GRAM-negative hosts like *E. coli*, secretion via these pathways leads to transport to the periplasm, as illustrated in Fig. 2.8b. Since SAV is toxic to *E. coli*, the choice of the Sec pathway seems advantageous, because the protein remains in an unfolded state during translocation. This may temporarily prevent the binding of biotin or biotinylated compounds, which potentially minimizes toxic effects.

Both pathways are available in GRAM-positive as well as -negative bacteria. However, Fig. 2.8a clearly shows that transport of the protein of interest strongly depends on the surface structure of the host. In GRAM-negative bacteria, the outer membrane and the lipopolysaccharide layer complicate secretion of proteins to the medium (indicated by the crossed out arrow in Fig. 2.8b), whereas this step is much easier in GRAM-positive hosts. This leads to a different fraction of proteins in the respective compartments. For *E. coli*, most of the secreted proteins are located in the periplasm, whereas for streptomycetes and other GRAM-positive bacteria secretion mostly leads to a release into the culture medium (Morosoli *et al.*, 1997).

Most studies on secretion by the genus *Streptomyces* focused on *S. lividans*, a host which is frequently applied for the production of heterologous proteins. For this host, observations indicated that

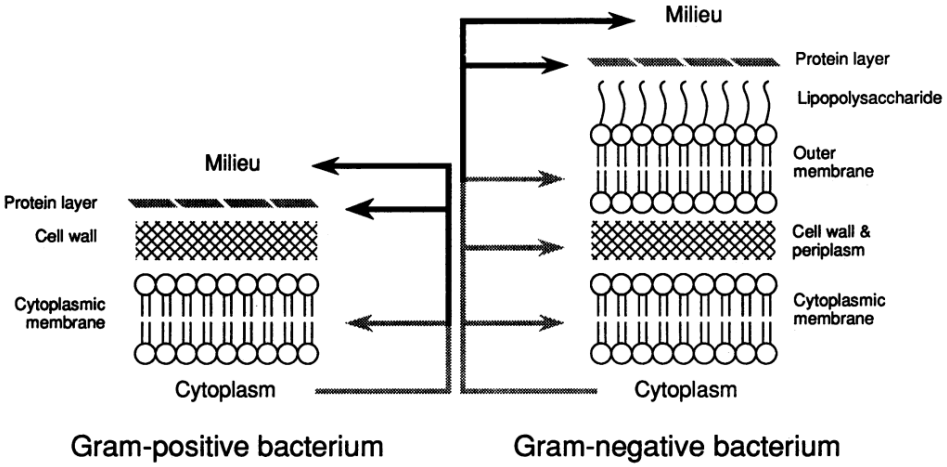

(a) Surface structure of GRAM-positive and GRAM-negative bacteria (Pugsley, 1993). Arrows indicate pathways of cellular targeting.

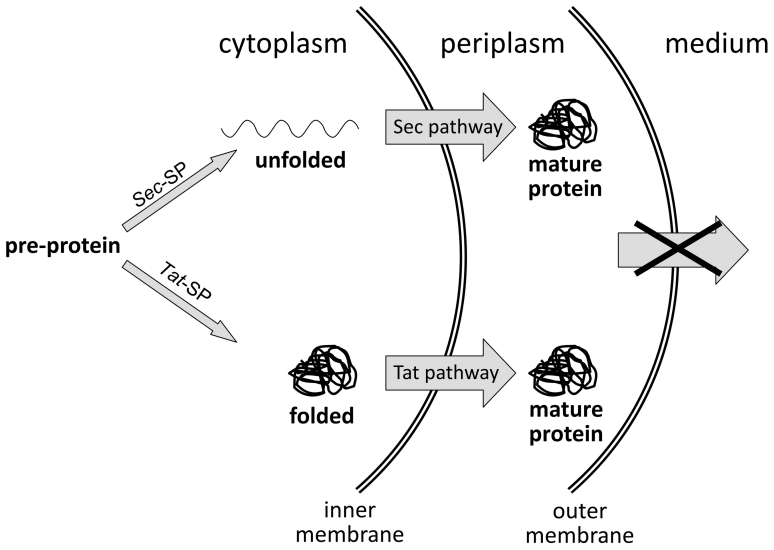

(b) Visualization of the Sec and Tat pathway in GRAM-negative bacteria (translated from Sommer, 2008). Abbreviation: SP = signal peptide.

Fig. 2.8: Cell wall structure of GRAM-positive and -negative bacteria (a) and visualization of the two main secretory pathways (b) in GRAM-negative bacteria.

the secretory efficiency is higher for homologous rather than heterologous secretion signal peptides (Rowland *et al.*, 1992) and for proteins of prokaryotic instead of eukaryotic origin (Anné *et al.*, 2012). Assuming that *S. avidinii* shows similar properties, a high secretory efficiency can be expected for the homologous production of SAV. As discussed in section 2.2 (p. 5), the native secretion signal peptide

for SAV from *S. avidinii* is most likely used for secretion via the Sec pathway. Thus, regulation of toxicity in the native producer may involve the avoidance of folded SAV in the cytoplasm. Generally, Anné *et al.* (2014) and Schaerlaekens *et al.* (2004) concluded that the overall secretory potential of *S. lividans* can be considered excellent. This may also apply to *S. avidinii*, but stands in contrast to *E. coli*.

Nevertheless, the utilization of secretory pathways for studies of heterologous expression based on GRAM-negative hosts like *E. coli* offers advantages towards cytosolic targeting: the risk of proteolytic degradation of the target protein is lowered towards cytoplasmic expression by periplasmic or extracellular targeting, typically with optimal results for the latter. However, the expression level of the gene has to be fine-tuned in order to avoid overloading of the export machinery. These aspects were reviewed by Makrides (1996). Furthermore, the proportion of contaminating proteins is lower when the target protein is transported to the periplasm, since this cellular fraction contains a fraction of only about 4 % of the total protein of the cell (Nossal & Heppel, 1966). Thus, use of the secretory pathways for periplasmic targeting seems favorable, even if the release of the target protein to the medium is difficult.

Consequently, Miksch *et al.* (2008) used a Sec-associated signal peptide for the secretion of SAV by *E. coli*. The transfer of the target protein from the periplasm to the surrounding medium was based on a bacteriocin release protein. Alternative approaches for the release of periplasmic SAV by *E. coli* may, e.g., focus on the application of periplasmic 'leaky mutants', i.e., strains with a decreased stability of the outer membrane.

Protein secretion in yeast

Due to a more complex cellular structure and various internal compartments, yeast-based expression systems offer a different way of cellular targeting. As summarized by Delic *et al.* (2013), proteins are secreted to the medium via co- or post-translational translocation to the lumen of the endpolasmic reticulum (ER), where they are folded in the presence of enzymes and chaperones. This step is followed by vesicular transport to the Golgi apparatus and medium via so-called COPII-vesicles. The process is shown in Fig. 2.9.

Taking this into account, the contact of folded and thus bioactive secreted proteins and the cytoplasm is minimized. This feature may be relevant for the expression of the SAV gene, since all four enzymes involved in the synthesis of long fatty acids in the *Saccharomyces cerevisiae* are located in the cytoplasm of the yeast (Schweizer *et al.*, 1978). Among these enzymes is the acetyl CoA carboxylase, which - like in bacteria - depends on a biocytin group (lysin-coupled biotin) for fatty acid synthesis. Assuming that the localization of biotinylated proteins in other yeast strains is comparable, transport of bioactive SAV to a different compartment than these biotinylated enzymes may be advantageous.

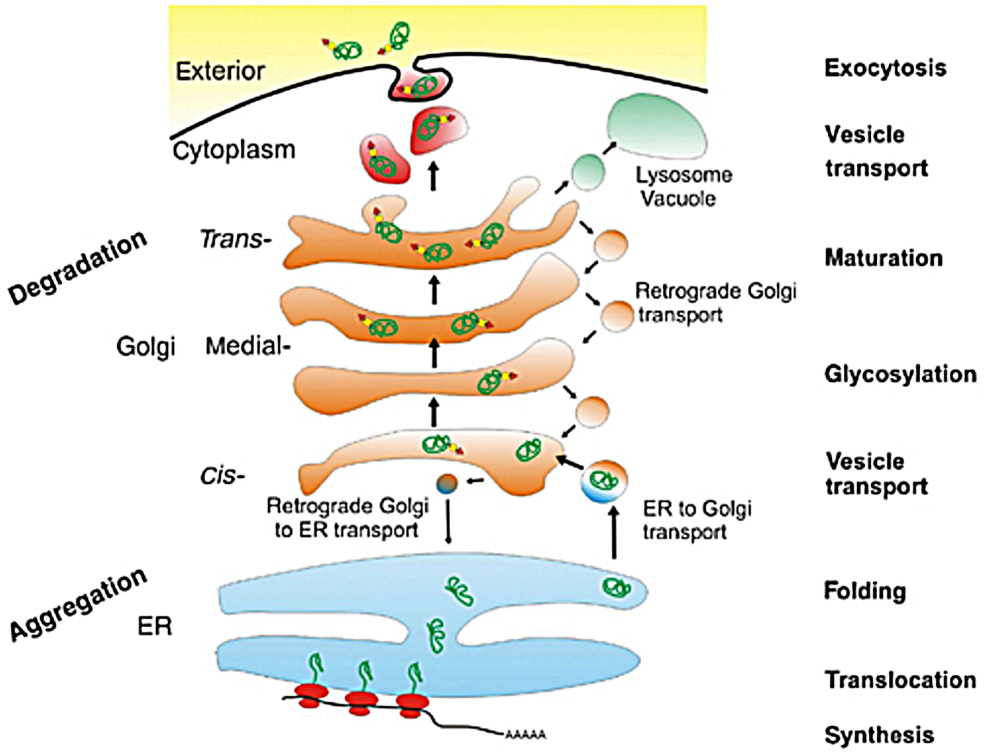

Fig. 2.9: Visualization of protein secretion in eukaryotes (Graf *et al.*, 2009). Proteins are either co- or post-translationally translocated from cytosol to ER.

2.5 Purification of SAV

A variety of methods has been applied for the purification of SAV. The standard procedure for the isolation of highly pure SAV is affinity chromatography based on iminobiotin columns (Hofmann *et al.*, 1980). The biotin derivative iminobiotin allows the pH-dependent binding and release of SAV and thus provides properties suited for a rapid purification of the protein. However, corresponding materials are costly and not very durable, leading to the necessity of replacement after a low number of cycles of purification and regeneration. Due to the strong affinity of SAV towards iminobiotin (see Table 2.1, p. 7), iminobiotin chromatography is superior to alternative chromatographic approaches. Therefore, genes for the heterologous expression of SAV usually don't contain additional functional sequences like the hexahistidine- (Hochuli *et al.*, 1988) or the maltose binding protein (MBP)-tag (di Guan *et al.*, 1988) for downstream processing. However, hydrophobic interaction chromatography has also successfully been applied for purification of the protein by Schwidop *et al.* (1990).

Other, less costly methods include precipitation by ammonium sulfate and dialysis (Suter *et al.*, 1988; Nogueira, 2013), and various combinations of dialysis in urea or guanidinium-HCl and precipitation by organic solvents like dimethyl ether, ethanol, and acetone, or direct precipitation by these solvents

(Nogueira, 2013). Due to the strong heat stability of SAV, heat incubation of SAV-containing supernatants and subsequent centrifugation has been used for the denaturing of contaminating proteins, followed by their removal via centrifugation (Gallizia *et al.*, 1998).

In respect to the heterologous production of SAV focusing on insoluble expression, Sørensen *et al.* (2003a) studied the purification of SAV via dialysis-based refolding and the accompanying removal of low molecular weight contaminants.

2.5.1 Aqueous two-phase extraction

Up to this point, aqueous two-phase extraction of SAV has not been studied. This procedure is based on the incompatibility of either a polymer towards another polymer (e.g., dextran and polyethylene glycol, abbreviated PEG) or of a polymer towards a salt (e.g., PEG and phosphate salts). When the concentration of both compounds exceeds a critical concentration, this incompatibility causes separation of the system into two phases (Albertsson, 1986). The separation behavior is typically depicted in the form of a binodal, which displays the concentrations necessary for phase separation, as shown in Fig. 2.10.

This binodal curve is specific for a defined composition of the system at a constant pH, temperature, and concentration of supplements like sodium chloride. Generally, compositions characterized by high concentrations of both polymer and salt, i.e., points in the upper right of Fig. 2.10, yield more stable two-phase systems than compositions close to the binodal. Phase formation for the latter systems is more susceptible towards changes of additional factors like pH and temperature.

Unlike methods based on organic extraction, aqueous two-phase systems (ATPS) can be used for the purification of proteins due to mild environmental conditions. Furthermore, the method is more economical due to the redundancy of explosionproof devices as well as more ecological because of the absence of organic solvents. The distribution of a protein in ATPS can be influenced by a variety of factors, including the adjustment of the chain length of the polymer, the pH value used for extraction, and the addition of supplements like sodium chloride (Albertsson, 1986). The extraction can furthermore be affected by the temperature, the use of charged or hydrophobic polymer derivatives or the coupling of affinity ligands to the polymer (Diamond & Hsu, 1992).

2.6 Focus of this dissertation

The major part of the studies performed for this dissertation focused on the expression of the SAV gene by a variety of host organisms. The natural producer *S. avidinii* (section 4, p. 60*ff.*) and several heterologous hosts (section 5, p. 91*ff.*) were analyzed with respect to their productive properties. Among other criteria, the hosts were selected based on different secretory pathways due to the toxic

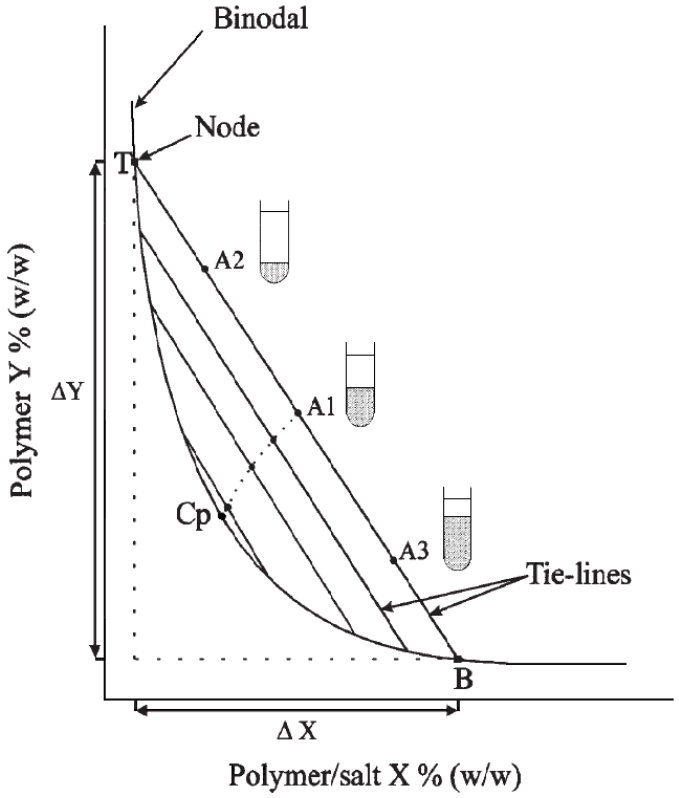

Fig. 2.10: Phase diagram of an aqueous two-phase system (Kaul, 2000). The binodal separates the one phase-region (bottom left) from the two-phase region (top right) of the plot. As illustrated by the sketches, the tie-lines sum up two-phase systems in which different phase ratios are achieved, but the concentrations of salt and polymer in the top- and bottom phase are constant. These constant concentrations refer to the end points of the tie-line, describing the composition of the top- (T) and bottom phase (B), respectively. C_p is the critical point of the phase system, which is gathered by extrapolation of the central points of the tie-lines.

properties of SAV and the secretory aspects discussed in the previous section. A summary of the hosts studied throughout this thesis is shown in Table 2.3.

Accompanying experiments were conducted to yield a more complete picture of the production process and to the process-dependent product quality by establishing a new method for the detection of biotin-blocked binding sites of SAV (section 3 p. 28*ff.*). Furthermore, studies targeting the replacement of the current downstream processing procedure, namely iminobiotin affinity chromatography, by a cheaper and simpler method (section 6, p. 144*ff.*), were performed.

Tab. 2.3: Summary of the hosts studied in this thesis.

host	class	strain(s)	secretion [1]	remarks
E. coli	Gammaproteobacteria	JW1667-5	Sec (UF), LM, M	GRAM-negative
		KRX	Sec (UF), PP	GRAM-negative
H. polymorpha [2]	Saccharomycetes	ATCC 34438	VT (F), M	yeast
		ATCC 26012 (DL-1)	VT (F), M	yeast
P. pastoris [3]	Saccharomycetes	GS 115	VT (F), M	yeast
		X-33	VT (F), M	yeast
S. avidinii [4]	Actinobacteria	CBS 730.72	Sec (UF) [5], M	GRAM-positive

[1] type of secretory pathway (see section 2.4.3.3, p. 18*ff.* for details): Sec = general secretory pathway, unfolded (UF); LM = periplasmic 'leaky mutant' for secretion from periplasm to medium; VT = vesicular transport via ER and Golgi apparatus to medium (folded (F) upon translocation to the ER). Targeting: PP = periplasm, M = medium.
[2] also known as *Ogataea polymorpha*
[3] also known as *Komagataella phaffii*
[4] natural producer
[5] suggested by an *in silico*-analysis of the signal peptide (Fig. 8.1, p. 180)

2.7 Software

The software that has been used for this thesis is shown in Table 2.4.

Tab. 2.4: Software used for this thesis.

application	software	version	reference / supplier [1]
pellet analysis	ImageJ	1.48v	Schneider *et al.* (2012)
cloning work	Clone Manager	9	Scientific & Educational Software
design of experiments	MODDE	10.1.0	Umetrics
flow chart creation	Dia	0.97.2	The Free Software Foundation
image processing [2]	PowerPoint 2010	14.0.7147.5001	Microsoft
image processing	GIMP	2.8.0	www.gimp.org
literature management	Zotero [3]	4.0.26.4	Center for History and New Media
modelling and simulation	CellDesigner	4.3	Funahashi *et al.* (2008)
	Scilab	5.5.0	Scilab Enterprises (2012)
parameter estimation	COPASI	4.10.55	Hoops *et al.* (2006)
plotting: contour plots	Ipython	2.7	Pérez & Granger (2007)
	Spyder	2.3.0rc	www.pythonhosted.org/spyder
	Matplotlib	1.4.3	Hunter (2007)
plotting: other plots	Gnumeric portable	1.12.17	www.gnumeric.org
text processing	MikTeX (LaTeX implementation)	2.9	www.miktex.org
text processing	TeXlipse (LaTeX editor)	1.5.0	texlipse.sourceforge.net

[1] if available/specified; otherwise: URL
[2] schematic representation of biochemical mechanisms
[3] Mozilla Firefox plugin

2.8 Abbreviations

The most important abbreviations and quantities used for this thesis are shown in Table 2.5 and 2.6. Abbreviations and quantities only applied in specific publications are not listed in the tables, but defined in the corresponding papers.

2.9 Structural remarks

Due to the modular structure of this thesis, the focus of this document was put on the research articles published in various journals and the summary of main findings of additional experiments. Additional methods and - in some instances - more detailed experimental descriptions are listed in the supplementary material, whereas the main body only contains brief experimental remarks.

Tab. 2.5: Important characteristic quantities and their dimensions used in this thesis.

abbreviation	quantity	dimension
η	dynamic viscosity	mPa s [a]
μ, μ_{max}	(maximal) specific growth rate	h^{-1}
μ_{set}	setpoint for μ for exponential feeding	h^{-1}
τ	residence time (=1/D)	h
$c_{SAV}, c_{SAV,app}$	(apparent) concentration of SAV [b]	nM
D	dilution rate	h^{-1}
$E-factor$	environmental factor	-
K_d	dissociation constant	M
k_{deg}	degradation constant	min^{-1}, h^{-1}
k_La	volumetric oxygen transfer coefficient	h^{-1}
K_S	Monod constant	$g\,L^{-1}$
L, L_{spec}	(specific) power input	W ($W\,L^{-1}$)
L_g, $L_{spec,g}$	aerated (specific) power input	W ($W\,L^{-1}$)
MW	molecular weight	kDa
n	rotary frequency of the stirrer	min^{-1}
p	volumetric productivity [c]	$nM\,h^{-1}$
p_{max}	volumetric productivity from t_0 to P_{max} [c]	$nM\,h^{-1}$
p_{spec}	specific (DCW-related) productivity [c]	$nmol\,g^{-1}$
P, P_{max}	(maximal) concentration of product [c]	nM, μM
Q	air flow rate	vvm
$Q_{blocked}$, Q_{bl}	proportion of biotin-blocked binding sites of SAV	-, %
Q_{SAV}	proportion of detectable SAV	-, %
rDO	relative dissolved oxygen saturation	%
s_{0S}	(substrate) saturation parameter (=S_0/K_S)	-
$s_{P/X}$	process selectivity (product per biomass)	$nmol\,g^{-1}$
S, S_0	(initial) concentration of substrate	$g\,L^{-1}$
t	time	h, min
$Y_{P/S}$	yield coefficient of product per substrate	-
$Y_{X/S}$	yield coefficient of biomass (DCW) per substrate	-

[a] $1\,mPa\,s = 10^{-3}\,\frac{N}{m^2}\,s = 1\,\frac{g}{s\,m}$

[b] Referring to the tetrameric concentration of SAV, if not stated otherwise.

[c] Referring to the extracellular, tetrameric concentration of SAV, if not stated otherwise.

Tab. 2.6: Abbreviations used in this thesis.

abbreviation	term
AA	amino acid(s)
AB	antibiotic(s)
ATPE	aqueous two-phase extraction(s)
ATPS	aqueous two-phase system(s)
B4F	biotin-4-fluorescein
BCCP	biotin carboxyl carrier protein
BSA	bovine serum albumin
DCW	dry cell weight
DF	diafiltration
DO	dissolved oxygen
DoE	Design of Experiments
DSP	downstream processing
ELP	elastin-like polypeptide(s)
ER	endoplasmic reticulum
HPLC	high performance liquid chromatography
IB	inclusion body/bodies
LMW	low molecular weight
MPEC	microparticle-enhanced cultivation
MW, MWCO	molecular weight (cut-off)
PEG	polyethylene glycol
PTVA	post-transformational vector amplification
RT	room temperature
SAV	streptavidin
SDS-PAGE	sodium dodecyl sulfate polyacrylamide gel electrophoresis
Sec	general secretory pathway
Tat	twin-arginine translocation pathway
UF	ultrafiltration
UV	ultraviolet
vvm	volume per volume and minute
WCW	wet cell weight

3 Development of an assay for the detection of biotin-blocked binding sites of SAV

In addition to the development of methods for the production and purification of SAV, an assay was designed for the rapid detection of biotin-blocked binding sites of the protein.

3.1 Motivation

The quality of isolates of SAV may be quantified based on a selection of parameters. The chain length of the protein varies depending on the host, the SAV gene used for expression, the presence of proteases, and the downstream processing procedure (Bayer *et al.*, 1989; Sano *et al.*, 1995). The molecular weight of SAV may therefore be valuable to differentiate between different isolates. Moreover, the purity of the protein - which is mainly influenced by the expression host, contaminating host proteins, the cultivation medium, and the method of purification - may be used for this purpose. While these two parameters can easily be assessed by standard laboratory techniques like SDS-PAGE analysis or terminal sequencing of the protein, another property is less readily accessible.

The bioactivity of different isolates of SAV varies depending on the proportion of bioactive binding sites. As biotinylated proteins, biotin or derivatives of the vitamin (see Fig. 2.7, p. 16) may bind to SAV during production, different production processes lead to a varying ratio of bioavailable and biotin-blocked binding sites. The biotin-free binding sites can easily be quantified by fluorescence quenching of biotin-4-fluorescein (B4F) (Kada *et al.*, 1999a,b). Fig. 3.1 depicts the procedure of this standard assay.

Despite advantageous properties in terms of experimental effort and expenditure of time, Kada's method is limited to biotin-free binding sites. Thus, complex procedures have to be applied to determine the proportion of blocked binding sites.

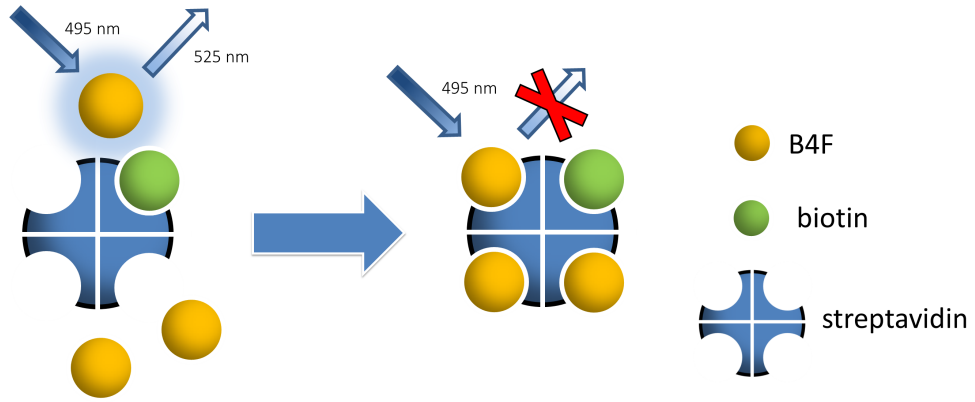

Fig. 3.1: Standard fluorescence quenching assay for the detection of biotin-free binding sites of SAV via biotin-4-fluorescein (B4F) according to Kada *et al.* (1999a,b).[1]

3.1.1 Goals of this study

To allow a simpler and more rapid measurement of biotin-blocked binding sites and therefore provide the basis for an analysis of this parameter during fermentations, a part of this project focused on the development of a corresponding assay.

3.2 Concept of the assay

The concept of the assay was based on results of Holmberg *et al.* (2005), who were able to dissociate the SAV-biotin interaction by incubation of the binding partners at elevated temperatures in non-ionic, aqueous solutions. As their studies were based on SAV coupled to magnetic beads and biotinylated DNA, the applicability of the method to free SAV and biotin had to be confirmed. Experiments of this part of the thesis therefore focused on the heat-induced displacement of SAV-bound biotin by biotin-4-fluorescein, as shown in Fig. 3.2.

Based on this strategy, the model-based development of an assay was performed. Experiments were carried out using a variety of supernatants of SAV producers, namely engineered clones of the yeast *P. pastoris*, the GRAM-negative bacterium *E. coli*, and the natural producer *S. avidinii*. The supernatants did not only vary in the concentration of contaminating proteins (see Fig. 6.1, p. 145), but also in the chain length of the SAV gene used for expression.

The optimization of assay conditions led to the successful, reproducible detection of the entire biotin-blocked binding sites in the samples.

[1] Figure created in PowerPoint (see Table 2.4, p. 24).

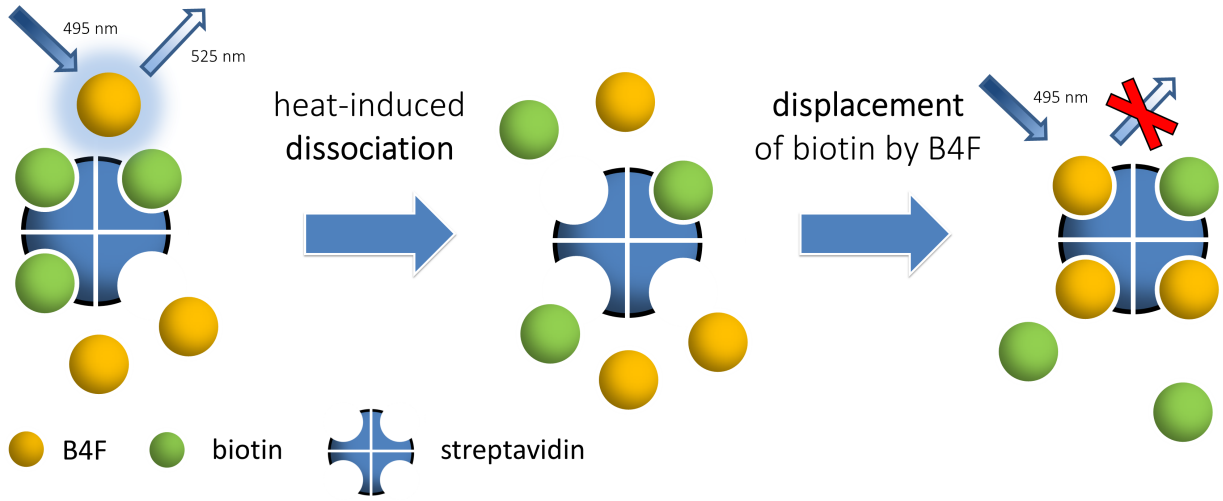

Fig. 3.2: Concept of a heat-based assay for the detection of biotin-blocked and biotin-free binding sites of SAV via displacement of biotin by B4F.[2]

3.3 Manuscript

The corresponding research article was published in Engineering in Life Sciences (Müller *et al.*, 2015) (Copyright Wiley-VCH Verlag GmbH & Co. KGaA. Reproduced with permission) and is shown on the following pages, including the accompanying supplementary material.

[2] Figure created in PowerPoint (see Table 2.4, p. 24).

Engineering in Life Sciences

Eng. Life Sci. **2015**, *15*, 627–639 www.els-journal.com

Jakob M. Müller
Joe M. Risse
Karl Friehs
Erwin Flaschel

Chair of Fermentation Engineering, Faculty of Technology, Bielefeld University, Bielefeld, Germany

Research Article

Model-based development of an assay for the rapid detection of biotin-blocked binding sites of streptavidin

The protein streptavidin (SAV) is applied in a large variety of molecular methods due to an extraordinarily strong binding to the vitamin biotin (BIO). The protein structure is homotetrameric, characterized by one binding site for BIO per subunit. Therefore, one of the major criteria to determine the quality of SAV isolates is the proportion of BIO-blocked binding sites per tetramer. A rapid analysis of BIO-free binding sites is achieved by fluorescence quenching of biotin-4-fluorescein (B4F). However, BIO-blocked binding sites can only be determined by costly and laborious procedures such as ELISA-based methods or radioactive labeling. This study describes the systematic, model-supported development of a method for the quick and simple detection of BIO-blocked binding sites, based on a short-term heat incubation of the sample in the presence of B4F. Kinetic modeling and parameter estimation yielded dissociation constants of $1.22 \pm 0.27 \times 10^{-11}$ M for the complex SAV–BIO and $5.16 \pm 0.70 \times 10^{-13}$ M for SAV–B4F at 70°C, allowing a displacement of SAV-bound BIO by B4F. This method allows the rapid monitoring of BIO-blocked binding sites in fermentation processes, independent from the chain length of SAV and the concentration of contaminating proteins, e.g. when optimizing the BIO concentration in cultivation media.

Keywords: Assay / Detection of biotin-blocked binding sites / Fermentation monitoring / Kinetic modeling / Streptavidin

Additional supporting information may be found in the online version of this article at the publisher's web-site

Received: November 11, 2014; *revised:* March 1, 2015; *accepted:* March 24, 2015

DOI: 10.1002/elsc.201400227

1 Introduction

Streptavidin (SAV) is a highly versatile molecular tool used for a large variety of applications. The homotetrameric protein was isolated from culture supernatants of *Streptomyces avidinii* and *Streptomyces lavendulae* in the early 1960 s [1, 2]. The nearly universal applicability of SAV is based on its ability to bind the vitamin BIO with an extraordinary dissociation constant K_d of up to 10^{-15} M [3], conveying a very high specificity when utilized. Furthermore, SAV exhibits a high tolerance toward extreme values of pH, temperature, and other environmental factors, especially upon BIO binding [4, 5]. This allows the application of SAV-based methods even in very harsh conditions. Molecular methods utilizing the SAV–BIO interaction include purification procedures for various macromolecules, e.g. for proteins by the Strep-tag technology [6], strategies for the containment of genetically engineered microorganisms by induced inactivation [7], numerous applications in molecular labeling, e.g. in the localization of tumors [8], and drug targeting approaches [9]. Recent discoveries suggest that the BIO-binding function of SAV and avidin, a protein of similar function from chicken egg white, is widely spread among a number of different proteins and species [10–12] and therefore not as unique as previously assumed.

1.1 Chain length and bioactivity of SAV

Several publications demonstrated that the terminal regions of SAV are not necessary for BIO binding [13, 14] and are even reported to result in a decreased stability of the protein. Moreover,

Correspondence: Jakob M. Müller (jmu@fermtech.techfak.uni-bielefeld.de), Chair of Fermentation Engineering, Faculty of Technology, Bielefeld University, Universitätsstraße 25, 33615 Bielefeld, Germany.

Abbreviations: B4F, biotin-4-fluorescein; **BIO**, biotin; **RT**, room temperature; **SAV**, streptavidin

the binding of biotinylated macromolecules to SAV is facilitated by the proteolytic removal of N- and C-terminal regions of the protein [15]. Therefore, some systems focus on the expression of N- and C-terminally truncated forms of the SAV gene. The corresponding protein variants are commonly referred to as core SAVs, typically ranging from 118 to 127 AA instead of the 159 AA of full-length mature SAV [15].

Apart from its chain length, SAV isolates can be characterized based on their bioactivity. Due to its homotetrameric structure, SAV is naturally capable of binding up to four molecules of BIO. However, depending on host, expression system and the presence of BIO and its derivatives in the medium, a fraction of the binding sites may be blocked by either of these compounds, which compromises the use of SAV e.g. as a crosslinking agent. While most SAV isolates from *S. avidinii* can typically be expected to be almost BIO-free [16], expression by *Bacillus subtilis* brings about proportions of BIO-blocked binding sites $Q_{blocked}$ in the range of 0.2, representing a relative BIO saturation of the binding sites of 20% [17, 18]. The production of SAV by the yeast *Pichia pastoris* leads to comparable results [19]. Insoluble intracellular production of SAV by *Escherichia coli* followed by resolubilization causes degrees of BIO saturation of 0.025–0.25 [20]. Commercial preparations of SAV are usually characterized by specific activities in terms of bound units of BIO per milligram of protein, not containing information on the concentration of BIO-blocked binding sites or incorporating potential variations of the chain length of SAV. Due to the large experimental effort necessary for the determination of BIO-blocked binding sites information on this parameter is often sparse.

1.2 Determination of the active binding sites of SAV

Kada et al. published an assay for the rapid detection of SAV in crude supernatants by static fluorescence quenching of biotin-4-fluorescein (B4F) [21, 22]. However, the assay is limited to binding sites, which are unblocked by BIO. To detect the blocked binding sites complex, time-consuming methods have to be applied. Potential strategies are the denaturing of SAV followed by measurements of released BIO, radioactive labeling of BIO or immunological methods (ELISA) in combination with active site determination by the quenching of B4F. However, these methods are costly and very laborious and therefore not suitable for a rapid monitoring of fermentation processes.

1.3 Motivation and theoretical concept of the assay

As our research group is currently screening a variety of heterologous expression systems for their potential to produce SAV, a method for the rapid detection of BIO-blocked binding sites was in the focus of interest. For an improved process performance, a fine-tuned optimization of the BIO concentration in fermentation media is desirable to maximize bioactivity of SAV without a major impact on cell growth. In this respect, the proportion of BIO-blocked binding sites provides essential information. A corresponding assay should be able to quickly quantify the blocked binding sites independent from the chain length of SAV and concentration of contaminating host proteins.

Holmberg et al. discovered to their surprise that a short-term incubation of biotinylated molecules at elevated temperatures in a nonionic, aqueous solution allows their release from SAV-coated magnetic beads [23]. Therefore, the goal of our studies was to combine this heat incubation step and the fluorescence quenching assay by Kada et al. [21, 22] in order to detect BIO-blocked binding sites. In theory, the elution of the SAV–BIO interaction should intermittently result in a fraction of unoccupied binding sites, which may be bound by B4F, a fluorescence derivative of BIO. Binding of B4F to SAV for its part should then lead to fluorescence quenching as described by Kada and coworkers. The key questions were if the elution of the SAV–BIO interaction would also be broken if SAV and BIO are in free suspension in an aqueous solution instead of being coupled to other molecules, because the coupling of SAV to beads leads to an increased dissociation constant and therefore a facilitated elution of the SAV–BIO interaction [24], and if the dissociation constants at elevated temperatures would allow a displacement of BIO by B4F.

The association rates of the complexes SAV–BIO and SAV–B4F differ only by a factor of 3.4 at 37°C with values of $k_{on,B4F}$ of $2.0 \pm 0.1 \times 10^7$ M^{-1} s^{-1} for B4F and a $k_{on,bio}$ of $6.7 \pm 0.5 \times 10^7$ M^{-1} s^{-1} for BIO (Supporting Information of [25]), which is achieved by the short ethylene diamine spacer between BIO and fluorescein [17]. Furthermore, the dissociation rate of the SAV–BIO complex $k_{off,bio}$ is known to increase exponentially upon temperature [26]. The investigation of a competition of B4F and BIO for the binding sites of SAV at elevated temperatures therefore seemed worthy of a detailed investigation.

2 Materials and methods

2.1 Standard procedure for the measurement of SAV by fluorescence quenching of B4F

SAV was quantified by the fluorescence quenching assay of Kada et al. [21, 22] using a calibration curve of B4F (GERBU, Heidelberg, Germany) in concentrations equivalent to 0–600 nM of tetrameric SAV. The calibration curve was gathered by a dilution of a 50 nM B4F solution in measurement buffer to final volumes of 1 mL at concentrations of 1, 5, 10, 20, 30, 40, 45, and 49 nM, respectively. The measurement buffer was composed of 100 mM of NaCl, 1 mM of EDTA, and 50 mM of NaH_2PO_4. The pH was adjusted to 7.5 by the addition of NaOH. Once per week, working volumes of this buffer solution were freshly supplemented with B4F and—to reduce unspecific binding to the reaction tube—BSA (GERBU) in concentrations of 50 nM and 0.1 g L^{-1}, respectively. Three technical replicates of samples of 20 μL were each added to 980 μL of measurement buffer (dilution factor: 1:50), vortexed for 1 s and incubated at room temperature (RT) for 30 min, followed by fluorescence measurement in disposable polystyrene semimicro cuvettes (BRAND, Wertheim, Germany). Measurements were performed five-fold in a RF-5301 PC fluorimeter (Shimadzu, Duisburg, Germany) at excitation and emission wavelengths of 495 and 525 nm, respectively. If not stated otherwise, all resulting molar concentrations refer to tetrameric SAV. A table for the calculation of the SAV

concentration based on the B4F calibration curve is attached in the Supporting Information, Table S1.

2.2 Procedure for the detection of BIO-blocked binding sites

The optimization procedure for the detection of blocked binding sites resulted in the following method: samples of 20 μL were mixed with 980 μL of measurement buffer including B4F and BSA by vortexing for 1 s, followed by an incubation at 70°C for 10 min in a standard laboratory heat block (VWR, Darmstadt, Germany) with water-filled wells to release SAV-bound BIO, inverting three times and a final incubation step at RT for 30 min. After the incubation, the fluorescence measurement was performed applying the conditions described in Section 2.1. All supernatants were analyzed in three replicates each, applying (i) the normal assay procedure and (ii) the heat incubation procedure. For the heat assay, samples were diluted to tetrameric concentrations of $c_{SAV,HT} \leq 300$ nM. A schematic representation of the assay is shown later in Fig. 4.

After conversion of the fluorescence signals to SAV concentrations according to Supporting Information, Table S1, the concentration of BIO-blocked SAV $c_{SAV,blocked}$ was calculated according to Eq. (1):

$$c_{SAV,blocked} = c_{SAV,HT} - c_{SAV,RT} \quad (1)$$

where $c_{SAV,RT}$ is the (tetrameric) concentration of SAV measured in the standard assay at RT (free binding sites) and $c_{SAV,HT}$ is the concentration measured after the heat incubation step (total binding sites—blocked and unblocked).

2.3 Production of SAV by different expression hosts

Measurements for the development of the assay were performed on supernatants from cultivations of different expression systems for the production of SAV. Supernatants for one part of the studies were acquired from bioreactor cultivations of the natural producer *S. avidinii*. Cultivation conditions were chosen according to the bioreactor batch experiments on M3 medium as described previously [27]. Furthermore, SAV derived from heterologous expression systems produced by two different hosts was analyzed in the experiments: core SAV (AA 13–139) secreted by a clone of the yeast *P. pastoris* GS115 (Invitrogen, Germany) carrying a chromosomal expression cassette and full-length SAV produced by an *E. coli* K-12 derivative transformed with a plasmid-based expression vector (unpublished expression systems).

2.3.1 Shake flask cultivation conditions

To demonstrate the application of the assay, a Mut^S (methanol utilization slow phenotype) clone of *P. pastoris* GS 115 producing and secreting core SAV (AA 13–139) under control of the alcohol oxidase 1 (AOX1) promoter was cultivated in baffled 500 mL shake flasks (Duran, Wertheim (Main), Germany) in three replicates, each filled with 50 mL, at 30°C at a shaking frequency of 160 min^{-1} and an eccentricity of 20 mm. The shake flasks were inoculated with an overnight culture on YPD medium [28] (p. 30) to an optical density OD_{600} of 0.5 after one washing step with sterile, demineralized water. Buffered MG medium (adjusted to pH 6.0) [28] (p. 57) with concentrations of BIO of 1 and 4 μM, respectively, was used. After the initial batch growth phase, sterile methanol was added to final concentrations of 0.2 and 0.4% v/v in the morning and evening, respectively. Samples of 1 mL were taken per sampling point and used for the determination of dry cell weight and substrate concentration according to standard laboratory procedures (differential weighing, HPLC analysis). The supernatants were used for the standard SAV assay (Section 2.1) and the determination of BIO-blocked binding sites (Section 2.2).

2.4 Software for simulation, data analysis, and evaluation

Parameter estimation for biochemical modeling was performed using the parameter estimation toolbox of COPASI (University of Manchester/Universität Heidelberg, UK/Germany, [29]), based on models developed in CellDesigner (Systems Biology Institute, Japan, [30]). The acquired parameters were used for simulations in Scilab (Scilab Enterprises, France, [31]). A polynomial model was developed in the design of experiments software MODDE (Umetrics, Sweden). If not stated otherwise, all plots were created using the Python plotting library Matplotlib [32].

3 Results and discussion

The results are divided into a section discussing the scope of SAV variants, which were used for the studies followed by steps describing the development and validation of the final assay procedure. Subsequently, the conditions used for the assay were evaluated by polynomial and kinetic modeling. Finally, the assay was tested in a shake flask cultivation of a SAV-producing clone of *P. pastoris*.

3.1 Characterization of the supernatants used for the experiments

The three different culture supernatants, namely samples from *S. avidinii*, *P. pastoris*, and *E. coli* cultivations, varied drastically concerning the proportion of contaminating proteins. While SAV was the dominant protein in the supernatants of both *P. pastoris* and *S. avidinii*, the supernatant of the *E. coli* producer contained a large fraction of unspecific SDS-PAGE bands. Furthermore, the SAV isolates varied in the chain length of SAV with 139 AA (core SAV) for the *P. pastoris* construct and the full 159 AA for the *E. coli* and *S. avidinii* supernatants, which was confirmed by SDS-PAGE analysis. Due to their variance in chain length and contaminating proteins these supernatants were chosen to represent typical extremes of supernatants used for the assay.

3.2 Heat stability of SAV and estimation of the heat-induced systematic error

First, an assay on the loss of activity of SAV samples at elevated temperatures was performed in order to find an appropriate time

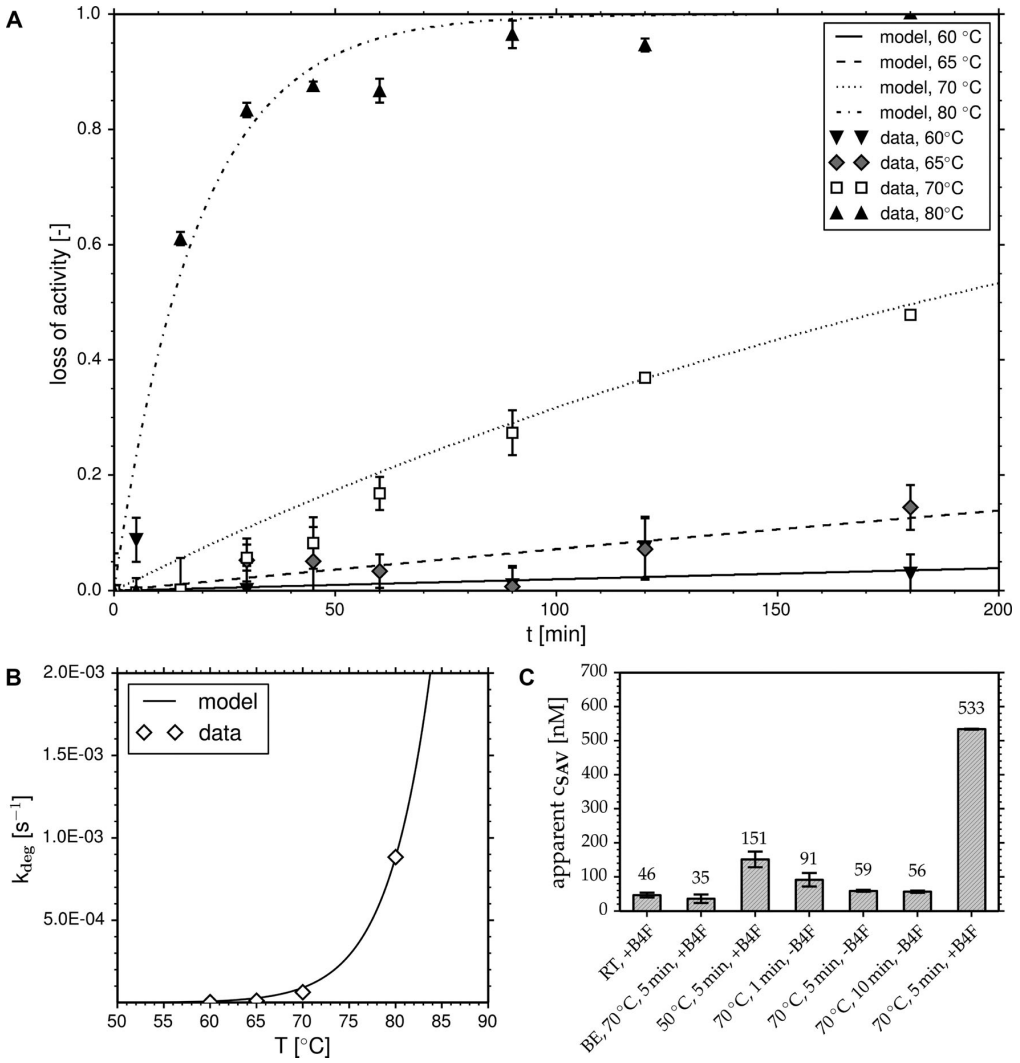

Figure 1. Development of a heat-based assay for the rapid quantification of biotin (BIO) blocked binding sites of streptavidin (SAV). Error bars represent SDs from three replicates. (A) Loss of activity by heat incubation: denaturing studies on a supernatant containing SAV derived from a bioreactor cultivation of *Streptomyces avidinii* on M3 medium incubated at elevated temperatures. The curves were acquired by a fit to the first order denaturation model of Eq. (2). The degradation constants k_{deg} were 3.31×10^{-6}, 1.24×10^{-5}, 6.36×10^{-5}, and 8.84×10^{-4} s^{-1} for 60, 65, 70, and 80°C, respectively. (B) Course of the degradation constant k_{deg} upon temperature, based on calculations according to Arrhenius' equation (Supporting Information, Eq. (S1)) with an activation energy E_a of 229 kJ mol^{-1} [34] and a preexponential factor $k_{deg,0}$ of 6.5395×10^{30} s^{-1}. (C) Condition variation to detect BIO-blocked binding sites of SAV. A supernatant containing BIO-blocked binding sites was incubated at different temperatures for different periods of time either in the presence (+B4F) or absence (−B4F) of biotin-4-fluorescein and fluorescence measurement buffer. A reference sample was incubated at room temperature. The second bar shows a control sample with an excess of BIO (abbreviated BE for biotin excess).

and temperature range for the assay. An SAV-containing supernatant from a cultivation of *S. avidinii* of a concentration of 5606 ± 11 nM was diluted 10-fold by demineralized water. Samples of 1 mL were incubated in a reaction tube at 60, 65, 70, and 80°C for 180 min for an analysis of heat-induced denaturation of SAV. Three samples of 20 μL each were taken after 0, 5, 15, 30, 45, 60, 90, 120, and 180 min of incubation at these temperatures, followed by a measurement after 30 min of incubation at RT. To quantify the results, the data sets were fit to the first-order model for an irreversible denaturation of SAV described in Eq. (2).

$$\frac{dc_{SAV}}{dt} = -k_{deg}\, c_{SAV} \qquad (2)$$

where t is the time and k_{deg} is the reaction rate of the irreversible denaturing step.

Experimental results and the regression curves acquired by parameter fits to Eq. (2) are shown in Fig. 1A. A meta-analysis of the degradation constants was performed according to Arrhenius [33] (see Section 2 of Supporting Information for details). A corresponding plot is shown in Fig. 1B. The plot does not incorporate denaturation of SAV at higher temperatures. According to the data, an incubation of SAV at temperatures above 70°C should be avoided in order to retain bioactivity of the protein. This result matches the data of González et al. [5], who observed a melting point of 75°C for BIO-free SAV in a phosphate buffer. The model curves predict the loss of 50 % of activity after 182 and 13 min of incubation at 70 and 80°C, respectively. For a short-time incubation of 10 min a proportion of 41.2% of SAV lost its BIO-binding ability during incubation at 80°C, whereas this proportion was only 3.7% at 70°C. Based on these results, temperatures above 70°C were not included in the following experiments.

The results of the parameter estimation suggest that 49 nM of monomeric, BIO-free SAV[1] lose 3.7% of activity after 10 min of incubation at 70°C. However, for measurements of BIO-containing samples it has to be taken into account that the stability of SAV increases in the presence of bound BIO [5]. Thus, the loss of activity should be even lower in the conditions provided by the assay. Considering the close structural relation of BIO and B4F, B4F is likely to stabilize SAV at elevated temperatures as well. This hypothesis seems to be confirmed by the results of the control curve shown in Fig. 2A, which shows no decrease of the SAV concentration for 15 min of incubation at 70°C. Taking into account the dissociation constants of 1.4×10^{-10} M for the B4F–SAV complex [35] and 1×10^{-15} M for the complex of BIO and SAV [3], the proportion of free and therefore less stabilized SAV in the presence of both of these molecules can be considered diminishingly small. Therefore, the loss of activity through heat-induced unfolding of SAV was neglected in the following studies.

3.3 Screening for conditions for the detection of BIO-blocked binding sites

In the next step, appropriate conditions for the determination of blocked binding sites of SAV were in the focus. A volume of 100 mL of a supernatant containing 3356 ± 65 nM of SAV was saturated with a strong excess (approximately 191 μM) of (+)-BIO (Fluka, Switzerland) and incubated at RT for 15 min to allow the binding of BIO to SAV. Unbound BIO was removed by a stepwise diafiltration applying a 5 kDa polyethersulfone filtration module (Pellicon XL-50, Millipore, Germany). The sample was diluted 10-fold for seven times, followed by a concentration step, in which the volume was reduced to the initial 100 mL.

For the detection of BIO-blocked binding sites, samples of the filtration retentate were incubated in a standard laboratory heat block (VWR) at elevated temperatures, followed by fluorescence measurement in the presence of B4F. Two temperatures (50 and 70°C) and three incubation times (1, 5, and 10 min) were analyzed. A volume of 980 μL of B4F containing assay buffer was either incubated in the heat block along with 20 μL of sample, or the sample was added to room-tempered, B4F-supplemented assay buffer directly after the heat incubation. A control sample with an excess of free BIO (abbreviated BE for biotin excess) was also measured to analyze the impact of a strong BIO surplus on the assay. As shown in Fig. 1C, the detection of 533 ± 1 nM of BIO-blocked SAV in a sample containing 3356 ± 65 nM of BIO-saturated SAV was possible for a temperature of 70°C and an incubation time of 5 min in the presence of B4F and measurement buffer. This corresponds to a proportion of detectable SAV Q_{SAV} of 0.16, where $Q_{SAV} = 1$ represents 100% detectability. The control sample incubated at RT allowed the detection of 46 ± 7 nM of SAV ($Q_{SAV} = 0.01$). Incubating only the sample at elevated temperatures and mixing it with room tempered, B4F-containing measurement buffer afterwards did not deliver satisfying results. These results indicate that the heat incubation caused displacement of BIO by B4F followed by fluorescence quenching, thus allowing a partial detection of BIO-blocked binding sites of SAV.

3.4 Analysis of BIO displacement

Two parameters were varied in the next step in order to improve the low proportions of detectable SAV. The incubation time at the elevated temperature (70°C) was altered to characterize the course of the assay signal over time. Moreover, the incubation time at RT after the heat incubation was changed to determine whether the assay signal is stable or subject to variations due to BIO-binding to B4F-blocked binding sites releasing B4F, once the temperature is lowered from 70°C to RT. An *E. coli* supernatant diluted to an SAV concentration of 596 nM was used for the experiments to fit the maximal concentration range of the assay. In contrast to the previous experiments this supernatant was characterized by a large number of contaminating proteins and a higher salt content.[2] No changes in the assay signal were observed when the incubation time at RT after the heat incubation was performed for 5, 15, 30, and 45 min, respectively (data not shown). The results of the variation of the incubation time at 70°C are shown in Fig. 2A.

The asymptotic course of the signal curve indicates robust assay conditions for incubation periods ≥7.5 min. A BIO-free control sample of SAV of 596 nM led to a constant assay signal in the analyzed time interval, indicating that SAV is sufficiently stable under these conditions. As SAV is further stabilized in the presence of BIO [4,5], it is highly improbable that denaturation took place in the partially and completely BIO-saturated SAV samples. The proportions of detectable SAV Q_{SAV} of 0.89 ± 0.01 and 0.82 ± 0.04, respectively, were still lower than 1 for both partially and completely BIO-blocked binding sites ($Q_{blocked}$ of 0.5 and 1.0, respectively). However, these proportions were larger than the ones observed for the approximately 3.4 μM sample (Q_{SAV} of 0.16) of the previous experiment.

In the next step, the general applicability of the displacement of BIO by B4F was tested on different fermentation supernatants.

[1] the maximal detectable concentration for a measurement applying a 50 nM B4F-buffer.

[2] NaCl concentration of the undiluted *E. coli*-supernatant: 2.5 g L^{-1} vs. approx. 0 g L^{-1} for the diafiltered supernatant.

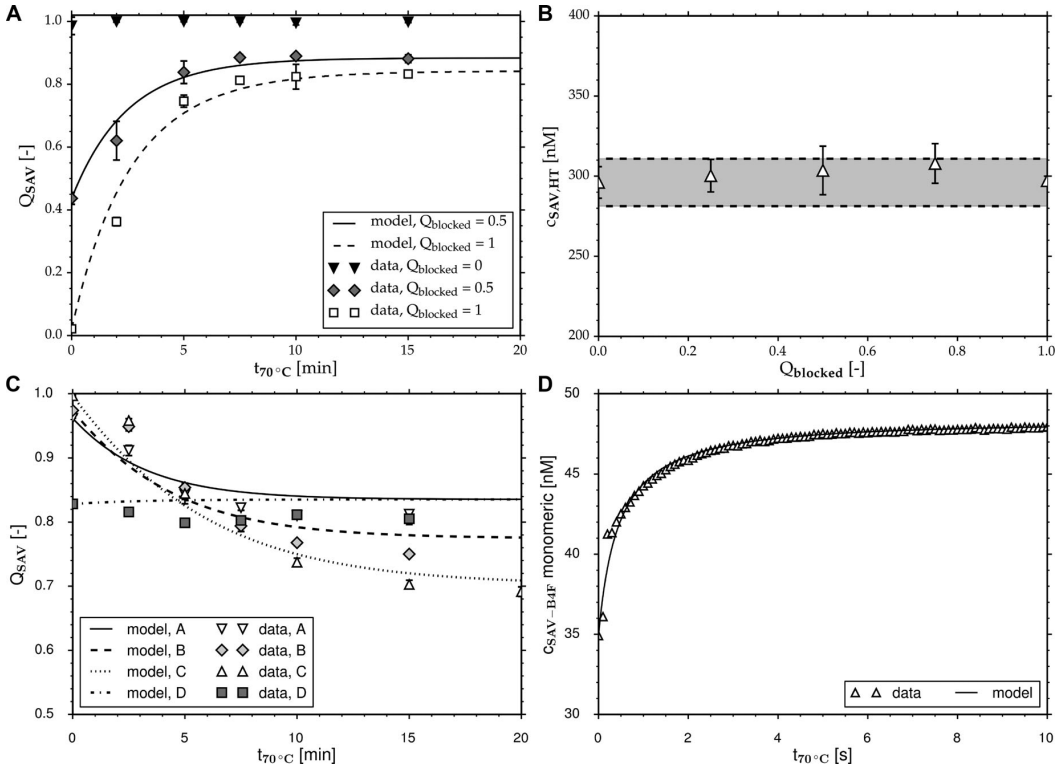

Figure 2. Variation of SAV concentration, biotin (BIO) saturation and time of heat incubation, and studies on the association and dissociation of the complexes SAV–BIO and SAV–B4F. Error bars represent SDs from three replicates. (A) Variation of the incubation time at 70°C in the heat assay for the detection of blocked binding sites of SAV. Samples characterized by different degrees of BIO saturation $Q_{blocked}$ were analyzed, where $Q_{blocked} = 1$ represents 100% of saturation of the available binding sites. Q_{SAV} is the proportion of detected SAV. The model curves were acquired by parameter optimization for Eqs. (4a) and (4b) in COPASI (see Section 3.7). (B) Heat assay results for a 296 nM SAV sample after an incubation at 70°C for 10 min. Degrees of BIO saturation vary from $Q_{blocked} = 0$ (all binding sites are BIO-free) to $Q_{blocked} = 1$ (complete saturation). All concentrations were within a range of ±5% of the signal for the unsaturated SAV sample, as is shown by the shaded gray area. (C) Kinetic data sets (symbols) and model curves (lines) for the parameter estimation based on BIO-free SAV samples that were preincubated in measurement buffer for the formation of the SAV–B4F complex. All samples contained 605 ± 24 nM of tetrameric SAV. Curve A: ratio of BIO to monomeric SAV: 1.06:1; B: 2.11:1; C: 4.23:1; D: 80% of BIO-free, B4F-blocked SAV and 20% of BIO-saturated SAV (ratio of total BIO—bound and unbound—to monomeric SAV: 1.06:1). (D) Comparison of model curve and kinetic experimental data of one of the five data sets used for the estimation of the association rate of the SAV–B4F complex at 70°C. The initial values for all species were chosen according to the data set. The $k_{on,B4F}$ and $k_{off,B4F}$ rates correspond to the results from the parameter estimation with 1.60×10^8 M^{-1} s^{-1} and 8.27×10^{-4} s^{-1}, respectively.

3.5 Variation of the culture supernatant

The supernatants were taken from cultivations on complex media without BIO supplementation, which according to our experience usually lead to low proportions of BIO-blocked binding sites. This was achieved by expression systems that allow the secretion of SAV into the medium. Fluorescence measurements on these samples after an incubation at 70°C for 10 min resulted in an unaltered fluorescence signal compared to the signal of a similar assay at RT, indicating a negligible proportion of blocked binding sites.[3]

The supernatants were diluted by demineralized water to adjust the concentration of SAV to 1.2 μM. The samples were then mixed with different volumes of an aqueous, 4.8 μM solution of BIO dissolved in a 50 mM phosphate buffer (pH 7.5), to reach a final tetrameric SAV concentration of 600 nM with degrees of BIO saturation $Q_{blocked}$ of 0, 0.25, 0.5, 0.75, and 1.0. All volumes were adjusted to 1 mL by the addition of demineralized water. After 15 min of incubation at RT, six aliquots of 20 μL of each sample were mixed with 980 μL of fluorescence measurement buffer. Three aliquots were measured at RT in the standard assay to determine the concentration of BIO-free binding sites, whereas the other three were analyzed after 10 min of incubation at 70°C and 30 min of incubation at RT to detect BIO-blocked binding sites.

The supernatants from the different expression hosts showed a similar signal pattern in the assay, indicating that neither the SAV chain length, nor the concentration of contaminating

[3]The hypothesis that small fractions of biotin-blocked binding sites can be detected by this procedure is confirmed by the following optimization procedure and by calculations based on the polynomial and the biochemical model discussed in sections 3.6 and 3.7.

Table 1. Proportions of detectable SAV Q_{SAV} for three different culture supernatants, different degrees of biotin saturation $Q_{blocked}$ and an incubation of the samples at 70°C for 10 min

Theoretical $Q_{blocked}$ [-]	$Q_{SAV,\ E.\ coli}$ [-]	$Q_{SAV,\ S.\ avidinii}$ [-]	$Q_{SAV,\ P.\ pastoris}$ [-]
0	1.01 ± 0.01	1.00 ± 0.02	1.00 ± 0.00
0.25	0.93 ± 0.00	0.92 ± 0.01	0.92 ± 0.01
0.5	0.89 ± 0.02	0.87 ± 0.01	0.87 ± 0.02
0.75	0.87 ± 0.01	0.85 ± 0.03	0.83 ± 0.01
1	0.82 ± 0.01	0.82 ± 0.01	0.80 ± 0.02

The *Escherichia coli* and *Streptomyces avidinii* supernatants contained full-length streptavidin (SAV), whereas the *Pichia pastoris* supernatant contained a core SAV consisting of AA 13–139 of full-length SAV. All samples were diluted to a tetrameric SAV concentration of approximately 600 nM with actual concentrations of 592 (*E. coli*), 593 (*S. avidinii*), and 604 nM (*P. pastoris*).

proteins has a major impact on the assay signal. Table 1 sums up the results from the variation experiments of the SAV-containing supernatants.

As was already observed in the kinetic measurements, the maximal detectable SAV concentration was again dependent on the degree of BIO saturation. Higher proportions of detected SAV were achieved for lower degrees of BIO saturation. The relative ratios of BIO, B4F, and available binding sites therefore had an impact on the assay signal and were varied in the next optimization step. Most of the following experiments were performed on the *E. coli* supernatant, because an SDS-PAGE analysis of this supernatant showed the largest proportion of contaminating proteins, representing the potentially most difficult conditions for the assay.

Additional experiments focused on the heat resistance of BIO, B4F, and the SAV–B4F complex at 70°C, indicating a sufficient stability of all of these compounds (Supporting Information, Sections 7 and 8). Moreover, the impact of salt ions on the result of the assay was identified to be negligible for the conditions tested (Supporting Information, Section 9). These results simplified the setup for the following experiments and modeling steps.

3.6 Variation of the B4F to BIO ratio and polynomial modeling

To provide a more favorable ratio of B4F toward BIO and SAV, respectively, the BIO-supplemented SAV samples were diluted two-fold for the next experiment. The heat incubation was performed for 10 min at 70°C to reach the constant region of the curves shown in Fig. 2A.

Figure 2B reveals that the problem of an only partial detection of SAV can be eliminated by a stronger excess of B4F toward BIO and SAV binding sites. A constant assay signal corresponding to the total concentration of available binding sites in the sample was detected independent of the degree of BIO saturation $Q_{blocked}$. Thus, the SAV sample should be diluted in order to yield valid results in the heat assay.

To determine the maximal concentration of BIO-saturated SAV to be used for the assay while minimizing the proportion of undetected binding sites, a systematic variation of the SAV concentration at different degrees of BIO saturation $Q_{blocked}$ was performed. The *E. coli* supernatant was diluted to concentrations from 300 to 600 nM in increments of 50 nM. The results were imported into the design of experiments software MODDE and evaluated by a partial least square fit to a polynomial model leading to the contour plot shown in Fig. 3A.

The model consisted of the factors c_{SAV} and $Q_{blocked}$ and their linear interaction ($c_{SAV} \times Q_{blocked}$), all of which were found to be highly significant (p-values for a confidence level of 0.95: 1.1×10^{-10}, 1.5×10^{-8}, and 2.1×10^{-4}). Model values of 0.855 and 0.811 for R^2 and predicted R^2, respectively, were achieved. Model Eq. (3) allows the calculation of the detectable SAV concentration $c_{SAV,det}$:[4]

$$c_{SAV,det} = 1.0074 - 0.137\ Q_{blocked} - 1.117 \times 10^{-5} c_{SAV} - 0.0006\ Q_{blocked}\ c_{SAV} \quad (3)$$

The plot in Fig. 3A, visualizing the results of Eq. (3) for typical SAV concentrations and degrees of BIO saturation, can be used to decide if a given sample should be diluted for valid results of the assay or if the undiluted sample may be used for the determination of blocked binding sites.

3.7 Kinetic modeling of the displacement of BIO by B4F at 70°C

To further characterize the detection of BIO-blocked binding sites and to provide biochemical insight into the displacement of SAV-bound BIO by B4F at 70°C, the data set was analyzed by the means of a competitive binding model using CellDesigner for model creation, COPASI for parameter optimization and Scilab for parameter variation, and simulation of various assay conditions. The competition reaction can be described by a system of the two differential Eqs. (4a) and (4b), each consisting of a term for the association (*on*) and the dissociation (*off*) of the respective complexes:

$$\frac{dc_{SAV-bio}}{dt} = c_{SAV}\ c_{bio}\ k_{on,bio} - c_{SAV-bio}\ k_{off,bio} \quad (4a)$$

$$\frac{dc_{SAV-B4F}}{dt} = c_{SAV}\ c_{B4F}\ k_{on,B4F} - c_{SAV-B4F}\ k_{off,B4F} \quad (4b)$$

where c_{SAV} is the concentration of free SAV, $c_{SAV\text{-}bio}$ the concentration of the SAV–BIO complex, $c_{SAV-B4F}$ the concentration of SAV–B4F complex, and c_{bio} and c_{B4F} the concentrations of the unbound concentrations of BIO and B4F, respectively. The net change of the complex concentration is determined by the complex formation and dissociation rates k_{on} and k_{off} for both complexes.

The equations are based on the assumption that an accurate description of the system is achieved by a pseudo-first order reaction model referring to monomeric concentrations instead of the SAV tetramer. Four data sets were used for the parameter estimation: the kinetic data set shown in the saturation curves in Fig. 2A was used to determine $k_{off,bio}$ by providing conditions in

[4] exact coefficients in order of appearance: 1.00736, 0.137313, –1.11701 × 10^{-5} and –0.000558038. Please use the tetrameric concentration of SAV in the sample for the calculation without taking into account the dilution by measurement buffer.

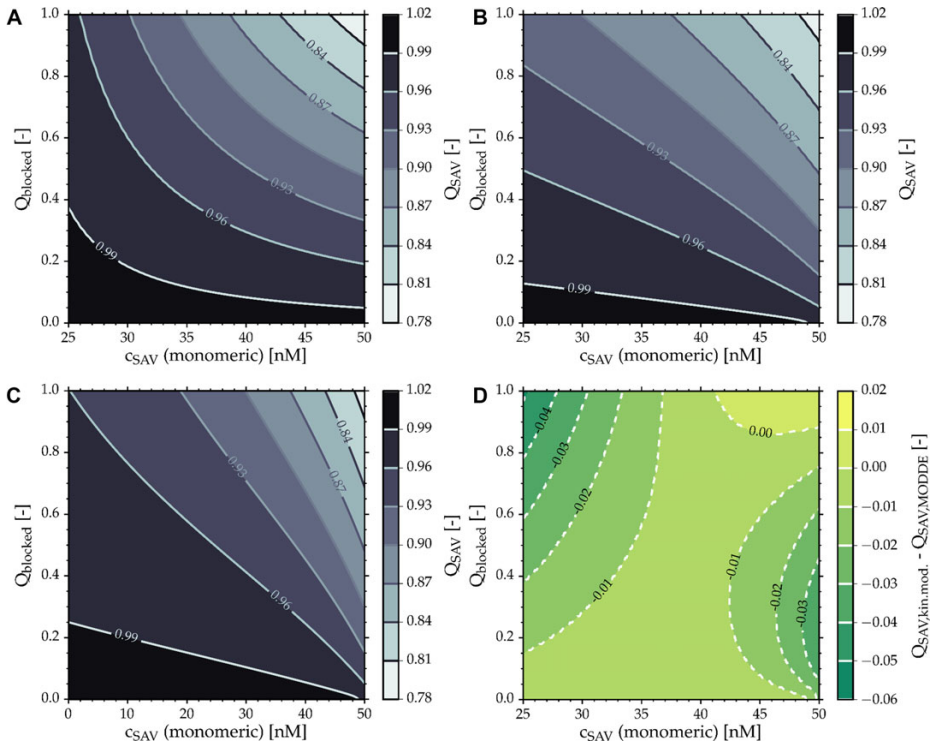

Figure 3. Contour plots for the proportion of detectable SAV Q_{SAV} in the heat assay at 70°C for an incubation for 10 min as a function of the final monomeric SAV concentration after the dilution in the measurement buffer c_{SAV} and the proportion of biotin-blocked binding sites $Q_{blocked}$. The plots are based on two different models. (A) Results of the model developed in MODDE. The data set was fit to the polynomial model described in Eq. (3). (B) Plot of simulation results based on the ordinary differential equation system of Eqs. (4a) and (4b), applying the parameters shown in Table 2 in the interval of 25–50 nM of monomeric SAV. (C) Plot of the ordinary differential equation simulation in the complete interval of 0–50 nM of SAV. (D) Direct comparison of the polynomial model (MODDE) and the biochemical model presented as the difference of the predicted concentrations of detectable SAV Q_{SAV} of the polynomial model $Q_{SAV,MODDE}$ and the biochemical model $Q_{SAV,kin,mod}$. Supporting Information, Fig. S2 contains two plots visualizing the deviations of both models toward the experimental data. A final monomeric SAV concentration of 48 nM in the measurement buffer corresponds to a tetrameric concentration of 600 nM in the sample used for the assay (dilution factor: 1:50 and conversion of tetrameric concentrations into monomers).

which BIO is displaced by B4F by an initially high concentration of the BIO–SAV complex. This was achieved by incubating the sample in measurement buffer at RT prior to the addition of BIO. An additional set of kinetic measurements was included for the calculation of the $k_{off,B4F}$ rate focusing on conditions characterized by high initial concentrations of the SAV–B4F complex. A selection of corresponding data sets is shown in Fig. 2C. Additionally, the data set of the concentration variation experiments used for the fit of the polynomial model was taken into account. Finally, kinetic binding measurements for the association of the B4F–SAV complex were performed using the *E. coli* supernatant. A corresponding data set is shown in Fig. 2D. All data sets were completed by calculations based on the mass balances of SAV, BIO, and B4F, from which the theoretical time courses for the SAV–BIO complex and free BIO and B4F were reconstructed. The calculations were performed assuming that the free SAV concentration is negligible, which seems reasonable considering the dissociation constants at RT and the full detectability of a 300 nM SAV sample at 70°C. Please refer to the Supporting Information, Section 3.1 for a detailed description of the parameter estimation. The results of the parameter estimation are shown in Table 2.

The dissociation constants $K_{d,bio}$ and $K_{d,B4F}$ at 70°C derived from the parameter optimization differ by a factor of 23.6 ± 6.1. In contrast to this ratio, usual dissociation constants for the B4F–SAV complex at RT are in the range of 1.4×10^{-10} M [35], whereas the constant for BIO is approximately 1×10^{-15} M [3], leading to a factor in the range of 10^{-5}. Therefore, unlike at RT, the heat assay provides conditions favoring the formation of the SAV–B4F complex instead of the complex of SAV and its natural ligand BIO. As the structures of B4F and BIO only vary in the modification on the valeric acid side chain, the difference in temperature dependence of the dissociation constants is likely to be an effect of this side chain rather than the core structure of the vitamin. Since the side chain is involved in dimer stabilization of SAV [3], the reason for the elution of BIO at elevated temperatures may be associated to a decreased dimer stability, rather than to an effect on a single SAV subunit. A comparison of the results

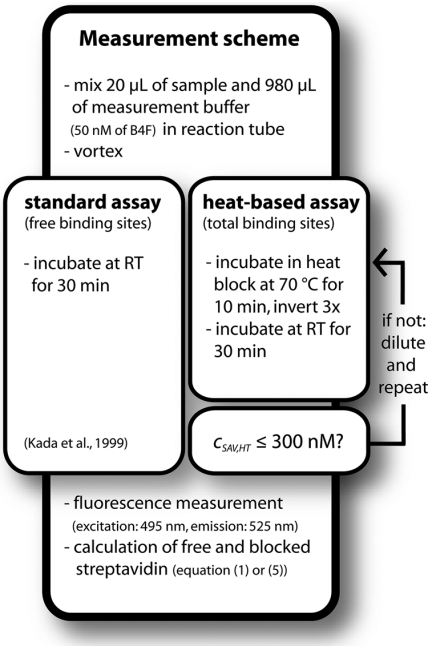

Figure 4. Schematic display of the final assay procedure. Either dilute the supernatant to a tetrameric $c_{SAV,HT} \leq 300$ nM or use Fig. 3A and B to choose an appropriate concentration. Equation (5) may be used for the correction of the assay signal for $c_{SAV,tetrameric} > 300$ nM.

Table 2. Parameter values and corresponding SDs acquired by the final parameter optimization in COPASI based on the ordinary differential equation system consisting of Eqs. (4a) and (4b) and additional binding measurements for the association of the B4F–SAV complex

Parameter	Value	CV [%]
$k_{on,bio}$	$4.46 \pm 0.93 \times 10^{7}$ M^{-1} s^{-1}	21.08
$k_{off,bio}$	$5.38 \pm 0.32 \times 10^{-3}$ s^{-1}	5.94
$k_{on,B4F}$ [a)]	$1.60 \pm 0.01 \times 10^{8}$ M^{-1} s^{-1}	0.60
$k_{off,B4F}$	$8.27 \pm 1.11 \times 10^{-4}$ s^{-1}	13.36
$K_{d,bio}$	$1.22 \pm 0.27 \times 10^{-11}$ M	21.90
$K_{d,B4F}$	$5.16 \pm 0.70 \times 10^{-13}$ M	13.37
Q_{Kd}	23.60 ± 6.05	25.66

All values refer to a temperature of 70°C. The dissociation constants were calculated according to $K_d = k_{off}/k_{on}$. The SDs are shown as absolute and relative values (coefficient of variation, CV). Deviations for the dissociation constants K_d and the ratio of the dissociation constants $Q_{Kd} = K_{d,bio}/K_{d,B4F}$ were calculated by Gaussian error propagation.
a) Parameter estimation based on binding measurements of only the SAV–B4F complex.

to the data of Chivers et al. [25] and Deng et al. [26] suggests that the results are feasible. A detailed analysis is performed in the Supporting Information, Section 3.2.

Based on the kinetic parameters in Table 2, the ordinary differential equation system of Eqs. (4a) and (4b) was solved covering the whole range of potential SAV concentrations in the assay (0–50 nM of monomeric SAV) and proportions of blocked binding sites $Q_{blocked}$ from 0 to 1 (0–100% of BIO saturation). The system was solved by Scilab's ordinary differential equation solver using its order 4 adaptive Runge–Kutta algorithm. The results are shown in Fig. 3B and C (Section 3.6). The results from the solver correlate well with the experimental data (see Supporting Information, Table S3 for a direct comparison), especially for high concentrations of SAV.

3.8 Discussion of model accuracy and specification of boundary conditions for the assay

According to the polynomial model, even very low concentrations of SAV lead to errors in the quantification of detectable SAV at high degrees of BIO saturation $Q_{blocked}$. For a maximal error of 5% the $Q_{blocked}$ value should not exceed 0.5 for intermediate tetrameric SAV concentrations of approximately 440 nM in the sample used for the measurement (see Fig. 3A in Section 3.6). This concentration corresponds to a final concentration of 35 nM of monomeric SAV in the measurement buffer. The prediction matches the data, as can be seen in Supporting Information, Table S4.

The biochemical model (Fig. 3B) deviates from the experimental data in several cases when the product in the sample is to be detected in its entirety (Q_{SAV} approaching 1). At a concentration of approximately 300 nM of tetrameric SAV in the sample, the detection of all binding sites is possible independent from the degree of BIO saturation (see Section 3.6, Fig. 2B). Figure 3B clearly indicates the lack of fit of the biochemical model for intermediate concentrations of SAV (24 nM of monomeric SAV in measurement buffer), with an increasing error for increasing degrees of BIO saturation. At 100% of BIO saturation, the predicted Q_{SAV} differs from the experimental data by 8.6%. Figure 3D shows a plot of the differences for the modeled values of Q_{SAV} of both models, indicating that in the corresponding parameter area (upper left part of the plot) the polynomial model developed in MODDE leads to more accurate results, because this part of the plot shows negative values, meaning that the polynomial model leads to higher proportions of detectable SAV. We therefore recommend the use of this model (Fig. 3A, Section 3.6) for an estimation of the detectable SAV concentration in this parameter area ($c_{SAV} \approx 300$ nM, high $Q_{blocked}$). However, the polynomial model shows an increasing lack of fit for high concentrations of SAV at low degrees of BIO saturation. The comparative plot in Fig. 3D once again shows a negative deviation, meaning that higher Q_{SAV} values are predicted by the polynomial model (MODDE). However, unlike for the upper left area of the plot the biochemical model (Fig. 3B) predicts the experimental data more accurately in the lower right area of the plot and should therefore be used for corresponding analyses. This can most easily be tracked by the two additional plots of the differences of modeled and experimental data for both models that are shown in Supporting Information, Fig. S1. Low/low and high/high combinations of c_{SAV} and Q_{SAV} along the diagonal of Fig. 3D also show slightly negative values. The biochemical model reflects the experimental results more accurately in this parameter area, as can be seen in Supporting Information, Fig. S1.

After characterizing the assay system and discussing the accuracy of both models, we can now define practical boundary conditions for the assay. For typical applications, a deviation of ≤5% of measured and actual SAV should be sufficient. As a consequence of both the biochemical and polynomial model and their accuracy discussed above, we suggest using maximal tetrameric SAV concentrations of 300 nM for the assay, corresponding to a ratio of monomeric SAV after dilution to B4F of approximately 1:2. This should provide favorable conditions for a complete detection of BIO-blocked as well as free binding sites. The practical measurements suggest that the actual error is next to zero, indicated by concentrations of 296 ± 10 nM at complete saturation vs. 297 ± 3 nM for a BIO-free sample (see Fig. 2B).

For a validation of this concentration range, the three different culture supernatants from cultivations of *E. coli*, *P. pastoris*, and *S. avidinii* were once again analyzed in different concentrations at complete BIO saturation. At 300 nM of SAV the detection of all of the available binding sites was possible independent from the chain length of SAV and the total protein concentration in the sample. The results of this final validation step are shown in the Supporting Information, Table S5. Moreover, the kinetic accuracy of the biochemical model was validated for the three supernatants. A plot of these experiments is shown in Supporting Information, Fig. S2. Both validation steps led to satisfying results. The final, validated assay procedure is visualized in Fig. 4. The following section describes a method for the mathematical correction of the assay signal without dilution of the sample for working concentrations of tetrameric SAV above 300 nM.

3.9 Mathematical correction of assay values for SAV concentrations larger than 300 nM

Although the dilution of the sample for concentrations of c_{SAV} > 300 nM is recommended, larger SAV concentrations measured at high degrees of BIO saturation may be corrected by the use of Eq. (5), if a dilution of the sample is not feasible.[5]

$$c_{SAV,corr} = -134\ \text{nM} + 0.117\ c_{SAV,RT} + 1.472\ c_{SAV,HT} - 0.001\ c_{SAV,RT}\ c_{SAV,HT} \quad (5)$$

where $c_{SAV,corr}$ is the corrected SAV concentration and $c_{SAV,HT}$ and $c_{SAV,RT}$ are the SAV concentrations calculated from the measurements at 70°C and RT, respectively. This equation is valid for tetrameric SAV concentrations in the range of 300 nM ≤ c_{SAV} ≤ 600 nM.

Equation (5) was derived from a partial least square fit in MODDE based on the measurement values for $c_{SAV,HT}$ and $c_{SAV,RT}$ and the theoretical concentration of SAV in the sample. The data was taken from the concentration variation experiments. Supporting Information, Table S6 shows exemplary results for SAV concentrations corrected according to this procedure, including the concentrations from the supernatant variation, which were not used for the parameter optimization in MODDE, therefore serving as an external control. Typical deviations of the theoretical and the corrected calculated concentration for the external validation are in the range of ±5%.

Additional simulations based on the kinetic model suggest, that comparable improvements of the assay result for c_{SAV} > 300 nM can be expected when the B4F concentration in the assay buffer is doubled (Supporting Information, Section 10, Fig. S3A). Minor improvements may also be achieved by prolonging the incubation period at 70°C (Supporting Information, Fig. S3B).

3.10 Monitoring of the production of SAV in shake flasks

After optimizing and characterizing the assay procedure, it was applied to a shake flask cultivation of a clone of *P. pastoris* expressing the core SAV gene under control of the methanol-inducible alcohol oxidase 1 (AOX1) promoter (see Section 2.3.1 for experimental details). A variation of the BIO concentration in buffered MG medium was performed with BIO supplements of 1 (label A) and 4 μM (label B), respectively. This did not influence the growth behavior of *P. pastoris* (Fig. 5B). Figure 5A demonstrates exemplarily that the standard assay by Kada et al. [21, 22] leads to biased results for cultivations applying media with high initial concentrations of BIO. Production of SAV started directly after induction at 24 h of cultivation. However, the standard assay allowed the detection of SAV only after 48 and 73 h of cultivation for concentrations of BIO of 1 and 4 μM in the medium, respectively. The heat-based results suggest that residual BIO was present in the medium after the initial growth phase, which subsequently was incorporated into the binding pockets of SAV after induction. Therefore, the accumulation of free binding sites was delayed by several hours. Overall, the volumetric productivities based on the heat assay amount to 4.2 (1 μM of BIO) and 6.7 nM h^{-1} (4 μM), as opposed to 2.8 and 1.9 nM h^{-1} (factors 1.5 and 3.5, respectively) based on the standard assay. Moreover, the course of product formation starting from induction can be described as linear, which is not reflected by the results from the standard assay. Both cultivations suggest that prolonging the induction period should lead to higher proportions of bioactive binding sites. These findings clearly show that the standard assay leads to biased results concerning the productive properties of the host, which can be avoided by an additional heat-based analysis.

4 Concluding remarks

By a systematic optimization of conditions, we demonstrated that BIO-blocked binding sites of SAV can be detected by a combination of the fluorescence quenching assay established by Kada et al. [21,22] and a prior incubation in a heat block at 70°C. The elution studies of Holmberg and coworkers [23] are therefore partially applicable to free SAV and BIO. The proportion of detectable binding sites depends on the ratio of B4F toward BIO and the concentration of available binding sites of SAV, respectively. If the dilution of the SAV-containing sample is strong

[5] exact coefficients in order of appearance: –133.96 (p = 0), 0.116972 (p = 1.46 × 10^{-8}), 1.47184 (p = 3.09 × 10^{-27}) and –0.000639386 (p = 0.003); model characterization: R^2 = 0.98; predicted R^2 = 0.976. Please use the tetrameric concentrations of SAV in the sample prior to mixing with measurement buffer for the calculation.

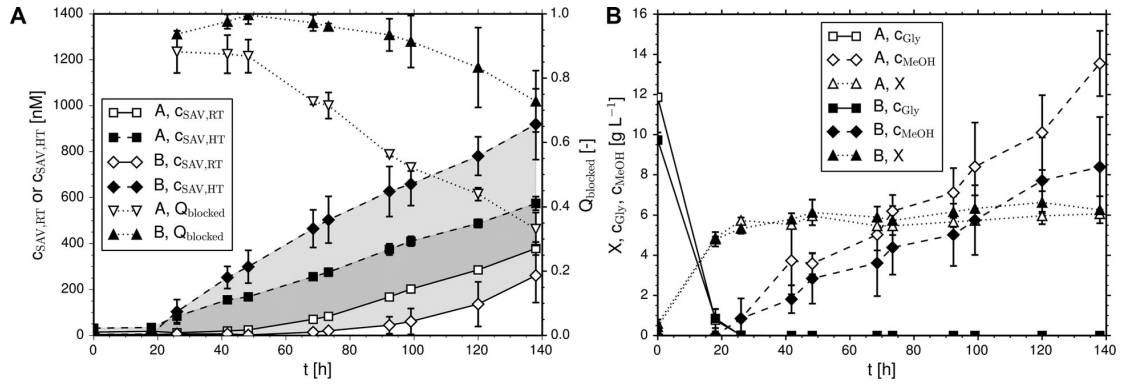

Figure 5. Shake flask cultivation of a clone of *Pichia pastoris* secreting core SAV in biotin-supplemented buffered MG-medium upon induction by methanol. The medium was supplemented with two concentrations of biotin: 1 μM (labeled A) and 4 μM (labeled B). Induction was started after 24 h of cultivation according to Section 2.3.1. All cultivations were performed in three biological replicates. (A) Plot of the SAV concentrations at room temperature and in the heat assay and corresponding proportion of biotin-blocked binding sites $Q_{blocked}$. The shaded area is a graphical representation of the biotin-blocked binding sites. (B) Course of the concentrations of dry cell weight X, methanol c_{MeOH}, and glycerol c_{Gly}.

enough (tetrameric $c_{SAV} < 300$ nM)[6], all of the binding sites in the sample can be detected, independent of the chain length of SAV, the total protein concentration in the sample, and the degree of BIO saturation. This allows the application of the assay for supernatants derived from a large variety of expression systems, which typically differ strongly in the chain length of SAV due to variable N- and C-termini [13, 14] and their content of contaminating proteins. Unlike for SAV, the assay procedure did not lead to displacement of bound BIO by B4F when applied to avidin (Supporting Information, Section 11).

Further studies provided insight into the kinetic parameters during heat incubation. A model-based analysis revealed that the dissociation constants for B4F and BIO at 70°C differ by a factor of approximately 23.60 ± 6.05 with values of K_d of 1.22 ± 0.27 × 10^{-11} M for SAV–BIO and of 5.16 ± 0.70 × 10^{-13} M for the SAV–B4F complex, thus favoring the association of the B4F–SAV complex. At RT this factor is in the range of 10^{-5} [5, 35]. This is due to larger association as well as smaller dissociation rates for the SAV–B4F complex toward the natural binding partners SAV and BIO at 70°C (see Table 2). The change in affinity causes a shift from the precise detection of free binding sites at RT to conditions that allow a reliable detection of BIO-blocked sites after a heat incubation step. The results indicate that B4F – like BIO – seems to stabilize SAV at 70°C. Additional studies (see Supporting Information) showed that neither the degradation of SAV, nor heat-induced damage on B4F and BIO at 70°C harm the outcome of the assay. This is caused by the very low proportion of free, more heat-susceptible SAV due to the small dissociation constants for the SAV–BIO and SAV–B4F complexes and the thermostability of BIO and its fluorescence derivative, respectively. No change in complex formation of SAV and B4F was observed for altered salt contents in the sample. Furthermore, the presence of free BIO did not cause a displacement of B4F in time intervals of up to 45 min after the heat incubation step, once the B4F–SAV complex was formed. These properties allow a robust and reliable measurement of the blocked binding sites. The assay was tested in a shake-flask cultivation, providing insight into the fermentative properties of a clone of *P. pastoris* producing core SAV and demonstrating its worth for a more detailed analysis of SAV producers.

The final optimized assay, characterized by an incubation at 70°C for 10 min prior to the fluorescence measurement (see Fig. 4), permits a rapid and reliable monitoring of BIO-blocked binding sites throughout the fermentation of different expression hosts. No additional equipment or material is required compared to the assay of Kada et al. [21, 22] except for a standard laboratory heat block.

Practical application

The assay herein developed may be useful for various applications, particularly the monitoring and optimization of SAV production. Unlike a standard assay, heat-based measurement of total SAV reveals the actual start of SAV biosynthesis and the unbiased fermentative properties of a producer, rather than the accumulation of free binding sites. Combined with measurements of BIO-blocked, cytoplasmic SAV after cell disruption, this information may be used to optimize the BIO concentration in media and to monitor strategies to reduce host toxicity by SAV, which is a central problem in heterologous production of the protein. In downstream processing, the assay may determine whether the proportion of BIO-blocked SAV is high enough to render its denaturing, diafiltration and refolding economically feasible. Furthermore, it may be useful to monitor the effectiveness of nondenaturing methods for the separation of BIO and SAV by quantifying the degradation of BIO-blocked sites.

[6] For the dilution of 20 μL of sample by 980 μL of a 50 nM B4F solution.

This study is dedicated to the memory of Prof. Dr. Erwin Flaschel (1949–2014), a brilliant scientist and intriguing personality.

This work was financially supported by the Scholarship Programme of the German Environmental Foundation (DBU).

The authors have declared no conflict of interest.

Nomenclature

$Q_{blocked}$	[-]	Degree of biotin saturation of SAV
Q_{SAV}	[-]	Detectable proportion of SAV
c_{SAV}	[nM]	SAV concentration
$c_{SAV,HT}$ and $c_{SAV,RT}$	[nM]	SAV concentration calculated from measurements at high temperature and room temperature, respectively
$c_{SAV,det}$ and $c_{SAV,corr}$	[nM]	Detectable and corrected concentration of SAV
$c_{SAV,blocked}$	[nM]	Concentration of biotin-blocked SAV
c_{B4F} and $c_{SAV–B4F}$	[nM]	Concentration of B4F and its complex with SAV
c_{bio} and $c_{SAV–bio}$	[nM]	Concentration of biotin and its complex with SAV
c_{Gly} and c_{MeOH}	[g L^{-1}]	Concentration of glycerol and methanol, respectively
$K_{d,bio}$ and $K_{d,B4F}$	[M]	Dissociation constants of biotin and B4F for the binding of SAV, respectively
k_{on} and k_{off}	[s^{-1}] and [M^{-1} s^{-1}]	Reaction constants for the association and dissociation of a complex, respectively
k_{deg}	[s^{-1}]	Degradation constant for the irreversible denaturation of SAV
Q_{Kd}	[-]	Ratio of the dissociation constants of the complexes SAV–biotin and SAV–B4F
X	[g L^{-1}]	Dry cell weight concentration

5 References

[1] Chaiet, L., Wolf, F. J., The properties of streptavidin, a biotin-binding protein produced by streptomycetes. *Arch. Biochem. Biophys.* 1964, *106*, 1–5.

[2] Stapley, E. O., Mata, J. M., Miller, I. M., Demny, T. C. et al., Antibiotic MSD-235. I. Production by *Streptomyces avidinii* and *Streptomyces lavendulae*. *Antimicrob. Agents Chemother. (Bethesda)* 1963, *161*, 20–27.

[3] Sano, T., Vajda, S., Reznik, G. O., Smith, C. L. et al., Molecular engineering of streptavidin. *Ann. N Y Acad. Sci.* 1996, *799*, 383–390.

[4] Katz, B. A., Binding of biotin to streptavidin stabilizes intersubunit salt bridges between Asp61 and His87 at low pH. *J. Mol. Biol.* 1997, *274*, 776–800.

[5] González, M., Argarana, C. E., Fidelio, G. D., Extremely high thermal stability of streptavidin and avidin upon biotin binding. *Biomol. Eng.* 1999, *16*, 67–72.

[6] Skerra, A., Schmidt, T. G. M., Applications of a peptide ligand for streptavidin: The strep-tag. *Biomol. Eng.* 1999, *16*, 79–86.

[7] Szafranski, P., Mello, C. M., Sano, T., Smith, C. L. et al., A new approach for containment of microorganisms: Dual control of streptavidin expression by antisense RNA and the T7 transcription system. *Proc. Natl. Acad. Sci. U S A* 1997, *94*, 1059–1063.

[8] Kalofonos, H. P., Rusckowski, M., Siebecker, D. A., Sivolapenko, G. B. et al., Imaging of tumor in patients with indium-111-labeled biotin and streptavidin-conjugated antibodies: Preliminary communication. *J. Nucl. Med.* 1990, *31*, 1791–1796.

[9] Nguyen, V. A. T., Huynh, H. A., Hoang, T. V., Ninh, N. T. et al., Killed *Bacillus subtilis* spores expressing streptavidin: A novel carrier of drugs to target cancer cells. *J. Drug Target.* 2013, *21*, 528–541.

[10] Bayer, E. A., Kulik, T., Adar, R., Wilchek, M., Close similarity among streptavidin-like, biotin-binding proteins from *Streptomyces*. *Biochim. Biophys. Acta* 1995, *1263*, 60–66.

[11] Nordlund, H. R., Hytönen, V. P., Laitinen, O. H., Kulomaa, M. S., Novel avidin-like protein from a root nodule symbiotic bacterium *Bradyrhizobium japonicum*. *J. Biol. Chem.* 2005, *280*, 13250–13255.

[12] Helppolainen, S. H., Nurminen, K. P., Määttä, J. A. E., Halling, K. K. et al., Rhizavidin from *Rhizobium etli*: The first natural dimer in the avidin protein family. *Biochem. J.* 2007, *405*, 397–405.

[13] Pähler, A., Hendrickson, W. A., Kolks, M. A., Argarana, C. E. et al., Characterization and crystallization of core streptavidin. *J. Biol. Chem.* 1987, *262*, 13933–13937.

[14] Bayer, E. A., Ben-Hur, H., Hiller, Y., Wilchek, M., Postsecretory modifications of streptavidin. *Biochem. J.* 1989, *259*, 369–376.

[15] Sano, T., Pandori, M. W., Chen, X., Smith, C. L. et al., Recombinant core streptavidins. A minimum-sized core streptavidin has enhanced structural stability and higher accessibility to biotinylated macromolecules. *J. Biol. Chem.* 1995, *270*, 28204–28209.

[16] Hofmann, K., Wood, S. W., Brinton, C. C., Montibeller, J. A. et al., Iminobiotin affinity columns and their application to retrieval of streptavidin. *Proc. Natl. Acad. Sci. U S A* 1980, *77*, 4666–4668.

[17] Wu, S.-C., Wong, S.-L., Engineering of a *Bacillus subtilis* strain with adjustable levels of intracellular biotin for secretory production of functional streptavidin. *Appl. Environ. Microbiol.* 2002, *68*, 1102–1108.

[18] Wu, S.-C., Qureshi, M. H., Wong, S.-L., Secretory production and purification of functional full-length streptavidin from *Bacillus subtilis*. *Protein Expr. Purif.* 2002, *24*, 348–356.

[19] Nogueira, E. S., Schleier, T., Dürrenberger, M., Ballmer-Hofer, K. et al., High-level secretion of recombinant full-length streptavidin in *Pichia pastoris* and its application to enantioselective catalysis. *Protein Expr. Purif.* 2014, *93*, 54–62.

[20] Sano, T., Cantor, C. R., Expression of a cloned streptavidin gene in *Escherichia coli*. *Proc. Natl. Acad. Sci. U S A* 1990, *87*, 142–146.

[21] Kada, G., Falk, H., Gruber, H. J., Accurate measurement of avidin and streptavidin in crude biofluids with a new, optimized biotin-fluorescein conjugate. *Biochim. Biophys. Acta* 1999, *1417*, 33–43.

[22] Kada, G., Kaiser, K., Falk, H., Gruber, H. J., Rapid estimation of avidin and streptavidin by fluorescence quenching or

fluorescence polarization. *Biochim. Biophys. Acta* 1999, *1427*, 44–48.

[23] Holmberg, A., Blomstergren, A., Nord, O., Lukacs, M. et al., The biotin-streptavidin interaction can be reversibly broken using water at elevated temperatures. *Electrophoresis* 2005, *26*, 501–510.

[24] Buranda, T., Jones, G. M., Nolan, J. P., Keij, J. et al., Ligand receptor dynamics at streptavidin-coated particle surfaces: A flow cytometric and spectrofluorimetric study. *J. Phys. Chem. B* 1999, *103*, 3399–3410.

[25] Chivers, C. E., Crozat, E., Chu, C., Moy, V. T. et al., A streptavidin variant with slower dissociation and increased mechanostability. *Nat. Methods* 2010, *7*, 391–393.

[26] Deng, L., Kitova, E. N., Klassen, J. S., Dissociation kinetics of the streptavidin-biotin Interaction measured during direct electrospray ionization mass spectrometry analysis. *J. Am. Soc. Mass Spectrom.* 2013, *24*, 49–56.

[27] Müller, J. M., Risse, J. M., Jussen, D., Flaschel, E., Development of fed-batch strategies for the production of streptavidin by *Streptomyces avidinii* based on power input and oxygen supply studies. *J. Biotechnol.* 2013, *163*, 325–332.

[28] Higgins, D. R., Cregg, J. M. (Eds.), *Methods in Molecular Biology: Pichia protocols*, Vol. *103*, Humana Press, New York City 1998.

[29] Hoops, S., Sahle, S., Gauges, R., Lee, C. et al., COPASI: A COmplex PAthway SImulator. *Bioinformatics* 2006, *22*, 3067–3074.

[30] Funahashi, A., Tanimura, N., Morohashi, M., Kitano, H., CellDesigner:A process diagram editor for gene-regulatory and biochemical networks. *BIOSILICO* 2003, *1*, 159–162.

[31] Scilab Enterprises, *Scilab: Free and open source software for numerical computation (OS, Version 5.5.0)*, 2012.

[32] Hunter, J. D., Matplotlib: A 2 D graphics environment. *Comput. Sci. Eng.* 2007, *9*, 90–95.

[33] Arrhenius, S., On the reaction rate of the inversion of non-refined sugar upon souring. *Z. Phys. Chem.* 1889, *4*, 226–248.

[34] Waner, M. J., Navrotskaya, I., Bain, A., Oldham, E. D. et al., Thermal and sodium dodecylsulfate induced transitions of streptavidin. *Biophys. J.* 2004, *87*, 2701–2713.

[35] Aslan, F. M., Yu, Y., Mohr, S. C., Cantor, C. R., Engineered single-chain dimeric streptavidins with an unexpected strong preference for biotin-4-fluorescein. *Proc. Natl. Acad. Sci. U S A* 2005, *102*, 8507–8512.

Model-based development of an assay for the rapid detection of biotin-blocked binding sites of streptavidin

Jakob M. Müller*[,1], Joe M. Risse[1], Karl Friehs[1], and Erwin Flaschel[1]

[1] *Chair of Fermentation Engineering, Faculty of Technology, Bielefeld University*
Universitätsstrasse 25, 33615 Bielefeld, Germany
** corresponding author: phone: +49-521-106-5299, fax: +49-521-106-6475,*
e-mail: jmu@fermtech.techfak.uni-bielefeld.de

Supplementary material

1. Calculation of the SAV concentration based on a B4F calibration curve

SAV concentrations were calculated according to Table S1.

Table S1 Calculation of the SAV concentration based on a B4F calibration curve. The fluorescence signals for different B4F concentrations (left row) were correlated to theoretical concentrations of quenched B4F, calculated from the concentration difference to the concentration in the measurement buffer of 49 nM. This maximal concentration results from the mixture of 980 µL of 50 nM B4F in measurement buffer with 20 µL of sample, therefore 50fold diluting the sample. This dilution factor was used for the conversion of $c_{B4F,quenched}$ in $c_{SAV,monomeric}$.

c_{B4F} [nM]	$c_{B4F,quenched}$ [nM]	$c_{SAV,monomeric}$ [nM]	$c_{SAV,tetrameric}$ [nM]
49	0	0	0
45	4	200	50
40	9	450	112.5
30	19	950	237.5
20	29	1450	362.5
10	39	1950	487.5
5	44	2200	550
1	48	2400	600

2. Estimation of the degradation constant of streptavidin according to Arrhenius

Based on the degradation reaction constants from the parameter fits the temperature-dependency of the irreversible denaturing step of SAV can be modeled according to Arrhenius [33] as described in equation (S1).

$$k_{deg} = k_{deg,0} \exp\left(-\frac{E_{a,deg}}{RT}\right) \quad \text{(S1)}$$

where $k_{deg,0}$ is the pre-exponential factor, $E_{a,deg}$ the activation energy for the denaturing step, R the universal gas constant and T the temperature in K.

An activation energy for the unfolding of SAV of about 229±16 kJ mol^{-1} has been reported [34]. Applying this activation energy, a parameter fit to the degradation rates acquired from the curves in Fig. 1 **A** resulted in an estimated $k_{deg,0}$ of 6.5395×10^{30} s^{-1}. The model curve for these parameters is shown in Fig. 1 **B** in the main document.

3. Parameter estimation for kinetic modelling

3.1 Steps of the parameter estimation

First parameter estimations were performed based on studies without detailed binding studies. Using the model described by equations (4a) and (4b), a parameter optimization based on the differential evolution algorithm of COPASI[1] led to the parameters shown in the supplements in Table S2. The values for the dissociation rates of both complexes determined by parameter estimation were characterized by small deviations. However, no accurate determination of the association rates was achieved. As long as the ratio of the dissociation constants K_d was not altered, they could be changed by several orders of magnitude without influencing the accuracy of the model.

Table S2 shows the results of the first iteration of the parameter estimation. The resulting dissociation rate for the SAV-B4F complex was used for the estimation of $k_{on,B4F}$.

Table S2 Parameter values and corresponding standard deviations for the first iteration of the parameter optimization for the heat incubation at 70 °C for 10 min acquired with COPASI and the ODE system consisting of equations (4a) and (4b). The standard deviations are shown as absolute and relative values (coefficient of variation).

Parameter	value	coeff. of variation [%]
$k_{on,bio}$	$6.94 \pm 84.0 \times 10^{8}$ M^{-1} s^{-1}	1210.42
$k_{off,bio}$	$5.37 \pm 0.15 \times 10^{-3}$ s^{-1}	2.86
$k_{on,B4F}$	$2.55 \pm 30.9 \times 10^{9}$ M^{-1} s^{-1}	1211.96
$k_{off,B4F}$	$8.33 \pm 0.54 \times 10^{-4}$ s^{-1}	6.50

To achieve a more reliable quantification of the association rates, additional kinetic experiments were performed in order to yield more reliable association rates.

An *E. coli* supernatant containing 1.21 µM of SAV was diluted onefold by demineralized water, resulting in a tetrameric concentration of 605 nM. A volume of 20 µL of the resulting, room-tempered solution was placed in a fluorescence measurement cuvette. Measurement buffer including B4F and BSA was tempered to 70 °C in a heat block. A kinetic measurement with scanning intervals of 0.1 s was started and 980 µL of the preheated measurement buffer were added directly into the cuvette. The fluorescence emission at 525 nm was measured for 60 s. This procedure was performed fivefold.

Two additional measurements were performed for calibration: to determine the maximal fluorescence at 70 °C, preheated measurement buffer supplemented with 20 µL of water instead of the sample was analyzed. The minimal fluorescence was determined at 70 °C for 2 min by mixing 20 µL of the sample with 980 µL of measurement buffer. These maximal and

[1] parameters: 2000 generations, population size: 10.

minimal values were used for the calibration of the kinetic data, representing 0 (no quenching) and 600 nM (maximal quenching) of tetrameric SAV in the undiluted sample, corresponding to 0 and approx. 48 nM of monomeric SAV diluted by measurement buffer, respectively.

The kinetic measurements were evaluated with a simple model representing complex formation and dissociation of the SAV-B4F complex according to equation (4b) in CellDesigner. The $k_{off,B4F}$ rate of 8.33±0.54 × 10^{-4} s^{-1} from the first iteration of the parameter estimation (Table S2) was used as a constant parameter for the estimation of the $k_{on,B4F}$ rate in COPASI based on the CellDesigner model and the five kinetic measurements. The mass balances of B4F and SAV were used for the calculation of the free species of these compounds in addition to the measured B4F-SAV concentrations.

The parameter estimation led to a $k_{on,B4F}$ rate of 1.60 × 10^{8} s^{-1} characterized by a drastically reduced coefficient of variation of 0.6 % as opposed to 1211.96 % for the first iteration of the estimation. The new value of the association rate for the SAV-B4F complex $k_{on,B4F}$ was reimported as a constant into the model consisting of equations (4a) and (4b) to recalculate the $k_{on,bio}$ rate and both dissociation rates. The complete results of this second parameter estimation are shown in Table 2 in the main document.

3.2 Comparison of results of parameter estimation and literature data

An Arrhenius-based estimation of the $k_{off,bio}$ rate of the SAV-biotin complex according to the data of Deng et al. [26] with activation parameters E_a of 31.7 kcal mol^{-1} (activation energy) and A of $10^{18.2}$ s^{-1} (pre-exponential factor) leads to a $k_{off,bio}$ rate of 1.03 × 10^{-2} s^{-1} at 70 °C. The parameter optimization resulted in a value of 5.38±0.32 × 10^{-3} s^{-1}, differing by a factor of 1.91. As the data of Deng and coworkers only covers temperatures from 15.3 to 44.8 °C an extrapolation to 70 °C is necessary. This is error-prone due to typically very large pre-exponential factors (A). Thus, the result of the parameter estimation seems feasible. Interestingly, the estimation suggests that the dissociation of the SAV-B4F complex at 70 °C is more than one order of magnitude slower than the dissociation of the SAV-biotin complex. Along with the 3.6fold higher association rate this results in conditions favoring the formation of the SAV-B4F complex, ultimately providing the conditions necessary for the assay.

Another interesting insight is provided in comparison to the data of Chivers et al. [25] who measured a $k_{on,B4F}$ rate of 2.0±0.1 × 10^{7} M^{-1} s^{-1} for the association of the B4F-SAV complex at 37 °C. Surprisingly, the value from the parameter estimation of 1.60±0.01 × 10^{8} M^{-1} s^{-1} at 70 °C (factor 8) suggests that an increase in temperature improves the association of this complex. Opposed to that, the association rate of the SAV-biotin complex determined at elevated temperatures (4.46±0.93 × 10^{7} M^{-1} s^{-1}) is slightly lower (factor 1.5), but in the same order of magnitude as the value of Chivers and coworkers at 37 °C (6.7±0.5 × 10^{7} M^{-1} s^{-1}).

4. Comparison of experimental data and model prediction

4.1 ODE-based model

To provide brief insight into the accuracy of the results from the ODE-based model (equations (4a) and (4b), Fig. 3 **B**) in comparison to the experimental results, Table S3 shows a summary of simulated and experimental data.

Table S3 Comparison of experimental data (exp) and simulated (sim) proportions of detectable SAV Q_{SAV} for different degrees of biotin saturation $Q_{blocked}$ and different initial SAV concentrations c_{SAV}. The abbreviations *SB* and *SB4F* refer to the complexes of SAV and biotin and SAV and B4F, respectively. The B4F concentration was kept constant at 49 nM for all experiments. Simulation and experimental data are based on an incubation at 70 °C for 10 min and refer to the actual, monomeric concentration of SAV in the assay buffer. 48 nM of monomeric SAV in measurement buffer correspond to 600 nM of tetrameric SAV in the initial sample.

c_{SAV} [nM]	$Q_{blocked}$ [-]	$c_{SB,sim}$ [nM]	$c_{SB4F,sim}$ [nM]	$Q_{SAV,sim}$ [-]	$c_{SB,exp}$ [nM]	$c_{SB4F,exp}$ [nM]	$Q_{SAV,exp}$ [-]
46.4	0.04	0.6	45.7	0.98	0.0	46.4	1.00
46.4	0.31	3.5	42.8	0.92	3.7	42.7	0.92
46.4	0.57	5.5	40.9	0.88	5.0	41.4	0.89
46.4	0.81	7.1	39.3	0.85	6.2	40.2	0.87
46.4	0.98	8.1	38.3	0.82	7.9	38.5	0.83
45.1	0.07	0.9	44.1	0.98	0.0	45.1	1.00
45.1	0.35	3.4	41.7	0.92	3.7	41.4	0.92
45.1	0.61	5.2	39.9	0.88	5.9	39.2	0.87
45.1	0.83	6.6	38.5	0.85	7.3	37.9	0.84
45.1	0.97	7.5	37.6	0.83	8.5	36.6	0.81
40.4	0.11	0.7	39.6	0.98	0.0	40.4	1.00
40.4	0.35	2.3	38.1	0.94	2.8	37.6	0.93
40.4	0.59	3.6	36.7	0.91	2.8	37.5	0.93
40.4	0.81	4.8	35.5	0.88	4.1	36.2	0.90
40.4	0.96	5.6	34.8	0.86	5.5	34.9	0.86
37.0	0.08	0.4	36.6	0.99	0.0	37.0	1.00
37.0	0.36	1.8	35.3	0.95	1.6	35.4	0.96
37.0	0.60	2.9	34.1	0.92	1.2	35.9	0.97
37.0	0.83	3.9	33.1	0.89	2.7	34.4	0.93
37.0	0.98	4.6	32.4	0.87	3.9	33.2	0.90
34.1	0.11	0.4	33.6	0.99	0.0	34.1	1.00
34.1	0.38	1.5	32.6	0.96	2.0	32.1	0.94
34.1	0.61	2.4	31.7	0.93	1.8	32.3	0.95
34.1	0.83	3.3	30.8	0.90	2.1	32.0	0.94
34.1	0.97	3.8	30.3	0.89	4.1	30.0	0.88
28.7	0.13	0.3	28.4	0.99	0.0	28.7	1.00
28.7	0.36	0.9	27.8	0.97	-0.2	28.9	1.01
28.7	0.61	1.6	27.1	0.94	2.1	26.6	0.93
28.7	0.82	2.2	26.5	0.92	1.0	27.7	0.97
28.7	0.97	2.7	26.0	0.91	2.8	25.9	0.90
23.6	0.05	0.1	23.5	1.00	0.0	23.6	1.00
23.6	0.36	0.6	22.9	0.97	0.5	23.1	0.98
23.6	0.61	1.1	22.4	0.95	1.2	22.4	0.95
23.6	0.82	1.5	22.0	0.93	-0.8	24.3	1.03
23.6	0.99	1.9	21.7	0.92	0.3	23.3	0.99

4.2 Polynomial model

A comparison of the model prediction of the polynomial model and the experimental data is shown in Table S4, summing up the predicted and experimental error of the measured SAV concentration for different concentrations of SAV in the sample at complete ($Q_{blocked}$ = 1) and 50 % of the maximal biotin saturation ($Q_{blocked}$ = 0.5). In addition to the theoretical $Q_{blocked}$ values (first row in the table), the table also contains calculated values for this parameter (fourth row, values in brackets). These refer to the concentration of SAV measured in the heat assay (70 °C, 10 min) prior to the saturation with biotin, corresponding to the total concentration of binding sites, and the free binding sites after the saturation procedure determined by a measurement at room temperature. The calculated $Q_{blocked}$ value is equal to the difference of the free and total concentration of binding sites divided by the total concentration of binding sites.

Table S4 Summary of the results of the optimization and prediction routines of MODDE. The table shows the maximal SAV concentrations $c_{SAV,max}$ which may be used in the heat assay for a desired maximal deviation dc_{SAV} of the actual SAV concentration in the sample. The predictions are compared to experimental results. The experimental data is divided into the actual SAV concentration and biotin saturation along with a prediction range and predicted value for dc_{SAV} for this actual concentration.

$Q_{blocked}$ [-]	$c_{SAV,max}$ [nM]	desired dc_{SAV} [%]	actual c_{SAV} ($Q_{blocked}$) [nM] / [-]	observed dc_{SAV} [%]	predicted dc_{SAV}-range for actual c_{SAV} (average value) [%]
1	285	-1	295 (0.99)	-1.1	0.7 ... -5.3 (-2.3)
1	341	-5	359 (0.97)	-9.9	-3.7 ... -7.9 (-5.8)
1	434	-10	426 (0.97)	-12.0	-8.0 ... -10.9 (-9.5)
1	600	-20	580 (0.98)	-17.0	-16.0 ... -20.3 (-18.2)
0.5	296	-1	295 (0.61)	-4.9 [a)]	0.4 ... -3.0 (-1.3)
0.5	434	-5	426 (0.61)	-5.2	-5.0 ... -6.7 (-5.9)
0.5	600	-10	580 (0.58)	-10.7	-9.4 ... -12.0 (-10.7)

[a)] This value is certainly too large. The deviation for this c_{SAV} was smaller for higher degrees of biotin saturation ($Q_{blocked}$ = 0.82: dc_{SAV} = +3.3 % (data not shown); $Q_{blocked}$ = 0.99: dc_{SAV} = -1.1 % (see first row)). It is therefore likely that this dc_{SAV} is caused by measurement problems due to the device or the experimental procedure.

4.3 Comparison of polynomial and ODE-based model

A graphical comparison of model and simulated data for both the polynomial and the biochemical model is shown in Fig. S1.

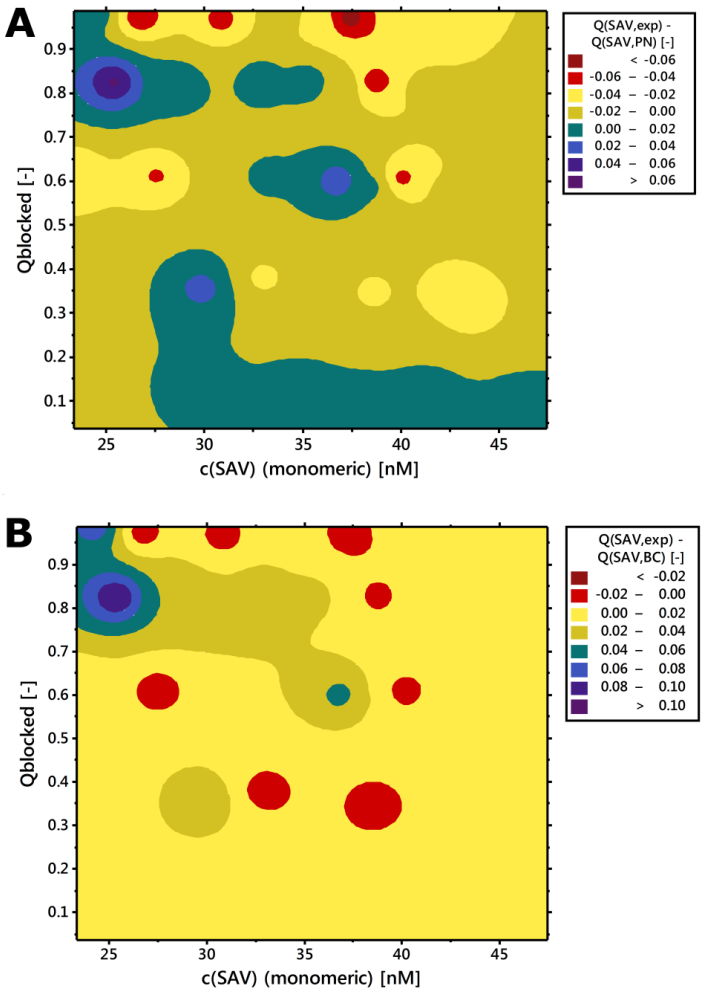

Fig. S1 Plots of the deviations of the proportion of detectable SAV Q_{SAV} from the **p**olynomial **m**odel ($Q_{SAV,PN}$) created by MODDE (**A**) and the **b**io**c**hemical model ($Q_{SAV,BC}$) acquired by parameter optimization for equations (4a) and (4b) (**B**) from the experimental data $Q_{SAV,exp}$. Negative values represent model values larger than the experimental data and vice versa. Please note that the color coding differs in the two plots. Spots differing from their surroundings and occuring in both plots are likely to result from measurement problems. The dark blue spot in the upper left of both plots serves as an example. The plots were created with Minitab 17.

5. Validation of the selected concentration range for the assay

Table S5 sums up the results of the final experimental validation of the assay procedure (section 3.11).

Table S5 Results of the final validation of the selected range of acceptable SAV for the assay. Supernatants from three different organisms were analyzed in different concentrations at complete biotin saturation. The concentrations of the supernatants were 1242±67, 1196±27 and 1227±49 nM of tetrameric SAV prior to the dilution for the assay. These concentrations were used as a reference point for the calculation of the detectable proportion of SAV Q_{SAV}. The highlighted rows show that a concentration of approximately 300 nM in the sample should allow the detection of all of the available binding sites, independent from the degree of biotin saturation $Q_{blocked}$ and the supernatant - and thus, the total protein concentration and the chain length of SAV.

supernatant	c_{SAV} [nM]	$c_{SAV,RT}$ [nM]	$Q_{blocked}$ [-]	$c_{SAV,HT}$ [nM]	Q_{SAV} [-]
E. coli	621	10±10	0.98	476±10	0.77±0.02
	466	11±6	0.98	424±6	0.91±0.01
	311	**6±6**	**0.98**	**305±6**	**0.98±0.02**
P. pastoris	598	56±2	0.91	484±0	0.81±0.00
	449	49±2	0.89	412±5	0.92±0.01
	299	**26±2**	**0.91**	**303±6**	**1.01±0.02**
S. avidinii	614	26±3	0.96	486±2	0.79±0.00
	460	21±7	0.96	417±6	0.91±0.01
	307	**9±5**	**0.97**	**302±3**	**0.99±0.01**

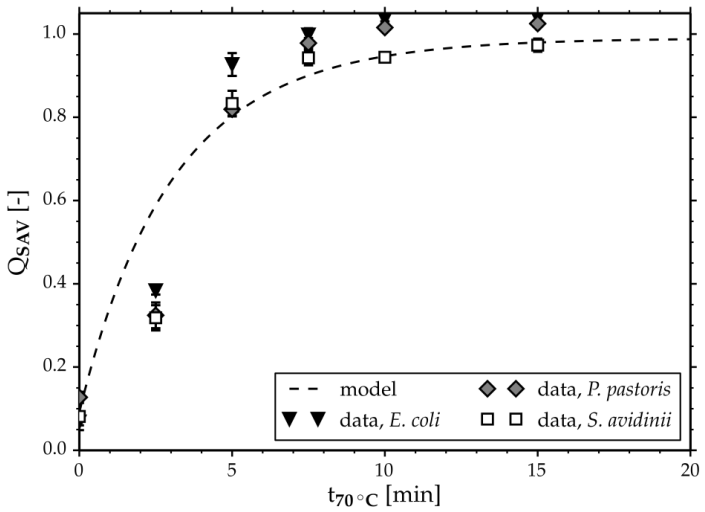

Fig. S2 Kinetic measurements on the three culture supernatants of *E. coli*, *P. pastoris* and *S. avidinii* incubated at 70 °C. The model curve was calculated for the average initial conditions for the three samples. The *S. avidinii*-curve shows slightly improved assay results for incubation times > 10 min, as is suggested by the biochemical model (Fig. S3).

6. Validation of equation (5) for the correction of the calculated SAV concentration

Equation (5) was validated by comparison of calculated data and expected concentrations according to Table S6. Two data sets were used for the calculations: The data set from the concentration variation leading to equation (5) and the data set from the supernatant

variation. The latter was not used for the calculation of equation (5) and therefore serves as an external control.

Table S6 Comparison of SAV concentrations corrected according to equation (5) based on the deviation dc_{SAV} of the theoretical SAV concentration $c_{SAV,theo}$ and the calculated corrected concentration $c_{SAV,corr}$. The sample-row shows the origin of the sample, which was either part of the concentration variation experiment (c-var) or used for the supernatant-variation (sup-var; external validation). The organisms used for the production are abbreviated *eco* (*Escherichia coli*), *ppa* (*Pichia pastoris*) and *str* (*Streptomyces avidinii*). The concentrations refer to tetrameric SAV in the initial sample.

$Q_{blocked}$ [-]	$c_{SAV,RT}$ [nM]	$c_{SAV,HT}$ [nM]	$c_{SAV,theo}$ [nM]	$c_{SAV,corr}$ [nM]	dc_{SAV} [nM]	sample
0.04	559	580	580	578	-2	c-var, *eco*
0.57	247	518	580	576	-5	
0.98	11	482	580	573	-7	
0.11	451	505	505	516	11	
0.59	209	469	505	518	14	
0.96	21	436	505	505	0	
0.11	377	426	426	434	8	
0.61	166	404	426	437	11	
0.97	14	375	426	416	-10	
0.01	587	592	592	584	-8	sup-var, *eco*
0.25	441	547	592	569	-23	
0.56	260	520	592	576	-16	
0.81	113	511	592	594	2	
0.98	13	484	592	576	-16	
0.00	592	593	593	584	-9	sup-var, *ppa*
0.23	459	546	593	563	-30	
0.51	289	516	593	564	-29	
0.75	146	505	593	580	-14	
0.91	52	485	593	570	-24	
0.00	606	604	604	592	-12	sup-var, *str*
0.22	473	557	604	573	-31	
0.49	310	529	604	576	-28	
0.77	139	505	604	581	-23	
0.95	30	486	604	575	-29	

7. Analysis of biotin and B4F stability during heat incubation

In addition to the stability of SAV and B4F during heat incubation (see section 3.2) biotin has to provide similar properties. A 4.8 µM biotin solution in 50 mM NaH_2PO_4 (pH 7.5) was incubated at 70 °C for up to 30 min to analyze the heat stability of the vitamin. After 0, 2.5, 5, 7.5, 10, 15, 20, 25 and 30 min, 500 µL of the vitamin solution were mixed with a culture supernatant containing 1.2 µM of tetrameric SAV. The following fluorescence measurements resulted in an unaltered binding of SAV for all of the samples (data not shown), indicating that biotin was not degraded. Due to the heat stability of the vitamin the ratio of biotin towards B4F and SAV can be assumed to be constant during the assay.

To rule out the effect of heat-induced degradation of the detection marker B4F in the assay, 1 mL of sample buffer was incubated at 70 °C for 5 min. The fluorescence emission signal at 525 nm was 261±1 for a sample incubated at room temperature as opposed to a signal of

262±2 for the heat-incubated buffer. A loss of fluorescence on B4F in the relevant period of time can therefore be ruled out. Furthermore, a subsequent binding test with the heat-incubated B4F-solution in the presence of SAV from a culture supernatant revealed that the quenching ability of B4F remained unaltered.

8. Analysis of the stability of the SAV-B4F-complex

In an additional experiment 20 µL of a 1.2 µM biotin solution were added at room temperature to a previously heat-incubated solution containing the usual 980 µL of measurement buffer and 20 µL of culture supernatant containing approximately 300 nM of tetrameric SAV. After vortexing, the sample was incubated at room temperature for 15 min. This did not lead to an increased fluorescence assay signal compared to a control sample to which water was added instead of biotin (data not shown). Additionally considering the results of section 3.4 (incubation at RT after the heat assay) the fluorescence signal in the presence of free biotin can be assumed to be stable in the relevant time interval.

9. Impact of additional parameters on the outcome of the assay

In the following section, two additional parameters are analyzed, which should be considered when working with the assay.

Fluorescence signals were larger than the maximal fluorescence emission of the calibration curve in several cases, when measurements were performed on samples with a strong excess of biotin towards SAV binding sites, resulting in large concentrations of free biotin. Results acquired for these conditions should therefore be treated with care. During a typical fermentation course the SAV concentration surpasses the biotin concentration already early in the cultivation process. Hence, this problem usually disappears in the course of cultivation.

In an additional variation, the impact of salt ions on the result of the assay was analyzed. Holmberg et al. observed a reduced elution efficiency of the SAV-biotin interaction for increasing salt concentrations in the eluent for an incubation at 70 °C for one second [23]. This extremely short incubation time was achieved by robot-assisted experiments, a mechanical separation of SAV-coated magnetic beads and by tempering the buffer solution to the corresponding temperature prior to the experiments. To analyze the influence of this factor a NaCl-free measurement buffer was tested in comparison to the unaltered buffer containing 100 mM of NaCl. This change resulted in a 3 % lower overall fluorescence emission and did not improve the proportion of detectable blocked binding sites. A partially biotin-saturated ($Q_{blocked}$ = 0.85), 580 nM tetrameric SAV sample allowed the detection of 460±6 nM of SAV for the NaCl-free and 459±8 for the NaCl-supplemented measurement buffer for an incubation at 70 °C for 5 min. Thus, the elution mechanism does not seem to depend strongly on sodium and chloride ions at 70 °C for prolonged incubation times (5 min vs. 1 s). Since the sample is diluted 50fold by measurement buffer prior to the fluorescence analysis in the standard measurement procedure, the impact of the salt content of the sample can be assumed to be negligible for the assay result, allowing a broad range of cultivation media without altering the outcome of the assay.

10. Simulation of increased B4F concentrations and increased incubation time

Two alternative strategies for the detection of biotin-blocked binding sites in concentrations > 300 nM were analyzed by simulation based on the biochemical model: doubling the B4F concentration in the assay buffer and increasing the incubation time at 70 °C. Results for these variations are shown in Fig. S3 **A** and **B**, respectively.

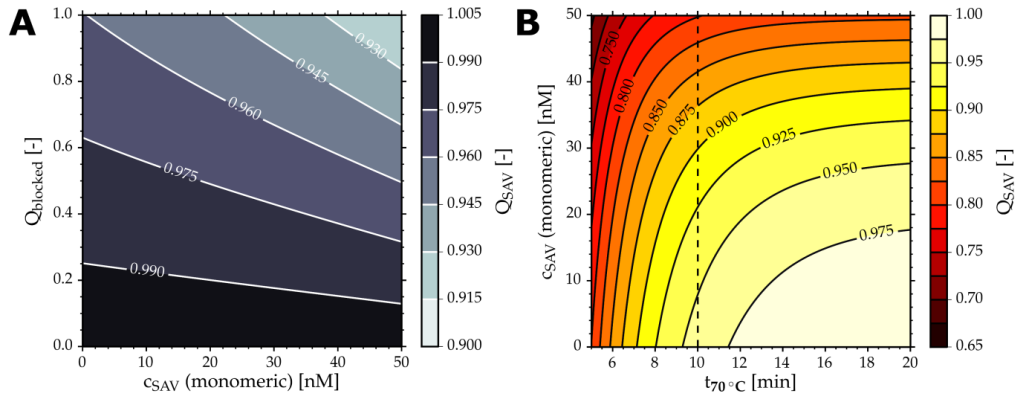

Fig. S3 Simulation-based evaluation of methods for improved assay results. **A** Plot for a variation of the SAV concentration c_{SAV} and the proportion of blocked binding sites $Q_{blocked}$ for a twofold concentrated B4F solution (100 instead of 50 nM). **B** Variation of the incubation time at 70 °C $t_{70\,°C}$ at various SAV concentrations for $Q_{blocked}$ = 1.0. The black, dashed line represents the standard assay conditions of 10 min of incubation at 70 °C..

The variation of the concentration of B4F in the assay buffer (Fig. S3, **A**) suggests that an increased concentration of B4F should lead to similar results as a twofold dilution of the sample. Therefore, doubling the B4F concentration may be a suitable strategy for the detection of SAV in concentrations > 300 nM if the increased fluorescence intensity is below the maximal detectable fluorescence emission of the fluorimeter, which was the case in our experiments. The model suggests errors < 5 % for concentrations of SAV of 600 nM (tetrameric, corresponding to 48 nM of monomeric SAV in the plot) for degrees of biotin saturation $Q_{blocked} \leq 0.7$.

The incubation time at 70 °C seems to be increasingly important for decreased SAV concentrations according to the biochemical model (Fig. S3, **B**). An expanded incubation time for low SAV concentrations and complete biotin saturation may result in slightly more adequate[2] results according to the simulation. The time course acquired for the *S. avidinii* sample in the final kinetic validation step (Fig. S2) supports this hypothesis.

11. Application of the assay to other biotin-binding proteins

Based on the high temperature stability of avidin from chicken egg white [5] and its detectability by B4F quenching [16] an additional study was performed on partially and completely biotin-blocked samples of this protein (Sigma, Germany). Neither measurements

[2] improving the accuracy of the measurement by about 2.5 % for monomeric SAV concentrations of < 30 nM.

at 70 °C, nor at 84 °C resulted in a displacement of biotin by B4F (data not shown). This is likely to be an effect of the very different AA sequences of avidin and SAV, showing a sequence identity of only 32 % according to a BLAST analysis. However, the assay may be suitable for more homologous biotin-binding proteins. Among many others, a sequence homology search for the full length sequence of SAV (159 AA) revealed hypothetical proteins from *S. violaceus, S. flavotricini*, and *S. lavendulae* showing 99, 96 and 96 % of sequence identity[3], respectively. Therefore, these proteins are suitable candidates for a further analysis.

[3] Sequence IDs: UniProtKB Q53532.1 (*S. violaceus*) and NCBI reference sequences WP_030030699.1 (*S. flavotricini*) and WP_030744339.1 (*S. lavendulae*).

3.4 Potential applications for the assay

The assay herein described is not only a useful tool to evaluate the quality of SAV as a commercial product in the end of a fermentation process.

When cultivating strains of biotin auxotrophic hosts like *P. pastoris* for the inducible production of SAV, the assay may be used to determine the optimal point of time for induction to minimize the residual concentration of free biotin after the growth phase and thus improve bioactivity of the product. *Vice versa*, the method may be used to identify potential biotin-limiting effects in the culture accompanying SAV production, which should be detectable by increased proportions of biotin-free SAV without the necessity of an additional method of measurement for the vitamin.

Optimizing the concentration of biotin in the medium to achieve maximal bioactivity without a major impact on growth has been tested for the production of core SAV by *P. pastoris* (section 5.3, p. 116*ff.*).

For a better understanding of SAV-induced host toxicity, intracellular measurements of biotin-blocked binding sites may prove beneficial. This strategy could provide insight into the intracellular biotin deprivation of the host, allowing the detection of potential bottlenecks for the secretion efficiency of SAV. Corresponding measurements have been performed for the expression of the SAV gene by *E. coli* (section 5.2, p. 93*ff.*).

In addition to these applications, the assay has been used in a study on the recovery of biotin-blocked binding sites of SAV, as discussed in the following section.

3.5 Recovery of biotin-blocked binding sites of SAV

The assay was applied for the evaluation of methods for the non-denaturing removal of biotin from the binding pocket of SAV. In this context, it permits the detection the overall concentration (blocked and free binding sites) of the protein in a sample, which - combined with the regular assay of Kada *et al.* (1999a,b) - in turn allows quantification of the degradation of biotin-blocked SAV. A short summary of the corresponding experiments is given below.

3.5.1 Motivation

As only biotin-free binding sites of SAV are available for applications of the protein, methods for the recovery of biotin-blocked binding sites of SAV are desirable. For this purpose, SAV can be denatured, washed via diafiltration for the removal of biotin, and refolded, but this method is costly, cumbersome, and leads to loss of product. Thus, methods for the non-denaturing removal of biotin were in the focus

of interest.

Biotin is sensitive to oxidative stress and ultraviolet radiation.[3] Oxidative treatment leads to oxidation at its probably most susceptible site, the sulfur atom of the head group of the vitamin, as shown in Fig. 2.7 (p. 16). Oxidative degradation - as can be expected in the presence of hydrogen peroxide - leads to biotin sulfoxide and biotin sulfone for the one- and twofold oxidation of the sulfur atom, respectively.

The high stability of SAV towards various environmental factors (see section 2.2, p. 5) suggests that SAV may be more resistant towards these factors than the vitamin. Thus, supernatants containing biotin-blocked SAV were treated with UV radiation and/or hydrogen peroxide.

To partially dissociate the SAV-biotin-complex both methods were combined with incubation at elevated temperatures (Holmberg *et al.*, 2005). For the choice of incubation temperature and duration, the thermal inactivation of SAV was simulated in Scilab based on the first order kinetics and the degradation parameters of Müller *et al.* (2015) (see Fig. 1 in the corresponding publication; section 3, p. 28*ff.*). The simulations led to the degradation curves shown in Fig. 3.3.

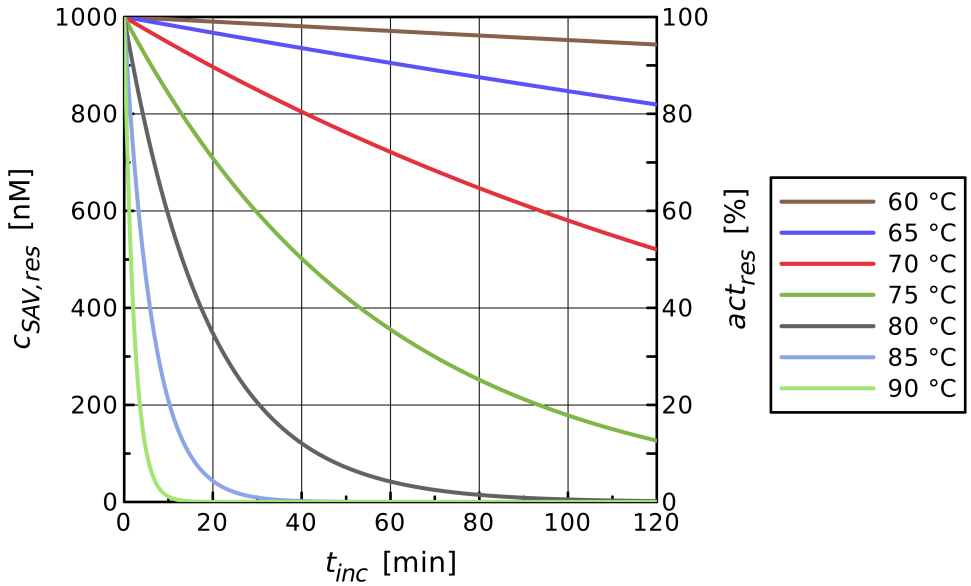

Fig. 3.3: Simulation of the heat-induced degradation of SAV depicted in the form of a plot of the relative residual protein activity act_{res} and active concentration of SAV $c_{SAV,res}$ over the incubation time t_{inc}. Simulation parameters: $c_{SAV,0} = 1000\,\mathrm{nM}$, $k_{deg,0} = 6.5395 \times 10^{30}\,\mathrm{s^{-1}}$, E_A 229 $\mathrm{kJ\,mol^{-1}}$, $R = 8.314\,\mathrm{J\,mol^{-1}\,K^{-1}}$ (Müller *et al.*, 2015).

[3] Product information sheet "Biotin in Cell Culture" by Sigma-Aldrich; http://www.sigmaaldrich.com/life-science/cell-culture/learning-center/media-expert/biotin.html

3.5.2 Brief summary of the results

Fig. 3.4 shows results of studies for the non-denaturing removal of biotin from the binding pocket of SAV from *S. avidinii* by hydrogen peroxide treatment at 60 °C. A detailed description of the experimental procedure is given in section 8.1.1 (p. 173) in the supplementary material.

The experimental results indicate that treatment of biotin-blocked SAV by hydrogen peroxide results in a partial recovery of blocked binding sites. The effect of hydrogen peroxide on the recovery of biotin-blocked binding sites in the initial period of incubation was found to be concentration-dependent, as shown in Fig. 8.2 (supplementary material, p. 180).

As shown in Fig. 8.4b (p. 182 in the supplements), treatment by UV radiation also resulted in the recovery of blocked binding sites. On the one hand, UV treatment of SAV caused a decrease of biological activity of the protein on the long term, while hydrogen peroxide seemed to bring about only minor damage to SAV. On the other hand, UV radiation allowed an increase of biotin-free binding sites of SAV at room temperature, whereas elevated temperatures were necessary for the hydrogen peroxide-based degradation of biotin. This may be due to protective effects of the binding pocket towards elements of oxidative stress (see Fig. 2.1, p. 3), which in turn may be reduced or neutralized by a partial dissociation of the SAV-biotin interaction (Holmberg *et al.*, 2005). UV radiation, however, may more easily target biotin located directly in the binding site.

Generally, both methods led to maximal proportions of recovered binding sites in the range of 30 % (Fig. 3.4a). This final proportion was nearly independent of the incubation period and concentration of H_2O_2. Moreover, a systematic variation of the degree of biotin saturation of a supernatant showed that blocked binding sites were only recovered for completely biotin-saturated samples (data not shown). If the degree of saturation was lower than 70 %, no positive effect of hydrogen peroxide was observed. These results may indicate a 'biochemical inequality' of the binding sites of SAV due to potential cooperative effects between two or more binding sites of the tetrameric protein.

Several experiments focused on alternative approaches to destabilize SAV. However, incubation at higher temperatures and pH values[4] did not bring about beneficial properties. Using cycles of UV or hydrogen peroxide treatment and incubation on ice did also not improve the results (data not shown). The same applied for the recovery of binding sites by combining the physical and chemical degradation of biotin via a combination of UV radiation and treatment by hydrogen peroxide, as shown in Fig. 8.4b (supplements). Neither supplementation of the supernatant with the denaturing agent urea, nor the addition of bovine serum albumin (BSA) (Fig. 3.4a) or UV-absorbing, aromatic amino acids (data not shown) as protective agents towards the damaging effects of the UV treatment increased the recovery of binding sites.

However, as shown in Fig. 3.4b, the addition of BSA reduced damage on biotin-free binding sites for

[4] E.g., to deprotonate the carboxyl group of biotin.

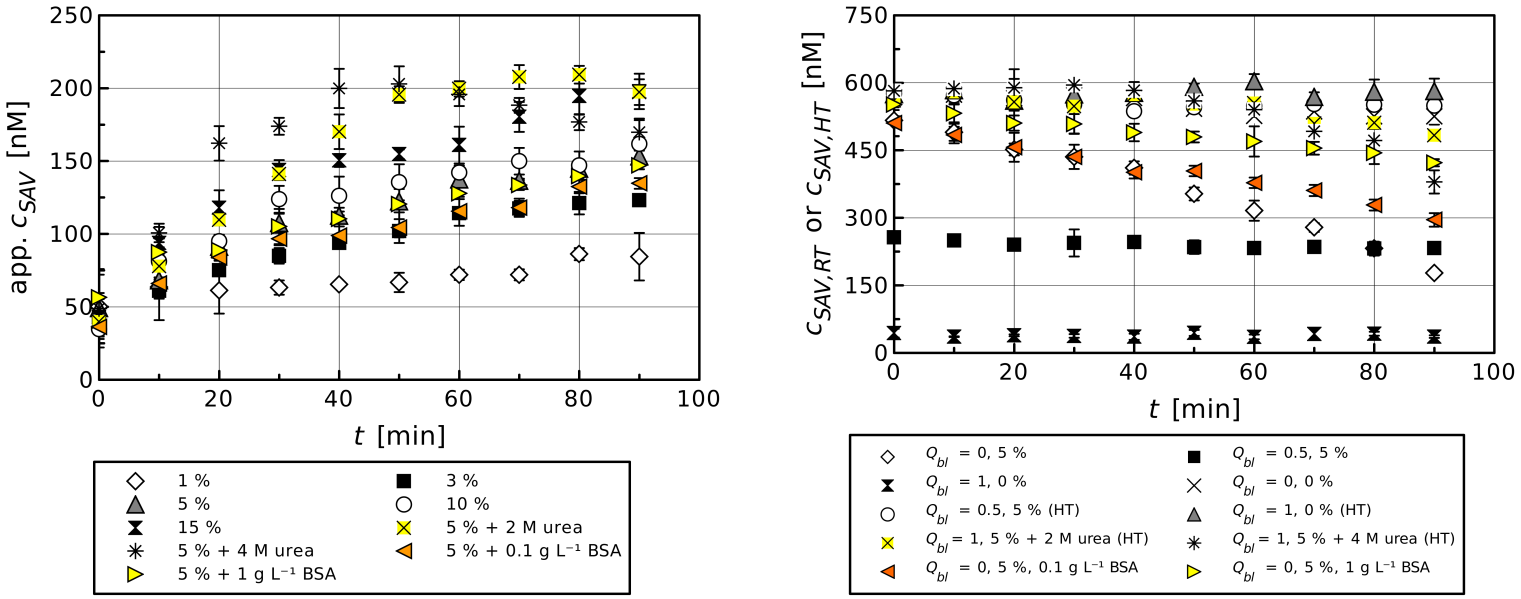

(a) Detection of free binding sites.

(b) Degradation of SAV.

Fig. 3.4: Results of studies for the non-denaturing degradation of SAV-bound biotin by hydrogen peroxide at 60 °C (n=3). An initial concentration of approx. 600 nM of biotin-saturated, tetrameric SAV was used for the studies. (a) Measurement of biotin-free binding sites in the assay at room temperature. (b) Results of measurements of the degradation of SAV. Labels for subfigure (a) indicate the concentration of hydrogen peroxide and of additional agents. The labels for subfigure (b) show the degree of biotin saturation Q_{bl} and the concentration of hydrogen peroxide and supporting agents. Concentrations of the oxidizing agent are given in % (w/w). Where indicated (HT), measurement of SAV was performed in the heat-based-assay (10 min, 70 °C).

samples with low proportions of blocked binding sites. Thus, this strategy may prevent the degradation of recovered binding sites in future studies. Furthermore, supplementation of urea was found to speed up the recovery of binding sites (Fig. 3.4a), but at the same time resulted in an increased degradation of SAV (Fig. 3.4b).

Two main conclusions can be drawn from the results. Firstly, the studies show that a non-denaturing recovery of biotin-blocked binding sites of SAV is possible. Similar observations were made for the recovery of binding sites of immobilized SAV (see supplementary material, Fig. 8.3, p. 181). Secondly, the experiments provide insight into the stability of SAV towards oxidation. Here, the findings indicate that the binding of biotin does not only cause a higher thermotolerance of SAV (González *et al.*, 1999), but also improves the resistance of the binding pocket or the whole protein towards oxidizing agents at elevated temperatures (see Fig. 3.4b).

If the degree of recovery can be increased, this procedure may lead to a method for the recycling of free or immobilized SAV for future applications. Moreover, an efficient method for the removal of SAV-bound biotin would massively simplify handling of the toxic properties of the protein. In this context, it would permit a non-denaturing recovery of biotin-blocked binding sites resulting from supplementation of cultivation media by an excess of biotin after fermentation. Potential strategies to achieve this goal may, e.g., include the application of an optical bandpass filter for the absorption wavelength of biotin, which may protect SAV while at the same time allowing a more targeted, UV-based degradation of biotin.

4 Production of SAV by *Streptomyces avidinii*

The following chapter sums up studies performed for the production of SAV by the native producer *S. avidinii*.

4.1 Motivation

To this date, *S. avidinii*, the native producer of SAV, has not been studied in a detailed manner. Therefore, the kinetic of product formation by the host in varying production media, cultivation conditions, and modes of operation is characterized either poorly or not at all. This lack of knowledge limits the final product concentration in current production processes. Furthermore, insufficient characterization of the complex morphology of the filamentous bacterium poses problems to its cultivation.

4.1.1 Goals of this study

Hence, the primary goal of this study was to establish methods for a reproducible cultivation of *S. avidinii* yielding high concentrations of SAV. In literature, processes are commonly performed batch-wise in shake flasks (Cazin Jr. *et al.*, 1988; Kolomiets & Zdor, 1998). Thus, the development of fed-batch processes in the bioreactor seemed highly promising for an improved production. Morphological aspects were less important in bioreactor cultivations due to stronger shearing of the mycelia by the stirrer and were therefore only analyzed in side projects in smaller scales (see section 4.4, p. 80*ff.*).

4.2 Manuscript

The results of fed-batch development were published in a research article in the Journal of Biotechnology (Müller *et al.*, 2013) (with permission from Elsevier, Copyright 2013), as shown on the following pages. The studies also focused on the effect of power input on SAV production. However, theoretical calculations (see section 4.3, p. 71) indicated that the original results for this parameter were inaccurate due to an insufficient experimental design. Thus, a *Corrigendum* for the article was submitted for publication in 2016 (with permission from Elsevier, Copyright 2016), containing corrected values for this parameter (Müller *et al.*, 2016b). The *Corrigendum* was based on considerations and calculations described in section 4.3 (pp. 71*ff.*).

Journal of Biotechnology 163 (2013) 325–332

Contents lists available at SciVerse ScienceDirect

Journal of Biotechnology

journal homepage: www.elsevier.com/locate/jbiotec

Development of fed-batch strategies for the production of streptavidin by *Streptomyces avidinii* based on power input and oxygen supply studies

Jakob Michael Müller, Joe Max Risse*, Daniel Jussen, Erwin Flaschel

Lehrstuhl für Fermentationstechnik, Technische Fakultät, Universität Bielefeld, PF 10 01 31, D-33501 Bielefeld, Germany

ARTICLE INFO

Article history:
Received 17 August 2012
Received in revised form 29 October 2012
Accepted 31 October 2012
Available online 8 November 2012

Keywords:
Fed-batch cultivation
Oxygen supply
Power input
Shear stress
Streptavidin production
Streptomyces avidinii

ABSTRACT

Streptavidin is a tetrameric protein with an extremely high affinity to biotin and different biotin-like peptide-tags. This characteristic causes its widespread use in biotechnology. Streptavidin is produced by the fermentation of wild type *Streptomyces avidinii* or by recombinant *Streptomyces lavendulae*, *Escherichia coli*, and *Bacillus subtilis* strains. However, little is known about the influence of power input and oxygen supply as well as feeding strategies on the production of streptavidin by *S. avidinii*. This paper provides a systematic analysis of the effect of rotary frequency of the stirrer, leading to a plateau-like streptavidin formation behaviour between 400 and 700 min^{-1}. This plateau was characterized by specific power inputs between 79 and 107 $W L^{-1}$ and corresponding maximal product concentrations of 6.90 μM in 6 days. Lower as well as higher rotary frequencies were not beneficial. Subsequently, a linear fed-batch procedure could be established reproducibly yielding 39.20 μM streptavidin in 14 days, characterized by a constant productivity of 114 nM h^{-1}. Fed-batch procedures based on dissolved oxygen were less efficient. The linear feeding strategy presented in this paper led to the highest streptavidin concentration ever reported and exceeded the maximal product level given in the literature drastically by a factor of 8.5.

1. Introduction

Streptavidin (SAV) was found in 1963 in the culture supernatants of *Streptomyces avidinii* and *Streptomyces lavendulae* (Chaiet and Wolf, 1964; Stapley et al., 1963). Like avidin from chicken egg white, SAV binds biotin with a dissociation constant (K_d) of up to 10^{-15} M. Each subunit of the tetrameric protein can bind one molecule of biotin. In contrast to avidin, SAV is not glycosylated and has an isoelectrical point near neutral pH (about 6.1). After cleavage of the signal peptide native SAV has a molecular mass of 65962.8 Da (4 times 16490.7 Da) and consists of four chains of 159 amino acids. Depending on the degree of proteolysis different molecular species can be found with the lowest molecular mass at 50.4 kDa (Bayer et al., 1989; Sano et al., 1995). The digestion down to a so-called "core streptavidin" consisting of 118 to 127 amino acids per subunit does not affect the binding properties to biotin or the isoelectric point of the protein, but leads to an increased solubility (Kopetzki et al., 1996; Pähler et al., 1987; Sano et al., 1995). In contrast to native SAV, core streptavidin interacts with the carboxyl carrier protein, which can reduce its number of available biotin-binding sites (Wang et al., 2005). Core streptavidin is commercially available in different molecular masses (Bayer et al., 1989). The monomers re-assemble autonomously even under slightly denaturing conditions (Warner et al., 2004). By changing amino acid residues, monomeric forms of SAV were constructed. These monomers showed significantly reduced binding constants (Howarth et al., 2006; Qureshi and Wong, 2002; Wu and Wong, 2005, 2006).

SAV is used for the detection, localization, quantification, and isolation of various macromolecules like DNA and proteins. For this purpose biotin or SAV itself are bound to the molecule of interest. The application of SAV was enhanced by the identification of several short peptide sequences with high affinity to the tetrameric protein. Strep-tag I®, Strep-tag II®, and Nano-tag are catchwords in this field of interest (Dumelin et al., 2006; Lamla and Erdmann, 2004; Skerra, 2003; Skerra and Schmidt, 1999). Molecules tagged with these peptides can be separated by SAV, which is immobilized on resins like agarose. Depending on the peptide sequence and length, dissociation constants of up to 4 nM are described. In the widespread Strep-tag II® technology a dissociation constant of about 1 μM is reported, although a SAV variant called streptactin is used, which had been modified in position 44–47 (Schlapschy and Skerra, 2010; Skerra, 2003). In comparison to the often-used His_6-tag technology the association constant (K_a) in Strep-tag II® technology is about three times

Abbreviation: SAV, streptavidin.

* Corresponding author.
E-mail address: jrisse@uni-bielefeld.de (J.M. Risse).

0168-1656/$ – see front matter © 2012 Elsevier B.V. All rights reserved.
http://dx.doi.org/10.1016/j.jbiotec.2012.10.021

higher (Dorn et al., 1998; IBA GmbH, 2003). The construction of proteins both fused with a His_6- and a Strep-tag, resulting in so-called "double-tagged" proteins, is a popular technique to yield proteins of extremely high purity in order to investigate their properties, e.g. for the analysis of unknown open reading frames (IBA GmbH, 2003).

1.1. Survey on the production of streptavidin

Although SAV is of great use in biology, medical science, and biotechnology only little has been published about its production by microorganisms. Cultivations are mostly performed in shake flasks (Cazin et al., 1988; Meade and Jeffrey, 1986; Stapley et al., 1963; Thompson and Weber, 1993; Wu and Wong, 2002, 2006). No data are available on the influence of shear stress and oxygen supply on SAV formation. Furthermore, techniques like fed-batch fermentation are not discussed in the literature. Besides the native producers *S. avidinii* and *S. lavendulae* three recombinant microorganisms are mentioned for the production of SAV: *S. lividans*, *Bacillus subtilis*, and *Escherichia coli*. While Gram-positive bacteria are able to secrete the product into the medium, SAV remains in the cyto- or periplasmatic space, when produced in *E. coli* (Gallizia et al., 1998; Sano and Cantor, 1990; Wu and Wong, 2006; Veiko et al., 1999).

Media optimization led to maximal SAV concentrations of up to 170 mg L^{-1} by the cultivation of wild type *S. avidinii* (Kolomiets et al., 1998). As shown in Table 1 a maximal productivity of approximately 82 nM h^{-1} can be calculated from the data given in the literature assuming a molecular mass of the product of 54 kDa derived from their SDS-PAGE analysis. A maximal concentration of up to 250 mg L^{-1} was reported for the cultivation of a recombinant *S. lividans* strain (Meade and Jeffrey, 1986). So far, no higher concentration during cultivation has been observed. However, details about the productivity of this process were not specified.

By using a recombinant *B. subtilis* for the production of SAV Wu et al. (2002) reached a maximal productivity up to 109 nM h^{-1}, but the SAV concentration was limited to 94 mg L^{-1} (Wu et al., 2002). The maximal molar concentrations of SAV during *E. coli* cultivations were similar to the ones obtained with *B. subtilis*, but productivities were much higher. Productivities up to 340 nM h^{-1} have been described in the literature (see Table 1). Although the productivities for *E. coli* refer to the time of induction, the values for the whole process were minored only insignificantly, because the induction was applied already at low cell densities, i.e. an OD_{600} of about 1 (Gallizia et al., 1998; Sano and Cantor, 1990; Wu and Wong, 2006). Intracellular accumulation of SAV produced by Gram-negative recombinant microorganisms in some cases has been associated with the formation of inclusion bodies. In order to express high levels of SAV in *E. coli* a synthetic core streptavidin with optimized codon usage was constructed (Thompson and Weber, 1993). Although the expression level was ten-fold higher in comparison to the corresponding native gene, the maximal concentration was only 3 mg L^{-1}. In order to overcome these drawbacks an *E. coli* strain with a bacteriocine release protein-mediated secretion of SAV into the medium was constructed by Miksch et al. (2008). They observed a maximal SAV concentration up to 2.12 μM.

1.2. Goals and experimental setup

The primary goal of our research is the development of a fed-batch strategy for the production of streptavidin by the natural producer *S. avidinii*. For a rational process design this strategy is developed on the basis of studies on shear stress resistance and oxygen demand of the organism. This is realized by a systematic variation of the rotary frequency of the stirrer. Along with results of shake flask based medium optimization efforts we want to obtain a long-term stable and highly productive process.

2. Material and methods

2.1. Strain

S. avidinii (DSMZ 40526; CBS 730.72) was ordered from CBS (Centraalbureau voor Schimmelcultures, Utrecht, Netherlands) and DSMZ (Deutsche Sammlung von Mikroorganismen und Zellkulturen GmbH, Braunschweig, Germany). In order to avoid a non-producing fraction of cells a selection of producer cells was performed by picking colonies from HM agar plates (4.0 g L^{-1} yeast extract, 10.0 g L^{-1} malt extract, 4.4 g L^{-1} D-glucose monohydrate, pH 7.2) for which 15 g L^{-1} agar were used for solidification. Each colony was used for the inoculation of 30 mL M3 medium (0.7 g L^{-1} yeast extract, 1.3 g L^{-1} casein hydrolysate, 10.0 g L^{-1} soy peptone, 10.0 g L^{-1} D-glucose monohydrate, 6.0 g L^{-1} NaCl, pH 7.0) in 300 mL baffled shake flasks. Cultivation conditions are described in Section 2.3. The best performing culture determined by SAV measurement (see Section 2.4) was used for strain maintenance.

2.2. Strain maintenance

Strain maintenance was based on cultures of *S. avidinii* incubated for 48 h in M3 medium followed by the addition of glycerol

Table 1
Microorganisms reported for the production of streptavidin (SAV). The molecular mass of the tetramer *M* is given more or less accurately by the literature. The maximal productivities are estimated from literature data. $c_{SAV,max}$: maximal SAV concentration, p_{max}: maximal productivity, and n.sp.: not specified.

Organism	$c_{SAV,max}$ [mg L^{-1}]	*M* [kDa]	$c_{SAV,max}$ [μM]	p_{max} [nM h^{-1}]	Reference
S. avidinii	53	72	0.74	10.3	Aldwin et al. (1990)
S. avidinii	145	70	2.07	10.4 (8.6 [c])	Cazin et al. (1988) and Suter et al. (1988)
S. avidinii	170	58 [d]	2.93[d]	82.0 [d](48.0 [c, d])	Kolomiets et al. (1998)
S. lavendulae	201	n.sp.	n.sp.	n.sp.	Zhang et al. (2007)
S. lividans [a]	**250**	54 [d]	**4.63** [d]	n.sp.	Meade and Jeffrey (1986)
B. subtilis [a]	50	66.0 [d] (80 [d])	0.76 [d] (0.63 [d])	37.0 [d] (31.5 [d])	Wu and Wong (2002)
B. subtilis [a]	94	66.0 [d] (80 [d])	1.42 [d] (1.18 [d])	109.2 [d] (90.8 [d])	Wu et al. (2002)
E. coli [a]	65	64	1.02	**340.0** [b]	Sano and Cantor (1990)
E. coli [a]	70	65.7	1.07	267.5 [b]	Gallizia et al. (1998)
E. coli [a]	70	16.6 [e]	1.05	843.0 [b, e]	Wu and Wong (2006)
E. coli [a]	127	60 [d]	2.12	265.0	Miksch et al. (2008)

[a] Recombinant microorganism.
[b] Productivity after induction by IPTG.
[c] Productivity referring to the maximal SAV concentration.
[d] *M* not clearly given.
[e] Monomeric SAV

to a final concentration of 13% (v/v), aliquotation in volumes of 1 mL, shock-freezing and finally storage at −80 °C.

2.3. Cultivation

S. avidinii was cultivated in 100 mL M3 medium in a 1 L baffled shake flask inoculated with 1 mL of a freshly thawed glycerol stock. Cultivation was performed on a rotary shaker at a frequency of 150 min^{-1}, an amplitude of 2.5 cm, and at 28 °C.

Fermentation experiments were carried out in a LAB bioreactor (MBR, Wetzikon, Switzerland) with a total volume of 7 L and a working volume of 5 L. The diameters of the fermenter and the stirrer were 150 and 70 mm, respectively. The bioreactor fulfilled the criteria of the DECHEMA reference stirred tank reactor (Rehm, 1982), except from the stirrer installation. Instead of three six-bladed Rushton turbines only two were used, which were placed in a distance of 125 mm and 250 mm from the bottom, respectively. Power input to the stirrer was achieved by magnetic coupling. The bioreactor was inoculated with 250 mL of a 48 h old shake flask culture in order to obtain comparable inoculation cell densities. For the preparatory and main cultivation M3 medium was used, however the D-glucose monohydrate supplement for the bioreactor cultivation was increased to 30 g L^{-1}. For shake flask and fed-batch studies medium variations were used as described in Table 3. For the latter a 400 g L^{-1} D-glucose monohydrate feed solution in two-fold demineralized water was applied. Fermentations were controlled at pH 7 by the automatic addition of 2 M NaOH and 20% (v/v) H_3PO_4. The air flow rate was set to 5 NL min^{-1}. Antifoam (PE 8100, BASF, Germany) was added automatically when required. For the batch-studies the dissolved oxygen concentration was not actively controlled. All cultivations were performed at a constant overpressure of 0.5 bar and 30 °C. For the fed-batch studies the rotary frequency of the stirrer was set to 350 min^{-1}.

Volumetric oxygen transfer coefficients k_La were determined in water for different rotary frequencies. Therefore, the values were not the exact k_La values for the crude fermentation broth, but relative values to compare the fermentations among each other. Furthermore, they only represent the oxygen transfer in the beginning of the fermentation, because the mycelial growth of streptomycetes can be expected to reduce the transfer rate in the cultivation course due to the increasing viscosity of the culture broth (Járai et al., 1969).

For determination of the power input by the two Rushton impellers into the bioreactor the motor current was measured by a system from Trainings Systeme, which was composed of a power quality analyzer (40 302) and an energy measuring adapter (40 303). The motor efficiency was estimated to be 90% (Wolf, 2000).

2.4. Analysis

Measurement of the SAV concentration was performed by fluorescence quenching as described by Kada et al. (1999a, 1999b). An assay mixture with a volume of 980 μL containing 50 nM biotin-4-fluorescein (Sigma–Aldrich), 0.1 g L^{-1} bovine serum albumin (BSA), 100 mM NaCl, 1 mM EDTA, and 50 mM NaH_2PO_4 (pH 7.5) was filled in 1 mL polypropylene assay tubes. Precoating of the tubes with BSA was omitted, since it had no influence on the results when BSA was added to the assay mixture instead. A sample volume of 20 μL was added to the assay mixture. After 2 s of vortexing and incubation for 30 min at 25 °C the samples were transferred into disposable plastic cuvettes and fluorescence was determined at 495 nm (excitation)/525 nm (emission) by a fluorimeter (Shimadzu RF-5301 PC). For the determination of streptavidin in culture supernatants samples were diluted to a final concentration of 0–600 nM (tetrameric form). For quantification a calibration curve was generated using different biotin-4-fluorescein concentrations.

Because of its mycelial growth the determination of dry *S. avidinii* biomass was performed by suction filtration (paper filter, ⌀110 mm MACHEREY-NAGEL MN 615) of 10 mL culture washed once with 10 mL tap water. After drying the filter at 50 °C to constancy of weight, the dry mass was measured by differential weighing. Microscopic analysis (10 μL of sample, 200-fold magnification) of the culture broth was performed every 24 h to rule out the effect of contaminations and, infrequently, of the filtration permeate to track mycelial fragmentation.

Glucose concentration was quantified utilizing ion-exchange HPLC, which was equipped with a Marathon Basic autosampler (Spark Holland) and an Irica Σ871 pump. A Nucleogel Ion 300OA (300 mm × 7.8 mm) column (MACHEREY-NAGEL) was used. The running buffer was composed of 2.5 mM sulphuric acid. The sample tray of the autosampler was tempered to 4 °C. Each sample was diluted five-fold with two-fold demineralized water and afterwards mixed with an equal volume of running buffer. D-Glucose monohydrate solutions of 0.5, 5 and 10 g L^{-1}, respectively, diluted with an equal amount of running buffer, were used as references. All samples and standards, each consisting of 1 mL volume, were finally supplemented with 5 μL of 4 mM sodium azide in order to inhibit microbial growth. These samples were injected on the column with a volume of 20 μL, followed by isocratic elution at a constant flow rate of 0.5 mL min^{-1}. The column was tempered to 70 °C. An RI detector (Irica ERC-7515 A, Erma CR. Inc.) was used for quantification.

3. Results and discussion

Medium optimization for the batch production of SAV by *S. avidinii* was already described by Kolomiets et al. (1998). Therefore, we initially focused on the optimization of bioprocess engineering by the systematic variation of the rotary frequency of the stirrer in the bioreactor. In order to identify an adequate basic medium composition for a fed-batch procedure shake flask cultivations were performed. The most promising medium variations were used for further batch experiments in the bioreactor. Finally, the combined results were integrated in the rational development of a fed-batch strategy.

3.1. Selection of streptavidin producing S. avidinii cells

Genetic instability is widespread within the mycelial growing genus *Streptomyces* (Birch et al., 1991). So, most of the analyzed *S. avidinii* cells obtained from DSMZ and CBS lost their ability to produce SAV. After the selection of SAV producing cells from CBS a glycerol stock was prepared.

3.2. Impact of rotary frequency on streptavidin production

The impact of shear stress on SAV production was analyzed in the MBR-bioreactor. Corresponding results of measurements of the oxygen transfer coefficients and power inputs are shown in Table 2.

Cultivation of *S. avidinii* in M3 medium with an initial D-glucose monohydrate concentration of 30 g L^{-1} each under the rotary frequencies given in Table 2 led to the data set presented in Fig. 1.

Rotary frequencies of the stirrer below 400 min^{-1} resulted in relatively low maximal streptavidin concentrations. This was most likely due to insufficiently low oxygen transfer rates indicated by drops in the relative dissolved oxygen saturation curves and low k_La-values as shown in Table 2. Very high frequencies between 1100 and 1500 min^{-1} seem to have a negative impact on SAV formation. In this context the increased mycelial fragmentation observed by microscopic analysis could be relevant.

Table 2
Measured values for specific power input L_{spec} and volumetric oxygen transfer coefficient k_La for different rotary frequencies of the stirrer n. All measurements were performed using the following conditions: 1.5 bar static pressure, 30 °C and an air flow rate of 5 NL min^{-1} in 5 L of demineralized water.

n [min^{-1}]	L_{spec} [W L^{-1}]	k_La [h^{-1}]
200	54.8	18.6
300	67.5	39.9
350	72.7	55.5 (66.2 [a])
400	79.1	75.6
500	88.1	90.4
700	106.6	95.0
900	119.7	109.5
1100	143.4	133.3
1300	161.1	161.9
1500	177.6	181.3

[a] For an air flow rate of 10 NL min^{-1}

Table 3
Results of the shake flask medium optimization. 300 mL baffled shake flasks (degree of filling: 10%) were used on a rotary shaker with an eccentricity of 2.5 cm and a frequency of 150 min^{-1}. All experiments were carried out for 144 h in three biological replica, applying a D-glucose monohydrate concentration of 10 g L^{-1}. Abbreviations: $c_{SAV,max}$: maximal streptavidin concentration; X_{max}: maximal mycelial dry mass concentration; p_{max}: productivity until $c_{SAV,max}$; process selectivity $S_{SAV/X}$: $c_{SAV,max}$ $X_{max^{-1}}$. The media used are abbreviated with M3 (standard M3 medium); SP3 (M3 medium with three times the amount of soy peptone); CH3 (M3 medium with three times the amount of casein hydrolysate and yeast extract) and 2 N/0.5 N (M3 medium with twice/half the amount of soy peptone; casein hydrolysate and yeast extract).

Label	$c_{SAV,max}$ [μM]	X_{max} [g L^{-1}]	p_{max} [nM h^{-1}]	$S_{SAV/X}$ [nmol g^{-1}]
M3	1.77 ± 0.09	5.0 ± 0.2	12.3 ± 0.6	354
SP3	1.71 ± 0.40	**7.4 ± 0.0**	11.9 ± 2.8	231
CH3	1.14 ± 0.07	5.8 ± 0.2	7.9 ± 0.5	195
2 N	**3.37 ± 0.78**	4.9 ± 0.3	**23.4 ± 5.4**	**693**
0.5 N	0.68 ± 0.22	3.0 ± 0.1	4.7 ± 1.5	226

A product formation plateau between 400 and 700 min^{-1}, corresponding to a specific power input between 79 and 107 W L^{-1}, respectively, was observed, characterized by maximal SAV concentrations of 6.93 ± 0.07 μM. Applying a frequency of 900 min^{-1}, which corresponds to 120 W L^{-1}, already resulted in a slight decrease of the maximum product concentration to 6.58 μM.

This suggests that on the one hand an increase of oxygen supply improves SAV formation whereas on the other hand mycelial fragmentation induced by high shear stress affects this process.

Exemplarily, Fig. 2 shows the fermentation at a rotary frequency of 700 min^{-1}.

The course of the mycelial dry mass was representative for all fermentations with rotary frequencies above 350 min^{-1}. After a strong increase in the beginning of the cultivation it reached its climax after two days. Afterwards a nearly instantaneous concentration decline could be observed. Similar observations were made by Torres-Bacete et al. (2005) for the cultivation of *S. lavendulae* in shake flasks. To show that this concentration decline was not an effect of biomass degradation we determined the overall cell dry mass concentration by centrifugation in order to take into account small mycelial fragments as well. The latter did not show a significant decrease after correlating with the mycelial dry mass concentration during the first two days of cultivation. Moreover, short mycelial fragments in the permeate of suction filtration were detected after the initial growth period, suggesting that the mycelium is rather fragmented than completely degraded. This effect was apparently correlated with the limitation of glucose after 56 h of cultivation as shown in Fig. 2. Glucose limitation and mycelial fragmentation, however, did not seem to affect the accumulation of streptavidin in the fermentation supernatant, the rate of which remained approximately linear in the evaluated time period for all rotary frequencies. The observed productivities from cultivation start to the maximal SAV concentration $c_{SAV,max}$ were very similar to those reported by Kolomiets et al. (1998).

3.3. Shake flask cultivation of *S. avidinii*

After the optimization of bioprocess engineering, medium variation was carried out to further improve the maximal SAV concentration. These experiments were performed in 300 mL baffled glass shake flasks (Schott Duran). The results are shown in Table 3.

As was already observed in the bioreactor batch experiments (see Table 2), the data show no direct correlation between biomass and SAV formation.

Neither higher eccentricities with corresponding higher oxygen transfer rates, nor an increase in glucose content of the medium

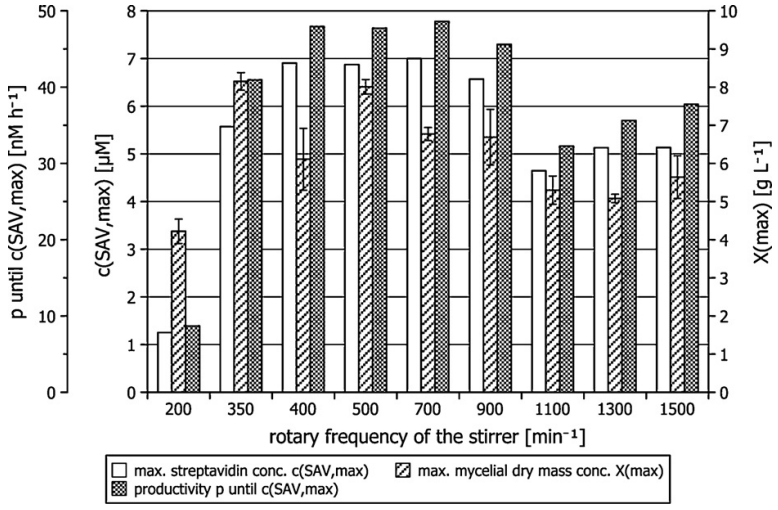

Fig. 1. Productivity p (referring to $c_{SAV,max}$), maximal mycelial dry mass X_{max}, and maximal SAV concentration $c_{SAV,max}$ of fermentations of *S. avidinii* at different rotary frequencies of the stirrer in a period of 6 days on M3 medium supplied with 30 g L^{-1} of D-glucose monohydrate at 30 °C, pH 7, 1.5 bar static pressure and at an air flow rate of 5 NL min^{-1}.

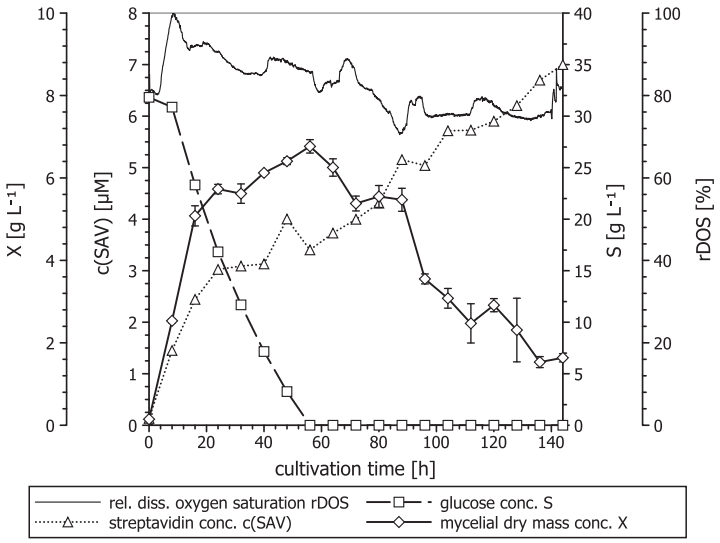

Fig. 2. Batch fermentation with a constant rotary frequency of the stirrer of 700 min^{-1}, 30 °C, pH 7, 1,5 bar static pressure and an air flow rate of 5 NL min^{-1} on M3 medium with 30 g L^{-1} of D-glucose monohydrate.

resulted in higher productivities or improved maximal product concentrations (data not shown). Moreover, decreasing the level of nitrogen-containing compounds in the medium (0.5 N-variation) was tested, assuming an improved oxygen supply for the cells relative to the lower mycelial concentrations. However, this did not lead to a better performance.

The 2N-variation of the M3 medium seemed to be suitable for a higher productivity, selectivity ($S_{SAV/X}$; ratio of maximal product concentration and maximal mycelial dry mass concentration), and product concentration, whereas the SP3-variation yielded a high mycelial dry mass concentration, suggesting its use in pre-cultures for fermentations. Therefore, both of these variations were used for subsequent fed-batch studies.

3.4. Fed-batch production of streptavidin

Two approaches for the fed-batch production of SAV were evaluated: A feed strategy dependent on the relative dissolved oxygen signal, characterized by the initiation of feeding above a relative dissolved oxygen saturation of 60%, and a linear feed profile with a constant glucose mass flow into the fermentation vessel.

Based on the shake flask experiments (see Section 3.3) and the glucose-limitation occurring in all batch processes after approximately two days, conditions were selected as follows: 2 N and SP3 medium were chosen as basic media, whereas 1 L of a 400 g L^{-1} D-glucose monohydrate solution in two-fold demineralized water was used as feed solution. To prevent mycelial fragmentation and to ensure the long-term stability necessary for fed-batch processes, the rotary frequency of the stirrer was chosen as low as 350 min^{-1}. All other default values like pH, temperature, and the initial filling volume of 5 L were carried over from the rotary frequency variation experiments (see Section 3.2).

First fed-batch fermentations were controlled by an on-off system using the dissolved oxygen signal to initiate the glucose feed. An exemplary process (see Table 4, FB 2 N, 60% #1) with a feed initiation above a setpoint of 60% is shown in Fig. 3. Glucose mass flow into the vessel began after 38 h and amounted to 2.3 g h^{-1} on average during the whole feed phase. For this process a maximal SAV concentration of 12.70 µM after 216 h was observed.

The oxygen-controlled processes were characterized by linear glucose feed profiles and SAV concentrations above the values reached for batch fermentation, as shown in Table 4. However, towards the end of cultivation the oxygen concentration exceeded the setpoint permanently, supposedly due to a reduced metabolic activity of the cells and a corresponding decreased oxygen demand. This resulted in a feed of the entire remaining feed solution accompanied by an unregulated increase in glucose concentration (see Fig. 3 after 120 h). In order not to intensify this problem higher air flow rates were not applied, although the variation experiments on the rotary frequency of the stirrer suggested that higher oxygen transfer rates are beneficial for the productivity. Raising the setpoint to 70% did prevent uncontrolled feeding, but lowered the maximal SAV concentration to 9.04 µM after 232 h (see Table 4, FB 2 N, 70%). As a consequence of these results the feed profiles observed in the oxygen-controlled fermentations were used to develop a linear fed-batch process. In detail the average glucose flow rate in the feed interval of the oxygen-controlled processes was used to estimate the glucose demand of the culture. In the case of Fig. 3, for example, this demand was calculated in the interval between the initiation of feeding and the permanent transgression of the oxygen setpoint. An exemplary fermentation course applying this strategy is shown in Fig. 4. Here, the linear feed profile permitted to set the air flow rate to 2 vvm (10 NL min^{-1}). A maximal product concentration of 40.41 µM was reached after 336 h (see Table 4, FB 2 N, lin #2).

As can be concluded from Fig. 4 the linear feed strategy as well as the improved oxygen supply by a doubled air flow rate resulted in higher product concentrations as well as productivities than the comparable processes with oxygen-controlled feed. SAV accumulation remained linear even after 300 h of cultivation time, suggesting a sufficiently high genetic stability of the organism and low or no product inhibition. Table 4 shows a summary of all fed-batch as well as several reference batch processes. In contrast to the 2 N medium the M3 and SP3 medium generated less promising results.

The change of strategy from an oxygen-controlled to a linear feed profile along with the increased oxygen supply provided the basis for the reproducible accumulation of 19.25 ± 0.86 µM (n = 3; FB 2 N, lin#1-3) SAV in 7 days. Compared to the 11.43 ± 1.27 µM

Table 4
Overview on all fed-batch processes. If not declared otherwise, air flow was set to 5 NL min^{-1}. 2 N, M3 and SP3 symbolize the basic medium composition as described in Table 3 The percentages indicate the relative dissolved oxygen saturation-setpoint for the oxygen-controlled fed-batch processes. The linear processes are entitled "lin". Reference batch processes are labelled "B", fed-batches "FB". For all fed-batches 1 L of a 400 g L^{-1} D-glucose monohydrate feed solution was used. Further abbreviations: $c_{SAV,max}$: maximal SAV concentration, t_{max}: cultivation time when reaching $c_{SAV,max}$, t_{feed}: cultivation time when feed was initiated, X_{max}: maximal mycelial dry mass concentration p_{max}: productivity until $c_{SAV,max}$, process selectivity $S_{SAV/X}$: $c_{SAV,max}$ $X_{max^{-1}}$, p_{feed}: average productivity in feed phase, $\dot{m}_{Glc}$: glucose mass flow rate into the vessel during feed phase.

Label	$c_{SAV,max}$ [μM]	t_{max} (t_{feed}) [h]	X_{max} [g L^{-1}]	p_{max} [nM h^{-1}]	$S_{SAV/X}$ [nmol g^{-1}]	p_{feed} [nM h^{-1}]	$\dot{m}_{Glc}$ [g h^{-1}]
B M3	5.57	136 (–)	8.2	41.0	679	–	–
B 2 N	4.40	128 (–)	9.6	34.4	458	–	–
B SP3	3.12	88 [a] (–)	9.4	35.4	333	–	–
FB 2 N, 60% #1	12.70	216 (34)	16.1	58.8	788	63.6	2.7
FB 2 N, 60% #2	10.15	184 (70)	16.0	55.2	634	80.2	2.0
FB 2 N, 60% #3	11.44	144 (38)	10.8	79.4	1062	54.9	2.3
FB 2 N, 70%	9.04	232 (52)	14.1	38.9	641	22.2	2.8
FB M3, 60%	6.04	128 (50)	6.7	47.1	897	16.2	1.6
FB SP3, 60%	6.99	152 (57)	15.1	46.0	464	34.9	1.1
FB 2 N, lin #1 [b]	18.54	184 (49)	19.8	100.8	936	100.1	1.8
FB 2 N, lin #2 [b]	**40.41**	336 (48)	23.8	**120.3**	**1698**	**123.2**	1.7
FB 2 N, lin #3 [b]	38.00	336 (37)	**25.2**	113.8	1507	101.5	1.7

[a] The streptavidin concentration showed a logarithmic course and didn't increase after this time period until the process was aborted after 168 h.
[b] Air flow rate: 10 NL min^{-1}.

(n = 3) obtained on average in 8 days for the processes with a feed based on the oxygen signal (see Table 4, FB 2 N, 60% #1-3), the maximal product concentration was increased by the factor 1.7. After 14 days of cultivation the concentration of SAV even reached 39.20 μM (n = 2) for the linear feed processes (see Table 4, FB 2 N, lin #2 and #3). The characteristic mean productivity of 64 nM h^{-1} (n = 3) in the oxygen-controlled processes was improved by a factor of 1.8, corresponding to 114 nM h^{-1} (n = 3). Furthermore, the new strategy showed a more favourable process selectivity. Although the selectivities of the single processes varied significantly, the observed overall tendency to a higher product to mycelial dry mass-ratio for the linear feed profiles is beneficial. Unlike for many other biotechnological processes the results reveal no indication for a strong positive correlation between biomass and product formation as shown in Table 3 and Table 4. The maximal mycelial dry mass concentration for the linear processes was increased compared to the oxygen-controlled processes. However, this was partially due to the longer cultivation time for the former. By using the feed data from the oxygen-controlled processes to develop a linear feed profile, the use of which allowed decoupling of the improved oxygen input achieved through the doubled air flow rate and glucose feed. This permits an independent adjustment of these process variables, which is very challenging for oxygen-controlled processes. In case of a suboptimal choice of feed control parameters in oxygen-controlled processes a strong oxygen signal fluctuation can occur, whereas linear feed strategies have the potential of providing a more stable environment for the cells.

The reference processes for the fed-batch experiments show that neither simple modification of the basic medium nor the implementation of the glucose feed solution alone are sufficient for a strong increase in productivity, but only the combination of both leads to high product yields. This suggests that the inferior product formation in the rotary frequency batch experiments was caused by insufficient carbon as well as nitrogen supply.

To sum up the process which led to the development of the linear fed-batch strategy, five main aspects have to be considered:

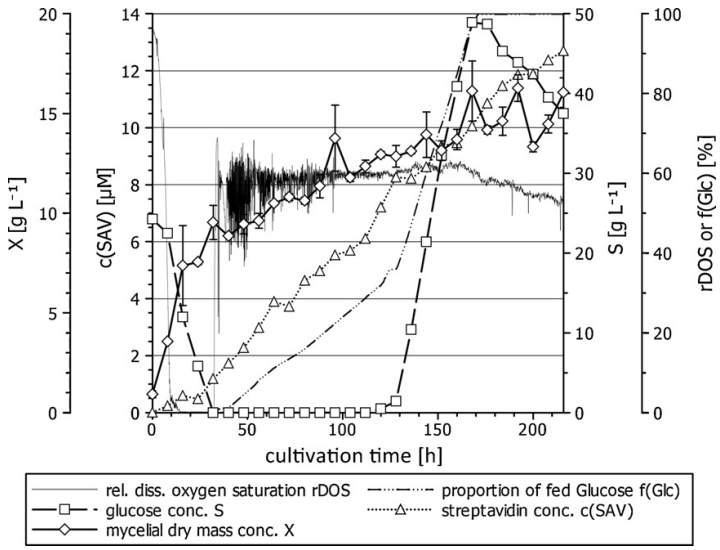

Fig. 3. Fed-batch cultivation with an oxygen-controlled feed of a 400 g L^{-1} D-glucose monohydrate solution on 2 N medium supplemented with 30 g L^{-1} D-glucose monohydrate above a feed-setpoint of 60% relative dissolved oxygen saturation and an air flow rate of 5 NL min^{-1}.

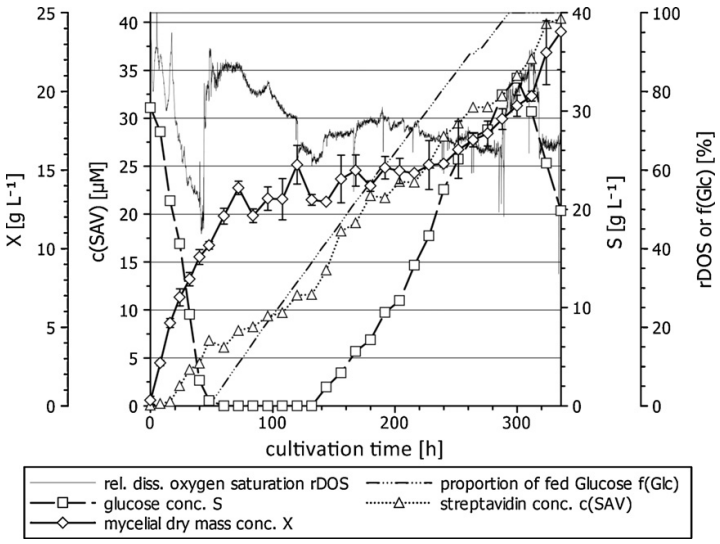

Fig. 4. Fed-batch fermentation of *S. avidinii* based on a linear feed of a 400 g L^{-1} D-glucose monohydrate concentrate on 2 N medium supplemented with 30 g L^{-1} D-glucose monohydrate. The air flow rate was set to 10 NL min^{-1}. Glucose mass flow into the vessel was initiated after 48 h and amounted to a feed rate of 1.7 g h^{-1} on average.

1) The observation of glucose limitation accompanied by mycelial instability at rotary frequencies above 350 min^{-1} resulted in the decision to use a glucose concentrate as feed solution. 2) Mycelial fragmentation was determined to be a main drawback at high rotary frequencies of the stirrer. Hence, a low frequency of 350 min^{-1} was chosen in order to guarantee long-term stability of the mycelium during fed-batch experiments. 3) The shake flask medium variation experiments resulted in two potentially beneficial modifications of the M3 standard medium, 2 N and SP3. These were therefore used in subsequent fed-batch experiments, where the 2 N modification turned out to be suitable. 4) Control problems in the oxygen-controlled fed-batch processes could be avoided efficiently by the development of a linear feed profile. 5) Oxygen supply seemed to be a second important parameter for SAV production by *S. avidinii*. To provide sufficient oxygen supply during the fermentation without an alteration in power input, the air flow rate was doubled in the linear fed-batch fermentations.

4. Conclusions

In this paper the influence of stirrer induced shear stress on the production of streptavidin (SAV) was examined using the natural producer *S. avidinii*. In 6 day-fermentations maximal concentrations of 6.93 ± 0.07 µM were achieved for rotary frequencies of the stirrer between 400 and 700 min^{-1}, correlated with a specific power input of 79 and 107 W L^{-1}, respectively. Both higher and lower frequencies affected the product formation. The former suggested shear stress induced damage on the mycelium for an immoderately high power input. The latter caused insufficient oxygen supply. This clearly indicated the importance of an appropriate choice of this process variable for the fermentation of *S. avidinii*.

Based on these results feed studies with a 400 g L^{-1} D-glucose monohydrate concentrate on 2 N medium resulted in the development of a linear fed-batch process reproducibly yielding 39.20 µM ($n = 2$) of streptavidin in 14 days. This product concentration by far exceeds all maximal concentrations reported in literature for SAV production. Furthermore, it outperformed the highest maximal productivity of 82 nM h^{-1} described for *S. avidinii* by Kolomiets et al. (1998) (see Table 1) by the factor 1.4 with a linear productivity of 114 nM h^{-1} ($n = 3$) during the whole process.

Compared to processes in rapidly growing recombinant bacteria like *E. coli*, production of streptavidin by *S. avidinii* shows lower productivities. The productivity for heterologous SAV production in *E. coli* described by Sano and Cantor (1990) of approximately 340 nM h^{-1} (see Table 1), is still much higher than the one obtained by the linear fed-batch strategy presented here. However, the productivity is limited to a short time interval due to product toxicity, causing a maximal concentration of only 1.02 µM of SAV. In contrast to recombinant SAV expression no product inhibition even for concentrations as high as 40 µM was observed using *S. avidinii* (see Fig. 4). Furthermore, in the recombinant process the product accumulated in the cytoplasm partly as inclusion bodies, causing the necessity of refolding accompanied by poor product recovery. In addition, considering the down time necessary for process preparation and shut-down, the productivity of the whole process has to be corrected to lower values. To avoid these drawbacks, long-term processes with constant productivities are desirable due to low down times relative to their process length. The process strategy described here implements the idea of a long-term stable productivity and at the same time outbalances all absolute productivities described for SAV production by *S. avidinii* to date.

This paper for the first time provides a protocol for a complex process strategy for SAV production by *S. avidinii*. Therefore, upcoming studies can now be realized much more rationally, allowing targeted process optimization. In particular, the application of different feed media and higher oxygen transfer rates as well as experiments with varied feed profiles are now in the focus of interest. Furthermore, the high stability of the organism observed during linear fed-batch cultivation can be exploited by the application of long-term process strategies like continuous cultivation and repetitive fermentation.

Acknowledgement

We would like to thank the DBU (Deutsche Bundesstiftung Umwelt) for the financial support.

References

Aldwin, L., Toso, R., Goodson, R., Hunter, J., 1990. Improvement of production, assay and purification of streptavidin. Journal of Industrial Microbiology 5, 239–246.

Bayer, E.A., Ben-Hur, H., Hiller, Y., Wilchek, M., 1989. Postsecretory modifications of streptavidin. Biochemical Journal 259, 369–376.

Birch, A., Häusler, A., Rüttener, C., Hütter, R., 1991. Chromosomal deletion and rearrangement in *Streptomyces glaucescens*. Journal of Bacteriology 173, 3531–3538.

Cazin Jr., J., Suter, M., Butler, J.E., 1988. Production of streptavidin obtained in a synthetic medium. Journal of Immunological Methods 113, 75–81.

Chaiet, L., Wolf, F.J., 1964. The properties of streptavidin a biotin-binding protein produced by streptomycetes. Archives of Biochemistry and Biophysics 106, 1–5.

Dorn, I.T., Neumaier, K.R., Tampé, R., 1998. Molecular recognition of histidine-tagged molecules by metal-chelating lipids monitoring by fluorescence energy transfer and correlation spectroscopy. Journal of the American Chemical Society 120, 2753–2763.

Dumelin, C.E., Scheuermann, J., Melkko, S., Neri, D., 2006. Selection of streptavidin binders from a DNA-encoded chemical library. Bioconjugate Chemistry 17, 366–370.

Gallizia, A., de Lalla, C., Nardone, E., Santambrogio, P., Brandazza, A., Sidoli, A., Arosio, P., 1998. Production of a soluble and functional recombinant streptavidin in *Escherichia coli*. Protein Expression and Purification 14, 192–196.

Howarth, M., Chinnapen, D.J.-F., Gerrow, K., Dorrestein, P.C., Grandy, M.R., Kelleher, N.L., El-Husseini, A., Ting, A.Y., 2006. A monovalent streptavidin with a single femtomolar biotin binding site. Nature Methods 3, 267–273.

IBA GmbH, 2003. Expression and purification of proteins using Strep-tag and/or 6xHis-tag: a comprehensive manual. Version PR02-0003, Last date of revision: November 03.

Járai, M., Győry, E., Tombor, J., 1969. Oxygen transfer in *Streptomyces* fermentation broths. Biotechnology and Bioengineering 11, 605–622.

Kada, G., Falk, H., Gruber, H.J., 1999a. Accurate measurement of avidin and streptavidin in crude biofluids with a new, optimized biotin-fluorescein conjugate. Biochimica et Biophysica Acta 1417, 33–43.

Kada, G., Kaiser, K., Falk, H., Gruber, H.J., 1999b. Rapid estimation of avidin and streptavidin by fluorescence quenching or fluorescence polarization. Biochimica et Biophysica Acta 1427, 44–48.

Kolomiets, E.I., Zdor, N.A., Vashkevich, I.I., Pryadko, A.G., Svirid, V.D., Ermolenko, M.N., Sviridov, O.V., 1998. Streptavidin a product of the strain *Streptomyces avidinii* VKM Ac1047: synthesis, purification and use in immunoassay technology. Russian Biotechnology 2, 1–8.

Kopetzki, E., Rudolph, R., Grossmann, A., 1996. Recombinant core-streptavidin. Patent: Boehringer Mannheim GmbH, US 5489528.

Lamla, T., Erdmann, V.A., 2004. The nano-tag a streptavidin-binding peptide for the purification and detection of recombinant proteins. Protein Expression and Purification 33, 39–47.

Meade, H.M., Jeffrey, J.L., 1986. Production of streptavidin-like polypeptides. Patent: Biogen N.V., WO 86/02077.

Miksch, G., Risse, J.M., Ryu, S., Flaschel, E., 2008. Factors that influence the extracellular expression of streptavidin in *Escherichia coli* using a bacteriocin release protein. Applied Microbiology and Biotechnology 81, 319–326.

Pähler, A., Hendrickson, W.A., Gawinowicz Kolks, M.A., Argarana, C.E., Cantor, C.R., 1987. Characterization and crystallization of core streptavidin. Journal of Biological Chemistry 262, 13933–13937.

Qureshi, M.H., Wong, S.-L., 2002. Design production and chracterization of a monomeric streptavidin and its application for affinity purification of biotinylated proteins. Protein Expression and Purification 25, 409–415.

Rehm, H.J., 1982. Arbeitsmethoden für die Biotechnologie, Dechema-Fachausschuss Biotechnologie, in Dechema-Studien zur Forschung und Entwicklung, Frankfurt a.M.

Sano, T., Pandori, M.W., Chen, X., Smith, C.L., Cantor, C.R., 1995. Recombinant core streptavidins. Journal of Biological Chemistry 270, 28204–28209.

Sano, T., Cantor, C.R., 1990. Expression of a cloned streptavidin gene in *Escherichia coli*. Proceedings of the National Academy of Sciences 87, 142–146.

Schlapschy, M., Skerra, A., 2010. Purification and analysis of strep-tagged antibody fragments. In: Kontermann, R., Dübel (Eds.), Antibody Engineering, vol. 2, second ed. Springer Verlag, Berlin/Heidelberg.

Skerra, A., 2003. Das Strep-tag als molekulares Werkzeug zur Hochdurchsatz-Proteinreinigung in der Proteomforschung. BIOspektrum 9, 189–192.

Skerra, A., Schmidt, T.G.M., 1999. Applications of a peptide ligand for streptavidin: the strep-tag. Biomolecular Engineering 16, 79–86.

Stapley, E.O., Mata, J.M., Miller, I.M., Demny, T.C., Woodruff, H.B., 1963. Antibiotic MSD-235. I. Production by *Streptomyces avidinii* and *Streptomyces lavendulae*. Antimicrobial Agents and Chemotherapy (Bethesda) 161, 20–27.

Suter, M., Cazin Jr., J., Butler, J.E., Mock, D.M., 1988. Isolation and characterization of highly purified streptavidin obtained in a two-step purification procedure from *Streptomyces avidinii* grown in synthetic medium. Journal of Immunology Methods 113, 83–91.

Thompson, L.D., Weber, P.C., 1993. Construction and expression of a synthetic streptavidin-encoding gene in *Escherichia coli*. Gene 136, 243–246.

Torres-Bacete, J., Arroyo, M., Torres-Guzmán, R., De La Mata, I., Acebal, C., Pilar Castillón, M., 2005. Optimization of culture medium and conditions for penicillin acylase production by *Streptomyces lavendulae* ATCC 13664. Applied Biochemistry and Biotechnology 126, 119–131.

Veiko, V.P., Gul'ko, L.B., Okorokova, N.A., Dýakov, N.A., Debabov, V.G., 1999. Cloning and expression of the streptavidin gene from *Streptomyces avidinii* in *Escherichia coli* and secretion of streptavidin by *E. coli* cells. Russian Journal of Bioorganic Chemistry 25, 184–188.

Wang, W.W.-S., Das, D., Suresh, M.R., 2005. Biotin carboxyl carrier protein co-purifies as a contaminant in core streptavidin preparations. Molecular Biotechnology 31, 29–40.

Warner, M.J., Navrotskaya, I., Bain, A., Oldham, E.D., Mascotti, D.P., 2004. Thermal and sodium dodecylsulfate induced transitions of streptavidin. Biophysical Journal 87, 2701–2713.

Wolf, K.H., 2000. Rührfermenter-Dimensionierung, first ed. Vulkan-Verlag, Essen.

Wu, S.-C., Wong, S.-L., 2002. Engineering of a *Bacillus subtilis* strain with adjustable levels of intracellular biotin for secretory production of functional streptavidin. Applied Environmental Microbiology 68, 1102–1108.

Wu, S.-C., Qureshi, M.H., Wong, S.-L., 2002. Secretory production and purification of functional full-length streptavidin from *Bacillus subtilis*. Protein Expression and Purification 24, 348–356.

Wu, S.-C., Wong, S.-L., 2005. Engineering soluble monomeric streptavidin with reversible biotin capability. Journal of Biological Chemistry 280, 23225–23231.

Wu, S.-C., Wong, S.-L., 2006. Intracellular production of a soluble and functional monomeric streptavidin in *Escherichia coli* and its application for affinity purification of biotinylated proteins. Protein Expression and Purification 46, 268–273.

Zhang, L., Liu, C.Q., Gao, Z.H., Cao, Y., Bai, G., 2007. Research on the classification of *streptomyces* strain ZG0429 and purification of streptavidin. Acta Microbiologica Sinica 47 (1), 7–10.

Journal of Biotechnology 226 (2016) 76–77

Contents lists available at ScienceDirect

Journal of Biotechnology

journal homepage: www.elsevier.com/locate/jbiotec

Corrigendum

Corrigendum to "Development of fed-batch strategies for the production of streptavidin by *Streptomyces avidinii* based on power input and oxygen supply studies" [J. Biotechnol. 163 (2013) 325–332]

Jakob Michael Müller, Joe Max Risse*, Daniel Jussen, Erwin Flaschel

Lehrstuhl für Fermentationstechnik, Technische Fakultät, Universität Bielefeld, PF 10 01 31, D-33501 Bielefeld, Germany

The authors regret mistakes in the original version of the article.

Power input

Measurements of the specific power input L_{spec} with the original experimental setup brought about incorrect results. Theoretical calculations according to Briel and Wittig (1998) based on the given bioreactor system yielded drastically lower values for this parameter. This suggested that measuring L_{spec} only for the final filling volume of 5 L resulted in an overestimation of power input due to load-dependent effects of mechanic friction, heat dissipation, and electrical loss of power (Briel and Wittig, 1998). The motor efficiency typically increases upon load of the motor until it reaches its optimum in the range of 50–100% of the rated load (McCoy et al., 1993). The maximal power of the given motor (80G-4, Elektromotoren Brienz AG, Brienz, Switzerland) was 1.5 kW, but the motor was operated at a much lower load (see Table 2 in the original paper). Thus, the efficiency of the motor was probably lower than the maximal rated efficiency of 77% (information of the supplier), leading to a large contribution of factors like friction for operation in the lower range of frequencies, which falsified the results. Therefore, the measurements were repeated with a new experimental design for a differential calculation of power input.

Table 2
Volumetric oxygen transfer coefficient k_La and corrected values for the specific power input L_{spec} for different rotary frequencies of the stirrer n for the bioreactor described in section 3.2. Measurements of the k_La were performed applying 1.5 bar static pressure, 30 °C and an air flow rate of 5 NL min^{-1} (1 vvm) in 5 L of demineralized water, whereas only n and the air flow rate were controlled for the estimation of power input.

n [min^{-1}]	L_{spec} [W L^{-1}][a]	k_La [h^{-1}]
200	0.1[b]	18.6
300	0.2[b]	39.9
350	0.4[b]	55.5 (66.2[c])
400	0.5[b]	75.6
500	1.0	90.4
700	2.3	95.0
900	4.5	109.5
1100	7.6	133.3
1300	11.9	161.9
1500	17.4	181.3

[a] Acquired from fitting to a power function (see Fig. 5); the values refer to aerated conditions.
[b] Experimental value close to lower detection limit.
[c] For an air flow rate of 10 NL min^{-1}.

All measurements of L_{spec} were performed without regulation of pH, temperature or pressure to minimize interfering factors.[1] Firstly, power input (a) was measured for a filling volume of 1 L, for which both stirrers were surrounded by air, whereas the bottom part of the

DOI of original article: http://dx.doi.org/10.1016/j.jbiotec.2012.10.021.
* Corresponding author.
E-mail address: jri@fermtech.techfak.uni-bielefeld.de (J.M. Risse).
[1] No effect of the slight increase of temperature on power input during the measurements (+3 °C) was observed.

http://dx.doi.org/10.1016/j.jbiotec.2016.03.048

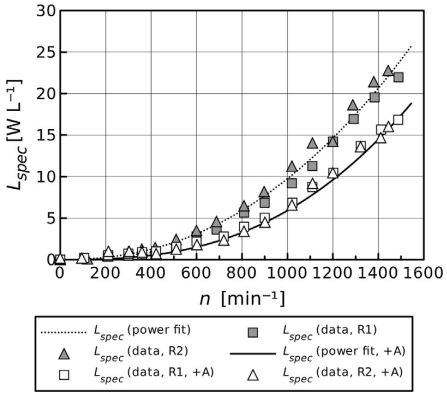

Fig. 5. Results of the power input measurements of two identical bioreactors (R1 and R2) as specified in section 3.2. The plot shows the course of specific power input L_{spec} over the rotary frequency of the stirrer n. Data for measurements in aerated conditions (1 vvm) are labelled "+A". Experimental data and results from the fit to the two-parameter power function $L_{spec} = n^a \times b$ (power fit) are shown (parameters: without aeration: $a = 2.23$, $b = 2 \times 10^{-6}$; aerated: $a = 2.66$, $b = 6.22 \times 10^{-8}$).

stirrer shaft including the magnetic coupling was submerged in water. This configuration was used for the evaluation of load-dependent, friction-related effects. Secondly, measurements for a volume of 5 L (b), for which both stirrers were submerged in the liquid, were used for estimation of the overall power input. Calculation of the specific power input was then based on subtraction of (a) from (b), relating to the filling volume of 5 L,[2] and assuming that 90% of the energy was dissipated in the fluid (Wolf, 2000). Two identical bioreactors were analyzed in this way. All measurements were performed in aerated and unaerated conditions. The course of the specific power input L_{spec} was fit to a power function to allow more accurate predictions for low values of n. Resulting values are shown in the corrected version of Table 2 of the original paper and the additional Fig. 5.

The new values for L_{spec} are in the expected range for lab scale bioreactors and follow the typical course over the frequency of the stirrer (Hortsch and Weuster-Botz, 2010). The corrected values also apply to the streptavidin formation plateau (abstract, p. 328, p. 331) mentioned in the paper. The plateau observed for rotary frequencies of the stirrer between 400 and 700 min^{-1} is therefore correlated to a range of L_{spec} between 0.5 and 2.3 W L^{-1}.

The given method does, however, not allow quantification of the volume-dependent change of slippage of the motor and the corresponding loss of energy, which may lead to lower values of L_{spec} for increasing frequencies of the stirrer. Slippage of electrical motors is typically proportional to the motor load (McCoy et al., 1993), reaching a maximal value of 6.7% for the given motor (information of the supplier). This maximal error would only apply in the worst case, i.e. when slippage is negligible for the low filling volume whereas it reaches its maximal value for the working volume of 5 L, and for operation at full motor load (which was not the case).

Strategy of feeding

An imprecise term was used for the strategy of feeding in the original article ('linear fed-batch'; abstract, pp. 328–331). The correct term is 'constant feeding', as the feed rate was kept constant over time.

The authors would like to apologise for any inconvenience caused.

References

Briel, R., Wittig, A. (Eds.), 1998. Mischen und Rühren – Grundlagen Und Moderne Verfahren für Die Praxis. , first ed. VDI-Gesellschaft Verfahrenstechnik und Chemieingenieurwesen (GVC), Düsseldorf.
Hortsch, R., Weuster-Botz, D., 2010. Power consumption and maximum energy dissipation in a milliliter-scale bioreactor. Biotechnol. Prog. 26, 595–599.
McCoy, G.A., Litman, T., Douglass, J.G., 1993. Energy-Efficient Electric Motor Selection Handbook, third revision. U.S. Department of Energy, Washington.
Wolf, K.H., 2000. Rührfermenter-Dimensionierung, first ed. Vulkan-Verlag, Essen.

[2] Assuming that no power was dissipated in the liquid volume of 1 L for the first measurement.

4.3 Theoretical analysis of the accuracy of the power input measurements

A comparison of measured values for the specific power input L_{spec} and literature data suggested that this parameter was not quantified accurately in the original manuscript. For typical reactors on the laboratory scale, power input can be estimated to be in the range of 100-500 W (van't Riet & Tramper, 1991, p. 315). Related to a typical reactor volume of 5 L, this would yield a specific power input of 20-100 W L^{-1}. Specific power input has been reported to be <44 W L^{-1} for bioreactors with a working volume of 50 L (Menkel, 1992, p. 128).

However, the power input measurements performed for this study yielded surprisingly high values of L_{spec} in the range of 54.8 to 177.6 W L^{-1} in the variation interval of the stirring frequency from 200 to 1500 min^{-1} (Müller *et al.*, 2013). Moreover, the course of power input for increasing stirring frequencies did not resemble a power function as expected (refer, e.g., to Hortsch & Weuster-Botz, 2010).

The discrepancy of literature values and experimental data indicated problems for the measurement of L_{spec} by motor current and amperage as performed in the original paper. Generally, the method is error-prone, because varying proportions of the measured current may be released not in the form of motion but friction-induced heat (GVC-Fachausschuss 'Mischvorgänge', 1998).

Theoretical calculations according to the following sections were performed for an estimate of realistic values of L_{spec} for the given bioreactor. Correlations and equations for this purpose were obtained from GVC-Fachausschuss 'Mischvorgänge' (1998) (p. 44*ff.*).

4.3.1 Dimensions of the MBR bioreactor.

The characteristic dimensions of the 5 L MBR bioreactor used in Müller *et al.* (2013) are shown in Table 4.1.

4.3.2 Reynolds number and power equation

In general, the definition of the Reynolds number of mixing Re_M is

$$Re_M = \frac{n \cdot d^2 \cdot \rho}{\eta} \tag{4.1}$$

where n is the stirring frequency, d the diameter of the stirrer, and ρ and η the density and dynamic viscosity of the fluid, respectively.

Tab. 4.1: Dimensions of the 5 L MBR bioreactor.

dimension/ratio	value
stirrer type	6-bladed Rushton turbine
number of turbulence promoters	4
d/D[1]	70 mm/150 mm = 0,47
H/D[2]	300 mm/150 mm = 2
w[3]	15 mm
installation height of the stirrer	125 mm and 250 mm
working volume	5 L

[1] ratio of stirrer diameter d and bioreactor diameter D
[2] ratio of height H to diameter of the bioreactor D (assuming a working volume of 5 L)
[3] blade with of the stirrer

The power input L can be calculated from the power equation:

$$L = Ne \cdot \rho \cdot n^3 \cdot d^5 \tag{4.2}$$

where Ne is the Newton number and d is the diameter of the stirrer.

4.3.3 Performance characteristics of different stirrers

The Newton number Ne which was used for the following calculations was derived from Fig. 4.1.

The Newton number for Rushton turbines and vessels with turbulence promoters (curve gs, 'Scheibenrührer' = Rushton turbine) converges towards a constant value of 5 upon transition from an ordered laminar to a turbulent flow regime. This feature can be utilized for the calculation of L by equation 4.2.

4.3.4 System-based modifications

Several modifications of Ne apply due to the configuration of the bioreactor, as discussed in the following sections.

4.3.4.1 Impact of the ratio d/D

An increase of the ratio of stirrer- to bioreactor diameter d/D from 0.2 to 0.5 is correlated to a decrease of the Newton number by approx. 20% (GVC-Fachausschuss 'Mischvorgänge', 1998). The

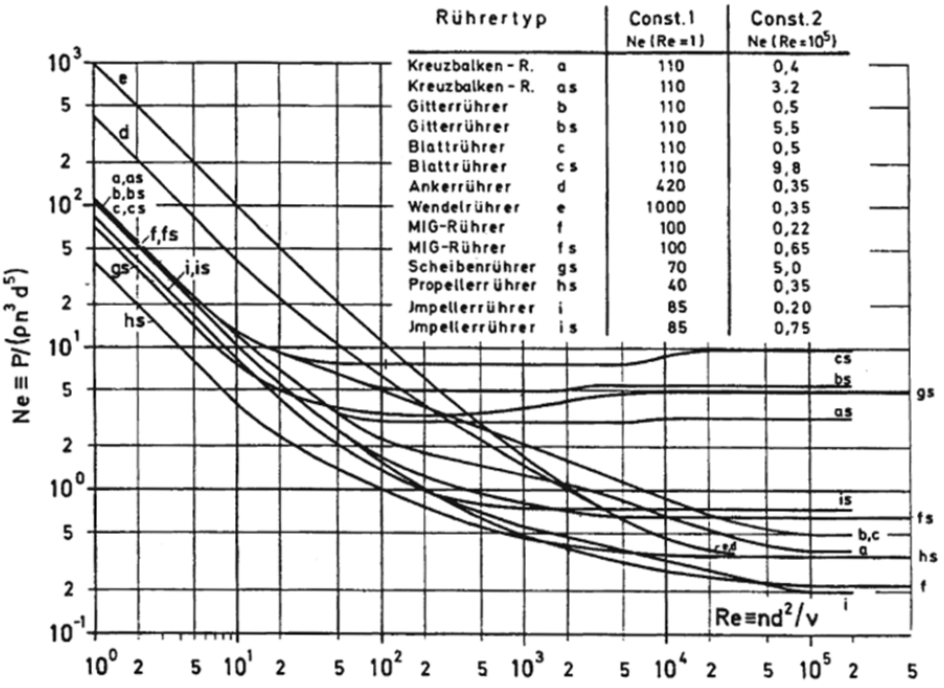

Fig. 4.1: Plot of Newton number versus Reynolds number for different types of stirrers according to Zlokarnik (1999) (p. 35).

reference system with a Rushton turbine depicted in Fig. 4.1 ($Ne = 5$) was characterized by a ratio d/D of 0.3. In the system used for this study, this ratio was 0.47 (see Table 4.1). The difference of the d/D ratio of the reference system and the applied reactor thus amounts to 0.47-0.3 = 0.17, corresponding to approx. 50% of the interval 0.2 to 0.5. The Newton number used for the following calculations was therefore reduced by 10% assuming a linear decrease of Ne in the given interval. This yielded a value of Ne=4.5.

4.3.4.2 Heigth of filling

For a ratio of height of filling to diameter of the bioreactor (H/D) $\geq$ 0.8 the Newton number can be considered constant (GVC-Fachausschuss 'Mischvorgänge', 1998). This condition was fulfilled by the given system.

4.3.4.3 Systems with multiple stirrers

If several stirrers are installed in a bioreactor, the distance between the stirrers on the stirrer axis is of central importance for the calculation of the overall power input. This distance should 1.2fold exceed the diameter of the stirrer to assume an additive behavior of the power input by each stirrer

(GVC-Fachausschuss 'Mischvorgänge', 1998).

This distance was 125 mm in the present case (see Table 4.1, p. 72), corresponding to 1.8 times the stirrer diameter (70 mm). Thus, calculation of power input by the two Rushton turbines was calculated by simple addition of the input by each stirrer.

4.3.5 Calculation of flow regime and power input

Estimations of the dynamic viscosity at the maximal biomass concentration of the cultivations by a falling ball viscometer[1] yielded values in the range of 7.3 mPa s.[2] Calculations based on the previous paragraphs brought about the theoretical values for the power input L for various configurations of the system given in Fig. 4.2. All configurations yielded Reynolds numbers larger than 100 (limit of the Reynolds number for turbulent flow in systems with turbulence promoters) as shown in Table 8.3 in the supplementary material (p. 184). Therefore, turbulent flow in the reactor can be assumed. However, in the case of the biomass suspension, Re_M was in the transition zone from partially developed to a fully turbulent flow ($Re_M > 10^3$ or 10^4, Doran, 1995). This type of flow regime may - as shown in Fig. 4.1 - result in slightly lower actual values of Ne for low rotary frequencies of the stirrer.

4.3.6 Estimation of aerated power input

Generally, power input can be assumed to be lower in aerated than in unaerated conditions. To calculate the effect of aeration on power input a correlation of Hughmark (1980) was used. The ratio of aerated L_g to unaerated power input L was estimated according to Eq. 4.3.

$$\frac{L_g}{L} = 0.1 \left(\frac{Q}{n \cdot V} \right)^{-0.25} \left(\frac{n^2 \cdot d^4}{g \cdot w \cdot V^{0.67}} \right)^{-0.2} \tag{4.3}$$

where Q is the volumetric gas flow rate, V is the volume of liquid in the bioreactor, g is the gravitational acceleration, and w is the blade width of the stirrer.

Based on the characteristic proportions of the bioreactor of Table 4.1 and the experimental volumetric flow rate of 1 vvm, the correlation yields factors for the decrease of L by aeration for different rotary frequencies of the stirrer.

[1] See section 8.1.2.1, p. 174 in the supplements for a detailed description of the method.

[2] This estimate is based on the assumption that the flow behavior of the fluid is close to Newtonian, which may be feasible considering the low dry cell weight concentrations.

4.3.7 Comparison of experimental and theoretical values

Based on these theoretical calculations, a new experimental setup was designed, which led to the values presented in the *Corrigendum* of the article (see p. 69). Fig. 4.2 shows a comparison of calculated values and experimental data acquired for the new experimental design.

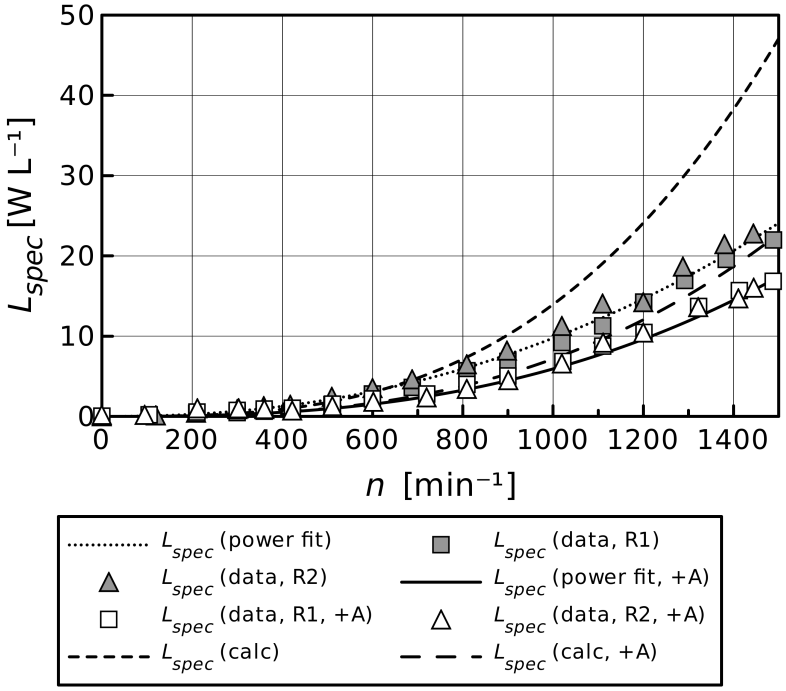

Fig. 4.2: Comparison of theoretical and experimental values of the specific power input L_{spec} for the new experimental design for the given bioreactor configuration for stirring in water. Aerated conditions are labelled "+A". The figure is an extended version of the plot used in the *Corrigendum* (Müller *et al.*, 2016b).

4.3.8 Load-dependent efficiency of electric motors - an error analysis

The motor applied in the study was a 3-phase current motor of the type DAS 80G-4 (Elektromotoren Brienz AG, Brienz, Switzerland), operating at a frequency of 50 Hz and a current of 400 V. It was characterized by a power of 1.5 kW and a rated maximal rotary frequency of 1400 min^{-1} (operation above this frequency was possible).

Electric motors are usually designed to run at 50-100 % of their rated load with a maximal efficiency at about 75 % load (McCoy *et al.*, 1993). Generally, motor efficiency for electric motors rises upon increasing load and dimension of the motor. Moreover, the relative efficiency of smaller motors shows a stronger dependency on load. Both aspects are illustrated in Fig. 4.3.

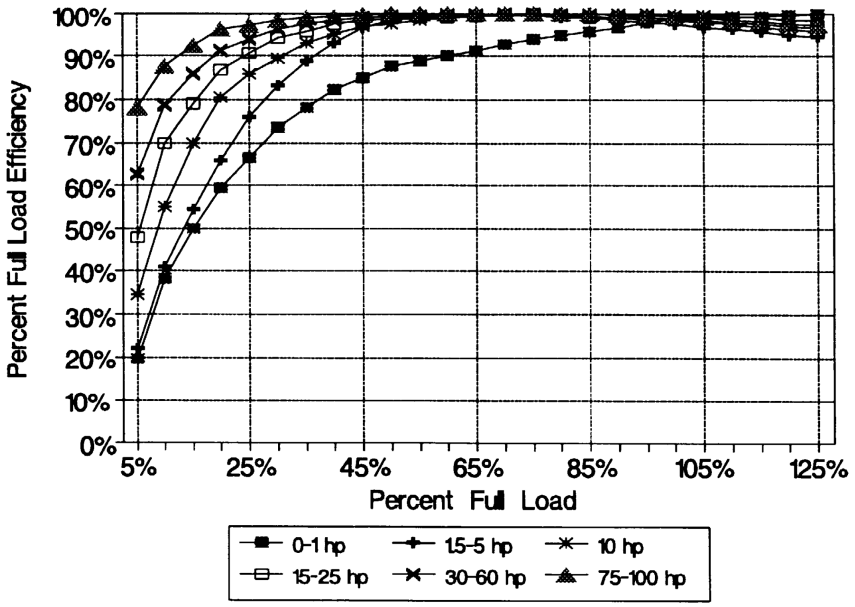

Fig. 4.3: Relative efficiency of electric motors versus load (McCoy *et al.*, 1993). Please note that the load does not only depend on the frequency of the stirrer, but also on the flow resistance arising from the stirred liquid.

The category for the motor used is 1.5-5 hp.[3] Its efficiency can thus be considered to be strongly dependent on motor load. It was operated in a frequency range of 200 to 1500 min^{-1}, leading to a maximal power consumption of the whole system in the range of 0.48 kW.[4] This corresponds to only 32 % of the maximal power of 1.5 kW.

It therefore seems reasonable to assume that the motor was operated in underloaded conditions even for intermediate rotary frequencies of the stirrer, resulting in a strong contribution of factors like friction. The proportional influence of these factors on the overall power consumption can be expected to be successively smaller for increasing frequencies of the stirrer. This leads to a non-linear deviation of experimental data and actual power input, which explains the atypical linear course of L_{spec} over n observed in the original paper. The differential method of measurement used for the *Corrigendum* should circumvent this error, as friction-related effects were analyzed and compensated by a separate measurement for a low filling volume.

[3]hp = horsepower, 1 hp $\approx$ 735.5 W.
[4]This includes power used for the console of the bioreactor and for control of the stirring frequency.

4.3.8.1 Limitations of the differential method of measurement

As discussed in the *Corrigendum*, the optimized method is not able to quantify effects of volume-dependent changes of slippage on power input despite eliminating friction-related effects from the outcome of the measurement. A comparison of the rotary frequency of the rotor and the stator of the motor may illustrate this feature.

The rated maximal rotation frequency n of the rotor according to the supplier is 1400 min^{-1}. The rotation of the stator - the so-called synchronous speed n_s - can be calculated according to equation 4.4.

$$n_s = \frac{f}{p} \tag{4.4}$$

where f is the frequency of the motor supply and p - always given in integer numbers - is the number of magnetic poles .

For the given motor, f equals 50 Hz and p equals 2. Thus, the synchronous speed is 25 s^{-1} or 1500 min^{-1}. From this information, slippage s of the motor can be calculated according to equation 4.5.

$$s = \frac{n_s - n}{n_s} \tag{4.5}$$

This leads to the maximal slippage of the motor of 6.7 % (as specified by the supplier), which corresponds to the maximal error arising from this factor. However, the actual rotary frequencies measured for both bioreactors for the working volume of 5 L at a setpoint of 1500 min^{-1} were 1445 and 1489 min^{-1}, respectively. These results suggest that the actual maximal error is lower, i.e., in the range of 0.7 to 3.7 %. Moreover, even these smaller errors would only apply assuming no slippage for the measurement at a low filling volume and maximal contribution of this factor for the working volume of 5 L, which seems unlikely.

4.3.9 Correlation of k_La and L_{spec}

Literature offers many correlations of the volumetric oxygen transfer coefficient k_La and the aerated specific power input $L_{spec,g}$, typically resembling the form of equation 4.6.

$$k_L a = k \left(\frac{L_g}{V} \right)^x {v_s}^y \tag{4.6}$$

where v_s is the superficial air velocity [m s^{-1}] and k, x, and y are the specific parameters of the equation.

In a study of van't Riet (1983) the parameters k, x, and y were estimated to be 0.026, 0.4, and 0.5, respectively. These parameters were acquired by comparing literature values from different publications for water-based measurements. The parameters were found to be within a range of $\pm$40 % of these values.

In addition to this absolute description of $k_L a$ and $L_{spec,g}$, van't Riet (1983) also proposed a relative correlation of the two parameters, as shown in equation 4.7.

$$k_L a \propto \left(\frac{L_g}{V} \right)^z \tag{4.7}$$

where L_g is the aerated power input and the model parameter z is 0.5 for coalescing, aqueous systems.

The experimental values of aerated specific power input $L_{spec,g}$ and $k_L a$ were compared to theoretical courses acquired from these equations as shown in Fig. 4.4. The superficial air velocity v_s was calculated according to equation 4.8.

$$v_s = \frac{Q}{A} \tag{4.8}$$

where Q is the gas flow rate [m^3 s^{-1}] and A is the cross-sectional area of the fermenter (0.018 m^2).

Fig. 4.4a shows that the data set of Müller *et al.* (2013) and the corrected values of $L_{spec,g}$ published in the *Corrigendum* lie within a range of $\pm$40 % of the model curve based on the parameters of van't Riet (1983). Generally, a comparison to the study of van't Riet (1983) suggests that the $k_L a$ values achieved for the given bioreactor are relatively low. Parameter estimation of the parameters of equation 4.6 led to the parameter set depicted in the caption of Fig. 4.4a, yielding a more accurate fit. The fitted curve suggests a limited effect of an increase of $L_{spec,g}$ beyond 5 W L^{-1}, corresponding to a stirring frequency of about 900 min^{-1}. Fig. 4.4b indicates similar effects: the increase of $k_L a$ over L_{spec} can more accurately be described by applying an exponent in the range of 0.3 (parameter estimation) for equation 4.7 rather than 0.5 as suggested by van't Riet (1983).

The $k_L a$ can be taken as a measure for different aspects of mass and heat transfer in the vessel. This leads to the conclusion that increased values of L_{spec} are not only detrimental for cultivations of *S. avidinii* from a biological perspective due to the fragmentation of mycelia (Müller *et al.*, 2013).

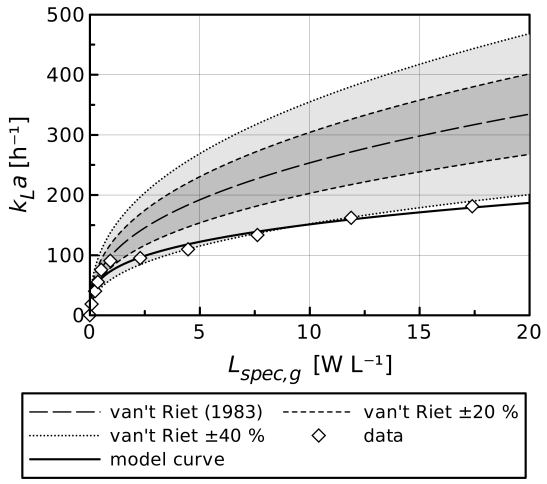

(a) Quantitative evaluation based on equation 4.6. Modelling according to van't Riet (1983) with confidence intervals of ±20 and ±40 % . Parameter fitting yielded the parameters k=0.046, x=0.306, y=0.418 for the experimental data.

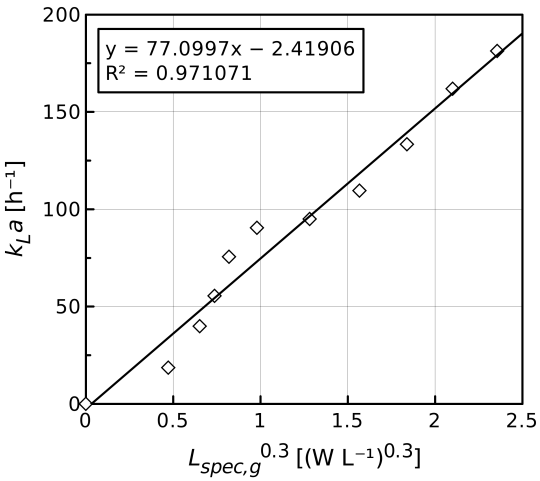

(b) Relative correlation of aerated specific power input and k_La based on equation 4.7. Parameter estimation yielded a value of 0.296≈0.3 for z.

Fig. 4.4: Comparison of experimental and theoretical values of $L_{spec,g}$ and k_La based on van't Riet (1983).

They also drastically increase power consumption with only slight benefits for homogenization of the broth and improved oxygen supply. This decreased efficiency, visualized in Fig. 4.4a, has already been described, e.g., by Winkler (1990).

4.3.10 Power input and streptomycetes in literature

Since the publication of the paper, the impact of power input on the morphology of streptomycetes has been studied by Gamboa-Suasnavart *et al.* (2013). The authors analyzed the production of a protein from *Mycobacterium tuberculosis* by *S. lividans*. They investigated the correlation of pellet diameter and theoretical power input and found a decreasing pellet diameter d_p from approx. 0.35 to 0.1 mm for increasing stirring frequencies of up to 400 min^{-1}, followed by only minor changes of d_p for higher frequencies. The specific power input of the study was in the range of 0.15-9.4 W L^{-1} for frequencies of the stirrer between 250 and 999 min^{-1} in a 1.5 L bioreactors with two turbulence promoters and a volumetric air flow rate of 0.5 L min^{-1} (0.33 vvm). The authors successfully used this data for purposes of up-scaling to achieve a comparable morphology in shake flasks and bioreactors.

In the study by Müller *et al.* (2013) applying *S. avidinii*, macroscopic pellets were only observed in the initial growth phase, whereas the culture shifted to filamentous growth later in the process.

However, microscopic analysis may contribute to improved scalability of the results for this organism, too.

4.4 Summary of additional experiments applying *S. avidinii*

Supplementing experiments focused on the impact of additional factors on the production of SAV. These experiments included the evaluation of strategies for the control of morphology, a design of experiments (DoE)-approach for the optimization of the growth medium, and studies of continuous cultivation. Furthermore, genetic engineering of *S. avidinii* was analyzed. Results are briefly summed up in the following sections.

4.4.1 Control of the morphology of *S. avidinii*

Pellet formation posed problems to the reproducibility of shake flask cultivations of *S. avidinii* especially for a low inoculum size and the application of highly concentrated media, as exemplified in Fig. 4.5. Hence, strategies for the control of morphology of *S. avidinii* were evaluated to minimize corresponding complications.

Fig. 4.5: Formation of small pellets in a shake flask culture of *S. avidinii*. The pellets shown here are relatively small compared to further experiments.

4.4.1.1 Control of morphology by the addition of microparticles

Kaup *et al.* (2008) analyzed the impact of the supplementation of microparticles to cultivation media on a variety of filamentous organisms, revealing positive effects on their morphology by a reduction of the pellet diameter and an improved metabolite production. The method was called 'microparticle-enhanced cultivation' (MPEC). As morphological problems remained an issue in shake flask cultivations throughout this thesis, this method was tested in several experiments.

Generally, particles and the remaining media compounds were always prepared and sterilized separately. The experiments indicated that the addition of talc powder (hydrous magnesium silicate) and aluminum oxide to the cultivation medium contributes to a more homogeneous culture broth when highly concentrated media are applied. These media typically led to a strong pellet formation in the absence of particles. The impact of talc particles on the morphology in the bioreactor seemed to be smaller, which is most likely due to strong shearing by the blades of the stirrer in this system. However, the production of SAV was increased by a factor of 1.6 in this cultivation system towards a reference culture, as illustrated in Fig. 4.6.

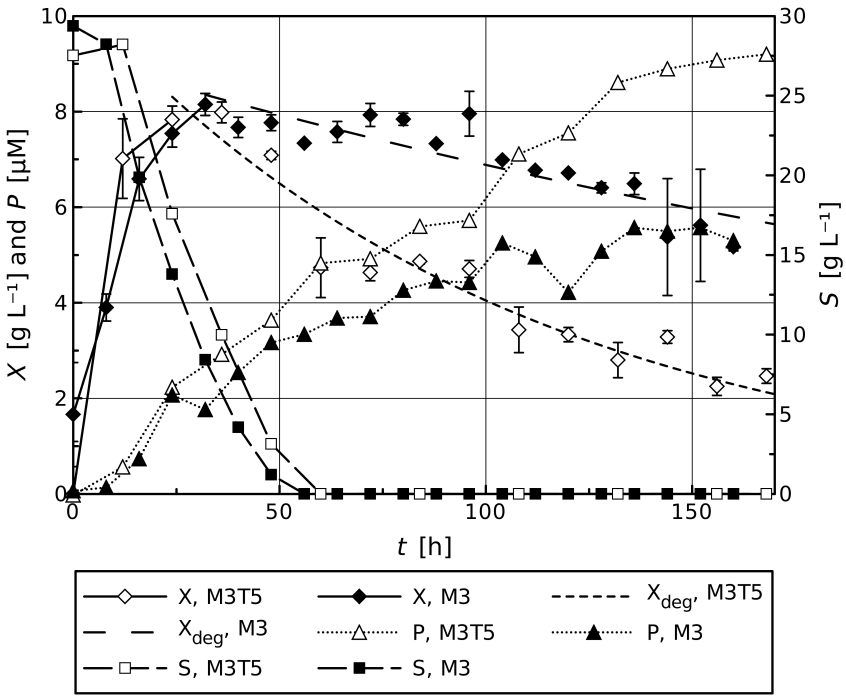

Fig. 4.6: Microparticle-enhanced cultivation of *S. avidinii* in the presence of talc particles in the bioreactor. Fermentation courses for cultivation at 30 °C at a stirring frequency of 350 min^{-1} in talc-supplemented (M3T5) and talc-free (M3) M3 medium are shown. Abbreviations: X = conc. of dry cell weight, P = conc. of SAV, S = conc. of glucose. The 'deg'-labels refer to regression curves acquired by a fit of X to equation 4.9.

The courses of the dry cell weight (DCW) concentration X shown in Fig. 4.6 were evaluated based on the first order degradation model of equation 4.9

$$-\frac{\mathrm{d}X}{\mathrm{d}t} = k_{deg} \cdot X \tag{4.9}$$

where k_{deg} is the characteristic constant of degradation.

Parameter estimation yielded degradation constants of 0.00284 h^{-1} for the talc-free and 0.00946 h^{-1} (factor 3.3) for the talc-supplemented culture, indicating less stable filaments for the microparticle-supplemented system. This may be due to the collision of particles and mycelia, as discussed by Kaup *et al.* (2008). Interestingly, like observed for the un-supplemented cultures analyzed in Müller *et al.* (2013), the feeding of glucose prevented the degradation of biomass for a talc-based fed-batch process and seemed to stabilize the mycelia (data not shown). This could be the result of morphological changes upon substrate depletion of the culture, as suggested by the growth-dependent viscosity of the culture broth (see Fig. 8.5, p. 183).

Hence, advantageous properties regarding the production of SAV were achieved by the addition of talc particles. However, additional studies in shake flasks suggested that particle supplementation may also improve the tolerance of *S. avidinii* towards fluctuations of the cultivation temperature. Cultivation at 25 instead of 30 °C brought about problems of reproducibility for talc-free cultures, whereas supplementation of talc speeded up the initial growth phase and resulted in a more homogeneous growth among different replicates (data not shown).

Additional MPEC-based experiments were performed in cooperation with the DECHEMA Research Institute (Research Group 'Biochemical Engineering', Dr. Dirk Holtmann, Felicitas Vernen) to study the impact of talc particles on the pellet size in unbaffled shake flasks. The morphology of the pellets was evaluated via a USB microscope and the image analysis software ImageJ (see Table 2.4, p. 24) as described in the supplements (section 8.1.2.2, p. 175). This analysis yielded a lower median of the pellet diameter for talc-supplemented cultures especially in the early stage of cultivation, as shown in Fig. 4.7.

Overall, a step-wise reduction of the pellet area was observed throughout the cultivation for both the talc-supplemented and the reference culture. However, the course of the median of the pellet area of *S. avidinii* indicates that talc has a major impact on the morphology of *S. avidinii* in the first days of cultivation. This impact is becoming successively smaller throughout the cultivation.

Reduction of the pellet diameter in the early stage of cultivation was also possible by the addition of small glass beads (0.25 to 0.5 mm) to the shake flasks. However, unlike for the supplementation of talc, this did not improve the final concentration of product (results in publication).

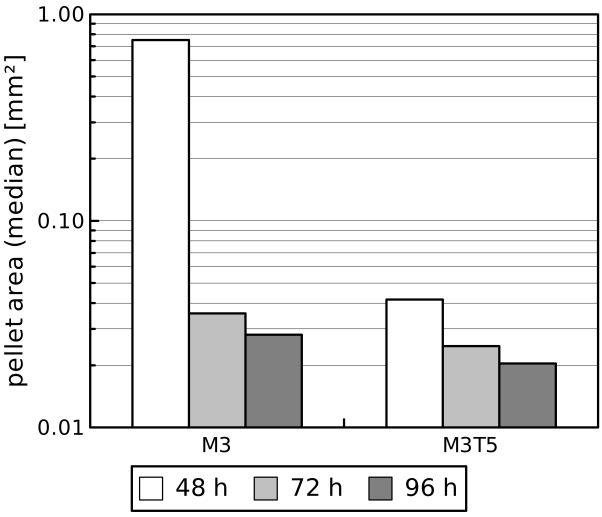

Fig. 4.7: Median value of the pellet area of *S. avidinii* over time for the cultivation in unbaffled shake flasks (y-axis scaled logarithmically). M3 = reference culture, M3T5 = talc-supplemented culture. Please refer to Fig. 4.8 for the impact of talc on the production of SAV. Number of analyzed pellets after 48, 72, and 96 h, respectively: M3: 211, 1096, 1282; M3T5: 608, 2236, 1599.

4.4.1.2 Control of morphology by further methods

Further strategies were evaluated for the control of the morphology of *S. avidinii* in shake flasks and microplates. Fig. 4.8 shows a brief summary of results from various shake flask studies. Cultivation conditions were chosen to provoke pellet formation by the application of shake flasks without baffles, a low shaking frequency of 120 min^{-1}, and a low inoculum size.

The effects of oxygen limitation on the morphology of filamentous fungi was studied by Hockenhull (1980). This study indicated that upon ageing of the culture - and accompanying lower concentrations of dissolved oxygen due to increased oxygen consumption of in the culture broth - a switch from pellets to filamentous growth can be observed. Therefore, one of the configurations shown in Fig. 4.8 was based on an artificial limitation of oxygen early in the culture based on sealing of shake flasks via a sterile sealing film. This led to increased product concentrations for media typically resulting in strong pellet formation, but was detrimental to media which are optimized for *S. avidinii*. The latter may partially be due to the limitation of the DCW concentration to $2.78 \pm 0.04\,g\,L^{-1}$ by the enclosed air volume. This could be avoided by removing the film after the initial growth phase in future experiments.

Co-sterilization of glucose and other compounds of M3 led to an increase of productivity. This may be due to potentially beneficial effects of Maillard products on the morphology of *S. avidinii*. These arise from the reaction of glucose and peptides in the complex compounds of M3 medium. The

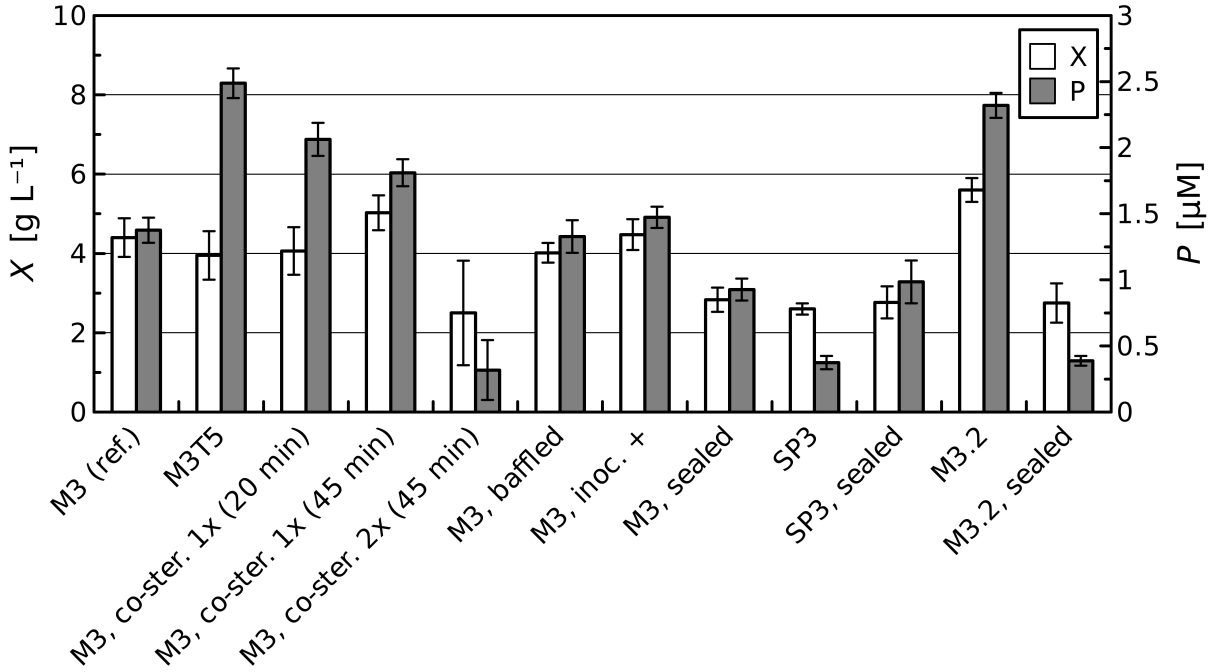

Fig. 4.8: Summary of shake flask studies on control of the morphology of *S. avidinii* ($n \geq 3$). The plot shows concentrations of DCW X and SAV P after 6 days of cultivation at 28 °C. If not indicated otherwise, experiments were performed in unbaffled 300 mL shake flasks with a filling volume of 30 mL using an inoculum of 60 μL per flask (inoc. + = 300 μL per flask). Designations refer to the medium used (M3, SP3, M3.2), the addition of talc powder (M3T5), cycles and time of co-sterilization of glucose and other compounds of M3 (coster.), and sealing of the flasks by an oxygen-impermeable sealing film. M3 and SP3 medium were composed as described in Müller *et al.* (2013), whereas the optimized M3.2 medium resulted from the optimization procedure discussed in section 4.4.2.

hypothesis is supported by the results from continuous cultivation of *S. avidinii* (see section 4.4.3). Surprisingly, an increased inoculum size and the application of baffled shake flasks did not improve the production of SAV. However, the volume percentage of 1 % (v/v) used for high inoculation was still rather low, meaning that a further increase may actually improve growth and production. Moreover, inoculation was always performed by a mycelial glycerol stock instead of a spore suspension.

In summary, the results emphasize the impact of morphology on the formation of SAV in shake flasks, since strongly differing concentrations of the protein were achieved for identical concentrations of DCW in several cases. Generally, filamentous growth was essential for high product concentrations.

The adequacy of the method of morphological control depends on the cultivation system used. This was, e.g., the case for the improved performance upon talc-supplementation of media in shake flasks,

whereas this strategy did not yield improvements for its application in squared v-bottom microplates due to sedimentation. Opposed to this result, supplementation of shake flask cultures of *S. avidinii* by 3 mm-glass beads showed no effect, whereas it reduced pellet formation in microplates as discussed in the next section.

4.4.2 Medium optimization

The experiments performed up to this point led to remarkable concentrations of SAV in several cases, but yielded rather limited concentrations of biomass. Thus, the major compounds of the M3 growth medium, namely yeast extract, soy peptone, casein hydrolysate, and glucose, were varied in a DoE-approach designed in the software MODDE (Umetrics) to optimize the process outcome.

Cultivations were performed in MOPS[5]-buffered media in 24-well deepwell microplates in the presence of 6 glass beads ($\varnothing$ 3 mm) per well to minimize pellet formation based on a method for *S. coelicolor* published by Sohoni *et al.* (2012). A detailed description of the method is given in the supplements (section 8.1.2.3, p. 175).

The results indicate that the concentration of soy peptone in the standard medium may inhibit a rapid formation of biomass and product. Optimized production media therefore contained elevated concentrations of yeast extract and lower proportions of soy peptone.

Subsequent experiments in shake flasks based on pulse-wise feeding of additional substrates (glucose, yeast extract, meat extract) resulted in 7.3$\pm$0.1 μM of SAV and a concentration of DCW of 15.5$\pm$0.6 g L^{-1} in 144 h, strongly surpassing the results for 2N medium described in Müller *et al.* (2013) (3.37$\pm$0.78 μM of SAV, 4.9$\pm$0.3 g L^{-1} of DCW). Among other suitable compositions, the optimization resulted in the medium shown to the right in Fig. 4.8 (M3.2), consisting of (per L) 5 g of NaCl, 2 g of soy peptone, 3.75 g of yeast extract, 2 g of casein hydrolysate, and 15 g of glucose.

These results now have to be transferred to the bioreactor scale in order to analyze, whether the improved performance also applies for this system.

Additional fed-batch fermentations in the bioreactor based on glycerol brought about lower concentrations of SAV than the glucose-based processes. These results were contrary to previous shake flask cultivations, in which glycerol yielded comparable or slightly advantageous results. Thus, glucose seems to be a more suitable carbon source for the production of SAV by *S. avidinii* in the bioreactor.

[5] 3-(N-morpholino)propanesulfonic acid

4.4.3 Continuous cultivation

Since detailed knowledge on the properties of *S. avidinii* regarding biochemical engineering is sparse, the organism was cultivated in chemostat operation using M3 medium to characterize the growth rate-dependent production of SAV by the organism. Please refer to section 8.1.2.4 (p. 176) in the supplementary material for a detailed description of the experimental setup.

Briefly, experiments were performed in the same bioreactor as the fed-batch studies of Müller *et al.* (2013) in M3 medium. All ingredients of this complex medium were sterilized simultaneously for 45 min (see Fig. 4.8 for results of this variation in shake flasks), and two peristaltic pumps were used to adjust the dilution rate of the culture. The fermenter was operated for 5-10 residence times τ [6] at each dilution rate D to achieve steady state conditions ($\mu = D$). The results are shown in Fig. 4.9.

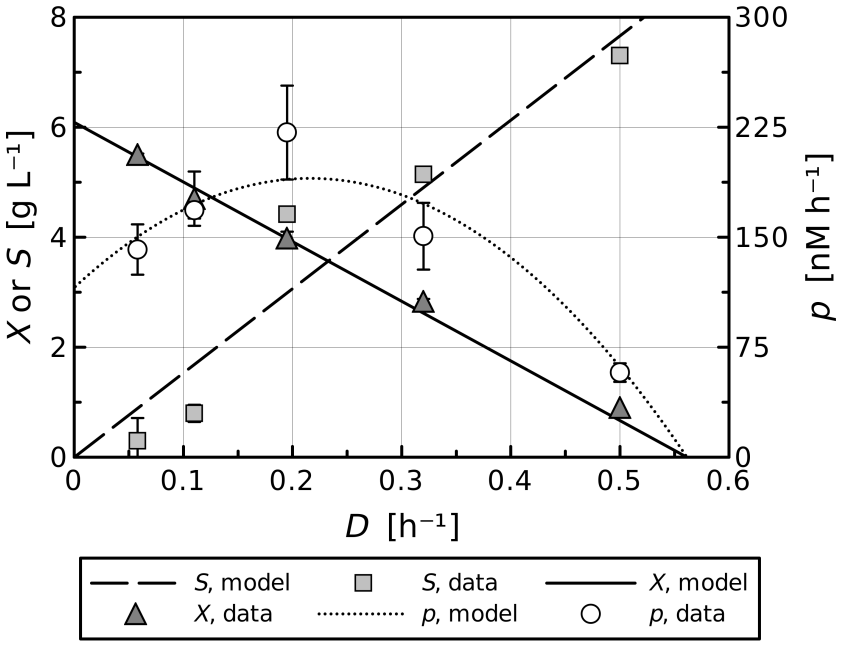

Fig. 4.9: Continuous cultivation of *S. avidinii* in the bioreactor at 30 °C, pH 7.0, and a stirring frequency of 500 min^{-1} at different dilution rates D. The plot shows the residual substrate concentration S, the volumetric productivity p, and the DCW concentration X. Model curves were derived by a fit to a Monod-like growth model and the three-term, biomass-based model of productivity used in Müller *et al.* (2016c) based on a modified Luedeking-Piret equation (Luedeking & Piret, 1959).

For the model-based evaluation of the data, the Monod constant K_S was set to a constant value of approximately 8.6 g L^{-1} (equal to the inflow concentration of substrate) based on an estimated

[6] Times, in which the working volume is replaced once. Residence time $\tau = 1/D$.

saturation parameter s_{0S}[7] of 1.0 for the parameter fit. This adjustment was performed to account for the linear decrease of X over D, indicating a low affinity of *S. avidinii* for the substrate glucose. The course is therefore only a rough estimate. Detailed batch studies would be more suitable for a more precise determination of K_S due to a larger number of data points.

Parameter estimation brought about a yield coefficient $Y_{X/S}$ of biomass per substrate in the range of 0.71 and a maximal specific growth rate μ_{max} of 0.53 h^{-1}, matching the data of several neutrophile streptomycetes analyzed by Flowers & Williams (1977) (μ_{max} between 0.56 and 0.64 h^{-1}).

These results indicate that *S. avidinii* is capable of growing much faster than suggested by all previous experiments. Cells were not washed out until the setpoint for the flow rate was adjusted to 0.6 h^{-1}.

Surprisingly, the culture formed small pellets at very high dilution rates, whereas for low rates filamentous growth was observed. This is seemingly contradictory to the lower surface to volume-ratio of pellets towards filaments, as nutrient limitation may occur for the former (see Fig. 2.5 p. 12) with a corresponding impact on the growth rate.

Very high volumetric productivities were achieved at intermediate dilution rates of 0.2 to 0.3 $^{-1}$, reaching an experimental maximum of 221±32 nM h^{-1} at a DCW concentration of only 4.0±0.5 g L^{-1} for D = 0.195 h^{-1} and a maximum of the model-based regression curve of 190 nM h^{-1} for D = 0.22 h^{-1} (see Fig. 4.9).

Due to the mode of operation, even low dilution rates resulted in low concentrations of SAV (2.4±0.3 µM of SAV for D = 0.058 h^{-1}). Chemostat operation for the production of SAV would therefore require the processing of very large volumes. Exponential feeding using a setpoint for μ (μ_{set}) in the range of these growth rates could thus be a more suitable alternative to further improve SAV production by *S. avidinii*. Slightly lower growth rates (e.g., μ_{set} = 0.1 h^{-1}) may allow prolonged processes at a constant μ_{set}, while reducing the volumetric productivity to an only small extent. The specific (biomass-related) productivity was even higher for very high dilution rates in the range of μ_{max}, but corresponding values of μ_{set} will be difficult to implement due to constraints imposed by factors like oxygen input.

Alternatively, further optimization may focus on cell retention or the cultivation of immobilized biomass of *S. avidinii* in continuous cultivation to achieve higher cell densities at high flow rates.

4.4.4 Analysis of the effect of oxygen supply

As the results of Müller *et al.* (2013) suggested a positive impact of high concentrations of oxygen on the formation of SAV, additional fermentations focused on aeration by concentrated oxygen. These

[7] $s_{0S} = S_0/K_S$, where S_0 is the inflow concentration of substrate.

studies indicate, however, that aeration by pure oxygen is as harmful as oxygen depletion (data not shown), which may be due to oxidative damage to the cells. Another potential explanation of this phenomenon is described by Wongwicharn *et al.* (1999), who observed that a lower concentration of oxygen in the culture resulted in prolonged filaments, whereas more aggregates occurred for an increased oxygen saturation for the cultivation of *Aspergillus niger*. Thus, the detrimental effects of high concentrations of oxygen observed here may be also be the result of undesired morphological changes, negatively effecting the formation of SAV. This hypothesis is supported by the improvements of product formation for the cultivation in sealed shake flasks (Fig. 4.8, p. 84). Therefore, control of the oxygen saturation at intermediate setpoints - as performed for the studies of continuous cultivation - is a more suitable method than supplying pure oxygen at high volumetric flow rates not only from the economical, but also from the biological perspective.

4.4.5 Determination of mycelial growth by viscosity measurements

The analytical methods for several bioreactor studies included measurements of the dynamic viscosity η according to section 8.1.2.1 (p. 174*ff.* in the supplementary material). The viscosity usually increased for growing mycelia and dropped to a biomass-dependent base value for a stationary culture. This behavior is common for filamentous organisms, since the viscosity of corresponding fermentation broths is typically correlated to the growth rate and concentration of biomass of the culture (Olsvik & Kristiansen, 1994). An example for corresponding measurements is shown in the supplementary material, Fig. 8.5 (p. 183). The overall course roughly resembled the concentration of carbon dioxide in the exhaust air, but was more sensitive towards small changes of the DCW concentration. It may therefore be a useful parameter for a sensitive determination of the decelerated and stationary growth phase of a cultivation or an at-line analysis of the effect of different feeding strategies on growth.

4.4.6 Genetic engineering of *S. avidinii*

A final set of experiments targeted the genetic modification of *S. avidinii* to determine if genetic optimization of the host may serve as a tool for further optimization of SAV production. For this purpose, a collaboration with the research group 'Microbial Genomics and Biotechnology' at the CeBiTec at Bielefeld University (Prof. Dr. Jörn Kalinowski, Tetiana Gren) was established.

Sporulation of *S. avidinii* was successfully induced on oatmeal agar (40 g L^{-1} of oatmeal, 20 g L^{-1} of agar, pH 8.0). An analysis of the antibiotic (AB) resistances of the organism on oatmeal agar plates revealed that the strain is sensitive to apramycin and resistant to nalidixic acid. This would allow the killing of vector transferring strains of *E. coli* by the latter and selection of transformants of *S. avidinii* by the former antibiotic. A summary of the AB resistance tests is shown in Table 4.2.

Transformation by the standard broad host range vector pSET152 (NCBI ID 173260) conferring resistance to apramycin applying an *E. coli* helper strain yielded colonies after selection by the antibiotic. In conclusion, *S. avidinii* seems to fulfill the basic requirements for genetic engineering. However, due to time restrictions no subsequent experiments were performed.

These preliminary results may be useful for future attempts to integrate additional copies of the SAV expression cassette into the genome of *S. avidinii*.

Tab. 4.2: Analysis of antibiotic resistances of *S. avidinii* by Oxoid™ Antimicrobial Susceptibility Discs (Thermo Scientific).

antibiotic	mass [μg] [a]	AB resistance
ampicillin	25	+
bacitracin	10 units	- [b]
ceftazidime	30	+
chloramphenicol	10	-
colistin sulfate	10	+
cycloserine	200 mg L^{-1} [c]	+
gentamicin	10	-
kanamycin	30	-
lincomycin	15	-
nalidixic acid [d]	30	+
norfloxacin	5	+
phosphomycin [d]	50 μg mL^{-1} [e]	+
polymyxin B	300 units	+
rifampicin	30	-
spectinomycin	10	-
streptomycin	10	-
sulphonamide	300	+
tetracyclin	30	-
trimethoprim	5	+
vancomycin	5	-

[a] mass of AB per disc
[b] weak inhibition zone, partially overgrown
[c] analyzed in liquid culture
[d] suitable for the killing of *E. coli* helper strains
[e] supplied in liquid form (100 μL)

5 Heterologous expression of the SAV gene

5.1 Motivation

Heterologous production of proteins offers a large variety of advantages over conventional expression systems. Only 0.1-10 % of all microorganisms are estimated to be cultivable in laboratory conditions (Zeyaullah *et al.*, 2009). However, many of the strains not belonging to this minority host a diverse range of metabolic properties which are of interest, e.g., for medical or biotechnological purposes. Heterologous expression based on metagenomics offers a way of making some of the corresponding pathways or gene products available for corresponding purposes (Zeyaullah *et al.*, 2009). Moreover, heterologous studies may maximize product concentration and minimize process time based on established process strategies (Lee, 1996) and a large number of host/vector-combinations suited for the production of a highly diverse range of proteins (Abelson *et al.*, 1990). Exploiting these properties, product concentrations ranging from hundreds of milligrams to several grams per liter can be obtained (Cos *et al.*, 2006; Georgiou & Segatori, 2005), often surpassing the concentrations achieved by cultivation of the native host. However, in the case of SAV, product toxicity complicates common strategies of gene expression (see section 2.4.3, p. 15*ff.*). As these aspects are often host-specific, several hosts were optimized for the production of this protein throughout this thesis.

5.1.1 Strategies of heterologous expression used for this project

Three promising hosts were selected for heterologous expression of the SAV gene. The enterobacterium *E. coli* was chosen representing GRAM-negative hosts as it is the most frequently used prokaryotic expression system (Chen, 2012; Hannig & Makrides, 1998; Hockney, 1994) and has already been used for expression of the SAV gene in multiple studies (Sano & Cantor, 1990b; Gallizia *et al.*, 1998; Miksch *et al.*, 2008).

As discussed in section 2.4.3.3 (p. 20*ff.*), yeasts generally offer a more elaborate compartmentalization and a highly efficient secretory pathway. Moreover, these eukaryotes are typically capable of rapidly growing to high cell densities in simple, defined media. Advantageous properties for post-translational processing are not relevant for SAV, but may prove beneficial for other target proteins (Abelson *et al.*, 1990). Due to these attributes, two yeast-based expression systems were applied.

Firstly, experiments focused on the methylotrophic yeast *P. pastoris* (Macauley-Patrick *et al.*, 2005; Cregg *et al.*, 2000), which is becoming increasingly popular in the last decade and has already been identified as a suitable host for the production of SAV (Casteluber *et al.*, 2012; Nogueira *et al.*, 2014). However, for *P. pastoris* only methanol-based processes have been applied, which - among other downsides - increases process cost due to safety regulations for the flammable and toxic organic solvent. This will be discussed in detail in section 5.3 (p. 116).

Secondly, a novel expression system was constructed applying the yeast *Hansenula polymorpha*, which in many aspects of growth, metabolism, and production of heterologous proteins resembles *P. pastoris* (Gellissen, 2000).

5.1.2 Experimental remarks

During the final stages of evaluation of the cultivations performed for this thesis theoretical considerations and measurements of the k_La for different experimental setups indicated that the choice of the gas flow rate for the cultivations of *H. polymorpha* and *E. coli* in the Sixfors bioreactor system (Infors HT, Bottmingen, Switzerland) was not always optimal. For a fraction of experiments, very high volumetric flow rates of 5 or 3 vvm, respectively, were applied. Effects of evaporation were avoided by pre-saturation of the inflowing air by water vapor. However, dynamic measurements of the volumetric oxygen transfer coefficient k_La according to Bandyopadhyay *et al.* (1967) resulted in no improvements for this parameter for these flow rates towards lower setpoints. The results are consistent with literature, as can be seen in Fig. 5.1.

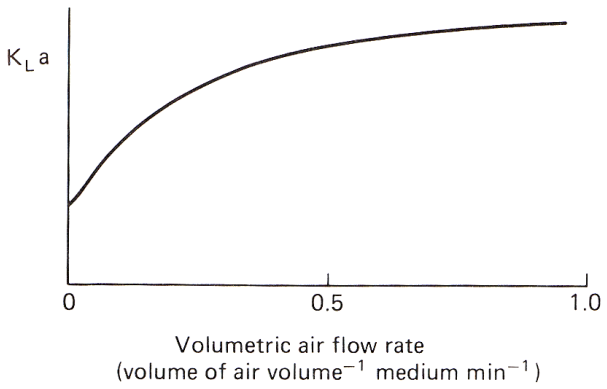

Fig. 5.1: Qualitative dependency of volumetric oxygen transfer coefficient k_La and volumetric air flow rate according to Stanbury *et al.* (1995) (Fig. 9.12).

According to Stanbury *et al.* (1995), air flow rates larger than 1.5 vvm typically don't improve the k_La. Additionally, power input may decrease in these conditions (see equation 4.3 in section 4.3.6,

p. 74), which may in turn negatively contribute to the overall process, e.g., by decreasing heat transfer. Thus, lower volumetric flow rates should be applied especially for further experiments in larger scales.

5.2 Production of SAV by *Escherichia coli*

E. coli is a GRAM-negative model bacterium and a biotechnological workhorse. Due to relatively simple and well-established procedures of genetic and biochemical engineering, the organism is employed for a large variety of biotechnological production processes (Sørensen & Mortensen, 2005). It has particularly been shown to be highly suited for the production of short proteins in the range of 100-200 AA, which applies to SAV monomers. Corresponding proteins typically simplify recombinant production as direct expression often leads to a soluble product without the necessity of fusion partners (Abelson *et al.*, 1990). In addition to these protein-specific properties, progress has been made for the secretion of heterologous proteins by *E. coli* despite an unfavorable structure of the cell wall (see Fig. 2.8a, p. 19) (Mergulhao *et al.*, 2005; Ni & Chen, 2009). Secretion has been - and to some degree still is - a major bottleneck, especially when the target protein produced is not secreted by its native host (Abelson *et al.*, 1990).

Heterologous production of SAV has been tested in many studies applying *E. coli*. Due to the natural properties of the host, overexpression of the SAV gene often led to intracellular, inactive inclusion bodies (Sano & Cantor, 1990b; Thompson & Weber, 1993; Chen *et al.*, 2014), partially overcoming its toxicity. Only Miksch *et al.* (2008) achieved soluble extracellular accumulation of the protein by the use of the general secretory pathway (Sec) and a bacteriocin release protein.

5.2.1 Goals of this study

The goal of this study was to get a more holistic view of the productive properties of *E. coli* regarding the soluble and secretory production of SAV. For this purpose, a novel expression system was established based on the periplasmic 'leaky mutant' JW1667-5 (Δ*lpp::kan*). This mutant is commercially available from the Coli Genetic Stock Center (Keio Knockout Collection, Yale University, USA). A combined analysis of various genetic, biochemical, and technical factors was performed.

5.2.2 Manuscript

The results were published in the Journal of Biotechnology (Müller *et al.*, 2016c) (with permission from Elsevier, Copyright 2016). Paper and accompanying supplementary material are shown below.

Journal of Biotechnology 221 (2016) 91–100

Contents lists available at ScienceDirect

Journal of Biotechnology

journal homepage: www.elsevier.com/locate/jbiotec

Constitutive production and efficient secretion of soluble full-length streptavidin by an *Escherichia coli* 'leaky mutant'

Jakob Michael Müller*,[1], David Wetzel[1], Erwin Flaschel, Karl Friehs, Joe Max Risse

Lehrstuhl für Fermentationstechnik, Technische Fakultät, Universität Bielefeld, PF 10 01 31, D-33501 Bielefeld, Germany

ARTICLE INFO

Article history:
Received 24 October 2015
Received in revised form 18 January 2016
Accepted 22 January 2016
Available online 25 January 2016

Keywords:
Escherichia coli
Periplasmic leaky mutant
Chain length of streptavidin
Temperature
Secretion
Fed-batch cultivation

ABSTRACT

Due to its various applications the protein streptavidin is a highly interesting target for heterologous production. This study focuses on different *Escherichia coli*-based constructs targeting a high-level expression and secretion of streptavidin to the medium. The effect of various promoters, variants of the target gene, leader sequences and host strains on expression and secretion into the culture broth was analyzed. Constitutive production of full-length streptavidin fused with the leader sequence of the *bglA* gene from *Bacillus amyloliquefaciens* by the periplasmic 'leaky mutant' *E. coli* JW1667-5 (*Δlpp-752:kan*) at 30 °C generated the highest yield of the conditions tested, surpassing the extracellular concentration of a conventional T7-based expression system. Supplementation of the medium by the non-ionic surfactants Triton® X-100 and X-45 led to an improved secretion of the protein to the culture supernatant. Tetrameric concentrations of streptavidin of 2790 ± 166 nM were reached in shake flasks at a productivity of 49.6 nM h^{-1}. Optimization of conditions led to a successful transfer to the bioreactor, yielding a maximal concentration of 2608 ± 169 nM and a productivity of 65.2 nM h^{-1} in fed-batch operation. The proportion of biotin-blocked binding sites of 8.3 ± 4.3% indicated a highly bioactive product.

1. Introduction

The homotetrameric protein streptavidin (SAV) binds one molecule of the vitamin biotin per monomer characterized by a dissociation constant K_d of 4×10^{-14} M (Green, 1990) to 10^{-15} M (Bayer and Wilchek, 1990). Being one of the strongest noncovalent biological interactions the biotin-binding ability of SAV can be used in a large variety of applications. Among them are the recovery of biotinylated (Rösli et al., 2008) or peptide-tagged (Skerra and Schmidt, 1999) proteins, the localization and detection of various proteins (Zwart and Lewis, 2008), and strategies for drug targeting (Muzykantov et al., 1999). Due to its biotin-binding properties SAV is known to be toxic to bacteria (Chaiet and Wolf, 1964). This antibiotic effect probably is the reason for its natural occurrence but complicates its heterologous production using *Escherichia coli*, especially for strategies based on intracellular expression.

In contrast to avidin from chicken egg white SAV has no sulfur-containing amino acids (Argaraña et al., 1986), a lower isoelectric point (Chaiet and Wolf, 1964), and is not glycosylated which offers advantages concerning applications of SAV due to less nonspecific interactions with substances other than biotin (Bayer and Wilchek, 1990).

The native SAV gene codes for 159 amino acids (16.5 kDa per monomer). However, various N- and C-terminally shortened species naturally occur due to limited proteolysis (Bayer et al., 1989; Sano et al., 1995). The so-called 'core streptavidins', smallest forms of SAV still maintaining the biotin-binding properties of full-length SAV, consist of 118-127 amino acids and show increased solubility (Pähler et al., 1987; Sano et al., 1995). Lacking the nonfunctional termini, core SAV may exhibit advantageous properties in production by reducing the metabolic burden for the host as well as for applications due to an improved accessibility of the binding site for biotinylated macromolecules.

Various expression systems for the heterologous production of SAV are described in literature. Most of them are based on the biotechnological model bacterium *E. coli* (Sano and Cantor, 1990; Miksch et al., 2008; Gallizia et al., 1998; Wu and Wong, 2006; Chen et al., 2014). These systems usually lead to the intracellular accumulation of the protein and inclusion body formation. Others report soluble intracellular SAV partly overcoming its toxicity. Only Miksch et al. (2008) achieved extracellular accumulation of the protein in its active form. In regard to the necessity of cell disruption, additional purification steps and possibly renaturation for

Abbreviations: SAV, streptavidin; vvm, volume per volume and minute.

* Corresponding author.
E-mail address: jmu@fermtech.techfak.uni-bielefeld.de (J.M. Müller).

[1] Both authors contributed equally.

http://dx.doi.org/10.1016/j.jbiotec.2016.01.032
0168-1656/

intracellular products the secretion of bioactive SAV to the medium is desirable. Other studies focus on production of SAV by *Pichia pastoris* (Casteluber et al., 2012; Nogueira et al., 2014) and *Bacillus subtilis* (Wu et al., 2002; Wu and Wong, 2002). Homologous production has been reported using the natural producers *Streptomyces avidinii* (Kolomiets and Zdor, 1998; Müller et al., 2013) and *Streptomyces lavendulae*.

Using inducible expression systems the metabolic burden is reduced during bacterial growth, which commonly leads to higher growth rates compared to constitutive systems. This difference is even more pronounced if the target protein is toxic (Baneyx, 1999). Approaches based on the inducible T7 expression system are well-established and frequently used for heterologous protein production by *E. coli*. A typical, commercial system consists of *E. coli* KRX, a strain characterized by low basal expression (Hartnett et al., 2006), and plasmids from the pET-series (Novagen, Madison, Wisconsin, USA). Uncoupling of growth and production can also be achieved by the use of stationary phase promoters.

However, for the production of SAV Miksch et al. (2008) obtained best results using a constitutive promoter (P_{bglA}). Secretion to the culture broth was achieved by the *phoA* signal sequence for periplasmic localization of the target protein and a gene coding for a bacteriocin release protein (BRP) driven by the stationary phase promoter P_{stat52} (Miksch et al., 2005) in order to permeabilize the outer membrane in the stationary growth phase. This active disruption of the outer membrane may be avoided by the use of periplasmic 'leaky mutants'. The K12-derived *E. coli* strain JW1667-5 (*Δlpp-752:kan*) was created by a single knockout of the murein lipoprotein gene *lpp*, affecting the integrity of its cell envelope (Baba et al., 2006; DiRienzo et al., 1978). For similar strains lacking the *lpp* gene, Ni et al. (2007) describe enhanced permeability of the outer membrane, but no significant change in cell growth, carbon metabolism or fatty acid composition compared to the wild type. The strain of Ni et al. (2007) has already been used for the production and secretion of a maltose binding protein, a xylanase and a cellulase (Shin and Chen, 2008). Thus, the system seems promising for secreting small proteins like SAV to the cultivation medium.

Transport of target proteins to the periplasm has several advantages compared to intracellular localization, e.g., reduced protease activity (Choi and Lee, 2004). In *E. coli*, this can be achieved by using signal peptides for the general secretory pathway (Sec). In the case of toxic proteins like SAV this pathway is advantageous because the protein remains (partially) unfolded during transport (Pugsley, 1993), reducing the concentration of bioactive intracellular product. However, secretion efficiency strongly depends on target protein, signal sequence, and host strain (Choi and Lee, 2004). For the secretion of SAV Miksch et al. (2008) used the signal sequences of the *phoA* gene for the alkaline phosphatase from *E. coli* and of the *bglA* gene for the β-glucanase from *Bacillus amyloliquefaciens*. The application of the *phoA* signal sequence led to secretion efficiencies of almost 100%.

1.1. Performance of selected expression systems

Müller et al. (2013) used the natural producer *S. avidinii* for production, yielding 39.2 μM of extracellular, tetrameric SAV in 14 days (114 nM h^{-1}) in a fed-batch process. However, due to the complex morphology and sensitivity of the organism and long cultivation times an efficient heterologous expression system for the SAV gene is desirable.

Miksch et al. (2008) reported a maximal concentration of 1.6 μM of extracellular SAV in 8 h (200 nM h^{-1}) using *E. coli* in a stirred tank bioreactor. Recently, heterologous expression systems were published based on the yeast *P. pastoris* and complex methanol-based fermentation processes (Nogueira et al., 2014; Casteluber et al., 2012). Nogueira et al. (2014) reached a final extracellular SAV concentration of 11 μM in 164 h (67 nM h^{-1}) in the bioreactor. Casteluber et al. reported even higher concentrations in the range of 71 μM in spinner flasks.[1]

1.2. Goals of this study

The system of Miksch et al. (2008) as mentioned above led to remarkable productivities in short cultivation periods. However, maximal biomass concentrations were low (<10 g L^{-1}, OD_{600} < 25). Furthermore, the system contained an Ω-Cm transposon (Miksch et al., 1997) to avoid uncontrolled expression of the bacteriocin release protein-encoding gene, causing serious problems in the genetic stability of the producer strains. To achieve higher dry cell weight (DCW) concentrations and a more stable expression over longer periods of time, this study focused on an a novel secretion strategy avoiding an active disruption of the outer membrane of *E. coli* based on the application of the periplasmic 'leaky mutant' JW1667-5. Comparable deletion mutants have not been used for the production of SAV before.

On the genetic level, several promoters, leader peptides, and a variety of SAV genes differing in chain length and codon usage were applied. One of the research questions in this context was if shortened genes (core SAV) can be used for SAV production by *E. coli*. Based on an optimized genetic configuration, the performance of the new construct was compared to a conventional producer strain (*E. coli* KRX).

So far, none of the studies performed targeting expression of the SAV gene by *E. coli* contained detailed investigations on the optimization of process conditions. Corresponding experiments where therefore integrated in the work plan applying various culture conditions and cultivation parameters (medium, temperature, supplements) in batch and fed-batch operation. Thus, factors on all major levels of the development of recombinant production processes were part of this study to get a more holistic view of *E. coli*'s potential for the production and secretion of SAV.

2. Materials and methods

2.1. Bacterial strains and plasmids

The strain *E. coli* KRX (Promega, Fitchburg, Wisconsin, USA) was used for cloning work and as a host for heterologous gene expression based on the T7 system. The K12 BW25113-derived strain *E. coli* JW1667-5, purchased from the Coli Genetic Stock Center (CGSC, Keio Knockout Collection, Yale University, New Haven, Connecticut, USA), was used as a second expression host. *S. avidinii* (CBS 730.72; DSM 40526) was ordered from CBS (Centraalbureau voor Schimmelcultures, Utrecht, Netherlands).

The plasmids constructed during this project are given in Table 1, which contains information on designations and features. The pET24a vector backbone was purchased from Novagen (Madison, Wisconsin, USA) and used in combination with *E. coli* KRX (plasmids 7–10). For plasmids 1–6 the pEL vector backbone was used, constructed and generously provided by Maurice Telaar of Bielefeld University (Germany). Both backbones are shown in Fig. S2 (Supplementary material).

2.2. Plasmid construction and verification of cloning steps

The plasmids used in this project were constructed as described by Gibson et al. (2009) using the isothermal reaction protocol (50 °C, 1 h) and a master mix purchased from NEB (Ipswich, Massachusetts,

[1] Assuming a molecular weight of the core SAV of 56 kDa per tetramer.

Table 1
Features and designations of plasmids used in this study.

Plasmid number	*E. coli* strain	Plasmid backbone[a]	Promoter[b]	Signal peptide[c]	SAV gene[d]	Type of secretion[e]
1	JW1667-5[f]	pEL	P_{bla}	*bglA*	nat	LM
2	JW1667-5	pEL	P_{bla}	*bglA*	CO	LM
3	JW1667-5	pEL	P_{bla}	*phoA*	nat	LM
4	JW1667-5	pEL	P_{bla}	*phoA*	CO	LM
5	JW1667-5	pEL	P_{stat69}	*bglA*	nat	LM
6	JW1667-5	pEL	P_{stat69}	*bglA*	CO	LM
7	KRX	pET24a	P_{T7}	*bglA*	nat	BRP
8	KRX	pET24a	P_{T7}	*bglA*	CO	BRP
9	KRX	pET24a	P_{T7}	*bglA*	nat + natSP[h]	BRP
10	KRX	pET24a	P_{T7}	*bglA*	CO, coreSAV[g]	BRP

[a] The antibiotic resistance marker used for selection was tetracycline for the pEL-based vectors and kanamycin for the pET24a-based vectors.
[b] Promoter for the expression of the SAV gene: P_{bla} = β-lactamase (*bla*) promoter from *E. coli*; P_{T7} = T7 promoter; P_{stat69} = stationary phase promoter 69 (Miksch et al., 2005).
[c] Secretion signal peptide: bglA-SP = β-glucanase (*bglA*) secretion signal peptide from *B. amyloliquefaciens*, phoA-SP = alkaline phosphatase (*phoA*) secretion signal peptide from *E. coli*.
[d] SAV gene variant: nat = native SAV gene from *S. avidinii*, CO = codon-optimized gene.
[e] Method of secretion to the medium: LM = leaky mutant (JW1667-5), BRP = Co-expression of the optimized LppBRP gene (Miksch et al., 2008) under control of the stationary phase promoter P_{stat52} (Miksch et al., 2005) for secretion of SAV.
[f] Native SAV gene and native secretion signal peptide in addition to the *bglA* leader.
[g] Codons 13–139 of the codon-optimized SAV gene (core SAV).
[h] Also used for *E. coli* KRX for the analysis of host strain-dependent secretory differences.

USA). The fragments for the assembly reaction were amplified by PCR based on primers with homologous overlaps of up to 30 base pairs (bp) and purified by clean-up from agarose gels. A volume of 3 μL of the Gibson Assembly mixture was used to transform *E. coli* by electroporation using standard laboratory procedures (Sambrook, 1989). Relevant plasmid sequences were confirmed by sequencing at Bielefeld University (IIT Biotech GmbH, Bielefeld, Germany). A detailed description of the cloning strategy and primer combinations is given in section S1 in the supplementary material (Tables S1–S4). Glycerol stocks (20% (v/v)) of the cultures were used for storage at −80 °C.

2.3. Media and supplements for cultivation

HSG medium was used as standard cultivation medium for *E. coli* containing glycerol (14.9 g L^{-1}), soy peptone (13.5 g L^{-1}), yeast extract (7.0 g L^{-1}), NaCl (2.5 g L^{-1}), K_2HPO_4 (2.3 g L^{-1}), KH_2PO_4 (1.5 g L^{-1}), and $MgSO_4 \cdot 7H_2O$ (0.249 g L^{-1}). The pH was set to 7.4 using 6 N NaOH.

SGA medium (Selvamani et al., 2014) was used as a supplement and prepared as a fivefold concentrated stock solution. Final concentrations of onefold concentrated SGA-medium were: glycerol (30 g L^{-1}) K_2HPO_4 (13.53 g L^{-1}), KH_2PO_4 (6.62 g L^{-1}), citric acid (1.7 g L^{-1}), EDTA (0.0084 g L^{-1}), $MgSO_4$ (0.585 g L^{-1}), $FeCl_3 \cdot 6H_2O$ (0.0108 g L^{-1}), $ZnSO_4 \cdot 7H_2O$ (0.00276 g L^{-1}), $MnSO_4 \cdot H_2O$ (0.0037 g L^{-1}), $CoSO_4 \cdot 7H_2O$ (0.00112 g L^{-1}), $CuCl_2$ (0.00034 g L^{-1}), H_3Bo_3 (0.002 g L^{-1}), $Na_2MoO_4 \cdot 2H_2O$ (0.005 g L^{-1}), and $(NH_4)_2SO_4$ (10 g L^{-1}).

Substances for supporting secretion of proteins localized in the periplasmic space were Triton® X-100, X-114, and X-45 (Sigma–Aldrich Chemie GmbH, Seelze, Germany) and glycine, each supplemented as 200 g L^{-1} stock solutions or added dropwise directly from an undiluted solution (bioreactor experiments). Isopropyl β-D-1-thiogalactopyrano-side (IPTG, 100 mM stock solution) and rhamnose (200 g L^{-1} stock solution) were used to induce transcription of the target gene in *E. coli* KRX carrying derivatives of the pET24-based plasmid (plasmids 7–10, Table 1). The antibiotics kanamycin (50 mg L^{-1}) and tetracycline (25 mg L^{-1}) were used to achieve segregational stability of plasmids.

2.4. Amplification of SAV gene and leader peptides

The SAV gene variants were either amplified from the genome of *S. avidinii* or from a codon-optimized gene, which was commercially synthesized by GeneArt® Gene Synthesis (Life Technologies, Carlsbad, California, USA; GenBank accession number: KT344129). The *bglA* and *phoA* leader peptides were amplified from constructs of Miksch et al. (2008).

2.5. Shake flask and microplate cultivation

Cultivations were carried out in 24-squared well deepwell plates (Axygen® 24 Well Clear V-Bottom, Corning, New York, USA) or in shake flasks inoculated to an optical density OD_{600} of 0.1. The cultivation volume for microplates was 3 mL. Plates were sealed by sterile sealing films (BREATHseal™, Greiner Bio-One International GmbH, Kremsmuenster, Austria) and incubated at 26, 30 or 37 °C on a rotary shaker (KS 4000 ic control, IKA-Werke GmbH & Co., KG, Staufen im Breisgau, Germany) using a frequency of 200 min^{-1} (shaking diameter: 20 mm). For shake flask cultivations, 500 mL baffled glass flasks (DURAN® baffled flask with membrane screw cap, Schott AG, Mainz, Germany) were filled with 50 mL of medium. The cultures were incubated at 30 °C on a rotary shaker (LS-X, Kühner AG, Birsfelden, Switzerland) using a frequency of 150 min^{-1} (shaking diameter: 50 mm).

2.6. Fermentations in the bioreactor

Fermentations in the bioreactor were performed in a Sixfors fermentation system (Infors HT, Infors AG, Bottmingen, Switzerland) with unbaffled glass vessels. Three six-bladed rushton turbines, one three-bladed propeller stirrer and one mechanic foam disruptor were equally distributed on 14.5 cm of the stirrer axis. The aspect ratio of the reactor was 2.77:1 and the ratio of stirrer to reactor diameter 0.4. Cultivation was performed at a stirring frequency of 1000 min^{-1}, 30 °C and pH 7.0, controlled by the automatic addition of 20% (v/v) H_3PO_4 and 25% (w/w) NH_3. The initial fermentation volume of 400 mL of HSG medium and variations thereof was adjusted to an optical density OD_{600} of 0.5 by an overnight culture grown in HSG medium. The vessels were aerated with air saturated by water vapor at a flow rate of 5 vvm (2 NL min^{-1}) or 1.2 vvm (0.48 NL min^{-1}). For fed-batch cultivations, a 870 g L^{-1} glycerol solution was fed at a constant rate of 0.98 mL h^{-1} after 20 h of cultivation. Samples were automatically taken in intervals of 6 or 8 h, cooled to 4 °C, and processed in intervals of 24 h. To avoid excessive foaming, media supplemented with the surfactant Triton® X-45 (9 drops per 400 mL ≈ 0.65 g L^{-1}) contained an additional supplement

(46 drops per 400 mL ≈ 4.13 g L^{-1}) of the antifoam agent Pluronic® PE 8100 (BASF, Ludwigshafen, Germany).

2.7. Determination of substrate (S) and biomass

The concentration of glycerol (*S*) was measured by ion-exchange HPLC as described previously (Müller et al., 2013).

For measurement of the optical density OD_{600} at 600 nm (BioPhotometer *plus*, Eppendorf AG, Hamburg, Germany) samples of cultures were diluted by a solution of NaCl (9 g L^{-1}) if required, i.e., if the optical density was higher than 0.8. The dry cell weight concentration *X* was determined by differential weighing after drying for 48 h at 60 °C using cell pellets acquired from 1 mL of culture volume washed twice in an aqueous NaCl solution (9 g L^{-1}).

2.8. Determination of the concentration (P) and the proportion of biotin-blocked binding sites of SAV ($Q_{blocked}$)

The concentration of soluble SAV was determined by fluorescence quenching of biotin-4-fluorescein as described by Kada et al. (1999a,b). The assay was performed in final volumes of 1 mL as specified elsewhere (Müller et al., 2013). Overall binding sites of SAV were quantified via heat-based displacement of biotin by B4F (Müller et al., 2015) by incubating the samples at 70 °C for 10 min prior to the fluorescence measurement. Samples were diluted to overall SAV concentrations ≤300 nM of tetrameric SAV to allow full detectability of the binding sites. The biotin-blocked sites were calculated from the difference of the room temperature- (free binding sites) and the heat-based measurement (overall binding sites) and scaled from 0 to 1.[2]

2.9. Fractional cell disruption

In order to separate medium, periplasmic and cytoplasmic cell fractions, the culture broth was treated by centrifugation followed by osmotic shock and sonication (Khosla and Bailey, 1989) as described by Miksch et al. (2008).

3. Results

3.1. Optimization of culture conditions using 24-well-plates

3.1.1. Effect of temperature (E. coli *JW1667-5*)

E. coli JW1667-5 carrying different plasmids (Table 1) was cultivated at 26 °C, 30 °C and 37 °C in microplates for 48 h. The results are shown in Fig. 1A and B.

Generally, at a cultivation temperature of 37 °C product concentrations (Fig. 1A, white bars) were relatively low. Only minor differences were observed for different plasmids. In contrast to that at lower temperatures of 26 °C (black bars) and especially at 30 °C (grey bars) plasmids 1 and 2 led to higher product concentrations compared to those achieved with plasmids 3–6. At 30 °C, the signal peptide of the *bglA* gene from *B. amyloliquefaciens* (plasmids 1 and 2, Table 1) caused improved results compared to the *phoA* signal peptide (plasmids 3 and 4) for the secretion of SAV. The codon-optimized SAV gene (plasmids 2, 4 and 6) did not improve production toward the native gene (plasmids 1, 3 and 5). Plasmids 1 and 2 providing the constitutive β-lactamase promoter from *E. coli* P_{bla} led to a higher extracellular product concentration than plasmids 5 and 6 for which SAV gene expression was controlled by the strong stationary phase promoter P_{stat69}. Best results were achieved for plasmid 1 at 30 °C (OD_{600} of 6.0 ± 0.3, 377 ± 9 nM of SAV in 48 h).

3.1.2. Effects of media supplements (E. coli *JW1667-5*)

Media supplements were tested in 24-well plates at 30 °C to increase the extracellular product concentration. Triton® X-100 (Yang et al., 1998), glycine (Miksch et al., 2008; Yang et al., 1998), and $ZnSO_4$ (Beshay et al., 2007; Baneyx et al., 1991) were applied to cultures of *E. coli* JW1667-5 carrying either plasmid 1 or plasmid 2 (Table 1) and compared to unsupplemented HSG medium. Triton® X-100 supplementation (1 g L^{-1}) of the strain carrying plasmid 1 led to a 2.5 fold higher extracellular product concentration after 24 h (730 ± 17 nM vs. 292 ± 48 nM) compared to the reference culture without decreasing the optical density of the culture (5.94 ± 0.25 vs. 5.58 ± 0.02). Combining this concentration of Triton® with 5 g L^{-1} of glycine caused even higher product concentrations (891 ± 92 nM), but also a strong decrease of the optical density (2.45 ± 0.07). The addition of glycine alone resulted in lower optical densities and unimproved SAV concentrations. Application of plasmid 2 generally brought about lower product concentrations. Detailed results are shown in Fig. S1 in the Supplementary material. When compared to the initial conditions (unsupplemented HSG medium, 37 °C), Triton® X-100 supplementation at 30 °C led to a 6.3 fold increase of the extracellular product concentration and a 12.7 fold increase of productivity. Thus, the following experiments were performed based on plasmid 1, cultivation at 30 °C, and Triton® supplementation.

3.1.3. Host-dependent efficiency of product secretion: E. coli *JW1667-5* vs. E. coli *KRX*

To calculate the efficiency of product secretion to the culture medium, cytoplasmic, periplasmic, and extracellular SAV concentrations were measured and compared. Based on the results of the previous sections, *E. coli* JW1667-5 carrying plasmid 1 (Table 1) was cultivated in microplates in 3 mL of HSG medium supplemented with 1 g L^{-1} of Triton® X-100. Samples were taken after 12, 24 and 48 h of cultivation. Periplasmic and cytoplasmic product concentrations were acquired by fractional cell disruption of cell pellets after 48 h of cultivation. A culture of *E. coli* KRX carrying plasmid 1 was treated similarly in order to compare the performance of the mutant JW1667-5 to an established production strain. Results are shown in Fig. 1C and D.

Cultivation of the strain KRX carrying plasmid 1 led to an OD_{600} of 10.0 ± 0.3 and an extracellular concentration of SAV of 439 ± 38 nM (Fig. 1C) after 48 h of cultivation. The strain JW1667-5 grew faster in the beginning of the cultivation and reached its final OD_{600} of 5.9 ± 0.10 already after 24 h of cultivation. The extracellular product concentration reached its maximum of 779 ± 24.7 nM after 24 h. In the culture of *E. coli* KRX carrying plasmid 1 containing no active secretion system (neither BRP, nor periplasmic knockout) 439 ± 38 nM of SAV (35%) were located in the supernatant, 543 ± 116 nM (43%) in the periplasmic fraction, and 277 ± 37 nM (22%) in the cytoplasm of the cells (Fig. 1D). In total the culture produced about 1259 nM soluble tetrameric SAV corresponding to a process selectivity $S_{P/X}$ of 126 nM per OD_{600} unit. The strain JW1667-5 carrying the same plasmid secreted more than 95% of the 783 nM of soluble SAV produced to the medium, leading to a selectivity of 137 nM per OD_{600} unit.

In conclusion, *E. coli* KRX led to higher overall product concentrations, but accumulated the majority of bioactive product in cytoplasm and periplasm due to the lack of a periplasmic secretion system. Regarding downstream processing the strain JW1667-5 therefore is beneficial.

[2] $Q_{blocked}$ = 0: all binding sites are biotin-free; $Q_{blocked}$ = 1: binding sites are completely biotin-blocked.

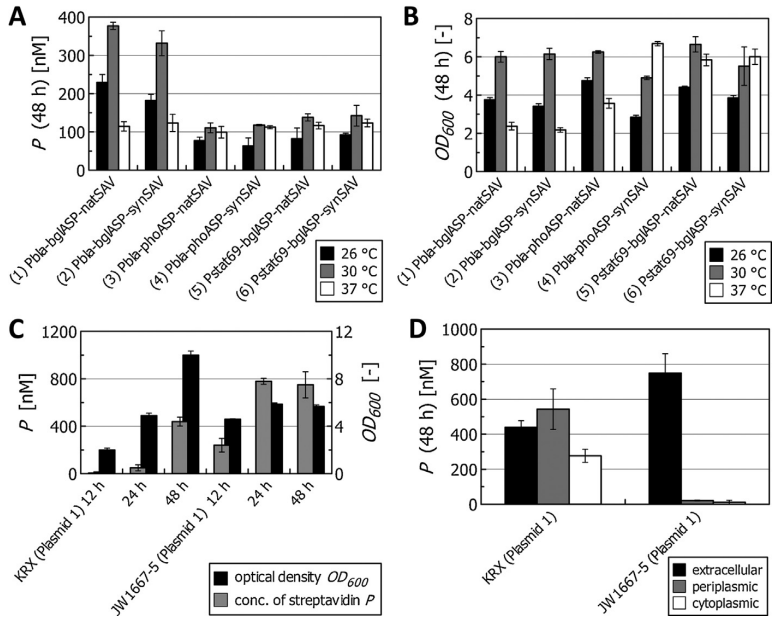

Fig. 1. Cultivation of *E. coli* JW1667-5 carrying variants of the pEL plasmid (Table 1) in 24-well plates in HSG medium at different cultivation temperatures. Designations refer to promoter, secretion signal peptide and target gene variant of the SAV expression cassette. Concentrations of tetrameric SAV in the culture supernatant *P* (A) and corresponding optical densities at 600 nm OD_{600} (B) 48 h post inoculation are shown. For plasmid 1, a comparison of the host strain was performed. (C, D) Comparison of *E. coli* JW1667-5 and *E. coli* KRX both carrying plasmid 1 in a 24-well deepwell plate in 3 mL of HSG medium supplemented by 1 g L^{-1} Triton® X-100 at 30 °C. (C) Optical density OD_{600} and extracellular concentration of extracellular tetrameric SAV *P* after 12, 24 and 48 h of cultivation. (D) Concentration of tetrameric SAV *P* in different fractions (extracellular, periplasmic space and cytoplasmic) after 48 h of cultivation.

3.1.4. *BRP-mediated secretion of SAV by* E. coli *KRX and expression of a core SAV gene*

For an active secretion of SAV by *E. coli* KRX, BRP-based secretion of the protein was analyzed by using plasmids 7–10 (Table 1). Screening in 24-well plates led to optimized cultivation conditions allowing the accumulation of soluble extracellular SAV. Using HSG medium supplemented with 1 g L^{-1} of rhamnose and 0.01 mM of IPTG for induction of expression, and 1 g L^{-1} of Triton® X-100 for improved secretion yielded a maximum of 550 nM of extracellular tetrameric SAV after 48 h of cultivation at 30 °C (data not shown), slightly surpassing the concentration of the KRX-based experiments applying plasmid 1 (Fig. 1C). Again, the native SAV gene (plasmid 7) led to higher productivities than the codon-optimized gene (plasmid 8). Remarkably, a codon-optimized core SAV gene (AA 13–139, plasmid 10) led to no detectable SAV, even upon Triton®-supplementation of the medium.

3.1.5. *Evaluation of additional constructs*

Two additional concepts were evaluated regarding their potential to reduce the toxicity of SAV to the host: a construct expressing the full-length SAV gene including its native secretion signal peptide (plasmid 9) and a co-expression-based construct (plasmid 11, Fig. S2(B) in the supplements) for the simultaneous expression of the SAV-binding Nanotag 15 (Lamla and Erdmann, 2004) under control of the strong, constitutive CP25 promoter (Jensen and Hammer, 1998). However, neither of the constructs led to improved SAV production (see Supplementary material, Section S3 for details).

3.2. *Shake flask cultivations*

The following experiments were based on *E. coli* JW1667-5 carrying plasmid 1. After optimization of culture conditions in 24-well plates, the next steps of process development were batch and fed-batch cultivations in baffled 500 mL shake flasks using a culture volume of 60 mL (Fig. 2). Different media were tested for this purpose, which were supplemented with Triton® X-100 due to the favorable effects on cell mass and product concentration (Section 3.1.2).

Firstly, the positive effect of Triton® X-100 on the SAV concentration described before was reproduced for cultivation in shake flasks. After 27 h of cultivation 863 ± 3 nM of tetrameric extracellular SAV was measured in Triton®-supplemented culture (productivity $p = 32.0$ nM h^{-1}, medium composition (b) in Fig. 2) compared to 484 ± 56 nM ($p = 17.9$ nM h^{-1}, medium composition (a)) in Triton®-free HSG medium. A drawback was the decrease of the DCW concentration after 12 h of cultivation upon Triton® supplementation.

Secondly, an SGA supplement in the basic medium increased both the optical density and product concentration. After the batch phase of the cultivation at 36.5 h a maximum of 1778 ± 31 nM of extracellular tetrameric SAV was achieved in the culture with 48 mL of HSG and 12 mL of fivefold concentrated SGA medium, corresponding to a productivity *p* of 48.7 nM h^{-1}. A reduced SGA supplement (6 mL) led to 1587 ± 21 nM after 36.5 h of cultivation ($p = 43.5$ nM h^{-1}).

Thirdly, adding 10% (v/v) of fivefold concentrated SGA medium after 37.8 h of cultivation to the culture grown in the 48 mL HSG/12 mL SGA-combination (medium composition (d), Fig. 2) resulted in a further boost of the extracellular product concentration. This fed-batch strategy led to a maximum

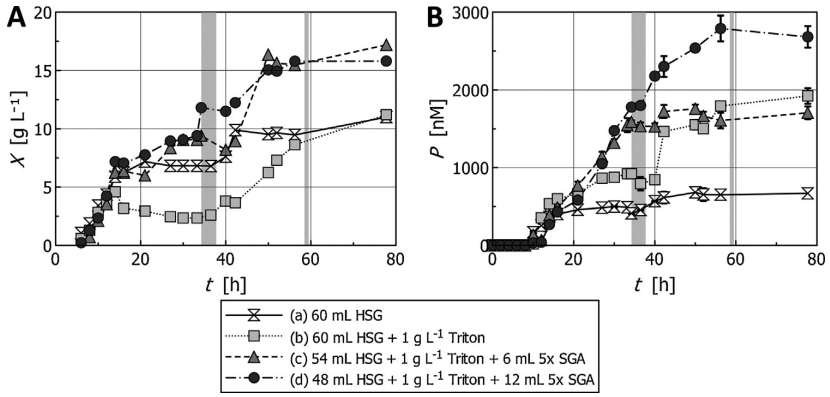

Fig. 2. Cultivation of *E. coli* JW1667-5 carrying plasmid 1 (Table 1) at 30 °C in three replicates in shake flasks using different cultivation media. Labels refer to the basic medium composition. (A) Plot of the dry cell weight concentration X over the cultivation time t. (B) Plot of the extracellular tetrameric SAV concentration P. All cultures were supplemented two times with 10% (v/v) of fivefold concentrated SGA medium indicated by the grey, shaded areas. Biomass measurements were performed onefold due to small cultivation volumes.

of 2790 ± 166 nM of tetrameric extracellular SAV after 56.3 h (p = 49.6 nM h^{-1}).

3.3. Transfer to the bioreactor

The non-ionic surfactant Triton® X-100 caused excessive foaming in the initial bioreactor experiments. To avoid this problem, foaming of the surfactant was titrated by an antifoam agent (Pluronic® PE 8100) in shake flask experiments. A detailed analysis led to the conclusion that shorter-length variants of Triton® like Triton® X-45 are more suitable for bioreactor cultivations (see Section S3 in Supplementary material for an elaborate discussion). Combining Triton® X-45 and Pluronic® PE 8100 in the bioreactor resulted in negligible amounts of foam on the gas–liquid interface even for high volumetric flow rates due to low foam stability. The properties were particularly advantageous for high rotary frequencies of the stirrer, resulting in a rapid disruption of emerging foam, an essential feature for an efficient control of pH and feeding during fermentation. Therefore, Triton® X-45 was used for the subsequent studies in the bioreactor. The concentration of surfactant was reduced from 1 g L^{-1} to 0.65 g L^{-1}, because shake flask studies indicated that this concentration is sufficient for an efficient secretion.

3.4. Bioreactor fermentation

Various batch and fed-batch strategies were evaluated in bioreactor experiments. The preparation of concentrated SGA medium regularly resulted in precipitates, which cause abrasive effects on the stirrer in the bioreactor. This factor, the complex preparation procedure and composition of SGA medium, and occasional, inexplicable intermediary lag phases for combinations of HSG and SGA medium led to the decision not to apply SGA-based media in the bioreactor. Variations of HSG medium were used instead. Feeding of 870 g L^{-1} glycerol was applied for fed-batch studies. Fig. 3 shows a selection of batch fermentations.

Fig. 3D shows that twofold concentrated HSG medium was most suitable for an increased production of SAV. A higher C/N-ratio (Fig. 3B and C) led to improved SAV formation for an initial glycerol concentration of 40 g L^{-1}, but yielded worse results and residual glycerol in the end of cultivation for an additional increase to 80 g L^{-1}. A maximal SAV concentration of 1570 ± 77 nM was reached for the cultivation using twofold concentrated HSG medium after 36 h of cultivation (Fig. 3D), corresponding to a productivity of 43.6 nM h^{-1} as opposed to 944 ± 34 nM after 42 h (22.5 nM h^{-1}) in the reference culture (Fig. 3A). Using a threefold concentrate of HSG medium did not result in further improvements (see Supplementary material, Fig. S3). The proportion of biotin-blocked binding sites measured by heat-based fluorescence quenching of B4F was in the range of 5–10% for all of the cultivations (data not shown), indicating a high bioactivity of the product. Glycerol depletion after 24 h suggested the application of a glycerol feeding after the initial growth phase for improved product concentrations.

Thus, feeding of glycerol was applied to twofold concentrated HSG medium, leading to the fermentation course shown in Fig. 4. To ensure scalability of the process the air flow rate was reduced from 5 to 1.2 vvm. The constant fed-batch process led to an SAV concentration of 2607 ± 169 nM after 40 h of cultivation, corresponding to a productivity of 65.2 nM h^{-1}. The heat-based assay for the determination of total binding sites of SAV yielded a proportion of biotin-blocked binding sites of 8.3 ± 4.3% in the interval 40–56 h. The process additionally led to the highest specific productivity p_{spec} (3.8 nmol g^{-1} h^{-1}) of this study.

Table 2 sums up the results of the bioreactor and shake flask experiments, highlighting maximal values for both the batch and the fed-batch studies.

3.5. Analysis of product toxicity and secretion efficiency in the bioreactor

Cell fractions of different bioreactor cultivations were analyzed by fractional cell disruption and determination of the proportion of biotin-blocked binding sites $Q_{blocked}$ (Section 2.8). Fig. 5A sums up the results. The sum of the concentration of SAV in all of the fractions was set to 100%. Like for the shake flask cultivations, the majority of SAV (91 ± 5%) accumulated as extracellular product facilitating the purification of the protein without cell disruption and emphasizing the secretory potential of the strain. The proportion of biotin-blocked SAV was approximately 3.3 fold higher in the cytoplasmic fraction than in the other fractions, independent from the time of sampling.

3.6. Summary of the results

Several factors on the level of cultivation conditions and the genetic composition of the producer strain were analyzed in this

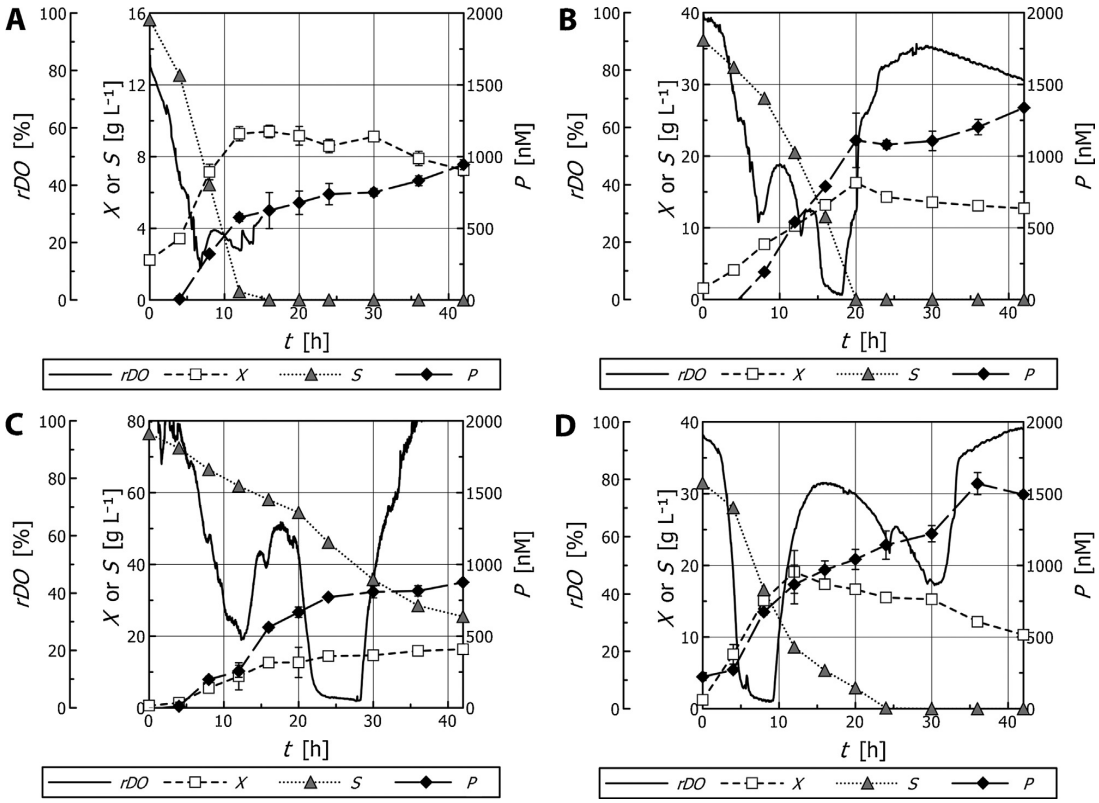

Fig. 3. Batch cultivations of *E. coli* JW1667-5 carrying plasmid 1 (Table 1) in the bioreactor using different cultivation media supplemented by Triton® X-45 (0.65 g L^{-1}). (A) standard HSG medium (reference), (B) HSG with 40 g L^{-1} of glycerol, (C) HSG with 80 g L^{-1} of glycerol, (D): twofold concentrated HSG medium. Abbreviations: *rDO* = relative dissolved oxygen saturation, *X* = dry cell weight concentration, *S* = substrate concentration (glycerol), *P* = extracellular SAV concentration, *t* = cultivation time. Due to technical problems no signal of the oxygen electrode is available for the reference cultivation (A) after 15 h onwards.

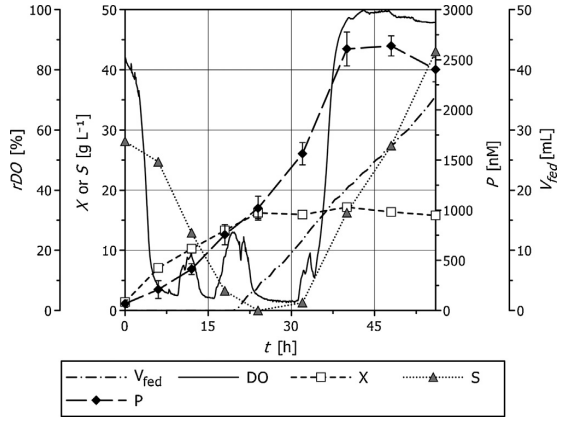

Fig. 4. Fed-batch cultivation of *E. coli* JW1667-5 carrying plasmid 1 (Table 1) in the bioreactor in twofold concentrated HSG medium supplemented by Triton® X-45 (0.65 g L^{-1}). A 870 g L^{-1} glycerol solution was used for feeding. Abbreviations: *r*DO = relative dissolved oxygen saturation, *X* = dry cell weight concentration, *S* = substrate concentration (glycerol), *P* = product concentration (SAV), V_{fed} = fed volume (feed solution), *t* = cultivation time. Glycerol was added to the culture medium after 20 h at a constant flow rate of 0.98 mL h^{-1} (on an initial cultivation volume of 400 mL).

study in respect to their potential to improve SAV production by the *E. coli* leaky mutant JW1667-5.

The characterization of various producer strains resulted in the following optimal genetic configuration of the producer strain: maximal extracellular product concentrations were achieved for (i) a native full-length SAV gene (ii) under control of the relatively weak constitutive promoter of the *bla* gene (iii) fused to the *bglA* signal peptide. The leader peptide was of increased importance

Table 2
Summary of the production processes using *E. coli* JW1667-5 carrying plasmid 1 (Table 1) in the bioreactor. Maximal bioreactor values for the batch and fed-batch experiments or shake flask cultivations are printed in bold face.

Medium[a]	Cultiv. mode[b]	X_{max} [g L^{-1}][c]	P_{max} [nM][c]	$p_{SAV,max}$ [nM h^{-1}][d]	$s_{P/X}$ [nmol g^{-1}][e]	p_{spec} [nmol g^{-1} h^{-1}][f]
HSG	B	9.40 ± 0.35 (16 h)	944 ± 34 (42 h)	22.5	**100**	**2.4**
HSG c_{Gly}: 40 g L^{-1}	B	16.28 ± 0.31 (20 h)	1337 ± 18 (42 h)	31.8	82	2.0
HSG c_{Gly}: 80 g L^{-1}	B	16.34 ± 0.24 (42 h)	875 ± 20 (42 h)	20.8	54	1.3
2x HSG	B	19.08 ± 2.98 (12 h)	**1570 ± 77** (36 h)	**43.6**	82	2.3
3x HSG	B	**30.78 ± 0.55 (36 h)**	311 ± 3 (36 h)	8.6	10	0.3
2x HSG	FB	**17.17 ± 0.31 (40 h)**	2608 ± 169 (40 h)	**65.2**	152	**3.8**
HSG/SGA	FB SF	15.80 (56 h)	**2791 ± 166 (56 h)**	49.8	**177**	3.2

[a] Batch medium for the cultivation; c_{Gly} refers to the initial glycerol concentration (14.9 g L^{-1} for onefold concentrated HSG medium, if not specified otherwise). All bioreactor-based processes were performed applying a Triton® X-45 supplement of 0.65 g L^{-1}. For shake flask results (FB SF), 1 g L^{-1} of Triton® X-100 was applied.
[b] Cultivation mode: B = batch, FB = fed-batch. For the fed-batch process a 870 g L^{-1} glycerol concentrate was fed at a constant feed rate of 0.98 mL h^{-1} after 20 h. FB SF refers to the shake flask fed-batch cultivation of Fig. 3, medium composition (d) (HSG/SGA medium combination with feeding of 5x SGA concentrate).
[c] Maximal dry cell weight (X) or product concentration (P). The number in brackets refers to the cultivation time at which the maximum was reached.
[d] Productivity in the time interval from start of cultivation to the maximal product concentration.
[e] Process selectivity $s_{P/X} = P_{max}/X_{max}$.
[f] Specific productivity $p_{spec} = p_{SAV,max}/X_{max}$.
t

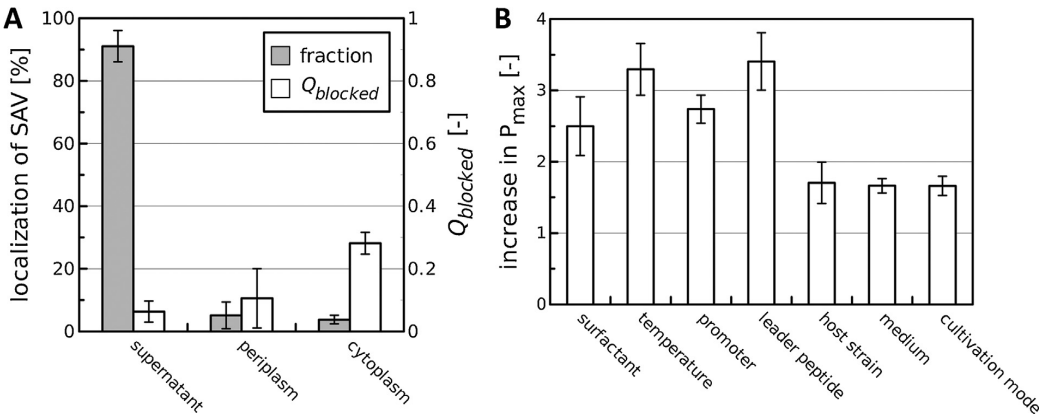

Fig. 5. Cellular localization of SAV upon optimization (A) and summary of the results of the optimization procedure (B). (A) Evaluation of the fractional localization of SAV and the proportion of biotin-blocked SAV $Q_{blocked}$ acquired by fractional cell disruption of *E. coli* JW1667-5 carrying plasmid 1 (Table 1) cultivated in the bioreactor. The bars represent average values of three cultivations and three time points ($n = 3 \times 3$). (B) Relative improvement of the maximal extracellular product concentration caused by selected parameters in comparison to a reference cultivation procedure. Error bars were derived from gaussian error propagation. The parameters of optimization (labels) refer to: (a) surfactant: HSG + 1 g L^{-1} Triton® X-100 (optimized) vs. HSG (microplate, reference), (b) temperature: 30 °C vs. 37 °C (microplate), (c) promoter: P_{bla} vs. P_{stat69} (microplate), (d) leader peptide: *bglA*-natSAV vs. *phoA*-natSAV (microplate), (e) host strain: *E. coli* JW1667-5 vs. KRX (microplate), (f) medium: 2x HSG vs. HSG (bioreactor), and (g) cultivation mode: fed-batch (glycerol feed) vs. batch (bioreactor).

for a cultivation temperature of 30 °C, indicating interactions of these two factors. Finally, (iv) the host used for SAV production had a strong impact on the accumulation of extracellular SAV, leading to improved results for the *E. coli* leaky mutant JW1667-5 in comparison to *E. coli* KRX. Codon-optimization of the SAV gene did not improve SAV production, whereas no free binding sites were detectable in the supernatant for the application of a core SAV gene. The native, full-length SAV gene from *S. avidinii* thus seems to be the most suitable for heterologous expression by *E. coli*.

On the level of process optimization, two key factors were identified. Supplementation of the medium by Triton® X-100 led to a nearly complete (95%) secretion of SAV from the periplasm to the medium by the leaky mutant JW1667-5 containing plasmid 1. The portion of secreted SAV was much lower (35%) for the established producer strain *E. coli* KRX in the presence of the detergent, which emphasizes the inherent properties of the knockout mutant used in this study. The cultivation temperature was of equal importance in the optimization procedure. Lowering it from 37 to 30 °C not only improved SAV production but also increased the optical density of the culture. These results indicate reduced host toxicity, which has been a central issue for expression of the SAV gene by *E. coli*.

Up-scaling of the process to the bioreactor resulted in foaming issues due to the detergent Triton® X-100. Foam formation was efficiently avoided by using the lower chain-length variant Triton® X-45 in combination with addition of antifoam agent without negatively affecting product secretion. In the presence of both supplements (Triton® and antifoam agent), the producer strain was successfully employed for bioreactor fermentation.

4. Discussion

This study shows that *E. coli* JW1667-5 is a suitable strain for the preparative heterologous production of SAV. The impact of the single parameters optimized throughout this study on the maximal extracellular concentration of SAV produced by this strain is shown in Fig. 5B. The addition of surfactants to the medium, the optimization of cultivation temperature, and the choice of promoter and leader peptide had a major effect (factor larger 2) on the product concentration. All of these factors contribute to a more efficient secretion of unfolded product (Sec pathway) and thus potentially reduce the toxicity of SAV for the host. The improved results for the *bglA* signal peptide are in in contrast to the findings of Miksch et al.

(2008), who reported improved results for the *phoA* signal peptide for a different vector backbone and *E. coli* BL21(DE3). Generally, the codon-usage of the SAV gene had an only minor impact on the product concentration, which may be due to the relatively weak promoter. The lack of active streptavidin in the core SAV-based construct may be an effect of binding of core SAV to the biotin carboxyl carrier protein (Wang et al., 2005), which potentially reduces the proportion of bioavailable binding sites.

Combinations of optimized conditions for the genetic parameters allowed the development of more sophisticated process strategies. In this context, direct optimization of the biomass concentration (3x HSG) turned out to be inefficient, whereas a well-balanced process (mediocre biomass concentration) led to an improved product concentration, process selectivity, and specific productivity. Overall, the optimization procedure improved the productivity and the extracellular product concentration by factors of 31.5 ± 5.3 and 26.3 ± 4.4, respectively (*E. coli* JW1667-5 carrying the P_{bla}-phoA-natSAV construct in HSG medium at 37 °C in a batch process in the microplate vs. the same strain carrying P_{bla}-bglA-natSAV in Triton®-supplemented 2x HSG medium at 30 °C in a fed-batch process in the bioreactor). In general, Triton®-supported cultivation may be a useful tool for future expression studies applying *E. coli* periplasmic leaky mutants, since secretion efficiency is strongly protein-dependent for *lpp*-knockout strains (Shin and Chen, 2008).

To our best knowledge, the product concentrations achieved in this study are the highest concentrations for the soluble, extracellular production of SAV by *E. coli* reported to date. The maximal extracellular product concentration of 2608 ± 169 nM in the bioreactor after 40 h of cultivation (Fig. 4) surpasses the reference bioreactor concentration of 1600 nM given in literature (Miksch et al., 2008) by a factor of 1.63. The maximal concentration of 2790 ± 166 nM achieved in shake flask fed-batch experiments (Fig. 2(d)) corresponds to an increase toward the reference value of 1715 nM (Miksch et al., 2008) by a factor of 1.63, emphasizing the potential of the construct. However, the data of Miksch et al. (2008) is based on batch experiments, whereas the results of this study refer to fed-batch cultivations.

P. pastoris seems to offer advantageous properties for the production of streptavidin, since the studies of Casteluber et al. (2012) (71 μM) and Nogueira et al. (2014) (11 μM) led to significantly higher product concentrations. However, both of these publications were based on the flammable and highly toxic organic solvent methanol, causing strong heat evolution, and oxygen demand, as well as increased cost for transport and storage on the industrial scale. The functionality of Casteluber's process has only been demonstrated for spinner flasks aerated through a porous stone at an air flow rates of 4 vvm. This system is not characterized regarding technical properties like power input and oxygen transfer, drastically complicating scale-up. Furthermore, the process was based on a washing step between growth and production, preventing a single-vessel fermentation and bearing the risk of contamination. Thus, a direct comparison of the bioreactor data of this study is only possible toward Nogueira's process, which was also performed in a standard bioreactor. Their product concentration was 4.2 fold higher, but the process led to a higher proportion of biotin-blocked binding sites (20% vs. 8.3 ± 4.3% in this study). Due to comparable productivities (67 vs. 65 nM h^{-1}), Nogueira's process was much longer (overall 10 vs. 3 days). The productivity in this study was achieved for a drastically lower dry cell weight concentration of 17.2 ± 0.3 g L^{-1} instead of the surprisingly high 235 g L^{-1} in Nogueira's process (for the given medium, DCW concentrations are typically in the range of <160 g L^{-1} for the medium applied; Jahic et al., 2002), resulting in a 3.3 fold improved process selectivity (47 (*P. pastoris*) vs. 152 nmol g^{-1} (*E. coli*)). This corresponds to a more efficient conversion of the substrates to the actual product. From the engineering point of view, the process described here was performed in conditions of poor oxygen supply by the use of un-baffled vessels and aeration with regular air, whereas Nogueira's process was dependent on supplementation with pure oxygen. Overall, the choice of host and process may therefore primarily depend on the properties of the available fermentation system (oxygen supply, cooling, safety properties) rather than the productive properties of the host.

Heat-based evaluation of the overall binding sites of SAV indicates that the extracellular product in the supernatant of the leaky mutant was highly bioactive. Although only small proportions of SAV were located in the cytoplasm for optimized culture conditions (see Fig. 5A), the high proportion of biotin-blocked binding sites in this compartment (3.3 fold increased toward medium and periplasm) suggests that toxic effects on the host observed for the expression of the SAV gene by *E. coli* may primarily be the result of cytoplasmic biotin binding. However, further investigations are necessary, e.g., to determine whether leakage of folded, biotin-blocked SAV from the cytoplasm to other cellular fractions takes place throughout cultivation.

To further enhance the systems' productivity the promoter may be exchanged as P_{bla} is known to be relatively weak (Liang et al., 1999). Optimization may also be performed on the host strain, e.g., by the knockout of protease genes, supported by the higher overall concentration of SAV in *E. coli* KRX.

Conflict of interest

The authors declare that they have no conflict of interest.

Acknowledgements

This work was financially supported by the Scholarship Program of the German Environmental Foundation (Deutsche Bundesstiftung Umwelt, DBU) and the Bielefelder Nachwuchsfonds.

Appendix A. Supplementary data

Supplementary data associated with this article can be found, in the online version, at http://dx.doi.org/10.1016/j.jbiotec.2016.01.032.

References

Argaraña, C.E., Kuntz, I.D., Birken, S., Axel, R., Cantor, C.R., 1986. Molecular cloning and nucleotide sequence of the streptavidin gene. Nucleic Acids Res. 14, 1871–1882.

Baba, T., Ara, T., Hasegawa, M., Takai, Y., Okumura, Y., Baba, M., Datsenko, K.A., Tomita, M., Wanner, B.L., Mori, H., 2006. Construction of *Escherichia coli* K-12 in-frame, single-gene knockout mutants: the Keio collection. Mol. Syst. Biol. 2, 1–11.

Baneyx, F., Ayling, A., Palumbo, T., Thomas, D., Georgiou, G., 1991. Optimization of growth conditions for the production of proteolytically-sensitive proteins in the periplasmic space of *Escherichia coli*. Appl. Microbiol. Biotechnol. 36, 14–20.

Baneyx, F., 1999. Recombinant protein expression in *Escherichia coli*. Curr. Opin. Biotechnol. 10, 411–421.

Bayer, E.A., Ben-Hur, H., Hiller, Y., Wilchek, M., 1989. Postsecretory modifications of streptavidin. Biochem. J. 259, 369–376.

Bayer, E.A., Wilchek, M., 1990. Application of avidin-biotin technology to affinity-based separations. J. Chromatogr. A 510, 3–11.

Beshay, U., Miksch, G., Friehs, K., Flaschel, E., 2007. Improved β-glucanase production by a recombinant *Escherichia coli* strain using zinc-ion supplemented medium. Eng. Life Sci. 7, 253–258.

Casteluber, M.C.F., Damasceno, L.M., da Silveira, W.B., Diniz, R.H.S., Passos, F.J.V., Passos, F.M.L., 2012. Cloning and expression of a functional core streptavidin in *Pichia pastoris*: strategies to increase yield. Biotechnol. Prog. 28, 1419–1425.

Chaiet, L., Wolf, F.J., 1964. The properties of streptavidin, a biotin-binding protein produced by *Streptomycetes*. Arch. Biochem. Biophys. 106, 1–5.

Chen, X., Xu, F., Peng, F., Xu, H., Luo, W., Xu, H., Xiong, Y., 2014. High-yield production of streptavidin with native C-terminal in *Escherichia coli*. Afr. J. Biotechnol., 8250–8258.

Choi, J.H., Lee, S.Y., 2004. Secretory and extracellular production of recombinant proteins using *Escherichia coli*. Appl. Microbiol. Biotechnol. 64, 625–635.
DiRienzo, J.M., Nakamura, K., Inouye, M., 1978. The outer membrane proteins of gram-negative bacteria: biosynthesis, assembly, and functions. Annu. Rev. Biochem. 47, 481–532.
Gallizia, A., de Lalla, C., Nardone, E., Santambrogio, P., Brandazza, A., Sidoli, A., Arosio, P., 1998. Production of a soluble and functional recombinant streptavidin in *Escherichia coli*. Protein Expr. Purif. 14, 192–196.
Gibson, D.G., Young, L., Chuang, R.-Y., Venter, J.C., Hutchison III, C.A., Smith, H.O., 2009. Enzymatic assembly of DNA molecules up to several hundred kilobases. Nat. Methods 6, 343–345.
Green, N.M., 1990. Avidin and streptavidin. Methods Enzymol. 184, 51–67.
Hartnett, J., Gracyalny, J., Slater, M.R., 2006. The single step (KRX) competent cells: efficient cloning and high protein yields. Promega Notes 94, 27–30 http://www.promega.com/pnotes/94/14410.27/14410.27.pdf.
Jahic, M., Rotticci-Mulder, J., Matrinelle, M., Hult, M., Enfors, S.-O., 2002. Modeling of growth and energy metabolism of *Pichia pastoris* producing a fusion protein. Bioprocess Biosyst. Eng. 24, 385–393.
Jensen, P.R., Hammer, K., 1998. The Sequence of Spacers between the Consensus Sequences Modulates the Strength of Prokaryotic Promoters. Appl. Environ. Microbiol. 64, 82–87.
Kada, G., Falk, H., Gruber, H.J., 1999a. Accurate measurement of avidin and streptavidin in crude biofluids with a new, optimized biotin-fluorescein conjugate. BBA—Gen. Subjects 1427, 33–43.
Kada, G., Kaiser, K., Falk, H., Gruber, H.J., 1999b. Rapid estimation of avidin and streptavidin by fluorescence quenching or fluorescence polarization. BBA – Gen Subjects 1427, 44–48.
Khosla, C., Bailey, J.E., 1989. Evidence for partial export of *Vitreoscilla* hemoglobin into the periplasmic space in *Escherichia coli*. Implications for protein function. J. Mol. Biol. 5, 79–89.
Kolomiets, E.I., Zdor, N.A., 1998. A product of the strain *Streptomyces avidinii* VKM Ac1047: synthesis, purification and use in immunoassay technology. Russ. Biotechnol. 2, 1–8, ISSN 1068-3682.
Lamla, T., Erdmann, V.A., 2004. The Nano-tag, a streptavidin-binding peptide for the purification and detection of recombinant proteins. Protein Expr. Purif. 33, 39–47.
Liang, S.-T., Bipatnath, M., Xu, Y.-C., Chen, S.-L., Dennis, P., Ehrenberg, M., Bremer, H., 1999. Activities of constitutive promoters in *Escherichia coli*. J. Mol. Biol. 292, 19–37.
Miksch, G., Neitzel, R., Fiedler, E., Friehs, K., Flaschel, E., 1997. Extracellular production of a hybrid β-glucanase from *Bacillus* by *Escherichia coli* under different cultivation conditions in shaking cultures and bioreactors. Appl. Microbiol. Biotechnol. 47, 120–126.
Miksch, G., Bettenworth, F., Friehs, K., Flaschel, E., 2005. The sequence upstream of the −10 consensus sequence modulates the strength and induction time of stationary-phase promoters in *Escherichia coli*. Appl. Microbiol. Biotechnol. 69, 312–320.
Miksch, G., Ryu, S., Risse, J.M., Flaschel, E., 2008. Factors that influence the extracellular expression of streptavidin in *Escherichia coli* using a bacteriocin release protein. Appl. Microbiol. Biotechnol. 81, 319–326.
Muzykantov, V.R., Christo Christofidou-Solomidou, M., Balyasnikova, I., Harshaw, D.W., Schultz, L., Fisher, A.B., Albelda, S.M., 1999. Streptavidin facilitates internalization and pulmonary targeting of an anti-endothelial cell antibody (platelet-endothelial cell adhesion molecule 1): a strategy for vascular immunotargeting of drugs. Proc. Natl. Acad. Sci. U. S. A. 96, 2379–2384.
Müller, J.M., Risse, J.M., Jussen, D., Flaschel, E., 2013. Development of fed-batch strategies for the production of streptavidin by *Streptomyces avidinii* based on power input and oxygen supply studies. J. Biotechnol. 163, 325–332.
Müller, J.M., Risse, J.M., Friehs, K., Flaschel, E., 2015. Model-based development of an assay for the rapid detection of biotin-blocked binding sites of streptavidin. Eng. Life Sci. 15, 627–639.
Ni, Y., Reye, J., Chen, R.R., 2007. lpp deletion as a permeabilization method. Biotechnol. Bioeng. 97, 1347–1356.
Nogueira, E.S., Schleier, T., Dürrenberger, M., Ballmer-Hofer, K., Ward, T.R., Jaussi, R., 2014. High-level secretion of recombinant full-length streptavidin in *Pichia pastoris* and its application to enantioselective catalysis. Protein Expr. Purif. 93, 54–62.
Rösli, C., Rybak, J.-N., Neri, D., Elia, G., 2008. Quantitative recovery of biotinylated proteins from streptavidin-based affinity chromatography resins. Methods Mol. Biol. 418, 89–100.
Pähler, A., Hendrickson, W.A., Kolks, M.A., Argaraña, C.E., Cantor, C.R., 1987. Characterization and crystallization of core streptavidin. J. Biol. Chem. 262, 13933–13937.
Pugsley, A.P., 1993. The complete general secretory pathway in gram-negative bacteria. Microbiol. Rev. 57, 50–108.
Sambrook, J., 1989. Molecular Cloning: A Laboratory Manual. Cold Spring Harbor Laboratory Press, New York.
Sano, T., Cantor, C.R., 1990. Expression of a cloned streptavidin gene in *Escherichia coli*. Proc. Natl. Acad. Sci. U. S. A. 87, 142–146.
Sano, T., Pandori, M.W., Chen, X., Smith, C.L., Cantor, C.R., 1995. Recombinant core streptavidins. J. Biol. Chem. 270, 28204–28209.
Selvamani, R.S.V., Telaar, M., Friehs, K., Flaschel, E., 2014. Antibiotic-free segregational plasmid stabilization in *Escherichia coli* owing to the knockout of triosephosphate isomerase (tpiA). Microb. Cell Fact. 13, 58.
Shin, H.D., Chen, R.R., 2008. Extracellular protein production from an *Escherichia coli* lpp deletion mutant. Biotechnol. Bioeng. 101, 1288–1296.
Skerra, A., Schmidt, T.G.M., 1999. Applications of a peptide ligand for streptavidin: the strep-tag. Biomol. Eng. 16, 79–86.
Wang, W.W.-S., Das, D., Suresh, M.R., 2005. Biotin carboxyl carrier protein co-purifies as a contaminant in core-streptavid in preparations. Mol. Biotechnol. 31, 29–40.
Wu, S.-C., Wong, S.-L., 2002. Engineering of a *Bacillus subtilis* strain with adjustable levels of intracellular biotin for secretory production of functional streptavidin. Appl. Environ. Micobiol. 68, 1102–1108.
Wu, S.-C., Qureshi, M.H., Wong, S.-L., 2002. Secretory production and purification of functional full-length streptavidin from *Bacillus subtilis*. Protein Expr. Purif. 24, 348–356.
Wu, S.-C., Wong, S.-L., 2006. Intracellular production of a soluble and functional monomeric streptavidin in *Escherichia coli* and its application for affinity purification of biotinylated proteins. Protein Expr. Purif. 46, 268–273.
Yang, J., Moyana, T., MacKenzie, S., Xia, Q., Xiang, J., 1998. One hundred seventy-fold increase in excretion of an FV fragment-tumor necrosis factor alpha fusion protein (sFV/TNF-alpha) from *Escherichia coli* caused by the synergistic effects of glycine and triton X-100. Appl. Environ. Microbiol. 64, 2869–2874.
Zwart, S.R., Lewis, B.J., 2008. Optimization of detection and quantification of proteins on membranes in very high and very low abundance using avidin and streptavidin. Methods Mol. Biol. 418, 25–34.

Journal of Biotechnology

Supplementary material to

Constitutive production and efficient secretion of soluble full-length streptavidin by an *Escherichia coli* 'leaky mutant'

Jakob Michael Müller [*,a,b], *David Wetzel* [a,b], *Erwin Flaschel* [a], *Karl Friehs* [a], *and Joe Max Risse* [a]

[a] Lehrstuhl für Fermentationstechnik, Technische Fakultät, Universität Bielefeld, PF 10 01 31, D-33501 Bielefeld, Germany

[b] equal contribution

[*] e-mail: jmu@fermtech.techfak.uni-bielefeld.de · phone: +49 521 106 5299 fax: +49 521 106 6475 (secretary's office)

S1 – plasmid construction

The plasmids used for this study were created mainly by the isothermal assembly reaction described by Gibson et al. (2009). Primers used for the amplification of the fragments are shown in the following tables. Short descriptions of the cloning strategy are given below the tables. Gene sequences refer to coding sequences (CDS).

Tab. S1 Primers used for the construction of plasmids 7 to 10 (Tab. 1 in the main document). Primer pairs consisted of one forward (fwd) and one reverse (rev) primer.

primer designation	sequence (orientation: 5`→3`)	remark
primer 1 (fwd)	CCCCATCGGTGATGTCGGCGATATAGGC	Linearization of pET24a for insertion of LppBRP expression cassette
primer 2 (rev)	AAGATCGGGCTCGCCACTTCGGGCTCATG	
primer 3 (fwd)	GCCTATATCGCCGACATCACCGATGGGGAATTC GAGCTCGCTCTTGTCAAATTC	Amplification of P_{stat52} from plasmid p616 (Miksch et al. 2008)
primer 4 (rev)	CGCGCCCAGTACCAGTTTAGTAGCTTTCATAACT CGATCCTTATAAAATGAAAAG	
primer 5 (fwd)	ATGAAAGCTACTAAACTGGTACTGGGCGCGGTA ATCCTGGGTTCTACTCTGCTGGC	Amplification of LppBRP CDS from plasmid pBADLpp-BRPmalE, (Sommer et al. 2009)
primer 6 (rev)	CATGAGCCCGAAGTGGCGAGCCCGATCTTAGAG TTTGTAGAAACGCAAAAAGGCCATCC	
primer 7 (fwd)	ATGTATATCTCCTTCTTAAAGTTAAACAAAATTAT TTCTAGAGGGGAATTGTTATC	Linearization of pET24a for insertion of SAV CDS and secretion signal peptide
primer 8 (rev)	ACCACCACCACCACCACTGAGATCCGGCTGCTA ACAAAG	

Tab. S1 (continued) Primers used for the construction of plasmids 7 to 10 (Tab. 1 in the main document). Primer pairs consisted of one forward (fwd) and one reverse (rev) primer.

primer designation	sequence (orientation: 5`→3`)	remark
primer 9 (fwd)	TTGTGTGGGATCACTTCTAGTGTTTCGGCCGAC CCCTCCAAGGACTCGAAGGCCCAGGTC	Amplification of native SAV CDS from the genome of *S. avidinii*
primer 10 (rev)	GCCGGATCTCAGTGGTGGTGGTGGTGGTTTATT ACTGCTGAACGGCGTCGAGCGGGTTGC	
primer 11 (fwd)	TTATACCAAGTGCCAGTGATGCCAGCTTCAGCG GCCGAAACACTAGAAGTGATC	Amplification of *bglA* secretion signal sequence from plasmid p545 (Miksch et al. 2008)
primer 12 (rev)	CTTTAAGAAGGAGATATACATATGAAACGAGTGT TGCTAATTCTTGTCACCGG	
primer 13 (fwd)	GGCCGAAACACTAGAAGTGATCCC	Linearization of plasmid 7 (Tab. 1) for exchanging SAV CDS
primer 14 (rev)	ACCACCACCACCACCACTGAGATCC	
primer 15 (fwd)	GTGTGGGATCACTTCTAGTGTTTCGGCCCGCAA GATCGTCGTTGCAGCCATCG	Amplification of native SAV CDS including the native secretion signal peptide from *S. avidinii* genome
primer 10 (rev) (see also above)	GCCGGATCTCAGTGGTGGTGGTGGTGGTTTATT ACTGCTGAACGGCGTCGAGCGGGTTGC	
primer 16 (fwd)	GCCGGATCTCAGTGGTGGTGGTGGTGGTTTATT AGGACGCGGCAGATGGTTTCACTTTAG	Amplification of the codon-optimized core SAV gene from a vector synthesized by GeneArt
primer 17 (rev)	GCTGAAGCTGGCATCACTGGCACTTGGTATAAC CAGCTGGGTTCCACGTTCATTG	
primer 18 (fwd)	GTGTGGGATCACTTCTAGTGTTTCGGCCGATCC GTCCAAGGATTCTAAAGCGCAGGTATCTG	Amplification of the codon-optimized full length SAV gene from a vector synthesized by GeneArt
primer 19 (rev)	GATCTCAGTGGTGGTGGTGGTGGTTTATCACTG CTGTACCGCGTCCAGCGGATTACCGTTG	

Primers 1 to 19 (Tab. S1) were used to amplify fragments for plasmids 7 to 10 (Tab. 1). The general cloning strategy was to first introduce the LppBRP exression cassette inte the pET24 backbone. Primers 1 to 6 (Tab. 6) were used for this step. For construction of plasmid 7 (Tab. 1) the native SAV CDS and the *bglA* secretion signal were amplified as well as the plasmid backbone carrying the LppBRP expression cassette. Primers 7 to 12 were used for this second step. Starting from plasmid 7 (Tab. 1) plasmids 8 to 10 were constructed by introducing different variants of the SAV gene into the vector. For this purpose, primer 10 and primers 13 to 19 were used.

Tab. S2 Primers used for the construction of plasmid 1 to 6 (Tab. 1). Primer pairs consisted of one forward (fwd) and one reverse (rev) primer.

primer designation	sequence (orientation: 5`→3`)	remark
primer 20 (fwd)	ACTCTTCCTTTTTCAATATTATTGAAGCATTTATC	Linearization of plasmid backbone used for plasmids 1 and 2 (Tab. 1)
primer 21 (rev)	ATCCGGCTGCTAACAAAGCCCGAAAG	
primer 22 (fwd)	GGGCCTTCGAGTCCTTGGAGGGGTCGGCCGAA ACACTAGAAGTGATCCCACACAAAC	Amplification of *bglA* secretion signal sequence from plasmid p545 (Miksch et al. 2008)
primer 23 (rev)	CAATAATATTGAAAAAGGAAGAGTATGAAACGAG TGTTGCTAATTCTTGTCACCGGATTG	
primer 9 (fwd) (see also Tab. S1)	TTGTGTGGGATCACTTCTAGTGTTTCGGCCGAC CCCTCCAAGGACTCGAAGGCCCAGGTC	Amplification of native SAV CDS from the genome of *S. avidinii*
primer 24 (rev)	CTTTCGGGCTTTGTTAGCAGCCGGATTTATTACT GCTGAACGGCGTCGAGCGGGTTG	
primer 25 (fwd)	CGGTAAGAGTGCCAGTGCAATAGTGCTTTGTTTC ACACTCTTCCTTTTTCAATATTATTGAAGCATTTA TC	Linearization of plasmid 1 (Tab. 1) with deletion of *bglA* secretion signal sequence and introducing *phoA* secretion signal peptide using primer extensions
primer 26 (rev)	TTACTGTTTACCCCTGTGACAAAAGCCGACCCCT CCAAGGACTCGAAGGCCCAGGTCTC	
primer 27 (rev)	TTACTGTTTACCCCTGTGACAAAAGCCATGGATC CGTCCAAGGATTCTAAAGC	
primer 28 (fwd)	CAATACAGTATAGAACAAATTTGCAAATTTGGCA AGATGAATGTATTTAGAAAAATAAACAAATAGGG GTTCCGCGCACATTTC	Linearization of plasmid 1 (Tab. 1) with deletion promoter P_{bla} and introducing promoter P_{stat69} using primer extensions
primer 29 (rev)	AAGGAAGAGTATGAAACGAGTGTTGCTAATTCTT GTCACCGGATTG	
primer 16 (see also Tab. S1)	GCCGGATCTCAGTGGTGGTGGTGGTGGTTTATT AGGACGCGGCAGATGGTTTCACTTTAG	Amplification of the codon-optimized CDS coding for SAV
primer 30 (rev)	CTTTCGGGCTTTGTTAGCAGCCGGATTTATCACT GCTGTACCGCGTCCAGCGGATTACC	
primer 31 (fwd)	TGTATTTAGAAAAATAAACAAATAGGGGTTCCGC GCACATTTCC	Linearization of plasmid backbone used for plasmids 5 and 6 (Tab. 1)
primer 21 (rev) (see also above)	ATCCGGCTGCTAACAAAGCCCGAAAG	

Plasmids 1 to 6 (Tab. 1) were constructed starting with a different plasmid than before carrying the P_{bla} promoter as well as a tetracycline resistance marker. Primers used for this second set of plasmids are listed in Tab. S2. Cloning work started with plasmids 1 and 2 (Tab.1). Primers 20 and 21 were used for linearization of the backbone. In a first step primer 9 and primers 22 to 24 were used in order to introduce a native CDS coding for full-length SAV and the *bglA* secretion signal (plasmid 1, Tab. 1). For plasmid 2 (Tab. 1) primers 16 and 30 (Tab. S1 and S2) were used to amplify the condon-optimized SAV gene.

For construction of Plasmids 3 and 4 (Tab. 1) the *bglA* secretion signal sequence was exchanged by *phoA*. Therefore primers 28 and 29 were used before phosphorylation and self-ligation of the linearized plasmid (T4 polynucleotide kinase and T4 DNA ligase, Life Technologies GmbH, Darmstadt, Germany).

For introducing the P_{stat69} promoter (Miksch et al. 2005) instead of the P_{bla} promoter primers 28 and 29 were used resulting in plasmids 5 and 6 (Tab. 1) depending on which Plasmid was used for linearization (plasmid 1 oder 2, Tab. 1).

Tab. S3 Primers used for the construction of plasmid 11 (Fig. S2). Primer pairs consisted of one forward (fwd) and one reverse (rev) primer.

primer designation	sequence (orientation: 5`→3`)	remark
primer 31 (fwd)	AGAAGGAGATATACATATGGACGTCGAAGCCTG GCTTGGTGCGCGTGTACCGCTGGTGGAAACCTA ATAGTGCTCCAGGTACCCAAAAAACCCCTCAAG A	Linearization of plasmid 1 (Tab. 1) for introduction of promoter CP25 and Nanotag 15 CDS using primer extensions
primer 32 (rev)	TAAAAACAGTACTATGTGATTATACCAGCCCCCT CACTACATGTCAAGAATAAACTGCCAAAGCAAGA CTGGCCTCATGGGCCTTC	

Primers 31 and 32 (Tab. S3) were used for linearization of plasmid 1 (Tab. 1). Promoter CP25 and Nanotag 15-CDS were introduced using primer extensions. After phosphorylation the linearized plasmid was ligated. The resulting plasmid was plasmid 11 (Fig. S2).

S2 – effect of various media supplements on product concentration and biomass

Different supplements were tested to compare their effect on the formation of streptavidin and biomass. Results are shown in Fig. S1.

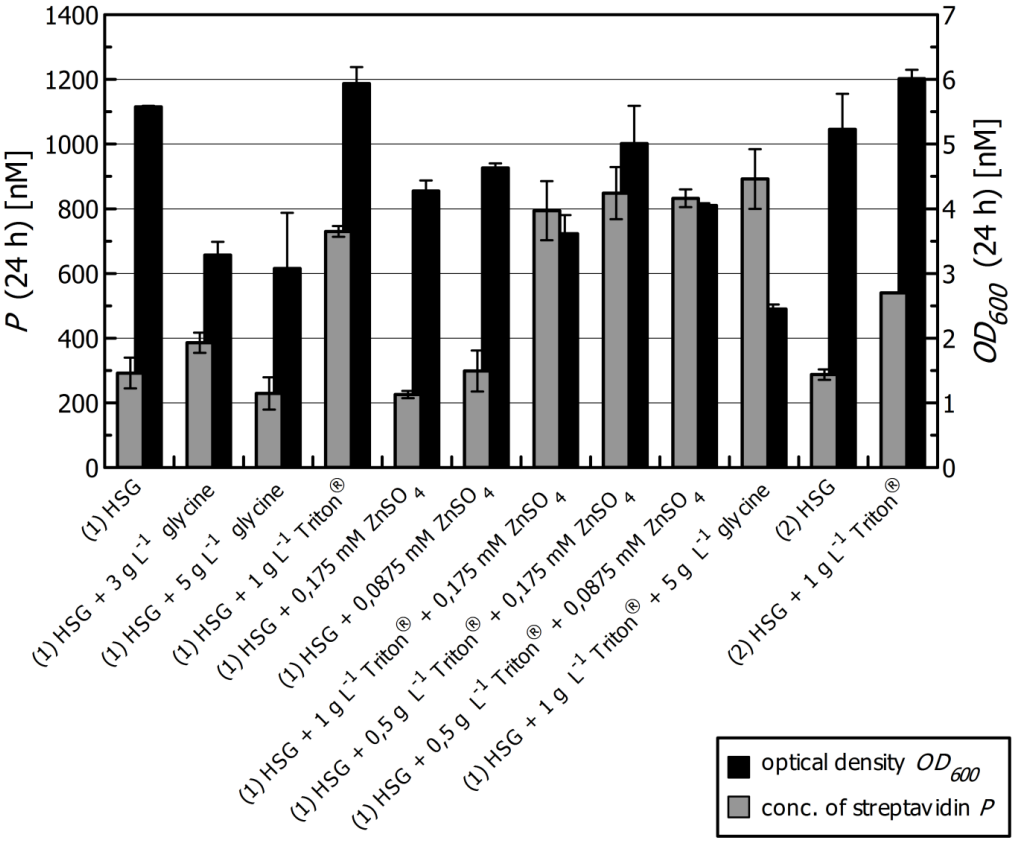

Fig. S1 Effect of permeabilizing compounds glycine, Triton® X-100 and $ZnSO_4$ on extracellular product concentrations. *E. coli* JW1667-5 carrying variants of a plasmid either containing the native (plasmid 1, Tab. 1) or the codon-optimized (plasmid 2) SAV gene was cultivated in 24-well plates in 3 mL of HSG medium supplemented by different permeabilizing substances at 30 °C. Reference cultures without supplements are designated 'HSG'. The cultures were harvested 24 h post inoculation. The bars show the extracellular concentration of biotin-free, tetrameric SAV *P* and the optical density at 600 nm OD_{600}. The number in parenthesis indicates the plasmid used.

In an additional experiment, glycine was supplemented to HSG medium in concentrations of 1 to 10 g L^{-1}, which did also not improve the streptavidin productivity (data not shown).

S3 – additional plasmid variants

Two additional concepts were tested for their potential to reduce the toxicity of streptavidin to the host *E. coli* JW1667-5: a construct expressing the full-length native streptavidin gene including its native secretion signal peptide and a co-expression-based construct for the simultaneous expression of the streptavidin-binding Nanotag 15 (Lamla and Erdmann 2004) under control of the strong constitutive promoter CP25 (Jensen and Hammer 1998). Both constructs were evaluated due to their potential ability to block fractions of the free binding

sites in the cytoplasm by either the native signal peptide or the streptavidin-binding peptide tag, thus potentially reducing the availability of the sites for biotin. The corresponding plasmid maps are shown in Fig. S2.

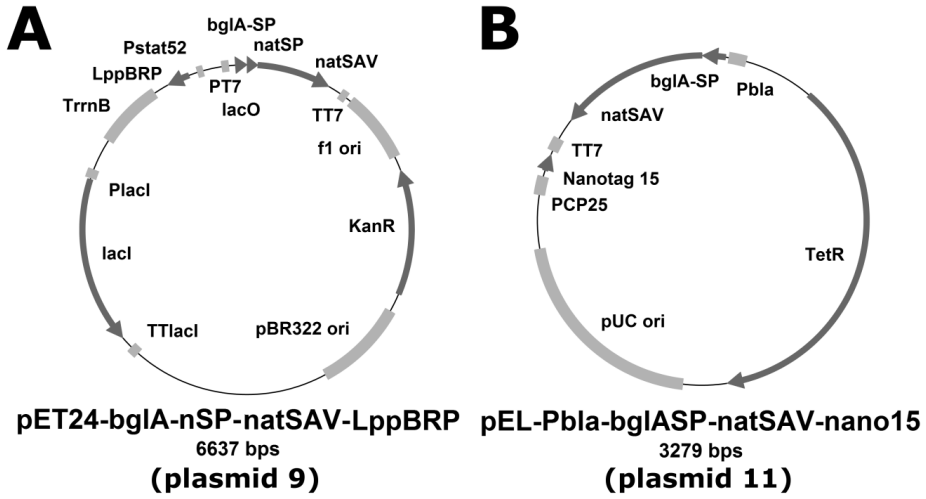

Fig. S2 Additional plasmid variants constructed and used for *E. coli* KRX (plasmid 9, A) and *E. coli* JW1667-5 (plasmid 11, B). The vectors contained either a kanamycin resistance gene (KanR, pET24) or a tetracycline (TetR, pEL). Origins of replication were either pBR322- (pET24) or pUC-based (pEL). Promoters are designated by P, terminators by T. Further relevant features: P_{bla} = *bla* promoter, P_{T7} = T7 promoter, bglA-SP = *bglA* secretion signal peptide from *B. amyloliquefaciens*, natSAV = native streptavidin gene from *S. avidinii*, T_{T7} = T7 transcription terminator, T_{rrnB} = *E. coli rrn*B transcription terminator (Brosius et al. 1981), P_{stat69} = stationary phase promoter 69 (Miksch et al. 2005), natSP = native SAV secretion signal peptide from *S. avidinii*, co-expression of peptide tag: P_{CP25} = CP25 promoter (Jensen and Hammer, 1998), Nanotag 15 = CDS for Nanotag 15 (Lamla and Erdmann 2004), co-expression of BRP gene: P_{stat52} = stationary phase promoter 52 (Miksch et al. 2005), LppBRP = optimized bacteriocin release protein (Miksch et al. 2008).

The plasmid variant based on the native signal peptide and SAV gene yielded 131 ± 7 nM in an expression study with *E. coli* KRX (24-well plate, 30 °C, 48 h of cultivation, HSG medium supplemented with 1 g L^{-1} of rhamnose, 0.01 mM of IPTG and 1 g L^{-1} of Triton® X-100) as opposed to 550 nM in the reference cultivation (see main document).

Co-expression of the Nanotag 15 led to reduced concentrations of SAV (100 ± 19 nM vs. 377 ± 9 nM after 48 h of cultivation) in 24-well plates at 30 °C in the absence of the surfactant when compared to the reference vector (plasmid 1 in the main document). Supplementation by Triton® X-100 led to an even more pronounced difference.

S3 – variation of surfactants in shake flasks for the scale-up to bioreactors

Due to excessive foaming in early bioreactor experiments, shake flask experiments were performed to analyze, whether titration of the foaming effect of the surfactant by an antifoam agent (Pluronic® PE 8100) was possible and if this strategy had an impact on product secretion.

To analyze the impact of the choice of surfactant on the performance of *Escherichia coli* JW1667-5 carrying plasmid pEL-Pbla-bglASP-natSAV (plasmid 1, Tab. 1 in the main

document), different surfactants were supplemented in a concentration of approximately 0.5 g L^{-1} to cultures of the strain in HSG medium in the presence of 25 mg L^{-1} of tetracycline. Cultivation was performed in 300 mL unbaffled shake flasks filled with 30 mL of medium at 28 °C and a shaking frequency of 150 min^{-1} (shaking diameter: 5 cm). The flasks were directly inoculated from a glycerol stock with a volume fraction of 0.1 % (v/v) (30 µL). Antifoam agent was supplied to shake flasks as indicated in the caption of Fig. S3. The concentration of necessary antifoam agent was derived from bioreactor experiments at high volumetric flow rates. Samples were taken after 20 and 46 h, respectively. Results are shown in Fig. S3.

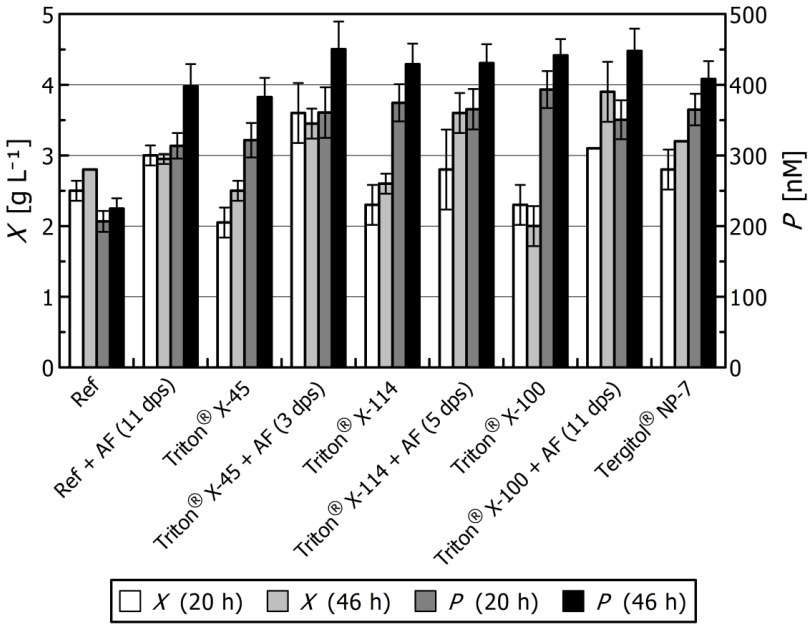

Fig. S3 Cultivation of *E. coli* JW1667-5 carrying plasmid 1 (Tab. 1) in unbaffled shake flasks at 28 °C in HSG medium in the presence of various surfactants. Abbreviations: Ref = reference culture (no surfactant), AF = antifoam agent (Pluronic® PE 8100), dps = drops of antifoam agent per 60 mL of medium. Cultivations were performed in duplicates. Each sample was analyzed twice (n = 2x2), resulting in standard deviations calculated from four measurements.

Studies applying Triton® X-100 caused the necessity of large amounts of the antifoam agent. Foam formation for 5 drops of surfactant was successfully avoided by the addition of 54 drops of Pluronic®. Moreover, the properties of foam formation and stability of Triton® X-100 were not optimal. Thus, a selection of Triton® variants was screened for less stable foam and reduced foam formation. Triton® contains a hydrophilic polyethylene oxide chain, which differs in length for different commercial agents. Triton® X-100 is characterized by an average chain length of 9.5. According to the supplier information, shorter chain lengths should result in a decrease of both foam formation and stability. The two surfactants Triton® X-114 (average chain length: 7.5) and Triton® X-45 (average chain length: 5) showed improved properties in this respect. Triton® X-45 showed the additional advantage that foam was rapidly mechanically disrupted by the impact of the foam disruptor in the bioreactor. Both surfactants needed less antifoam agent for reduced foaming. For Triton® X-45, 12 drops of antifoam agent were sufficient per 5 drops of the surfactant when mixed in 300 mL of medium in the bioreactor.

Triton® X-45 was chosen for the following studies in the bioreactor, since the smallest amount of antifoam agent was necessary to prevent foam formation and the extracellular product concentration was among the highest in the experiment.

Combinations of Triton® and antifoam agent were found to result in higher apparent biomass concentrations and a higher turbidity already in the beginning of cultivation. Furthermore, the initial biomass concentrations of fermentations in a bioreactor in the presence of both compounds were higher than expected when compared to the optical density of the inoculum. This effect is most likely due to insoluble aggregates formed by the two supplements, rather than to an actual increase of the biomass concentration.

S4 – Additional batch fermentation

S4.1 Batch experiments

Additional fermentations in the bioreactor were performed to characterize the performance of *Escherichia coli* JW1667-5 carrying plasmid 1 (Tab. 1). As the twofold concentrated HSG medium resulted in an improved performance of the strain, a threefold concentrate with twofold concentrated salts (sodium chloride, potassium phosphate and magnesium sulfate) was tested. The corresponding plot is shown in Fig. S4.

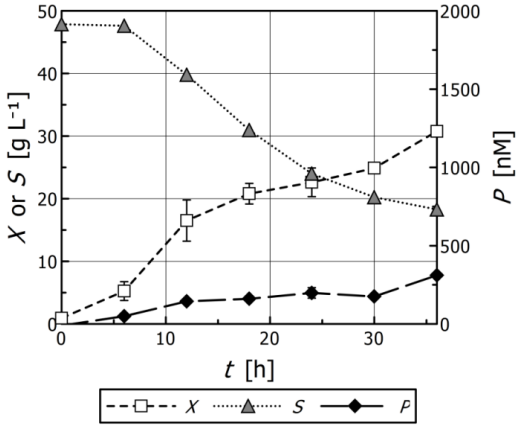

Fig. S4 Batch cultivation of *E. coli* JW1667-5 carrying plasmid 1 (Tab. 1) in 3fold concentrated HSG medium (twofold concentrated salts) in the bioreactor at 30 °C. Abbreviations: *X* = dry cell weight concentration, *S* = substrate concentration (glycerol), *P* = extracellular streptavidin concentration, *t* = cultivation time.

Fig. S4 shows that the 3fold concentrate results in an improved biomass production, but at the same time causes a decreased SAV concentration. Therefore, this medium was not used for further experiments.

Additional references

Brosius J, Ullrich A, Raker MA, Gray A, Dull TJ, Gutell RR, Noller HF (1981) Construction and fine mapping of recombinant plasmids containing the *rrn*B ribosomal RNA operon of *E. coli*. Plasmid 6:112-118

5.2.5 Additional information: coexpression of inhibitors

As described in the article, the production of SAV by *E. coli* typically leads to toxic effects on the host. Thus, parts of the experiments focused on the coexpression of potential inhibitors of toxicity. For this purpose, one of the constructs allowed the cytoplasmic coexpression of the Nano-tag$_{15}$ (Lamla & Erdmann, 2004) under control of the synthetic, strong, and constitutive promoter CP25 (Jensen & Hammer, 1998). This strategy was performed to prevent cytoplasmic biotin from binding to folded SAV in this cellular compartment by the competition of peptide tag and vitamin for the binding pocket of SAV (and ideally displacement of SAV-bound biotin). The inhibitor was chosen based on the favorable affinity for SAV and the low molecular weight of the peptide analogue towards potential nucleic acid-based inhibitors (see Table 2.1, p. 7).

To investigate on a theoretical basis whether this is a promising strategy, the concept was analyzed by modelling.

5.2.5.1 Modelling of the competition: model development

The model was based on the assumption that during competition for the binding pocket of SAV the species of free SAV and the complexes SAV-biotin, and SAV-inhibitor approach a steady state, in which all corresponding concentrations are constant. This assumption leads to the consequence that the respective association and dissociation terms have to level out. The change of concentrations of the complexes SAV-biotin c_{SB} and SAV-inhibitor c_{SI} can thus be described by the following differential equations:

$$\frac{\mathrm{d}c_{SB}}{\mathrm{d}t} = c_{SAV} \cdot c_B \cdot k_{b+} - c_{SB} \cdot k_{b-} \approx 0 \tag{5.1}$$

$$\frac{\mathrm{d}c_{SI}}{\mathrm{d}t} = c_{SAV} \cdot c_I \cdot k_{i+} - c_{SI} \cdot k_{i-} \approx 0 \tag{5.2}$$

where c_{SAV} is the concentration of free SAV and k_{i+} and k_{i-} are the rate constants for the association and dissociation for the binding and release of the inhibitor to SAV, respectively. Corresponding constants can be defined for biotin ($k_{b+/-}$).

Generally, association and dissociation of the SAV-inhibitor complex are characterized by equation 5.3.

$$SAV + I \underset{\mathrm{k}_{i-}}{\overset{\mathrm{k}_{i+}}{\rightleftharpoons}} SI \tag{5.3}$$

where SAV, I, and SI are the species of free SAV and inhibitor and SAV-inhibitor-complex, respectively.

Association and dissociation of the SAV-biotin complex can be depicted in a similar manner. In a steady state, both equations reach an equilibrium characterized by the corresponding dissociation constants $K_{d,i}$ and $K_{d,b}$, exemplarily shown for the SAV-inhibitor-complex:

$$K_{d,i} = \frac{k_{i-}}{k_{i+}} = \frac{c_{SAV} \cdot c_I}{c_{SI}} \tag{5.4}$$

as a ratio of the rate constants or the concentrations of dissociated and associated species.

The steady states of equations 5.1 and 5.2 may be combined with equation 5.4 and the analogous dissociation constant for the SAV-biotin-complex $K_{d,b}$ to yield:

$$\frac{\mathrm{d}c_{SB}}{\mathrm{d}t} = c_{SAV} \cdot c_B - c_{SB} \cdot K_{d,b} \approx 0 \tag{5.5}$$

$$\frac{\mathrm{d}c_{SI}}{\mathrm{d}t} = c_{SAV} \cdot c_I - c_{SI} \cdot K_{d,i} \approx 0 \tag{5.6}$$

where the new expressions are gathered via division of equations 5.1 and 5.2 by the rate constants k_{i+} and k_{b+} for the formation of the respective complexes.

In addition to this equilibrium, the mass balances for all species have to be fulfilled in the steady state. These balances are given in equations 5.7, 5.8 und 5.9.

$$n_{SAV,0} = n_{SAV} + n_{SI} + n_{SB} \tag{5.7}$$

$$n_{B,0} = n_B + n_{SB} \tag{5.8}$$

$$n_{I,0} = n_I + n_{SI} \tag{5.9}$$

where $n_{SAV,0}$, $n_{B,0}$, and $n_{I,0}$ are the overall (molar) amounts of SAV, biotin, and inhibitor, respectively, completed by the amounts of free and complex-bound species of these compounds in steady state conditions.

By combining these mass balances and equations 5.5 and 5.6 and assuming volume constancy,[1] a system of differential equations is acquired with the two unknown complex concentrations c_{SI} and c_{SB}:

$$\frac{\mathrm{d}c_{SB}}{\mathrm{d}t} = (c_{SAV,0} - c_{SI} - c_{SB}) \cdot (c_{B,0} - c_{SB}) - c_{SB} \cdot K_{d,b} \approx 0 \tag{5.10}$$

$$\frac{\mathrm{d}c_{SI}}{\mathrm{d}t} = (c_{SAV,0} - c_{SI} - c_{SB}) \cdot (c_{I,0} - c_{SI}) - c_{SI} \cdot K_{d,i} \approx 0 \tag{5.11}$$

Equations 5.10 and 5.11 can now be used for calculations of the steady state concentrations of both complexes for varying concentrations of biotin, SAV, and inhibitor as well as for different dissociation constants.

5.2.5.2 Modelling of the competition: results of the simulation

Simulation of the competition of biotin and the Nano-tag$_{15}$ ($K_{d,i} \approx 4$ nM, Lamla & Erdmann, 2004; see Table 2.1, p. 7) for the binding pocket of SAV was based on an intracellular concentration of biotin of 10 nM (data for *E. coli* K12, Prakash & Eisenberg, 1979) and a monomeric intracellular concentration of SAV of 50 nM, roughly based on the results of Miksch *et al.* (2008).

Three different scenarios for the dissociation constant of the SAV-biotin-complex were evaluated based on literature: $K_{d,b} = 10^{-12}$ M (Chivers *et al.*, 2010, 'best case'), $K_{d,b} = 2.5 \times 10^{-13}$ M (Reznik *et al.*, 1998, 'medium case'), and $K_{d,b} = 10^{-15}$ M (Sano *et al.*, 1996, 'worst case'). Results for the simulation are shown in Fig. 5.2.

Generally speaking, the model suggests that a quantitative displacement of biotin by the peptide tag is only probable for the two scenarios based on the data of Chivers *et al.* (2010) and Reznik *et al.* (1998). In these scenarios, cytoplasmic concentrations in the range of 1 g L^{-1} of inhibitor would suffice for the displacement of a majority of intracellular biotin. Based on Sano's scenario, however, the necessary concentration of inhibitor would be in the range of 10 to 100 g L^{-1}.

In addition to these problems, the strategy bears the risk of a leakage of inhibitor to the medium. This would cause blocked binding sites due to the peptide tag. Thus, the result that no improvements were visible for the coexpression of the peptide tag may either be due to insufficient intracellular concentrations of inhibitor or to blocking of secreted SAV. Therefore, this concept has to be rethought in detail for further investigations. Potential strategies to avoid leakage of the inhibitor may, e.g., involve fusion of the peptide tag to a protein or use of the larger SBP-tag (Keefe *et al.*, 2001) (see Table 2.1, 7) to achieve properties favoring retention of the inhibitor in the cytoplasm.

[1] allowing direct conversion of the mass balances to concentrations

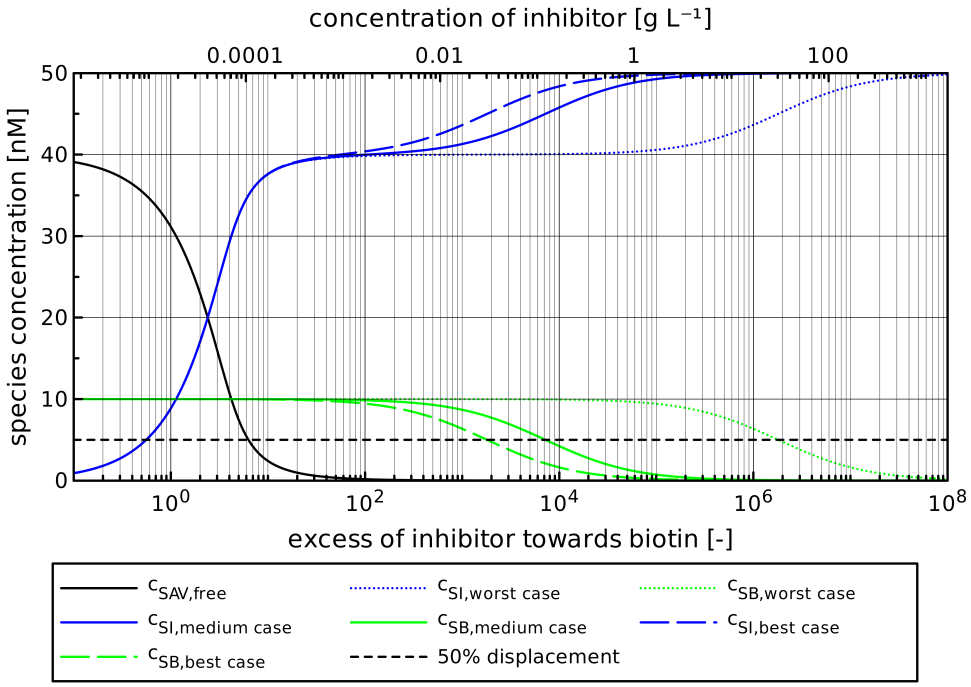

Fig. 5.2: Simulation of the competition of biotin and Nano-tag$_{15}$ for the binding pocket of SAV based on equations 5.10 and 5.11. Parameters: $c_{SAV,0} = 50\,\text{nM}$ (monomeric), $c_{B,0} = 10\,\text{nM}$ (Prakash & Eisenberg, 1979), worst case: $K_{d,b} = 10^{-15}$ (Sano *et al.*, 1996), medium case: $K_{d,b} = 2{,}5{\times}10^{-13}$ (Reznik *et al.*, 1998), best case: $K_{d,b} = 10^{-12}\,\text{M}$ (Chivers *et al.*, 2010). Abbreviations of the species concentrations: $c_{SAV,free}$: concentration of biotin-free SAV, c_{SI}: concentration of SAV-inhibitor-complex, c_{SB}: concentration of SAV-biotin-complex. The course of the concentration of free SAV was identical for all scenarios.

5.3 Production of SAV by *Pichia pastoris*

More than 600 genes have successfully been heterologously expressed by the yeast *P. pastoris* by the end of 2007 (Zhang *et al.*, 2009). The organism can thus be considered one of the key hosts for eukaryotic heterologous protein production. The popularity of *P. pastoris* is derived from various extraordinary properties like facile growth to DCW concentrations of up to $160\,g\,L^{-1}$ in fed-batch operation in synthetic media (Jahic *et al.*, 2002), the availability of the tightly regulated and very strong methanol-inducible AOX1 promoter (Ellis *et al.*, 1985), a high secretion efficiency for heterologous proteins (Cregg *et al.*, 2000), and a low number of contaminating extracellular host proteins (Cregg *et al.*, 1993). The host is also capable of performing various posttranslational modifications on the target protein (Cregg *et al.*, 2000). Typical extracellular concentrations of heterologous proteins range from several hundred milligrams to some grams per liter of supernatant, emphasizing the remarkable potential of this host (Cos *et al.*, 2006; Macauley-Patrick *et al.*, 2005; Cereghino *et al.*, 2002).

Unlike *E. coli*, *P. pastoris* naturally requires the supplementation of biotin to the cultivation medium, potentially complicating the heterologous production of biotin-binding proteins. Only recently, Gasser *et al.* (2010) created biotin prototrophic strains of *P. pastoris* by genetic engineering. Despite this fact, production of SAV by this host was successfully established by Nogueira *et al.* (2014) and Casteluber *et al.* (2012), applying common biotin auxotrophic producer strains. The general suitability for the production of biotin-binding proteins was furthermore demonstrated by the successful expression of avidin genes (Zocchi *et al.*, 2003; Jungo *et al.*, 2007a).

5.3.1 Goals of this study

The heterologous production processes of Nogueira *et al.* (2014) and Casteluber *et al.* (2012) were dependent on the flammable and toxic organic solvent methanol for induction (Zhang *et al.*, 2009). As corresponding processes cause problems of heat evolution (Niu *et al.*, 2013) and oxygen demand (Khatri & Hoffmann, 2006) on the industrial level, the goal of this study was to establish a methanol-free production system for SAV based on this yeast.

5.3.2 Manuscript

The results were accepted for publication in Biotechnology Progress (Müller *et al.*, 2016a) (Copyright Wiley-VCH Verlag GmbH & Co. KGaA. Reproduced with permission.). The revised manuscript used for submission and the supporting information are shown hereinafter.

GAP Promoter-Based Fed-Batch Production of Highly Bioactive Core Streptavidin by *Pichia pastoris*

Jakob Michael Müller
Lehrstuhl Für Fermentationstechnik, Technische Fakultät, Universität Bielefeld, PF 10 01 31, Bielefeld D-33501, Germany

Simon Bruhn
Lehrstuhl Für Fermentationstechnik, Technische Fakultät, Universität Bielefeld, PF 10 01 31, Bielefeld D-33501, Germany

Erwin Flaschel
Lehrstuhl Für Fermentationstechnik, Technische Fakultät, Universität Bielefeld, PF 10 01 31, Bielefeld D-33501, Germany

Karl Friehs
Lehrstuhl Für Fermentationstechnik, Technische Fakultät, Universität Bielefeld, PF 10 01 31, Bielefeld D-33501, Germany

Joe Max Risse
Lehrstuhl Für Fermentationstechnik, Technische Fakultät, Universität Bielefeld, PF 10 01 31, Bielefeld D-33501, Germany

DOI 10.1002/btpr.2283
Published online May 4, 2016 in Wiley Online Library (wileyonlinelibrary.com)

Streptavidin is a homotetrameric protein binding the vitamin biotin and peptide analogues with an extremely high affinity, which leads to a large variety of applications. The biotin-auxotrophic yeast Pichia pastoris *has recently been identified as a suitable host for the expression of the streptavidin gene, allowing both high product concentrations and productivities. However, so far only methanol-based expression systems have been applied, bringing about increased oxygen demand, strong heat evolution and high requirements for process safety, causing increased cost. Moreover, common methanol-based processes lead to large proportions of biotin-blocked binding sites of streptavidin due to biotin-supplemented media. Targeting these problems, this paper provides strategies for the methanol-free production of highly bioactive core streptavidin by* P. pastoris *under control of the constitutive* GAP *promoter. Complex were superior to synthetic production media regarding the proportion of biotin-blocked streptavidin. The optimized, easily scalable fed-batch process led to a tetrameric product concentration of up to* 4.16 ± 0.11 μM *of biotin-free streptavidin and a productivity of 57.8 nM* h^{-1} *based on constant glucose feeding and a successive shift of temperature and* pH *throughout the cultivation, surpassing the concentration in un-optimized conditions by a factor of 3.4. Parameter estimation indicates that the optimized conditions caused a strongly increased accumulation of product at diminishing specific growth rates (*$\mu \approx D < 0.01\ h^{-1}$*), supporting the strategy of feeding.* © 2016 American Institute of Chemical Engineers *Biotechnol. Prog.*, 32:855–864, 2016
Keywords: continuous shift of temperature and pH, biotin-free streptavidin, bioreactor fed-batch process optimization, proteolysis, parameter estimation

Introduction

The homotetrameric protein streptavidin (SAV) is used as a tool for various molecular applications. Originally isolated from culture supernatants of *Streptomyces avidinii* and *Streptomyces lavendulae* in the 1960s,[1,2] its nearly universal applicability results from extraordinary binding properties for the vitamin biotin. The SAV-biotin interaction is characterized by a dissociation constant K_d in the range of 10^{-15} M and a remarkable biochemical stability in respect to extremes of *pH*, temperature, and other factors.[3–5] The interaction therefore provides useful properties for the purification and detection of various macromolecules, e.g. for affinity chromatography of proteins by the peptide-based Strep-tag® technology.[6] The biotin-binding ability of SAV is shared by several proteins from various species like variants produced by *Streptomyces venezuelae*,[7] avidin from chicken egg white or bradavidin from *Bradyrhizobium japonicum*.[8]

Natural SAV contains a core sequence essential for biotin-binding[9,10] surrounded by *C*- and *N*-terminal regions that are reported to reduce the stability of the protein and may decrease the accessibility of the binding pocket for biotinylated macromolecules.[11] Thus, truncated forms of SAV, typically containing 118 to 127 amino acids (AA) instead of the 159 AA of mature full-length SAV, are commonly used for

Additional Supporting Information may be found in the online version of this article.

Correspondence concerning this article should be addressed to Jakob Michael Müller at jmu@fermtech.techfak.uni-bielefeld.de

heterologous expression. These are referred to as "core streptavidins."

Sano and Cantor[12] were the first to publish a heterologous expression system for the SAV gene in *Escherichia coli*. Since then, multiple studies were based on this host.[13–17] The production of SAV by *Bacillus subtilis* has also been studied extensively.[18–20] Due to limited secretory efficiency and/or cytoplasmic expression, these hosts commonly suffer from intracellular binding of biotin by SAV. As this vitamin is an important cofactor involved in carboxylation reactions in the central metabolism of pro- and eukaryotes,[21,22] biotin deprivation strongly limits growth and therefore the accumulation of SAV in most heterologous producers.

Although *Pichia pastoris* is known to be a suitable host for the expression of the biotin-binding protein avidin since the early 2000s,[23] the SAV gene has only recently been expressed in this yeast. Publications on the expression of both core[24] and full-length SAV[25] in *P. pastoris* resulted in remarkable concentrations of up to 4 g L^{-1} (71 μM)* and 0.65 g L^{-1} (11 μM) of SAV, respectively. Comparable product concentrations have so far only been reported for the secretion of the protein by the natural producer *S. avidinii*,[26] documenting the outstanding properties of *P. pastoris* as a host for heterologous protein production. However, both studies were based on the methanol-inducible alcohol oxidase 1 (*AOX*1, abbreviated *AOX* hereinafter) promoter. This causes high requirements for process management and safety due to the flammable and toxic properties of the organic solvent,[27] leading to increased cost. Furthermore, for the cultivation of Mut^+ (methanol utilization plus) strains containing an intact *AOX*1 gene, the use of methanol is accompanied by a strong increase in heat evolution[28,29] and oxygen demand, leading to challenges in fermentation processes.[30,31] Finally, methanol brings about specific by-products like formaldehyde and hydrogen peroxide.[32] Thus, production systems designed for a methanol-free expression of the gene of interest are desirable.

One of the major drawbacks for the expression of the SAV gene by *P. pastoris* is caused by the biotin auxotrophy of the commonly used wild type strains. Only recently engineered, biotin-prototrophic strains have been designed.[33] For that reason, fermentations typically rely on biotin supplementation of the media, resulting in a decreased yield of bioactive SAV due to biotin-blocked binding sites. Typical proportions of bioactive binding sites are in the range of 3.2 free binding sites per tetramer of SAV.[25]

Biotin-deficiency of the yeast *Saccharomyces cerevisiae* results in a reduced content of DNA, RNA and total protein,[34] and AA depletion.[35] These effects can partly be compensated by supplementation of media with aspartic acid, oleic acid or Tween 80 as a source of fatty acids.[36,37]

A commonly used, strong promoter for the methanol-independent gene expression by *P. pastoris* is the glyceraldehyde-3-phosphate (*GAP*) dehydrogenase promoter (P_{GAP}) from the central carbon metabolism.[38] Operational strategies for this promoter were recently reviewed.[39] Although constitutive, the expression level of P_{GAP} depends on the specific growth rate of the host[40] and the carbon source, showing stronger expression for glucose and glycerol than for methanol.[27,38,41] Fructose was identified as another promising candidate.[42]

This study addressed the two major challenges of SAV production by *P. pastoris*: The dependency on methanol when using the *AOX* promoter accompanied by the solvent-associated problems discussed above and the high proportion of inactive SAV due to its production in biotin-supplemented media. These problems were targeted by a P_{GAP}-based expression system and a step-wise optimization approach of culture conditions for increased concentrations of bioactive SAV.

Materials and Methods

Strains, vector construction, and transformation in E. coli

E. coli DH5α™ (Invitrogen/Life Technologies, Darmstadt, Germany) was used for vector manipulation and amplification. Expression of the SAV gene was performed by the *P. pastoris* strain X-33 (Life Technologies). The expression vector was constructed using the pUC-based pPpT4_GAP_αS vector backbone (*Pichia* Pool/TU Graz, Graz, Austria),[43] designed for the constitutive, secretory expression of the gene of interest in *P. pastoris* by use of the *GAP* promoter and the α-mating factor secretion signal from *S. cerevisiae*. Further elements include the *AOX* terminator after the gene of interest and a Zeocin™-resistance gene for selection of transformants of *P. pastoris* and *E. coli*, respectively.

The vector backbone was linearized by PCR and joined to a core SAV gene (AA 13-139), which was amplified from the genome of *S. avidinii* CBS 730.32 (Centraalbureau voor Schimmelcultures, Utrecht, Netherlands), by isothermal assembly at 50°C for 1 h, as described by Gibson et al.[44] The Gibson Assembly Mastermix was purchased from NEB (New England Biolabs, Frankfurt/Main, Germany).

The construct was used for electroporation of *E. coli* DH5α™ cells, which were prepared according to standard laboratory procedures.[45] Transformants were plated on selective LB agar (5 g L^{-1} yeast extract, 10 g L^{-1} tryptone, 10 g L^{-1} NaCl, 15 g L^{-1} agar) supplemented with 100 mg L^{-1} of Zeocin™ (Invivogen, Toulouse, France). The plates were incubated overnight at 37°C. Clones were characterized by plasmid isolation, restriction analysis, and DNA sequencing (Sequencing Core Facility, Bielefeld University, Bielefeld, Germany). Positive clones were cultivated overnight in 300 mL shake flasks with 30 mL of LB medium supplemented with Zeocin™ to a final concentration of 50 mg L^{-1} for plasmid isolation for the transformation of *Pichia pastoris*.

Transformation of P. pastoris *and clone characterization*

Competent *P. pastoris* X-33 cells were prepared, transformed and plated according to Lin-Cereghino et al.[46] For transformation, approximately 4 μg of plasmid DNA were linearized via overnight digestion by BamHI, purified by PCR clean-up, and concentrated by a vacuum concentrator (SpeedVac™, Thermo Fisher Scientific, Waltham, USA). Screening for producers was performed in 24 well v-bottom deepwell microplates (Axygen Scientific, Schwerte, Germany).

Bioreactor fermentation

Bioreactor experiments were performed in a sixfold fermentation system in unbaffled vessels (Sixfors, Infors HT,

*Homotetrameric concentration, calculation based on a molecular weight of 56 kDa.

Bottmingen, Switzerland) with a maximal volume of 500 mL and an initial filling volume of 400 mL. Three rushton impellers, one propeller impeller and one mechanical foam disruptor were installed in the vessels from bottom to top. Cells were cultivated at 30°C, 1000 min^{-1} and an air flow rate of 0.48 NL min^{-1} (1.2 vvm). The input air was pre-saturated by water vapor. The *pH* value was controlled by the automatic addition of 20% (w/w) H_3PO_4 and 25% (w/w) NH_3. The latter also served as nitrogen source. One drop per 100 mL of antifoam agent (Pluronic 8100, BASF, Ludwigshafen, Germany) was supplemented to the medium. Automatic sampling was performed by fraction collectors, instantly cooling the samples to 4°C. The bioreactors were inoculated to reach an OD_{600} of 0.2 or 0.5 by an overnight shake flask culture in Zeocin™-free YPD medium.

First cultivations were performed in synthetic basal salt medium (BSM)[47] supplemented with the PTM1 trace salt solution. BSM composition was 26.7 mL L^{-1} of 85% (w/w) H_3PO_4, 0.93 g L^{-1} $CaSO_4$, 18.2 g L^{-1} K_2SO_4, 14.9 g L^{-1} $MgSO_4 \cdot 7\ H_2O$, 4.13 g L^{-1} KOH, and 40.0 g L^{-1} glycerol or glucose. Glucose and the PTM1 solution were sterilized separately by autoclaving and sterile filtration, respectively. A volume of 4.35 mL of PTM1 was added per L of BSM medium. This solution contained 6.0 g L^{-1} $CuSO_4 \cdot 5\ H_2O$, 0.08 g L^{-1} NaI, 3.0 g L^{-1} $MnSO_4 \cdot H_2O$, 0.2 g L^{-1} $Na_2MoO_4 \cdot 2\ H_2O$, 0.02 g L^{-1} H_3BO_3, 0.5 g L^{-1} $CoCl_2$, 20.0 g L^{-1} $ZnCl_2$, 65.0 g L^{-1} $FeSO_4 \cdot 7\ H_2O$, 0.2 g L^{-1} biotin and 5.0 mL L^{-1} 98% (w/w) H_2SO_4. BSM-based processes usually were performed at *pH* 5.0.

Two complex media (YPD and MGY) were tested in further experiments at *pH* 6.0. YPD composition was (per L) 20 g soy peptone (UD Chemie, Wörrstadt, Germany), 10 g yeast extract (Ohly, Hamburg, Germany), 20 g glucose, *pH* 7.0. MGY medium[47] was additionally supplemented with 13.4 g L^{-1} of yeast nitrogen base without AA and with ammonium sulfate (YNB, Difco, BD, Heidelberg, Germany), which was sterile-filtered as a 10x concentrate and supplemented after sterilization. Glucose was sterilized separately.

Feed solutions were either based on concentrates of the medium or glucose and were supplemented with 2 mL per 100 mL of a biotin-free PTM1 solution in the latter case.

For the final fed-batch process strategy based on MGY medium, feeding of an aqueous 500 g L^{-1} solution of glucose was initiated after 20 h of cultivation at a constant flow rate of 2 mL h^{-1} (approx. 5 mL L^{-1} h^{-1} based on the initial cultivation volume). The setpoints of *pH* and temperature were successively shifted throughout the cultivation from 6.0 to 4.0 and 30°C to 24°C, respectively.

Analytical methods: Biomass, product and substrate

The dry cell weight (DCW) concentration X was determined by differential weighing of cell pellets in pre-dried and pre-weighed 1.5 mL reaction tubes acquired from 1 mL of culture washed twice in demineralized water (centrifugation at 13,000 min^{-1} for 10 min). Pellets were dried at 50°C until constancy of weight was reached (typically after 48 h).

SAV was quantified by the fluorescence quenching assay developed by Kada et al.[48,49] using a calibration curve of biotin-4-fluorescein (B4F, GERBU Biotechnik, Heidelberg, Germany) in concentrations equivalent to 0-600 nM of tetrameric SAV. The measurement buffer consisted of 100 mM NaCl, 1 mM EDTA and 50 mM NaH_2PO_4 adjusted to *pH* 7.5. Prior to measurements, the buffer was supplemented with 0.1 g L^{-1} bovine serum albumin (BSA, GERBU Biotechnik) and 50 nM of B4F. Samples of 20 µL were added to 980 µL of this solution, vortexed and incubated at RT for 30 min, followed by fluorescence measurement in a RF-5301 PC fluorimeter (Shimadzu Deutschland, Duisburg, Germany; excitation: 495 nm, emission: 525 nm) in disposable semi-micro PS cuvettes (BRAND, Wertheim, Germany).

HPLC analysis of glycerol and glucose was performed as described elsewhere.[26] Where indicated, glucose was analyzed by an enzyme-based kit (ENZYTEC™ D-Glucose/D-Fructose, R-Biopharm, Darmstadt, Germany).

Quantification of biotin-blocked binding sites

The quantification of biotin-blocked binding sites was performed by the displacement of SAV-bound biotin by B4F via heat incubation as described previously.[50] SAV-containing supernatants were diluted to tetrameric concentrations ≤ 300 nM. Samples of 20 µL were mixed with 980 µL of measurement buffer with BSA and B4F and vortexed for 1 s. The solution was incubated at 70°C for 10 min in a laboratory heat block (VWR International, Darmstadt, Germany) with water-filled wells to allow binding of B4F to biotin-blocked binding sites. After heat incubation the solution was inverted threefold, incubated at RT for 30 min and analyzed by fluorescence quenching as described above. The proportion of biotin-blocked streptavidin Q_{blocked} [-] in the sample was calculated by Eq. (1):

$$Q_{\text{blocked}} = \frac{P_{\text{blocked}}}{P_{HT}} = \frac{P_{HT} - P_{RT}}{P_{HT}} \tag{1}$$

where P_{blocked} [nM of tetrameric SAV] is the concentration of biotin-blocked binding sites, P_{HT} [nM] is the SAV concentration measured after heat incubation at 70°C (overall streptavidin), and P_{RT} [nM] is the SAV concentration measured at room temperature (biotin-free binding sites of SAV).

Quantitative analysis of fermentation courses: Modelling

For a quantitative analysis, the fermentation courses were evaluated on the basis of a four-parameter logistic growth model as described in Eq. (2):[51]

$$X(t) = \frac{a-d}{1+\left(\frac{t}{c}\right)^b} + d \tag{2}$$

where X [g L^{-1}] is the DCW concentration, t [h] is the time and a (minimal asymptote), b (slope), c (inflection point), and d (maximal asymptote) represent the specific parameters. Where indicated, this model was also applied to describe the degradation of biomass.

Based on the resulting regression curve for X, calculations of the specific growth rate μ [h^{-1}] were performed according to Eq. (3):

$$\mu = \frac{1}{X}\frac{dX}{dt} + D \approx \frac{1}{X}\frac{dX}{dt} + \frac{F}{V} \tag{3}$$

where D [h^{-1}], which was only part of the calculations for fed-batch processes, is the dilution rate, corresponding to the ratio of the feed rate F [mL h^{-1}] and momentary cultivation volume V [mL]. The flow rate for sampling (approx. 1.7 mL h^{-1}) was considered for the volume balance of the fermenter. Maximal specific growth rates μ_{max} were determined

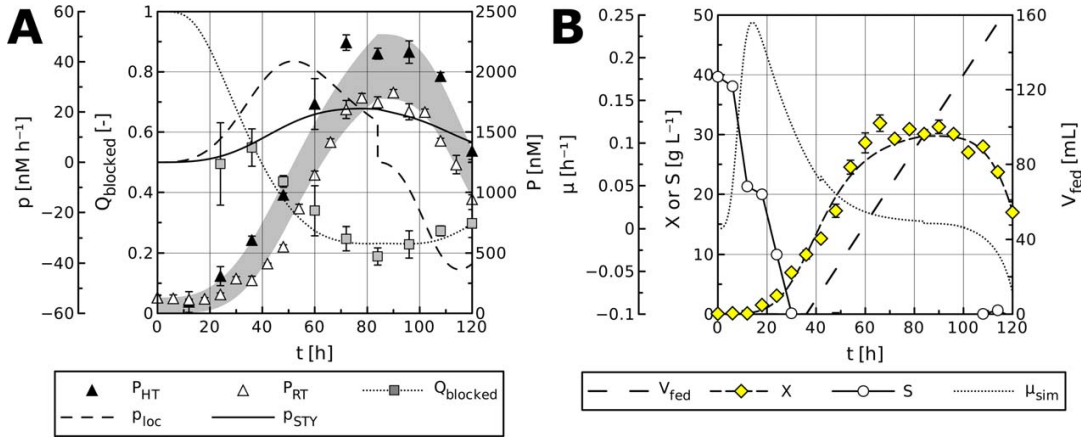

Figure 1. Fed-batch bioreactor cultivation of *P. pastoris* in BSM medium.

The standard biotin supplement, 40 g L^{-1} of glucose, and feeding of a 500 g L^{-1} glucose solution were applied. (A) Display of the productive properties. Product courses were directly fit to Eq. 2 to improve the accuracy of the local (p_{loc}) and overall productivity (p_{STY}). The shaded area represents the proportion of biotin-blocked SAV according to P_{HT} and P_{RT}, respectively (Eq. 1). (B) Feeding (fed volume V_{fed}) and consumption of substrate S, and specific growth rate μ. OD_{600} at inoculation: 0.2, μ_{max} ($X > 2$ g L^{-1}): 0.17 h^{-1}, end of the lag phase ($\mu > 0.01$ h^{-1}): 3.7 h.

for $X > 2$ g L^{-1} on the one hand to minimize errors for very small biomass concentrations and on the other hand to calculate 'macroscopic' growth rates. The lag phase was determined in the interval from inoculation to the cultivation time where μ surpassed 0.01 h^{-1}.

The courses of μ and X were used for the calculation of the local volumetric productivity p_{loc} [nM h^{-1}] based on Eq. (4), a variation of the Luedeking-Piret equation:[52]

$$p_{loc} = \underbrace{\mu * \sqrt{X} * f_r}_{P_{fr}} + \underbrace{\mu * X * f_{rX}}_{P_{frX}} + \underbrace{X * f_X}_{P_{fX}} \quad (4)$$

where f_r, f_X, and f_{rX} are growth- and/or biomass-related model parameters, corresponding to terms for a strongly growth-associated (f_r [nM]) (primary), growth-associated (f_{rX} [nmol g^{-1}]), and non-growth-associated (f_X [nmol g^{-1} h^{-1}]) (secondary) product formation. The initial product concentration P_0 [nM] was part of the parameter estimation. Product arising from each model term was evaluated according to the horizontal braces. Constraints for P_0 and X_0 [g L^{-1}] were chosen according to the Supporting Information, section S1. Confidence intervals for the parameters were determined as described in section S2. Two additional definitions of the productivity were used for a more detailed analysis:

$$p_{spec} = \frac{p_{loc}}{X_{loc}} \quad (5)$$

$$p_{STY} = \frac{P - P_0}{t} \quad (6)$$

where p_{spec} [nmol g^{-1} h^{-1}] is the (local) specific productivity related to the local biomass concentration X_{loc} and p_{STY} (**s**pace **t**ime **y**ield) [nM h^{-1}] is the overall productivity for the product concentration P at a given time point t. p_{loc} and p_{spec} therefore served as parameters for a kinetic analysis, whereas p_{STY} was used for the overall balance of the process. For courses of p_{spec}, the product concentration was directly fit to Eq. (2) to minimize deviations. Additionally, the process selectivity $s_{\mathrm{P/X}}$ [nmol g^{-1}] was considered for the balance as defined in Eq. (7):

$$s_{P/X} = \frac{P}{X} \quad (7)$$

If not specified otherwise, all of these parameters refer to extracellular tetrameric biotin-free streptavidin. Parameter estimation and simulation based on the acquired parameters was performed in Scilab 5.5.0[53] using the Levenberg-Marquardt-algorithm (*lsqrsolve*-function). Plots were created in Gnumeric 1.12.17.

Results and Discussion

Vector construction, transformation and screening

Construction of the *GAP* promoter-based vector pPpT4_GAP_αS-cSAV and transformation into *P. pastoris* X-33 yielded three producers. Microplate fed-batch characterization of the clones in YPD medium (YPD medium with glycerol instead of glucose) resulted in 2.52 ± 0.01 μM of streptavidin in 96 h, corresponding to a volumetric productivity p of 26 nM h^{-1}. As shake flask cultivation in YPD and YPG medium indicated slightly superior production kinetics for glucose instead of glycerol (Supporting Information Figure S3), glucose was used for the following studies.

Bioreactor experiments

Synthetic media. First bioreactor experiments were based on the synthetic BSM medium, commonly used for methanol-based expression.[54] The given bioreactor system did not contain baffles or allow the application of head pressure. Thus, glucose (500 g L^{-1}) was fed at a constant rate of 2 mL h^{-1} (5 mL L^{-1} h^{-1} relating to the initial cultivation volume of 400 mL) instead of exponentially to avoid oxygen limitation of the culture, as oxygen supply was only moderate ($k_La \approx 144$ h^{-1}, dynamic measurement[55]). This strategy of feeding was applied, e.g., by Gasser and coworkers.[56] It results in a steadily decreasing μ over time.

The initial fermentation conditions resulted in the process shown in Figure 1. The cultivation yielded 1.83 ± 0.03 μM of bioactive SAV in 90 h of cultivation, characterized by a

Table 1. Process Parameters for the Constitutive Production of SAV by *Pichia pastoris*

Medium	Carbon source/feed strategy[a]	*T*- and *pH*-profile[b]	p_{SAV}[c] [nM h^{-1}]	P_{max}[d] [μM] (t [h])	X_{max}[e] [g L^{-1}] (t [h])	$Q_{blocked}$[f] [-]	$s_{P/X}$[g] [nmol g^{-1}]
BSM	Glc: 2 mL h^{-1} from 42 h	C: 30°C, 5.0	20.3 (31.1)	1.83 ± 0.03 (90)	31.9 ± 1.4 (66)	0.26 ± 0.06*	57.4
BSM[h]	Glc: 2.5 mL h^{-1} from 72 h	C: 30°C, 5.0	19.4 (21.2)	1.51 ± 0.02 (78)	25.8 ± 0.4 (54)	0.17 ± 0.01*	58.5
BSM[i]	Glc: no feeding	C: 30°C, 5.0	4.4	0.32 ± 0.01 (72)	3.1 ± 0.5 (48)	−0.01 ± 0.09*	103.2
YPD	Glc: 2 mL h^{-1} from 24 to 60 h	C: 30°C, 6.0	10.7	0.77 ± 0.02 (72)	**45.6 ± 1.2 (72)**	0.03 ± 0.04*	16.9
YPD	5x YPD: 2 mL h^{-1} from 24 to 60 h	C: 30°C, 6.0	10.3	0.74 ± 0.03 (72)	23.0 ± 0.2 (66)	0.07 ± 0.10*	32.2
YPD	Glc: no feeding	C: 25°C, 5.0	5.7	0.34 ± 0.02 (60)	4.66 ± 0.33 (36)	0.06 ± 0.03*	73.0
MGY	5x MGY (2.5x YNB): 2 mL h^{-1} from 24 to 60 h	C: 30°C, 6.0	20.4	1.10 ± 0.05 (54)	26.9 ± 0.4 (60)	**−0.01 ± 0.11***	40.9
MGY[j]	Glc: 1.8 mL h^{-1} from 20 h	C: 30°C, 6.0	25.8	1.24 ± 0.02 (48)	36.3 ± 2.4 (42)	0.05 ± 0.02	34.2
BSM[j]	Glc: 2.9 mL h^{-1} from 44 h	D: 30°C/27°C (40 h); S: 5.0 → 3.5	27.1 (29.8)	1.95 ± 0.09 (72)	31.5 ± 0.8 (66)	0.11 ± 0.02	61.9
MGY[j]	Glc: 2.2 mL h^{-1} from 21 h	D: 30°C/27°C; D: 6.0 → 5.0 (24 h)	37.4	2.69 ± 0.03 (72)	31.8 ± 0.2 (72)	**0.03 ± 0.02**	84.6
MGY[j]	Glc: 2.1 mL h^{-1} from 20 h	D: 30°C/27°C; D: 6.0 → 5.0 (36 h)	20.5	0.87 ± 0.03 (42)	36.1 ± 0.4 (42)	0.06 ± 0.02	24.1
MGY[j]	Glc: 1.8 mL h^{-1} from 20 h	D: 30°C/27°C (24 h); S: 6.0 → 3.0	42.9	2.32 ± 0.07 (54)	22.3 ± 0.3 (54)	**−0.03 ± 0.03**	104.0
MGY[j]	Glc: 1.6 mL h^{-1} from 20 h	D: 30°C/27°C (24 h); S: 6.0 → 4.0	42.7	2.05 ± 0.07 (48)	30.8 ± 5.3 (42)	**0.02 ± 0.02**	66.6
MGY[j]	Glc: 2.1 mL h^{-1} from 20 h	S: 30°C/24°C; S: 6.0 → 4.0	**57.8**	**4.16 ± 0.11 (72)**	29.8 ± 1.2 (42)	**0.00 ± 0.02**	**140.0**

Fed-batch cultivation was performed in BSM, YPD and MGY medium in the bioreactor. Benchmark values are printed in **bold face**.

[a]Feeding strategy and carbon source used. All feed concentrates except for the media concentrates contained the PTM1 trace salt solution in a concentration of 2 mL per 100 mL. The PTM1-solutions for the processes on complex media were biotin-free. The concentration of the glucose feed solution was 500 g L^{-1}).

[b]Profile of *pH* and *T* for the fermentation process. C: both parameters were kept constant at the given setpoint. D: direct shift of the parameter at the indicated point of cultivation. S: successive shift of the parameter throughout the cultivation. If both parameters were directly shifted, the cultivation time in brackets relates to the shift of both parameters.

[c]Productivity from cultivation start to P_{max}. The productivity refers to bioavailable (biotin-free) SAV. If high proportions of SAV were biotin-blocked, the second productivity (given in brackets) refers to the maximal total SAV concentration.

[d]Maximal product concentration and corresponding cultivation time, referring to the bioavailable SAV-binding sites.

[e]Maximal DCW concentration and corresponding cultivation time.

[f]Proportion of biotin-blocked sites of the maximal SAV concentration according to Eq. (1). If P_{HT} was not determined at P_{max}, the value is an average of $Q_{blocked}$ of the neighboring values. If so, this is indicated by an asterisk (*).

[g]Process selectivity: Maximal (bioactive) product concentration divided by maximal DCW concentration.

[h]Biotin concentration lowered to 50% of standard BSM medium. A biotin-free PTM1-solution was applied for the feed.

[i]Biotin-free BSM medium supplemented with 2 g L^{-1} of yeast extract and soy peptone, respectively.

[j]Feeding was performed by the Sixfors pumps based on a step-wise adjustment of the mass flow of the feed solution. Average volumetric flow rates were calculated after the fermentation and therefore vary slightly.

proportion of biotin-blocked binding sites $Q_{blocked}$ of 0.26 ± 0.06 (26%) due to the strong biotin supplement of the medium.

Various strategies were tested in order to decrease $Q_{blocked}$. Cells neither grew in biotin-free BSM medium, nor in a medium in which biotin was substituted by oleic acid and aspartic acid as described for the production of avidin by *P. pastoris* (data not shown).[57] This may be the result of the carbon source glucose, which seems to inhibit the positive effects of the substitutes.[37] Replacement of biotin by small concentrations of complex supplements (soy peptone and yeast extract, 2 g L^{-1} each) allowed the accumulation of only small concentrations of both SAV and biomass. However, reducing the concentration of biotin to 50% resulted in improved bioactivity (1.51 ± 0.02 μM after 78 h, $Q_{blocked}$ = 0.17 ± 0.01). A summary of characteristic process parameters is given in Table 1.

Despite these improvements, the DCW concentration was low (31.9 ± 1.4 g L^{-1} for 1x biotin and 25.8 ± 0.4 g L^{-1} for 0.5x biotin) compared to typical high cell density cultivations of *P. pastoris*, which are usually in the range of 100 g L^{-1} for BSM medium.[54,58]

Complex media. Shake flask studies (Supporting Information, Figure S3) showed that SAV-producing clones of *P. pastoris* are capable of growing in complex media without biotin supplementation, potentially improving the bioactivity of SAV. Thus, bioreactor studies in YPD and MGY medium were performed, using either a glucose concentrate or concentrated cultivation media as feed solutions.

All of the experiments resulted in low proportions of biotin-blocked binding sites ($Q_{blocked} < 0.1$). YPD medium with glucose feeding resulted in the highest DCW concentration of this study (45.6 ± 1.2 g L^{-1}), but process selectivity and maximal SAV concentration were superior when glucose feeding was applied to MGY medium. Media concentrates brought about worse results (see Table 1). Thus, MGY medium and the glucose feed solution were chosen for the following studies.

As shown in Figure 1, cultivation in BSM medium resulted in a degradation of product towards the end of cultivation, which is potentially due to proteolysis. In methanol-based processes, this effect is commonly avoided by lowering *pH* or temperature for induction.[59–61] To analyze if this also applies to constitutive, P_{GAP}-based protein production in complex media, the producer strain was cultivated in YPD medium at a temperature of 25°C and a *pH* of 5.0. This led to very small concentrations of DCW and SAV (see Table 1), but improved the selectivity of the process. To exploit this property without harming the accumulation of biomass, *pH* and *T* were shifted to lower values with a delay in the

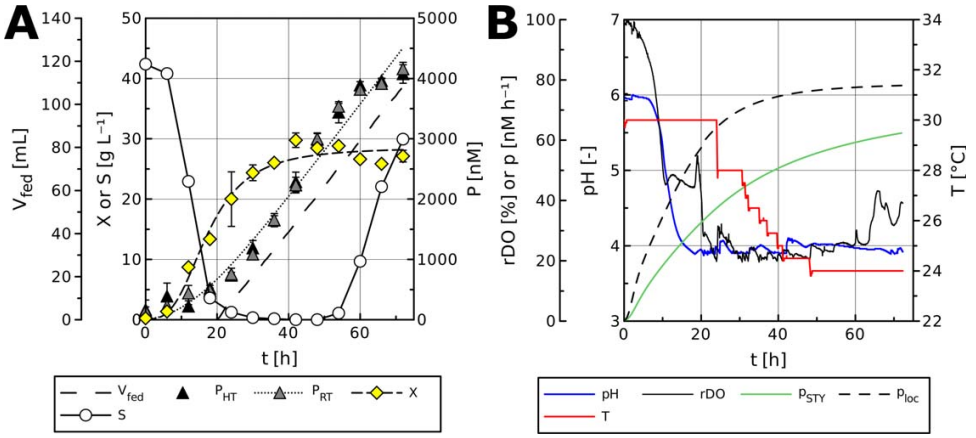

Figure 2. Optimized fed-batch bioreactor cultivation of *P. pastoris* in MGY medium.

Glucose was fed in a concentration of 500 g L^{-1} and initially supplemented in 40 g L^{-1}. *T* and *pH* were shifted to 24°C and 4.0, respectively, throughout the cultivation. (A) Consumption and feeding of substrate (fed volume V_{fed}) and production of biomass (*X*) and streptavidin (*P*). (B) Display of the volumetric streptavidin productivity (local p_{loc} and overall p_{STY}) and the process parameters dissolved oxygen (*rDO*), *pH* and temperature (*T*). OD_{600} at inoculation: 0.5, μ_{max} ($X > 2$ g L^{-1}): 0.37 h^{-1}, end of the lag phase ($\mu > 0.01$ h^{-1}): 0.3 h.

following experiments. The *pH* shift was either performed metabolically, i.e. without the addition of acid, or actively at a certain time of cultivation (i.e., after 24 or 36 h). The interval of variation for the *pH* value (3.0 to 6.0) was based on the data of Siegel et al.[59] To avoid the low DCW concentrations of the process at 25°C and *pH* 5.0, *T* was directly and moderately shifted from 30 to 27°C after 24 h, i.e. during early growth (high μ), or 36 h, i.e. in the decelerating growth phase of the culture.

A summary of the studies is given in Table 1. Only minor improvements were achieved for BSM-based cultivation. For MGY medium, lower maximal DCW concentrations were achieved for lower final *pH* values (36.3 ± 2.4 g L^{-1} for *pH* 6.0, 22.3 ± 0.3 g L^{-1} for *pH* 3.0). However, the strategy generally resulted in improved product concentrations, which were in the range of 2.05 ± 0.07 to 2.69 ± 0.03 µM as opposed to 1.24 ± 0.02 µM in the reference culture at *pH* 6.0. The cultivation time for the shift of *T* proved to be critical: improved product concentrations were only achieved for a shift after 24 h, whereas a shift after the initial growth phase (at 36 h) showed no effect.

For the final process strategy, the *pH* was therefore moderately shifted from 6.0 to 4.0 by metabolic acidification of the medium, avoiding the necessity of acid supplementation and allowing a successive adaptation of the culture to the new *pH*. The relative dissolved oxygen saturation *rDO* was used for regulation of the temperature. Whenever this parameter dropped below 20% the setpoint for *T* was lowered by 0.5°C to 24°C. The result of this optimized strategy is shown in Figure 2.

This final process led to a concentration of 4.16 ± 0.11 µM of practically biotin-free SAV ($Q_{\text{blocked}} = 0.00 \pm 0.02$) after 72 h of cultivation, corresponding to approx. 221 mg L^{-1} of SAV (assuming a theoretical MW of 53.1 kDa for the unglycosylated tetramer). The final space time yield p_{STY} of 57.8 nM h^{-1} and the process selectivity of 140 nmol g^{-1} surpassed all previous experiments. The concentration of ethanol throughout this final process was below 5 g L^{-1} for all time points of sampling.

Comparison to literature. In comparison to literature, the maximal concentration for the optimized process surpassed titers for *E. coli* (typically 1-2.6 µM), but was achieved for a lower productivity, as this parameter is usually in the range of 65 to 340 nM h^{-1} for this host.[12–14,16,17] The productivity was close to the p_{STY} of 67.9 nM h^{-1} achieved for *P. pastoris* by Nogueira et al.[25] The concentration of SAV was considerably lower than the reference concentrations for the methanol-based production processes for SAV by *P. pastoris* reported by Casteluber et al. (71 µM)[24] and Nogueira et al. (11 µM),[25] but was achieved in a shorter cultivation time (72 vs. 167 h and 162 h, respectively). Generally, Casteluber's process is difficult to compare or scale up, because it was performed in spinner flasks aerated through a porous stone at very high volumetric flow rates (4 vvm) and contained a washing step between growth and induction phase, bearing the risk of contamination. Due to this system, no measurement or control of parameters like *pH* or *rDO* was possible. In comparison to the study of Nogueira et al., which was performed in a standard bioreactor, the process selectivity of this study was increased (140 vs. 46.8 nmol g^{-1}), because Nogueira's process led to a surprisingly high DCW concentration of 235 g L^{-1} (usually up to 160 g L^{-1} for BSM-based processes).[58] From the perspective of bioactivity, Nogueira's study led to 20% of biotin-blocked binding sites, whereas this study resulted in a higher product quality by yielding SAV free of biotin or biotinylated proteins, which may offer advantages, e.g., for medical applications necessitating a pure product or the production of high capacity SAV columns for affinity chromatography.

Despite lower product concentrations and productivities, the process offers advantages compared to cultivation of the natural producer *S. avidinii*, since this organism is much more sensitive towards environmental factors, shows a complex morphology, slow growth and resulting long process times in an un-optimized environment, and imposes higher requirements for biochemical engineering.[26]

The new process strategy necessitates complex media compounds, which may result in batch-to-batch variability and the need for diafiltration during downstream processing. However, it is methanol-independent, thus eliminating central disadvantages of the application of P_{AOX} (see Introduction). This results in different demands for the fermentation

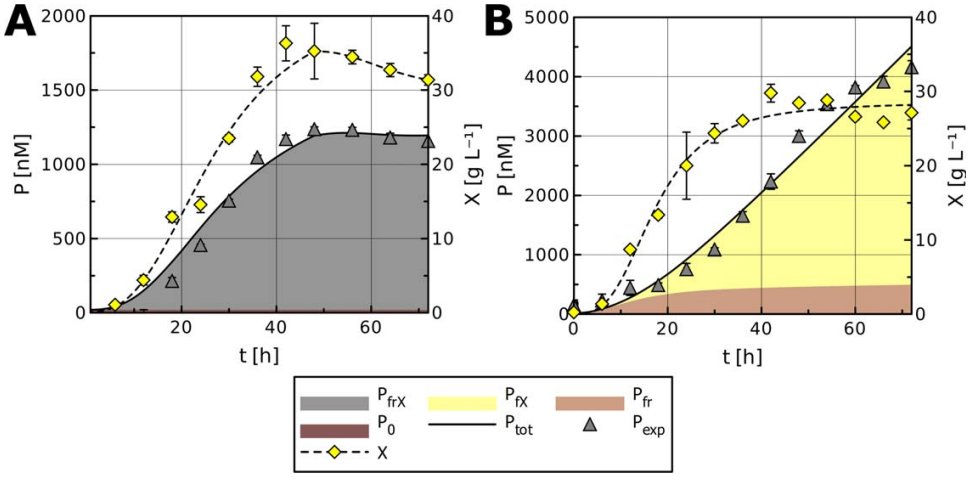

Figure 3. Analysis of the contribution of the model parameters of Eq. 4 (horizontal braces) to the overall product concentration P_{tot}.

Both processes shown were based on MGY medium and glucose feeding. (A) Reference fed-batch at constant T (30°C) and pH (6.0). Parameters (confidence interval of the parameter causing a maximal increase of the sum of squared errors by 5 % given in brackets): $P_0 = 20.4$ nM, $f_r = 0$, $f_{rX} = 29.39 \pm 0.89$ nM nmol g^{-1}, $fX = 0$ nmol g^{-1} h^{-1}. (B) Optimized fed-batch with a successive shift of T to 24°C and of the pH to 4.0 (Figure 3). Parameters: $P_0 = 20.4$ nM, $f_r = (0. . .)41.57$ nM, $f_{rX} = 0(. . .20.62)$ nmol g^{-1}, $f_X = 2.73 \pm 0.25$ nmol g^{-1} h^{-1}. P_{frX} and P_{fr} correspond to growth-related, primary product formation, whereas P_{fX} only depends on X (secondary product). P_0 and P_{exp} refer to the initial (parameter estimation) and experimental product concentration, respectively.

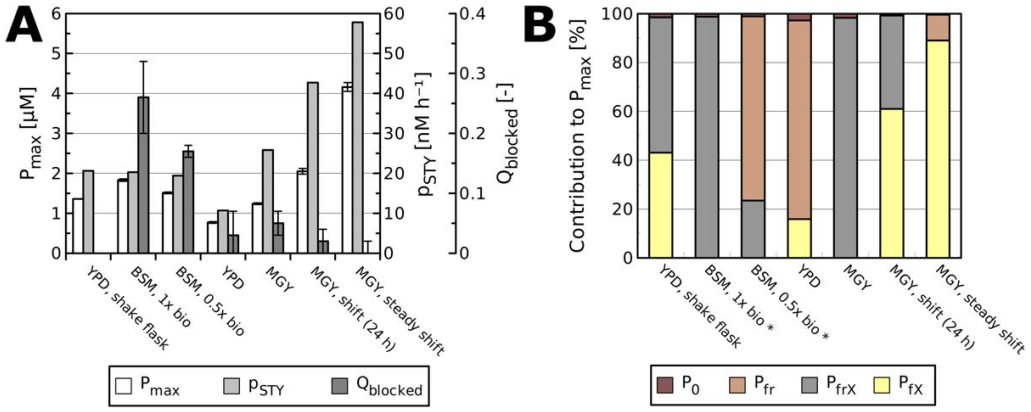

Figure 4. Results of the process optimization procedure.

Cultivations were based on glucose feeding and the media specified by the labels. YPD, shake flask refers to a shake flask batch cultivation (batch, pH uncontrolled; Supporting Information, Figure S3). BSM labels contain the relative concentration of biotin towards standard BSM medium. YPD and MGY correspond to fed-batches at constant T (30°C) and pH (6.0). For MGY, T-shift (24 h) T was shifted to 27°C after 24 h and the pH was not controlled until it reached 4.0. MGY, steady shift refers to the final procedure shown in Figure 3 (continuous shift of pH and T, respectively). (A) Productive properties: P_{max} = maximal (bioactive) product concentration, p_{STY} = productivity from 0 h to P_{max}, $Q_{blocked}$ = biotin-blocked binding sites (if determined). (B) Display of the contribution of the model terms of Eq. 4 to the final product concentration P_{max} (P_{fr}, P_{frX} = growth-associated, primary product formation, P_{fX} = secondary product). Color coding is identical to the areas shown in Figure 3. Where indicated (*), parameter estimation was based on measurements of the overall binding sites (P_{HT}).

equipment: Nogueira et al. had to apply concentrated oxygen due to the strong oxygen dependency during induction by methanol,[54] whereas conditions of low oxygen supply (vessels without turbulence promoters, atmospheric pressure, 1.2 vvm) were sufficient for this study. Generally, the use of concentrated oxygen poses the risk of explosion and increases process cost. As opposed to this, it has been reported that hypoxic conditions may actually increase the productivity of P_{GAP}-based processes.[62] With respect to process design, only two (batch, glucose feeding) instead of three (batch, glycerol feeding, methanol induction) process phases have to be prepared. Moreover, no optimization of the inducer concentration is necessary, which is critical for the methanol-based induction of P_{AOX}.[30,63]

Model-based evaluation of the optimized cultivation conditions. To characterize the optimized culture conditions, selected fermentation courses were compared by parameter estimation. Figure 3 visualizes the contribution of the model terms of Eq. (4) to the overall product concentration of the final process in comparison to the reference culture at pH 6.0 and 30°C. The regions of the plot were highlighted according to the three terms marked by the horizontal braces of the equation.

According to Figure 3, the optimized conditions led to an increased accumulation of SAV in the late phase of the process, characterized by diminishing growth rates ($\mu \approx D < 0.01$ h^{-1}). In contrast, production of SAV was strongly associated to biomass growth in the reference process, resulting in a stagnating product concentration towards the end of cultivation. In optimized conditions $89.0 \pm 6.1\%$ of SAV accumulated due to the P_{fX}-term of the model (secondary product), whereas only 10.5 to 16.6% were due to the growth-related P_{fr}- and P_{frX}-terms (primary product). In contrast, the P_{frX}-term was dominant in the reference culture, contributing to the final product concentration by a proportion of $98.3 \pm 0.1\%$.

To verify if the model accurately reflects the process, a protease study was performed for which cell-free supernatants of the reference and optimized cultivation were incubated at the final process *pH* and temperature in the presence of growth inhibitors (sodium azide). There was no loss of activity in 72 h of incubation for both processes (data not shown). This may be an effect of the media compounds yeast extract and peptone, which are known to reduce proteolytic degradation of the product.[64] Thus, the increased accumulation of SAV seems to be the result of an increase in production rather than a decrease in proteolysis.

Characteristic productive properties for selected steps of the process development are summed up in Figure 4A. Figure 4B shows the contribution of the model terms of Eq. (4) to the final product concentration P_{max} for each of these steps. A shift from growth-related (P_{fr} and P_{frX}) to growth-independent (P_{fX}) product formation can be observed throughout the optimization procedure. This shift is also visible for the reference shake flask batch cultivation, for which the *pH* was uncontrolled.

Conclusions

This study for the first time demonstrates that the protein streptavidin, which is toxic to many heterologous hosts due to the binding of biotin, can efficiently be produced in a constitutive manner by the biotin-dependent yeast *P. pastoris*, leading to 4.16 ± 0.11 μM of highly bioactive, extracellular tetrameric SAV in 72 h.

The production of SAV by *P. pastoris* was strongly dependent on the cultivation parameters *pH* and temperature. Commonly, P_{GAP}-based processes are performed at constant *T* and *pH* derived from preliminary screenings. Separation of fermentations into stages with different setpoints for the parameters is rarely applied.[32] Jahic et al. reported a temperature-limited fed-batch for P_{AOX}-based processes.[60] However, to our best knowledge, a continuous shift of *pH* and *T* throughout the cultivation has not been reported for the P_{GAP}-based expression of heterologous genes by *P. pastoris*. Despite causing lower DCW concentrations, the metabolic acidification and slow cooling of the medium improved the productivity by the factor 2.2 and the product concentration by the factor 3.4. The low μ-dependency of the specific productivity (Supporting Information, Figure S4) suggests that an active control of μ is not necessary for the optimized conditions due to improved productivities at lower growth rates. This simplifies processes based on constant instead of exponential feeding and allows the extension of the productive period of the culture. The strong accumulation of product in the final phase of the process ($\mu \approx D$) came as a surprise, because processes based on the *GAP* promoter typically rely on growth-associated production, as the specific product formation rate for this promoter is usually positively correlated to the specific growth rate.[40]

On the genetic level, further experiments may focus on stronger variants of the GAP promoter[65] and multiple integration of the expression cassette into the host genome.[64] From the perspective of medium optimization, further decreasing process cost by eliminating the complex media compounds via the development of a fine-tuned synthetic medium may be worthwhile. However, proteolytic activity has to be monitored carefully in this regard. Further improvements for the complex medium may be achieved by optimizing its C/N-ratio. In respect to bioengineering, the new process strategy should be reproduced and evaluated in larger scales. A comparison of the strategy applied here to exponential fed-batch cultivation applying a constant setpoint for μ and an oxygen-rich environment is also desirable.

Acknowledgements

This work was financially supported by the scholarship programs of the Deutsche Bundesstiftung Umwelt and the Bielefelder Nachwuchsfonds. We thank Yingfei Shi (Bielefeld University) for providing the optimized enzymatic glucose analysis procedure.

Notation

AA = amino acid
BSM = basal salt medium
DCW = dry cell weight
GAP = glyceraldehyde-3-phosphate
SAV = streptavidin

Literature Cited

1. Chaiet L, Wolf FJ. The properties of streptavidin, a biotin-binding protein produced by streptomycetes. *Arch Biochem Biophys*. 1964;106:1–5.
2. Stapley EO, Mata JM, Miller IM, Demny TC, Woodruff HB. Antibiotic MSD-235. I. Production by *Streptomyces avidinii* and *Streptomyces lavendulae*. *Antimicrob Agents Chemother (Bethesda)*. 1963;161:20–27.
3. Bayer EA, Wilchek M. Application of avidin-biotin technology to affinity-based separations. *J Chromatogr A*. 1990;510:3–11.
4. Katz BA. Binding of biotin to streptavidin stabilizes intersubunit salt bridges between Asp61 and His87 at low pH. *J Mol Biol*. 1997;274:776–800.
5. González M, Argarana CE, Fidelio GD. Extremely high thermal stability of streptavidin and avidin upon biotin binding. *Biomol Eng*. 1999;16:67–72.
6. Skerra A, Schmidt TGM. Applications of a peptide ligand for streptavidin: the strep-tag. *Biomol Eng*. 1999;16:79–86.
7. Bayer EA, Kulik T, Adar R, Wilchek M. Close similarity among streptavidin-like, biotin-binding proteins from *Streptomyces*. *Biochim Biophys Acta*. 1995;1263:60–66.
8. Nordlund HR, Hytönen VP, Laitinen OH, Kulomaa MS. Novel avidin-like protein from a root nodule symbiotic bacterium *Bradyrhizobium japonicum*. *J Biol Chem*. 2005;280:13250–13255.
9. Pähler A, Hendrickson WA, Kolks MA, Argarana CE, Cantor CR. Characterization and crystallization of core streptavidin. *J Biol Chem*. 1987;262:13933–13937.
10. Bayer EA, Ben-Hur H, Hiller Y, Wilchek M. Postsecretory modifications of streptavidin. *Biochem J*. 1989;259:369–376.
11. Sano T, Pandori MW, Chen X, Smith CL, Cantor CR. Recombinant core streptavidins. A minimum-sized core streptavidin has enhanced structural stability and higher accessibility to biotinylated macromolecules. *J Biol Chem*. 1995;270:28204–28209.

12. Sano T, Cantor CR. Expression of a cloned streptavidin gene in *Escherichia coli*. *Proc Natl Acad Sci USA.* 1990;87:142–146.
13. Gallizia A, de Lalla C, Nardone E, Santambrogio P, Brandazza A, Sidoli A, Arosio P. Production of a soluble and functional recombinant streptavidin in *Escherichia coli*. *Protein Expr Purif.* 1998;14:192–196.
14. Wu S-C, Wong S-L. Intracellular production of a soluble and functional monomeric streptavidin in *Escherichia coli* and its application for affinity purification of biotinylated proteins. *Protein Expr Purif.* 2006;46:268–273.
15. Risse JM, Flaschel E, Friehs K, Zillmer J. Gewinnung von Streptavidin mittels *Streptomyces avidinii* bzw. *Escherichia coli*. *Chemie Ingenieur Technik.* 2006;78:1383.
16. Miksch G, Risse JM, Ryu S, Flaschel E. Factors that influence the extracellular expression of streptavidin in *Escherichia coli* using a bacteriocin release protein. *Appl Microbiol Biotechnol.* 2008;81:319–326.
17. Müller JM, Wetzel D, Flaschel E, Friehs K, Risse JM. Constitutive production and efficient secretion of soluble full-length streptavidin by an *Escherichia coli* 'leaky mutant'. *J Biotechnol.* 2016;221:91–100.
18. Nagarajan V, Ramaley R, Albertson H, Chen M. Secretion of streptavidin from *Bacillus subtilis*. *Appl Environ Microbiol.* 1993;59:3894–3898.
19. Wu S-C, Wong S-L. Engineering of a *Bacillus subtilis* strain with adjustable levels of intracellular biotin for secretory production of functional streptavidin. *Appl Environ Micobiol.* 2002; 68:1102–1108.
20. Wu S-C, Qureshi MH, Wong S-L. Secretory production and purification of functional full-length streptavidin from *Bacillus subtilis*. *Protein Expr Purif.* 2002;24:348–356.
21. Lardy HA, Potter RL, Burris RH. Metabolic functions of biotin I. The role of biotin in bicarbonate utilization by *Lactobacillus arabinosis* studied with ^{14}C. *J Biol Chem.* 1949;179.
22. Lynen F, Knappe J, Lorch EJ, Ringelmann E, Lachance JP. Zur biochemischen Funktion des Biotins. 2. Reinigung und Wirkungsweise der beta-methyl-crotonyl-caboxylase. *Biochem Z.* 1961;335:123.
23. Zocchi A, Jobé AM, Neuhaus JM, Ward TR. Expression and purification of recombinant avidin with a lowered isoelectric point in *Pichia pastoris*. *Protein Expr Purif.* 2003;32:167–174.
24. Casteluber MC, Damasceno LM, da Silveira WB, Diniz RH, Passos FJ, Passos FM. Cloning and expression of a functional core streptavidin in *Pichia pastoris*: strategies to increase yield. *Biotechnol Prog.* 2012;28:1419–1425.
25. Nogueira ES, Schleier T, Dürrenberger M, Ballmer-Hofer K, Ward TR, Jaussi R. High-level secretion of recombinant full-length streptavidin in *Pichia pastoris* and its application to enantioselective catalysis. *Protein Expr Purif.* 2014;93:54–62.
26. Müller JM, Risse JM, Jussen D, Flaschel E. Development of fed-batch strategies for the production of streptavidin by *Streptomyces avidinii* based on power input and oxygen supply studies. *J Biotechnol.* 2013;163:325–332.
27. Zhang A-L, Luo J-X, Zhang T-Y, Pan Y-W, Tan Y-H, Fu C-Y, Tu F-Z. Recent advances on the GAP promoter derived expression system of *Pichia pastoris*. *Mol Biol Rep.* 2009;36:1611–1619.
28. Bertrand GL, Millero FJ, Wu C-H, Hepler LG. Thermochemical Investigations of the water-ethanol and water-methanol solvent systems. I. Heats of mixing, heats of solution, and heats of ionization of water. *J Phys Chem.* 1966;70:699–705.
29. Niu H, Jost L, Pirlot N, Sassi H, Daukandt M, Rodriguez C, Fickers P. A quantitative study of methanol/sorbitol co-feeding process of a *Pichia pastoris* Mut$^+$/pAOX1-lacZ strain. *Microb Cell Fact.* 2013;12:33.
30. Khatri NK, Hoffmann F. Impact of methanol concentration on secreted protein production in oxygen-limited cultures of recombinant *Pichia pastoris*. *Biotechnol Bioeng.* 2006;93:871–879.
31. Jungo C, Marison I, von Stockar U. Mixed feeds of glycerol and methanol can improve the performance of *Pichia pastoris* cultures: A quantitative study based on concentration gradients in transient continuous cultures. *J Biotechnol.* 2007;128:824–837.
32. Zhao W, Wang J, Deng R, Wang X. Scale-up fermentation of recombinant *Candida rugosa* lipase expressed in *Pichia pastoris* using the GAP promoter. *J Ind Microbiol Biotechnol.* 2008;35: 189–195.
33. Gasser B, Dragosits M, Mattanovich D. Engineering a biotin-prototrophy in *Pichia pastoris* for robust production processes. *Metabol Eng.* 2010;12:573–580.
34. Ahmad F, Rose AH, Garg NK. Effect of biotin deficiency on the synthesis of nucleic acids and protein by *Saccharomyces cerevisiae*. *Microbiology.* 1960;24:69–80.
35. Moat AG, Ahmad F, Alexander JK, Barnes IJ. Alteration in the amino acid content of yeast during growth under various nutritional conditions. *J Bacteriol.* 1969;98:573–578.
36. Ahmad F, Rose AH. Effect of biotin-sparing substances on growth of biotin-deficient *Saccharomyces cerevisiae* and on the synthesis of nucleic acids and protein. *Microbiology.* 1962;28: 147–160.
37. Adler JH, Gealt MA, Nes WD, Nes WR. Growth characteristics of *Saccharomyces cerevisiae* and *Aspergillus nidulans* when biotin is replaced by aspartic acid and fatty acids. *Microbiology.* 1981;122:101–107.
38. Waterham HR, Digan ME, Koutz PJ, Lair SV, Cregg JM. Isolation of the *Pichia pastoris* glyceraldehyde-3-phosphate dehydrogenase gene and regulation and use of its promoter. *Gene.* 1997; 186:37–44.
39. Çalık P, Atab Ö, Güneşa H, Massahib A, Boya E, Keskina A, Öztürk S, Zerzea GH, Özdamarc TH. Recombinant protein production in *Pichia pastoris* under glyceraldehyde-3-phosphate dehydrogenase promoter: From carbon source metabolism to bioreactor operation parameters. *Biochem Eng J.* 2015;95:20–36.
40. Maurer M, Kühleitner M, Gasser B, Mattanovich D. Versatile modeling and optimization of fed batch processes for the production of secreted heterologous proteins with *Pichia pastoris*. *Microb Cell Fact.* 2006;5:37.
41. Wang X, Sun Y, Ke F, Zhao H, Liu T, Xu L, Liu Y, Yan Y. Constitutive expression of *Yarrowia lipolytica* lipase LIP2 in *Pichia pastoris* using GAP as promoter. *Appl Biochem Biotechnol.* 2012;166:1355–1367.
42. Potvin G, Zhang Z, Defela A, Lam H. Screening of alternative carbon sources for recombinant protein production in *Pichia pastoris*. *Int J Chem React Eng.* 2016;14:251–257.
43. Ahmad M, Hirz M, Pichler H, Schwab H. Protein expression in *Pichia pastoris*: recent achievements and perspectives for heterologous protein production. *Appl Microbiol Biotechnol.* 2014; 98:5301–5317.
44. Gibson DG, Young L, Chuang RY, Venter JC, Hutchison CA, Smith HO. Enzymatic assembly of DNA molecules up to several hundred kilobases. *Nat Methods.* 2009;6:343–345.
45. Sambrook J, Russell DW. Molecular Cloning: A Laboratory Manual, 3rd ed. New York: Cold Spring Harbor Laboratory Press; 2000.
46. Lin-Cereghino J, Wong WW, Xiong S, Giang W, Luong LT, Vu J, Johnson SD, Lin-Cereghino GP. Condensed protocol for competent cell preparation and transformation of the methylotrophic yeast *Pichia pastoris*. *BioTechniques.* 2005;38:44. 46,48.
47. Cregg JM. Methods in Molecular Biology 389: Pichia Protocols, 2nd ed. Totowa: Humana Press; 2007.
48. Kad G, Falk H, Gruber HJ. Accurate measurement of avidin and streptavidin in crude biofluids with a new, optimized biotin-fluorescein conjugate. *Biochim Biophys Acta.* 1999;1417:33–43.
49. Kada G, Kaiser K, Falk H, Gruber HJ. Rapid estimation of avidin and streptavidin by fluorescence quenching or fluorescence polarization. *Biochim Biophys Acta.* 1999;1427:44–48.
50. Müller JM, Risse JM, Friehs K, Flaschel E. Model-based development of an assay for the rapid detection of biotin-blocked binding sites of streptavidin. *Eng Life Sci.* 2015;15:627–639.
51. Baud M. Methods of Immunological Analysis 1: Fundamentals, 1st ed. New York: VCH Publishers, Inc., 1993.
52. Luedeking R, Piret EL. A kinetic study of the lactic acid fermentation. Batch process at controlled pH. *J Biochem Microbiol.* 1959;1:393–412.
53. Scilab Enterprises. Scilab: Free and open source software for numerical computation (OS, version 5.5.0). Available at: www.scilab.org. 2012.

54. Invitrogen Co. Pichia fermentation process guidelines overview (Version B. 053002). Invitrogen Co., San Diego, USA. Available at: http://www.invitrogen.com/content/sfs/manuals/pichiaferm_prot.pdf. May, 2002. Accessed December 14, 2015.
55. Bandyopadhyay B, Humphrey A, Taguchi H. Dynamic measurement of the volumetric oxygen transfer coefficient in fermentation systems. *Biotechnol Bioeng*. 1967;9:533–544.
56. Gasser B, Maurer M, Gach J, Kunert R, Mattanovich D. Engineering of *Pichia pastoris* for improved production of antibody fragments. *Biotechnol Bioeng*. 2006;94:353–361.
57. Jungo C, Urfer J, Zocchi A, Marison I, von Stockar U. Optimisation of culture conditions with respect to biotin requirement for the production of recombinant avidin in *Pichia pastoris*. *J Biotechnol*. 2007;127:703–715.
58. Jahic M, Rotticci-Mulder J, Martinelle M, Hult K, Enfors S-O. Modeling of growth and energy metabolism of *Pichia pastoris* producing a fusion protein. *Bioprocess Biosyst Eng*. 2002;24:385–393.
59. Siegel RS, Buckholz RG, Thill GP, Wondrack LM. Production of epidermal growth factor in methylotrophic yeast cells. WO Patent 1990010697 A1, 1990.
60. Jahic M, Wallberg F, Bollok M, Garcia P, Enfors S-O. Temperature-limited fed-batch technique for control of proteolysis in *Pichia pastoris* bioreactor cultures. *Microb Cell Fact*. 2003;2:6.
61. Macauley-Patrick S, Fazenda ML, McNeil B, Harvey LM. Heterologous protein production using the *Pichia pastoris* expression system. *Yeast*. 2005;22:249–270.
62. Baumann K, Maurer M, Dragosits M, Cos O, Ferrer P, Mattanovich D. Hypoxic fed-batch cultivation of *Pichia pastoris* increases specific and volumetric productivity of recombinant proteins. *Biotechnol Bioeng* .2008;100:177–183.
63. Zhang W, Bevins MA, Plantz BA, Smith LA, Meagher MM. Modeling *Pichia pastoris* growth on methanol and optimizing the production of a recombinant protein, the heavy-chain fragment C of botulinum neurotoxin, serotype A. *Biotechnol Bioeng*. 2000;70:1–8.
64. Sreekrishna K, Brankamp RG, Kropp KE, Blankenship DT, Tsay JT, Smith PL, Wierschke JD, Subramaniam A, Birkenberger LA. Strategies for optimal synthesis and secretion of heterologous proteins in the methylotrophic yeast *Pichia pastoris*. *Gene*. 1997;190:55–62.
65. Qin X, Qian J, Yao G, Zhuang Y, Zhang S, Chu J. GAP promoter library for fine-tuning of gene expression in *Pichia pastoris*. *Appl Environ Microbiol*. 2011;77:3600–3608.

Manuscript received Dec. 17, 2015, and revision received Mar. 2, 2016.

Biotechnology Progress

Supporting information to

GAP promoter-based fed-batch production of highly bioactive core streptavidin by *Pichia pastoris*

*Jakob Michael Müller *[a], Simon Bruhn [a], Erwin Flaschel [a], Karl Friehs [a], and Joe Max Risse [a]*

[a] Lehrstuhl für Fermentationstechnik, Technische Fakultät, Universität Bielefeld, PF 10 01 31, D-33501 Bielefeld, Germany

[*] e-mail: jmu@fermtech.techfak.uni-bielefeld.de · phone: +49 521 106 5299 fax: +49 521 106 6475 (secretary's office)

S1 – constraints for parameter estimation

The parameters for modelling of the course of the product concentration P as well as the constraints used for the parameter estimation were chosen based on calculations and test-wise fitting to exemplary fermentations. As all of the cultures were inoculated to a specific OD_{600} and in order to avoid errors of the maximal specific growth rate caused by deviations of the initial biomass concentration X_0, this model parameter was calculated from the theoretical OD_{600} at the start of cultivation (0.5 or 0.2). A correlation factor of 0.228 g L^{-1} per absorption unit OD_{600} for the conversion of OD_{600} to X acquired from a corresponding correlation (see Fig. S1) was used. Furthermore, the initial product concentration P_0 was estimated applying an upper limit of 544 nM in the pre-culture. This concentration was measured in the YPD-based shake flask-cultivation of Fig. S3 A after 24 h of cultivation. A volume of up to 15 mL of this pre-culture was diluted by the initial fermentation volume of 400 mL. This results in a typical initial product concentration P_0 of up to 20 nM, which was therefore chosen as an upper limit for the estimation of this parameter.

For the kinetic course of the product concentration several models were evaluated. Three model variants of equation (4) were applied in Fig. S2. The removal of the strongly primary product-correlated f_r-term of the model (blue curve) resulted in a lack of fit in the initial growth period. When no upper limit for the initial product concentration P_0 was used, this lack of fit was partly compensated by an increased value for this parameter (green curve). However, expected initial product concentrations in the bioreactor are in the range of <20 nM of SAV as discussed above, indicating a lack of fit for the unconstrained parameter estimation. Therefore, (i) the model term based on the square root of the biomass

concentration X was included in the estimation procedure and (ii) P_0 was estimated in a constrained manner.

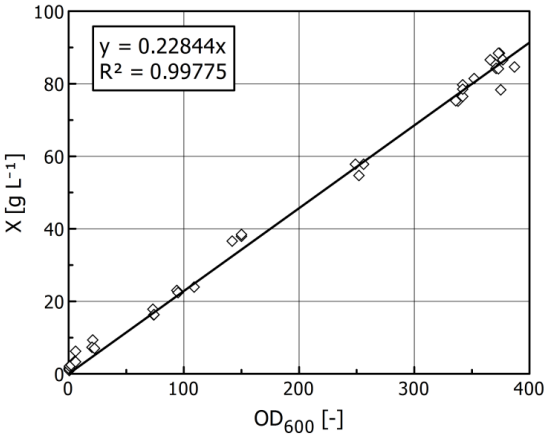

Fig. S1 Correlation of OD_{600} and dry cell weight concentration X for *Pichia pastoris* used for the calculation of the model parameter X_0 for the parameter estimations resulting in the biomass courses. The regression resulted in the correlation X = 0.22844 g L^{-1} * OD_{600}.

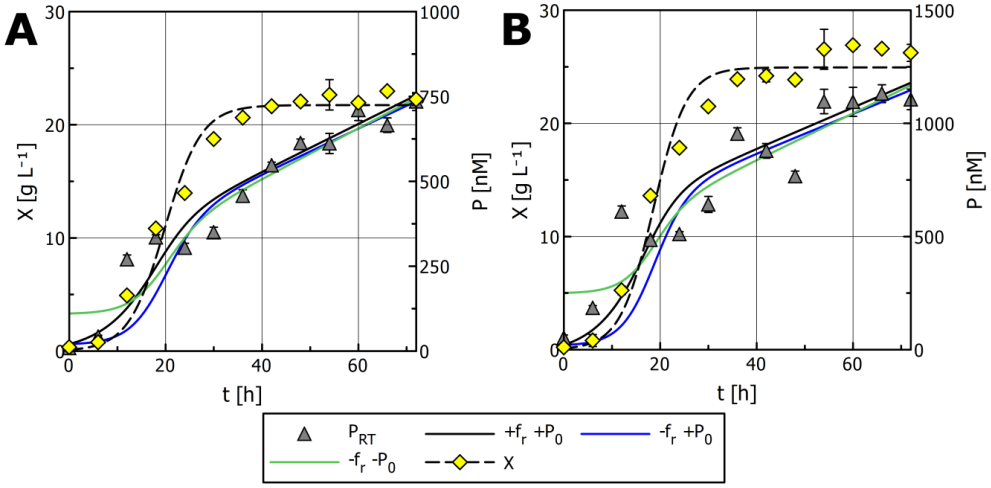

Fig. S2 Comparison of three parameter adjustments in respect to the outcome of parameter estimation for two fermentations. Parameters were either chosen according to equation (4) (+f_r) or the square root-term for biomass in combination with μ and f_r was removed (-f_r). Furthermore, the initial product concentration was estimated either constrained (+P_0) or unconstrained (-P_0), i.e. with or without an upper limit.

S2 – confidence intervals for the estimated parameters

Confidence intervals for the parameters were estimated manually by manually introducing constraints on a single model parameter and observing the change of fit quality (sum of squared errors). Intervals are based on a maximal reduction of the fit quality by 5 % caused by the change of each parameter. Confidence intervals for the resulting proportions of the

contribution of each model parameter to the final product concentration were derived from the resulting altered parameter set.

S3 – shake flask cultivation

Shake flask characterization of the clones was performed in YPD and YPG medium supplemented with 40 g L^{-1} of glucose and glycerol, respectively, in 1 L baffled glass shake flasks (Schott Duran, DURAN Group GmbH, Wertheim/Main, Germany). The degree of filling of the flasks was 15 %. Cultivations were performed on a rotary shaker at 200 min^{-1} (shaking diameter: 20 mm) and 30 °C. The inoculum was taken from an overnight culture in 30 mL of YPD medium grown in a 300 mL shake flask, inoculated with 300 µL of a freshly thawed glycerol stock. Samples were automatically taken and cooled to 4 °C every 2 h by a fraction collector. Results for this characterization step are shown in Fig. S3.

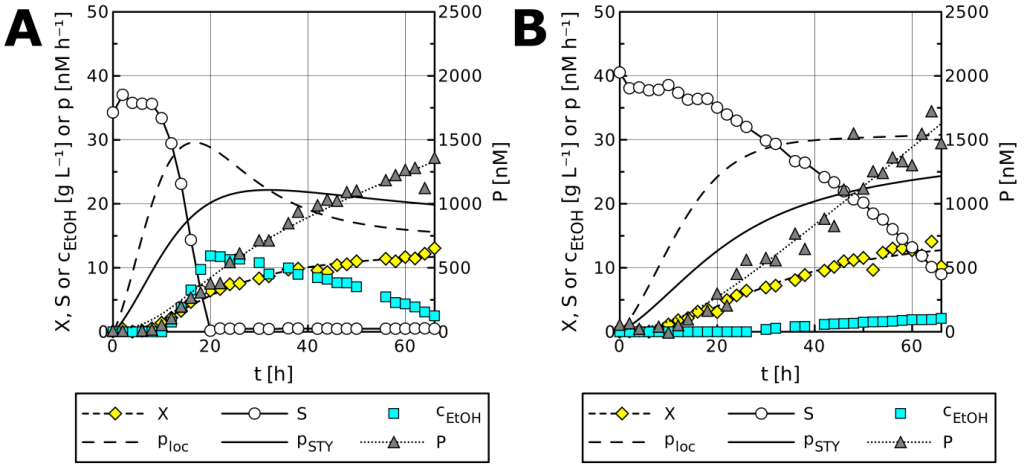

Fig. S3 Batch growth curves of *Pichia pastoris* X-33 clone B13 cultivated on YPD (A) and YPG (B) medium in baffled shake flasks (μ_{max} for X > 2 g L^{-1}: 0.18 and 0.14 h^{-1}, respectively). Due to limited sampling volumes all measurements were performed onefold. Process selectivities (62-66 h): $s_{P/X}$ = 102.6±9.8 and 132.2±11.2 nmol g^{-1}, respectively.

Biomass was formed more rapidly in YPD medium, leading to maximal specific growth rates μ of 0.18 h^{-1} and 0.14 h^{-1} for glucose and glycerol, respectively (determination for X > 2 g L^{-1}). Ethanol formation in both shake flasks indicates hypoxic conditions throughout the cultivation (Baumann et al. 2008). The phase of oxygen limitation can be expected to be more pronounced for glucose due to the faster substrate consumption and stronger ethanol formation. Despite the differences in growth, the resulting SAV concentrations after 66 h were comparable, reaching 1.36 µM on glucose vs. 1.47 µM on glycerol. However, the courses of the space-time-yield p_{STY} and the local productivity p_{loc} peaked earlier in the

glucose-based cultivation. Therefore, glucose was chosen as carbon source for the following bioreactor experiments

S4 – analysis of the specific productivity p_{spec}

An analysis of the biomass-related productivity p_{spec} (equation (5)) may contribute to a better understanding of the production in different growth phases. Fig. S4 shows plots of this parameter for the initial process conditions on MGY medium (*pH* 6.0, 30 °C) and the final, optimized process on MGY medium (steady shift of *pH* and *T* throughout the cultivation, Fig. 2 in the main document).

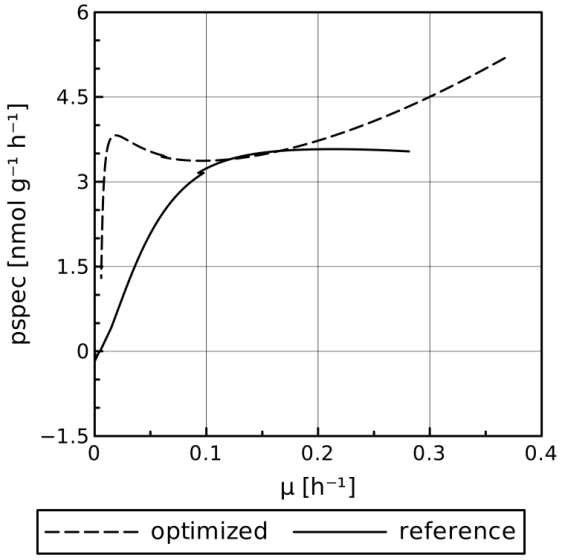

Fig. S4 Additional data for two fed-batch cultivations of *P. pastoris* X-33 clone B13 in the bioreactor on MGY medium with 40 g L^{-1} of glucose, glucose feeding and an initial OD_{600} of 0.5. The fermentations correspond to the plots in Fig. 3 in the main document. (A) Successive shift of the *pH* to 4.0 and direct shift of *T* to 27 °C after 24 h. (B) Successive shift of *pH* and *T* towards 4.0 and 24 °C, respectively. Parameters were acquired by direct fitting of biomass and product concentration to the four-parameter logistic model of equation (2) to minimize the deviations of data and model. Subsequently, the specific productivity (productivity per biomass) was calculated from the biomass course and the local productivity p_{loc}.

The plot reveals a steep decrease of the specific productivity for low specific growth rates for the initial process conditions, whereas p_{spec} remains nearly constant for the optimized process conditions in the same range of the growth rate.

5.3.5 Summary of additional experiments applying *P. pastoris*

Additional studies applying *P. pastoris* focused on multiple chromosomal integration of the GAP promoter-based expression cassette used in Müller *et al.* (2016a) and expression of SAV gene variants by use of the AOX1 promoter.

5.3.5.1 Methanol-based production of SAV by *P. pastoris*

In addition to the GAP promoter-based construct described in the publication, several expression cassettes using the AOX1 promoter were studied. One of the corresponding constructs was used for demonstration of the functionality of the assay for the detection of biotin-blocked binding sites as illustrated in section 3.3 (p. 30*ff.*; Fig. 5 in the corresponding article).

For the corresponding constructs, full-length as well as core SAV genes were applied. Furthermore, a sequence of the α-mating factor secretion signal modified according to Xiong *et al.* (2004) was used. Due to a relatively small number of clones no detailed conclusions can be drawn concerning the ideal genetic configuration of the expression cassette. However, microplate results (data not shown) indicated that the optimized secretion signal peptide may be slightly advantageous towards the unmodified peptide from *Saccharomyces cerevisiae* (factor in the range of 1.1 regarding the extracellular concentration of SAV). Furthermore, the application of a full-length gene seemed to result in improved production (factor 1.3 towards core SAV). These observations have to be confirmed in more detailed experiments. Moreover, scale-up to the bioreactor is essential for methanol-based induction due to the high oxygen demand in corresponding studies. These experiments were not a part of this thesis due to the high benchmark concentrations achieved for methanol-based production of SAV by *P. pastoris* by Casteluber *et al.* (2012) and Nogueira *et al.* (2014).

5.3.5.2 Multiple chromosomal integration of the expression cassette into the genome of *P. pastoris*

Multiple chromosomal integration of the gene of interest has been associated to increased production of heterologous proteins by *P. pastoris*. Based on the protocol by Sunga *et al.* (2008), the chromosomal expression cassette was amplified post-transformationally using the clone of the core SAV/GAP promoter construct applied for the studies in Müller *et al.* (2016a) by the exposure to increased selection pressure. Selection by increasing concentrations of Zeocin™ yielded clones resistant to up to $2\,\mathrm{g\,L^{-1}}$ of the antibiotic instead of the typically applied concentration of $100\,\mathrm{mg\,L^{-1}}$. The expression pattern for the cultivation of clones resulting from this selection procedure in 96-well plates is shown in Fig. 5.3.

Fig. 5.3 shows that the procedure yielded clones surpassing the average concentration of SAV from all wells by a factor of up to 2.4 (1.38 vs. 0.66±0.15 μM). Generally, the best results were achieved

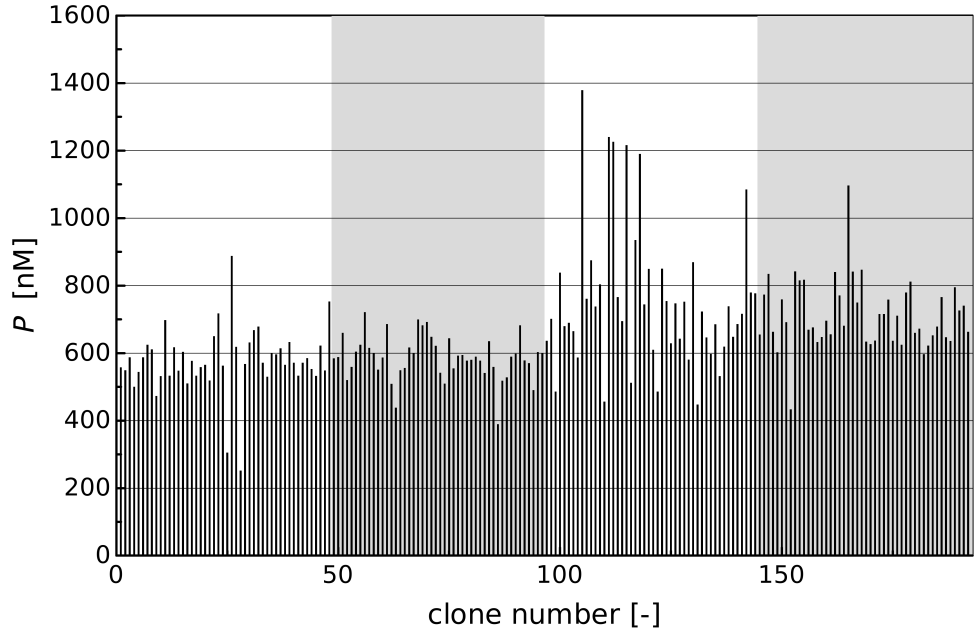

Fig. 5.3: Expression pattern of 192 clones of *P. pastoris* producing core SAV under control of the GAP promoter acquired by post-transformational vector amplification (PTVA) according to Sunga *et al.* (2008). Characterization was performed in 96-well plates. The highlighted blocks indicate increasing concentrations of Zeocin™ used for the selection procedure (from left to right: 200, 500, 1000 and 2000 mg L^{-1}).

for a concentration of 1 g L^{-1} of antibiotic (third section in the plot), which brought about 6 out of 7 clones accumulating more than 1 μM of SAV in the supernatant.

However, a subsequent characterization of the best-performing clones in 24-well plates without selection pressure resulted in concentrations of SAV resembling the productive properties of the original clone. This indicates problems of genetic stability of the clones acquired by PTVA. Multiple streaking of multi-copy integrants on plates supplemented by the increased concentration of Zeocin™ prior to the production study did not solve the issue. Thus, further studies should focus on the stabilization of multi-copy integrants.

If other strategies of stabilization are successful, the application of an optimized secretion signal peptide may also be a useful tool for further experiments in the context of multiple chromosomal integration, because the increased production may lead to a bottleneck in the secretory pathway of *P. pastoris*. This could cause problems of host toxicity, which is one potential reason for the loss of productive potential during the studies in the absence of the antibiotic.

5.4 Production of SAV by *Hansenula polymorpha*

The promising results from the studies of Casteluber *et al.* (2012) and Nogueira *et al.* (2014) on the production of SAV by *P. pastoris* suggested that yeast-based expression of the SAV gene may be superior to competing prokaryotic heterologous expression systems. This led to considerations of testing alternative yeasts for the expression of the gene.

Like *P. pastoris* (see section 5.3, p. 116), the methylotrophic yeast *H. polymorpha* is established in heterologous protein production for more than 20 years (Hollenberg & Gellissen, 1997; Stöckmann *et al.*, 2009) and has led to protein concentrations in the multi-gram per liter-range (Mayer *et al.*, 1999). It therefore seemed a suitable host for the production of SAV. Like *P. pastoris*, common production media for *H. polymorpha* contain a biotin supplement, indicating an auxotrophy for the vitamin (Mayer *et al.*, 1999).

5.4.1 Goals of this study

As *H. polymorpha* has not been used for a production of SAV before, this study focused on a variety of aspects on different levels of process development, including the evaluation of genetic factors, optimization of culture conditions, and scale-up to the bioreactor.

5.4.2 Manuscript

The results were published in the Journal of Biotechnology (Wetzel *et al.*, 2016) (with permission from Elsevier, Copyright 2016), as shown on the following pages. The section contains the research article and the corresponding supporting information.

Journal of Biotechnology 225 (2016) 3–9

Contents lists available at ScienceDirect

Journal of Biotechnology

journal homepage: www.elsevier.com/locate/jbiotec

Fed-batch production and secretion of streptavidin by *Hansenula polymorpha*: Evaluation of genetic factors and bioprocess development

David Wetzel[1], Jakob M. Müller*[,1], Erwin Flaschel, Karl Friehs, Joe M. Risse

Lehrstuhl für Fermentationstechnik, Technische Fakultät, Universität Bielefeld, Bielefeld, Germany

ARTICLE INFO

Article history:
Received 15 February 2016
Received in revised form 4 March 2016
Accepted 10 March 2016
Available online 14 March 2016

Keywords:
Bioreactor cultivation
Chain length of streptavidin
FMD promoter
MOX promoter
Methanol-free production
Biotin-blocked binding sites

ABSTRACT

Streptavidin – a protein secreted by the filamentous bacterium *Streptomyces avidinii* – is applied in a variety of methods, leading to numerous studies on its heterologous production. Development and characterization of a novel expression system for streptavidin genes by *Hansenula polymorpha* is described utilizing different target gene variants along with the two methanol-inducible promoters P_{MOX} and P_{FMD}. Extracellular product concentrations were higher for cultivation at 30 instead of 37 °C. The best performing strain carrying the full-length streptavidin gene under control of P_{FMD} was characterized in the bioreactor applying a synthetic medium and oxygen-controlled feeding of glucose. Derepression resulted in an extracellular concentration of 1.31 ± 0.07 μM of tetrameric streptavidin after 48 h (27.3 nM h^{-1}). Feeding of glycerol improved biomass formation, but lowered the product concentration. By combining derepression and methanol induction the final extracellular streptavidin concentration increased to 11.42 ± 0.22 μM (approx. 751 mg L^{-1}), yielding a productivity of 52.5 nM h^{-1}. Despite supplementing biotin the proportion of biotin-blocked binding sites in the supernatant dropped from 54.4 ± 5.0 % after 18 h to 17.2 ± 6.5 % towards the end of glucose feeding to a final value of 1.1 ± 3.8 %, indicating a highly bioactive product. Thus, *H. polymorpha* proved to be a suitable host for the production of streptavidin.

1. Introduction

The interaction of the homotetrameric protein streptavidin (SAV) and its natural ligand biotin is characterized by one of the smallest dissociation constants known in biological systems (K_d of 4×10^{-14} M; Green, 1990). This property is fundamental for the various applications of the interaction, including – among numerous others – the purification of peptide-tagged (Skerra and Schmidt, 1990) or biotinylated (Rösli et al., 2008) proteins. These applications are facilitated by the stability of SAV towards various environmental factors like *pH* (Sano and Cantor, 1995) and temperature (González et al., 1999).

Naturally occurring in the filamentous bacterium *Streptomyces avidinii* (Chaiet and Wolf, 1964), the SAV gene has been subject to many studies of heterologous expression since the 1980s. Various hosts were applied in the studies, ranging from *Escherichia coli* (Sano and Cantor, 1990; Gallizia et al., 1998; Miksch et al., 2008; Müller et al., 2016) to *Bacillus subtilis* (Wu et al., 2002), *Streptomyces lividans* (Meade and Jeffrey, 1984), and, more recently, to *Pichia pastoris* (Casteluber et al., 2012; Nogueira et al., 2014).

After cleavage of the native signal peptide, mature SAV monomers naturally consist of 159 amino acids, but often occur in shortened, bioactive forms in supernatants due to *N*- and *C*-terminal cleavage of the protein by proteases (Bayer et al., 1989). As only a core motif of 118–127 amino acids is necessary for the binding of biotin (Pähler et al., 1987; Sano et al., 1995), expression may focus either on truncated forms of the SAV gene, resulting in so-called "core streptavidins", or on full-length SAV.

Due to the biotin-binding ability of SAV, the protein exhibits toxic properties in heterologous expression, limiting the maximal product concentration especially for intracellular production of the protein. Nevertheless, studies with *P. pastoris* in methanol- and secretion-based production processes resulted in remarkable extracellular concentrations of 11 (full-length SAV, bioreactor culti-

Abbreviations: α-MF, α-mating factor; SAV, streptavidin; vvm, volume per volume and minute.

* Corresponding author.
E-mail address: jmu@fermtech.techfak.uni-bielefeld.de (J.M. Müller).

[1] Both authors contributed equally.

http://dx.doi.org/10.1016/j.jbiotec.2016.03.017
0168-1656/

vation; Nogueira et al., 2014) and 71 μM[1] (core SAV, cultivation in spinner flasks at 4 vvm, washing between growth and induction; Casteluber et al., 2012) of tetrameric SAV. Thus, despite typically being biotin-auxotrophic, yeast-based expression systems seem to be efficient for the production and secretion of the protein.

1.1. Goals of this study

The yeast *Hansenula polymorpha* is industrially established for heterologous protein production (Weydemann et al., 1995; Mayer et al., 1999) and thus seemed a promising host for the secreted production of SAV. Like *P. pastoris,* this yeast is accessible to methods of gene technology, established in fermentation engineering, able to secrete proteins to the supernatant in the grams per liter range and grows to dry cell weights of more than 100 g L^{-1} in standard fed-batch fermentations (Weydemann et al., 1995; Mayer et al., 1999). In the past the yeast was renamed several times. The two strains used in this study were classified as *Ogataea polymorpha* (ATCC 34438) and *Candida parapolymorpha* (ATCC 26012, DL-1) recently (Suh and Zhou, 2010). However, the designations *H. polymorpha* for the genus and DL-1 and ATCC 34438 for the strains, respectively, were used in this study, as they are still most widely employed in literature. The promoters of the methanol oxidase (*MOX*) (Ledeboer et al., 1985) and formiate dehydrogenase (*FMD*) (Hollenberg and Janowicz, 1987) genes were chosen for overexpression of the SAV gene. In addition to being strongly inducible by methanol both promoters allow heterologous gene expression upon derepression in the presence of growth limiting concentrations of carbon sources like glucose and glycerol (Weydemann et al., 1995; Mayer et al., 1999).

2. Materials and methods

2.1. Microbial strains and plasmids

The strain *E. coli* KRX (Promega, Fitchburg, Wisconsin, USA), which is optimized for recombinant protein production and cloning of DNA, was used for cloning work and vector amplification. *S. avidinii* (CBS 730.72) was ordered from CBS (Centraalbureau voor Schimmelcultures, Utrecht, Netherlands) and used for the amplification of the SAV gene. The *H. polymorpha* strains ATCC 34438 (DSMZ, German Collection of Microorganisms and Cell Cultures, Braunschweig, Germany) and DL-1 (ATCC 26012, ordered from CBS) were used for the study.

2.2. Plasmid construction, transformation and verification of cloning steps

Plasmids used for this study were assembled isothermally at 50 °C for 1 h as described by Gibson et al. (2009) using a master mix purchased from NEB (Ipswich, Massachusetts, USA). The plasmid fragments were amplified by PCR using primers with overlaps of up to 30 base pairs, followed by clean-up from agarose gels. *E. coli* was transformed by electroporation using 3 μL of the resulting solution according to standard laboratory procedures (Sambrook, 1989). The cloning steps were verified by sequencing at Bielefeld University (IIT Biotech GmbH, Bielefeld, Germany). After clone selection by Ampicillin and preparative plasmid isolation from positive clones, approx. 10 μg of linearized plasmid were used for the transformation of *H. polymorpha* by electroporation in general following the protocol from Faber et al. (1994), but using 1,5 kV, 50 μF and 100 Ω. Clone selection of was performed by Zeocin™ (Song et al., 2003).

[1] Assuming a tetrameric molecular weight of the core SAV of 56 kDa.

Table 1
Variants of expression vectors for the production of streptavidin by *Hansenula polymorpha*.

vector designation	promoter	streptavidin gene[a]
FMD-cSAV	FMD	core SAV
FMD-AP-cSAV	FMD	ala-pro core SAV
FMD-AP-SAV	FMD	ala-pro full-length SAV
MOX-cSAV	MOX	core SAV
MOX-AP-cSAV[b]	MOX	ala-pro core SAV
MOX-AP-SAV	MOX	ala-pro full-length SAV

[a] Variant of the streptavidin gene: core SAV = shortened streptavidin gene (AA 13–139), full-length SAV = AA 1–159. Variants labelled ala-pro contain an *N*-terminal alanine-proline-modification as described by Eilert et al. (2013).
[b] Transformation of ATCC 34438 with this vector did not yield producers.

Glycerol stocks of *H. polymorpha* were prepared applying a final concentration of 15% (w/v) of glycerol, freezing in liquid nitrogen and storage at −80 °C.

The expression vectors were constructed according to the detailed description in Section S1 (supplementary material). In brief, the pUC-based pAaZBgl vector backbone (Pichia Pool/TU Graz, Graz, Austria; Ahmad et al., 2014), designed for the AOX1 (alcohol oxidase) promoter-based expression of heterologous genes by *P. pastoris*, was modified for its application in *H. polymorpha*. The modified backbone allowed secretion of the target protein mediated by the α-mating factor (α-MF) secretion signal from *S. cerevisiae*, termination of transcription by the AOX1 terminator from *P. pastoris*, selection by a Zeocin™-resistance cassette and integration into the genome of *H. polymorpha* by a part of the 3′-UTR (untranslated region) of the FMD locus. The latter region was cut by the single cutter *Bgl*II prior to the transformation. The promoter region for the gene of interest was exchanged by the MOX or FMD promoters, which were amplified from a genome isolate of *H. polymorpha* ATCC 34438.

The final expression vectors (Table 1) contained different variants of the SAV gene. The gene variants were amplified from the genome of *S. avidinii* CBS 730.72, covering either the complete length of mature SAV (AA 1–159) or a core structure of the protein (AA 13–139). In some cases, the *N*-terminal amino acids were exchanged by an alanine-proline motif as described by Eilert et al. (2013) to improve processing of the α-MF signal sequence.-

2.3. Media and supplements for cultivation

HSG medium was used as standard cultivation medium for *E. coli* containing (per L) glycerol 14.9 g, soy peptone 13.5 g, yeast extract 7.0 g, NaCl 2.5 g, K_2HPO_4 2.3 g, KH_2PO_4 1.5 g, and $MgSO_4 \cdot 7H_2O$ 0.249 g. The *pH* was set to 7.4 using 6 N NaOH.

Microplate and shake-flask cultivations were performed using YPD or YPG medium (Cregg, 2007), containing (per L) 20 g soy peptone, 10 g yeast extract and 20 g of carbon source (D-glucose for YPD, glycerol for YPG), which was adjusted to *pH* 7.0.

Bioreactor cultivation was based on Mayer's synthetic medium (Mayer et al., 1999), consisting of (per L) 5 g KH_2PO_4, 10 g $NH_4H_2PO_4$, 5 g $(NH_4)_2SO_4$, 2.3 g KCl, 0.5 g NaCl, 0.75 g $CaCl_2 \cdot 2H_2O$, 0.1 g Na-EDTA, 0.1 g $(NH_4)_2Fe(SO_4)_2 \cdot 6H_2O$, and 4.5 g $MgSO_4 \cdot 7H_2O$, adjusted to a *pH* value of 4.6 and autoclaved in the fermenters. D-Glucose (10 or 30 g L^{-1}) was sterilized separately as a 10fold concentrate. Additionally, sterile-filtered thiamin and biotin were added to a final concentration of 100 and 0.3 mg L^{-1}, respectively, using 1000- and 500fold concentrates. A volume of 10 mL (1% (v/v)) of a 100fold trace salt solution was added after sterilization, consisting of (per L) 0.05 g H_3BO_3, 0.125 g $CuSO_4$, 3 g $ZnSO_4 \cdot 7H_2O$, 4 g $MnSO_4 \cdot H_2O$, 0.1 $NiSO_4 \cdot 6H_2O$, 0.1 $CoCl_2 \cdot 6H_2O$, and 0.1 $Na_2MoO_4 \cdot 2H_2O$, 0.1 g KI, acidified by the addition of 0.5 mL of 85% (w/w) H_2SO_4 per L for an improved solubility. Inoculation was

performed by an overnight culture applying a half-concentrated medium of the same composition, using the full amount of glucose (30 g L^{-1}), thiamin, biotin, and trace salts. Feed solutions were an aqueous glucose or glycerol solution (550 g L^{-1}) for biomass generation and sterile-filtered methanol (HPLC-grade, VWR, Darmstadt, Germany) for induction.

2.4. Characterization in microplates and shake flasks

Screening of transformants of *H. polymorpha* was performed in 96 well-deepwell plates (Deepwell Plate 96/2000 μL, Eppendorf AG, Hamburg, Deutschland) based on the methods for *P. pastoris* by Weis et al. (2004) and Hartner et al. (2008). A cultivation volume of 500 μL of YPD medium was inoculated by single colonies and sealed by a gas-permeable, sterile sealing film (BREATHseal™, Greiner Bio-One International GmbH, Kremsmuenster, Austria). After three days of incubation at 28 °C and a shaking frequency of 350 min^{-1} (shaking diameter 2.5 cm), the plate was used for the creation of glycerol stocks and 10 μL of the culture were used for the inoculation of a second 96 well plate (main culture) filled with 490 μL of YPG medium per well. After three additional days, the loss of water was compensated by the addition of sterile demineralized water (differential weighing) and induction was started by 1% (v/v) of sterile methanol. Cultivation was terminated after three more days and a final compensation of evaporation by sterile water. Where indicated, 24 squared well-deepwell-plates (Axygen® 24 Well Clear V-Bottom, Corning Inc., New York, USA) were used. The cultivation volume was increased to 3 mL for these experiments. All further steps were performed as described in the 96 well-protocol, but scaled according to the increased volume.

Shake flask cultivations were performed in YPG medium in baffled 500 mL-shake flasks (DURAN® baffled flask with membrane screw cap, Schott AG, Mainz, Germany) with a filling volume of 50 mL at 30 °C and a shaking frequency of 200 min^{-1} (shaking diameter: 2 cm). Upon sampling (every 24 h), methanol and glycerol were added for induction and derepression in concentrations of 0.5% (v/v) and 5 g L^{-1}, respectively. Flasks were inoculated to an OD_{600} of 0.1 by an overnight culture.

2.5. Fermentation in the bioreactor

Bioreactor fermentation took place in the Sixfors fermentation system by Infors HT (Infors AG, Bottmingen, Switzerland) with glass vessels without turbulence promoters and a maximal filling volume of 500 mL. The working volume was 400 mL. Three six-bladed rushton turbines, one three-bladed propeller stirrer and one mechanic foam disruptor were used as stirrers. Characteristic dimensions of the reactor were 2.77:1 (bioreactor aspect ratio) and 0.4 (ratio of stirrer to reactor diameter). Cultivations were performed at 30 °C, an air flow rate of 3 vvm (1.2 NL min^{-1}), and a stirring frequency of 1000 min^{-1}. The volumetric oxygen transfer coefficient k_La of the system was determined by dynamic measurement (Bandyopadhyay et al., 1967). Input air was saturated with water vapor. The *pH* value was metabolically shifted from 4.6 (initial *pH*) to 3.4 during the cultivation, followed by control at this value by the automatic addition of 20 % (w/w) H_3PO_4 and 25 % (w/w) NH_3. The initial fermentation volume of 400 mL was adjusted to an optical density OD_{600} of 1.0 at inoculation, using a shake flask overnight culture. A 550 g L^{-1} *D*-glucose or glycerol solution was fed pulse-wise to reach a glucose concentration of 1 g L^{-1} when the relative dissolved oxygen saturation *rDO* surpassed 50 %. After glucose feeding (48 h), the culture was induced by methanol based on the *rDO* in a similar manner, resulting in a methanol concentration of 0.5 % (v/v) per pulse.

Samples were automatically taken in intervals of 6 or 8 h, cooled to 4 °C and processed in intervals of 24 h. Media were supplemented with 1 drop of antifoam agent (Pluronic® PE 8100, BASF SE, Ludwigshafen, Germany) per 50 mL of medium (≈0.7 g L^{-1}).

2.6. Analysis of substrate (S) and biomass (X, OD_{600})

Glucose concentrations were determined by HPLC as described previously (Müller et al., 2013). For measurement of the optical density at 600 nm OD_{600} (BioPhotometer *plus*, Eppendorf AG, Hamburg, Germany) samples of cultures were diluted by a solution of NaCl (9 g L^{-1}) if required, i.e. if the optical density was higher than 0.8. The dry cell weight concentration *X* was determined by differential weighing after drying at 50 °C to constancy of weight. Cell pellets were acquired from 1 mL of culture broth washed twice in an aqueous NaCl solution (9 g L^{-1}).

2.7. Quantification of product (P) and the proportion of biotin-blocked binding sites ($Q_{blocked}$)

The tetrameric concentration of soluble SAV was determined by fluorescence quenching of biotin-4-fluorescein (Kada et al., 1999a, 1999b). The assay was performed in final volumes of 1 mL as specified elsewhere (Müller et al., 2013). The overall binding sites of SAV were quantified via heat-based displacement of biotin by B4F (Müller et al., 2015) by incubating the samples at 70 °C for 10 min prior to the fluorescence measurement. Samples were diluted to overall SAV concentrations ≤300 nM of tetrameric SAV to allow full detectability of the binding sites. The proportion of biotin-blocked sites $Q_{blocked}$ was calculated from the difference of the measurements at room temperature (free binding sites) and after heat incubation (overall binding sites) and scaled from 0 (biotin-free SAV) to 1 (product completely inactive).

3. Results

3.1. Clone characterization in microplates

The different expression constructs described in Table 1 were used for transformation of the two *H. polymorpha*-strains. Clones were analyzed in 96 well-plates. Results are shown in Fig. 1.

Generally, transformation efficiency was more than 12fold higher for *H. polymorpha* DL-1 than for ATCC 34438 (total number of clones: 478 vs. 38) which is probably due to the more efficient homologous recombination in the strain DL-1 (Rhee et al., 1999). According to the distribution of SAV concentrations, the expression pattern of the clones was rather inhomogeneous. This is particularly true for the DL-1 constructs FMD-cSAV and MOX-AP-SAV, for which the final product concentration ranged from 0 to 1766 nM (FMD-cSAV) and from 0 to 1287 nM (MOX-AP-SAV), respectively. ATCC 34438 transformed with the FMD-AP-SAV-vector led to a very narrow expression pattern and yielded by far (factor of >2.3 to all other combinations) the highest median of product concentrations (1601 nM). However, these results are only based on 5 clones due to low transformation efficiency.

The results for *H. polymorpha* DL-1 suggest that the alanine-proline-terminus fused to the core SAV gene (AP-cSAV) had a negative impact on the SAV concentration (median AP-cSAV = 41 and 121 nM for FMD and MOX; median cSAV = 541 and 224 for FMD and MOX). Thus, it would be desirable to analyze if removal of the AP-motif leads to improved SAV production for the full-length construct as well (not tested). No clear conclusions are possible for the choice of promoter and length of the SAV gene. However, the ATCC 34438 FMD AP-SAV construct showed the best overall performance of the combinations tested.

Three best-performing clones were taken to the next step of characterization in shake flasks. To provide comparable conditions,

only FMD-based constructs were evaluated, namely one clone of ATCC 34438 FMD-AP-SAV, DL-1 FMD-cSAV, and DL-1 FMD-AP-SAV, respectively.

3.2. Comparison of selected clones in shake flasks

The courses of product and biomass of the three clones were evaluated in shake flasks under conditions of induction and derepression. Results are shown in Fig. 2.

Generally, final product concentrations were 1.6- to 2.6fold improved by induction towards pure derepression of the same construct. Derepression was most effective for ATCC 34438 FMD-AP-SAV, yielding 523 nM of SAV after the initial growth phase (24 h). Remarkably, derepression of the corresponding clone led to a concentration of SAV surpassing or in one case (induction of DL-1 FMD-AP-SAV) matching the concentrations achieved by induction or derepression of all further constructs, implying a suitable genetic configuration for the heterologous production of SAV for subsequent studies. In comparison to the previous results, cultivation in microplates (Fig. 1) yielded higher concentrations of SAV than in shake flasks for *H. polymorpha* DL-1, whereas cultivation of the clone of ATCC 34438 led to comparable concentrations in both cultivation systems (microplate: 1601 nM, induction in shake flasks: 1782 nM). Upon induction, ATCC 34438 FMD-AP-SAV accumulated a maximal concentration of 1782 nM of SAV in the supernatant, surpassing the SAV concentration in all other cultures by a factor of at least 2.4.

Due to the favorable properties upon derepression and the higher overall product concentration, the corresponding clone (ATCC 34438 FMD-AP-SAV) was used for a more detailed characterization.

3.3. Impact of the cultivation temperature on SAV production

The cultivation temperature was varied in a microplate study, as this factor was of central importance in the optimization of SAV production by *E. coli* (Müller et al., 2016). Results are shown in Fig. 3. A cultivation temperature of 30 °C was favorable for the accumulation of SAV. The final OD_{600} and product concentration achieved at this temperature were 1.2 and 1.9fold increased towards cultivation at 37 °C, respectively. Thus, the temperature was adjusted to 30 °C for all following experiments.

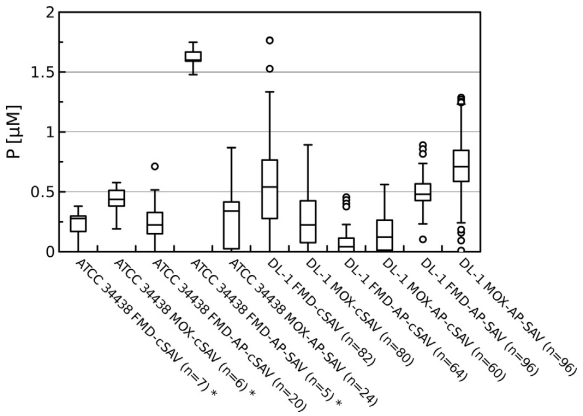

Fig. 1. Box plot for the effect of different host strains (ATCC 34438 and ATCC 26012 = DL-1) and combinations of promoter (MOX or FMD) and streptavidin gene (SAV = full-length, cSAV = core SAV (AA 13–139), AP-SAV/cSAV = alanine-proline-motif at *N*-terminus) on the extracellular concentration of streptavidin *P*. Outliers are shown as open circles. Expression was performed in 96 well-plates (YPG medium, induction by methanol). The number of clones analyzed is shown in brackets. Where indicated (*), cultivations were performed in 24 well-plates due to the small number of clones.

3.4. Effect of the carbon source on biomass and SAV production

Derepression of the promoter in fed-batch studies in microplates led to lower concentrations of biomass (factor 1.7 on average) and SAV (factor 1.6) for the carbon source glucose compared to pure glycerol (data not shown).

Moreover, as a byproduct of the continuously growing biodiesel industry glycerol may contribute to a more sustainable process. Quality and composition of crude glycerol vary depending on the manufacturer and the process established (Yang et al., 2012). In this study crude glycerol from Cargill GmbH (Krefeld, Germany) and Campa AG (Ochsenfurt, Germany) was used as carbon source for different batch and fed-batch cultivations instead of pure glycerol for laboratory use. The studies led to comparable results regarding final product concentration and productivity (data not shown). A process based on pure derepression applying crude glycerol may therefore be an ideal choice regarding sustainability.

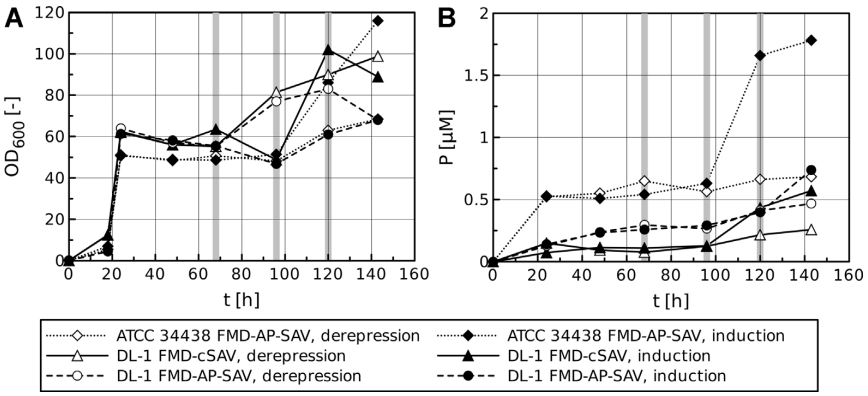

Fig. 2. Comparison of different producer strains of *H. polymorpha* in shake flasks as described in Section 2.4. Where indicated (once per gray area), cultures were either induced by 0.5% (v/v) of methanol (induction) or fed with 5 g L^{-1} of glycerol (derepression). (A) Optical density at 600 nm. (B) Product concentration *P*.

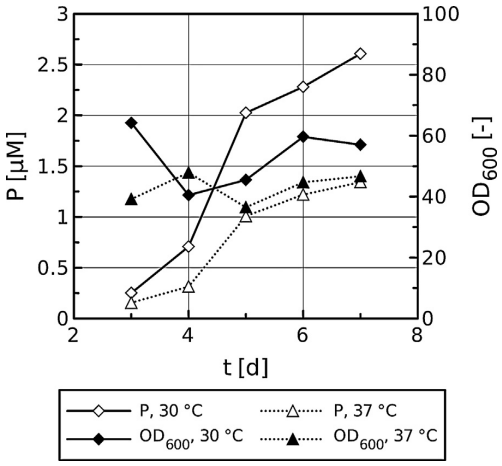

Fig. 3. Impact of the cultivation temperature on the concentration of streptavidin *P* and the optical density at 600 nM OD_{600} of *Hansenula polymorpha* ATCC 34438 FMD-AP-SAV grown in YPG medium in microplates in duplicates according to Section 2.4. Methanol was supplemented to the wells in a final concentration of 1.0 % (v/v) after sampling.

3.5. Production of SAV in the bioreactor

To ensure up-scalability of the system, the best-performing clone of ATCC 34438 based on the FMD promoter-based AP-SAV expression cassette was cultivated in the bioreactor. Dynamic measurement (Bandyopadhyay et al., 1967) yielded a volumetric oxygen transfer coefficient k_La of $129 \pm 19\,h^{-1}$ for the conditions applied (3 vvm, 1000 min^{-1}). Fermentation was performed as described in Section 2.5 applying a synthetic medium suitable for the production of dry cell weight concentrations larger than 100 g L^{-1} (Mayer et al., 1999). Glucose and glycerol were tested as carbon source. All of the substrates were fed pulse-wise based on the relative dissolved oxygen saturation *rDO*. The *pH* was shifted metabolically to 3.4 from an initial value of 4.6. The process was divided in three phases: batch phase on glucose, limiting feeding of glucose (derepression), and induction by methanol. Results are shown in Fig. 4. Regression curves of biomass and SAV (Fig. 4A) were acquired by fits to logistic models, resulting in courses of the local (p_{loc}) and overall (space time yield, p_{STY}) productivity as shown in Fig. 4B.

Biomass was formed primarily in the batch and glucose feed phase (derepression, 77.1%), whereas the majority of product (88.7%) accumulated upon induction by methanol. This is consistent with previous fed-batch experiments in microplates (data not shown). Derepression of the construct led to a concentration of SAV of 1.31 ± 0.07 µM (48 h, $p_{STY} = 27.3$ nM h^{-1}). This concentration further increased upon induction by methanol, reaching a maximum of 11.42 ± 0.22 µM (≈751 mg L^{-1}, assuming a theoretical MW of 65.8 kDa per un-glycosylated tetramer) of biotin-free, tetrameric SAV in 216 h ($p_{STY} = 52.5$ nM h^{-1}). The proportion of biotin-blocked binding sites (Fig. 4 B) dropped from 54.4 ± 5.0 % after 18 h to 17.2 ± 6.5% towards the end of the glucose feed phase (48 h), further decreasing to a diminishingly small proportion of 1.1 ± 3.8% in the end of the process (216 h), thus leading to a highly bioactive product. The final selectivity of the process (product per biomass) and specific productivity (productivity per biomass) were 244.5 nmol g^{-1} and 1.13 nmol g^{-1} h^{-1}, respectively.

A corresponding process applying glycerol instead of glucose in the batch- and first fed-batch phase yielded a 1.3fold higher concentration of biomass (60.1 ± 1.2 vs. 46.3 ± 1.3 g L^{-1} after 216 h), resembling the microplate results (section 3.4). However, due to a lower extracellular concentration of product (0.31 ± 0.02 vs. 1.31 ± 0.07 µM after 48 h upon derepression, 9.22 ± 0.26 vs. 11.42 ± 0.22 µM after 216 h upon induction) the strategy yielded a reduced process selectivity (153.3 nmol g^{-1}) and specific productivity (0.71 nmol g^{-1} h^{-1}).

Several additional fermentations were performed (data not shown). Further studies based on glucose feeding in pulses of 3 g L^{-1} brought about similar results for the derepression phase. Cultivation applying a constant *pH* of 4.6 without the metabolic shift from *pH* 4.6–3.4 resulted in a reduced overall product concentration. Optimization of the induction procedure by methanol was tested by step-wise reduction of the cultivation temperature or the feed volume per pulse to avoid relative dissolved oxygen saturations <10% (oxygen limitation). However, both of these strategies resulted in decreased product concentrations.

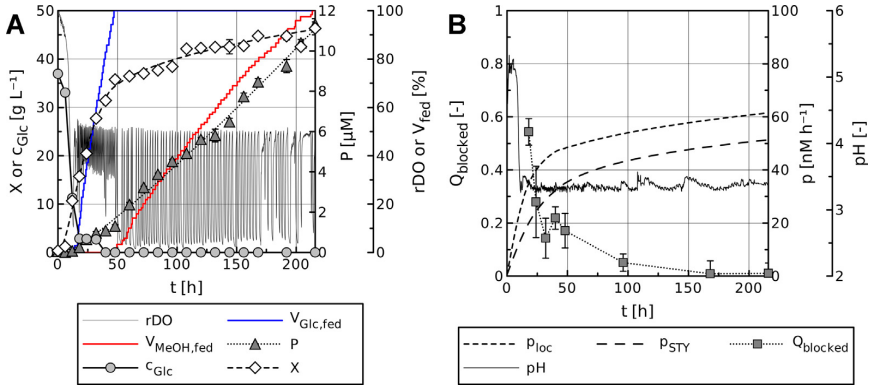

Fig. 4. Fed-batch bioreactor cultivation of *H. polymorpha* ATCC 34438 producing AP-SAV under control of the FMD promoter in a synthetic medium. The cultivation volume was 400 mL. Feeding was performed pulse-wise based on the dissolved oxygen signal, divided in a phase of glucose (14–48 h) and methanol feeding (48–216 h), respectively. The final volumes of the feed solutions were 32 mL of 550 g L^{-1} glucose and 173 mL of pure methanol, respectively. (A) Glucose (c_{Glc}) consumption, feeding (V_{fed}), and concentrations of dry cell weight (*X*) and SAV (*P*). (B) *pH*, proportion of biotin-blocked binding sites $Q_{blocked}$, and local (p_{loc}) and overall (p_{STY}) productivity. V_{fed} corresponds to the proportion of the final feed volume of both feed solutions (Glc = glucose, MeOH = methanol). The methanol concentration was <3 g L^{-1} for all sampling points (data not shown).

4. Discussion

The production of SAV by the yeast *H. polymorpha* was successfully established. According to the clone characterization in shake flasks, *H. polymorpha* ATCC 34438 is a more suitable host for the expression of the SAV gene than DL-1. A cultivation temperature of 30 °C improves SAV production towards 37 °C like previously observed for *E. coli* (Müller et al., 2016).

Cultivation was successfully scaled up from microplates via shake flasks to the bioreactor, showing suitable properties for industrial processes. As reported by Mayer et al. (1999), who produced a phytase under control of the FMD promoter, derepression using glucose instead of glycerol led to improved product formation. However, it remains unclear why methanol induction also resulted in lower product concentrations for the glycerol-based process, since this strategy was more efficient for biomass generation. This may be an effect of the pulse-wise feeding of methanol, potentially limiting the productive potential of the biomass. Experiments based on optimized induction by the use of methanol sensors and a constant concentration of methanol are therefore in preparation.

The final product concentration of 11.42 ± 0.22 μM for glucose-based cultivation is among the highest reported for the heterologous expression of a full-length SAV gene, surpassing maximal concentrations for secretion-based *E. coli* processes (2.60 ± 0.17 μM in bioreactor cultivations; Müller et al., 2016) by a factor of 4.4.

In contrast to the bioreactor study of Nogueira et al. (2014) using *P. pastoris*, the parameters for methanol induction were chosen to allow expression of the SAV gene under conditions of reduced oxygen supply for improved process scalability, i.e. without the application of concentrated oxygen. Nevertheless, the final product concentration was in the same range (11.42 ± 0.22 μM, this study vs. 11 μM of Nogueira and coworkers), although productivities were lower (52.5 vs. 67 nM h^{-1}). However, the concentration was reached for a much lower DCW concentration (46.3 ± 1.2 g L^{-1} vs. 235 g L^{-1}), leading to a drastically improved process selectivity (244.5 vs. 46.8 nmol g^{-1}). The proportion of biotin-blocked binding sites was reduced from 20% (Nogueira et al., 2014) to 1.1 ± 3.8% (this study). Furthermore, the derepression stage of the process shows that the construct allows the accumulation of SAV in the absence of methanol, which may be exploited to circumvent problems like high oxygen demand, flammability, and solvent toxicity accompanying the use of the organic solvent.

In summary, the properties indicate that *H. polymorpha* is a highly suitable host for the production of SAV. On the genetic level, multiple integration of the SAV expression cassette into the host genome may further improve SAV production (Sohn et al., 1996). The latter strategy may be useful in combination with derepression of the host to achieve higher concentrations of SAV without the use of methanol (Mayer et al., 1999). Furthermore, regarding the results for the core SAV gene a construct expressing a full-length gene of SAV without the AP-modification may futher improve SAV production. Finally, selected DL-1 clones should also be cultivated in the bioreactor to check, whether the production behavior in this cultivation system resembles the promising microplate results (Fig. 1) or brings about decreased concentrations of SAV like observed in shake flasks (Fig. 2).

Conflict of interest

The authors declare no financial or commercial conflict of interest.

Acknowledgements

The authors gratefully acknowledge financial support by the Scholarship Program of the German Environmental Foundation (Deutsche Bundesstiftung Umwelt, DBU) and the Bielefelder Nachwuchsfonds.

Appendix A. Supplementary data

Supplementary data associated with this article can be found, in the online version, at http://dx.doi.org/10.1016/j.jbiotec.2016.03.017.

References

Ahmad, M., Hirz, M., Pichler, H., Schwab, H., 2014. Protein expression in *Pichia pastoris*: recent achievements and perspectives for heterologous protein production. Appl. Microbiol. Biotechnol. 98, 5301–5317.
Bandyopadhyay, B., Humphrey, A., Taguchi, H., 1967. Dynamic measurement of the volumetric oxygen transfer coefficient in fermentation systems. Biotechnol. Bioeng. 9, 533–544.
Bayer, E.A., Ben-Hur, H., Hiller, Y., Wilchek, M., 1989. Postsecretory modifications of streptavidin. Biochem. J. 259, 369–376.
Casteluber, M.C.F., Damasceno, L.M., da Silveira, W.B., Diniz, R.H.S., Passos, F.J.V., Passos, F.M.L., 2012. Cloning and expression of a functional core streptavidin in *Pichia pastoris*: strategies to increase yield. Biotechnol. Prog. 28, 1419–1425.
Chaiet, L., Wolf, F.J., 1964. The properties of streptavidin: a biotin-binding protein produced by streptomycetes. Arch. Biochem. Biophys. 106, 1–5.
Cregg, J.M., 2007. Pichia Protocols. Humana Press, Totowa.
Eilert, E., Rolf, T., Heumaier, A., Hollenberg, C.P., Piontek, M., Suckow, M., 2013. Improved processing of secretory proteins in *Hansenula polymorpha* by sequence variation near the processing site of the alpha mating factor prepro sequence. J. Biotechnol. 167, 94–100.
Faber, K.N., Haima, P., Harder, W., Veenhuis, M., 1994. Highly-efficient electrotransformation of the yeast *Hansenula polymorpha*. Curr. Genet. 25, 305–310.
Gallizia, A., de Lalla, C., Nardone, E., Santambrogio, P., Brandazza, A., Sidoli, A., Arosio, P., 1998. Production of a soluble and functional recombinant streptavidin in *Escherichia coli*. Protein Expres. Purif. 14, 192–196.
Gibson, D.G., Young, L., Chuang, R.Y., Venter, J.C., Hutchison 3rd, C.A., Smith, H.O., 2009. Enzymatic assembly of DNA molecules up to several hundred kilobases. Nat. Meth. 6, 343–345.
González, M., Argaraña, C.E., Fidelio, G.D., 1999. Extremely high thermal stability of streptavidin and avidin upon biotin binding. Biomol. Eng. 16, 67–72.
Green, N.M., 1990. Avidin and streptavidin. Meth. Enzymol. 184, 51–67.
Hartner, F.S., Ruth, C., Langenegger, D., Johnson, S.N., Hyka, P., Lin-Cereghino, G.P., Lin-Cereghino, J., Kovar, K., Cregg, J.M., Glieder, A., 2008. Promoter library designed for fine-tuned gene expression in *Pichia pastoris*. Nucleic Acids Res. 36, e76.
C.P. Hollenberg, Z.A. Janowicz. DNA molecules coding for FMDH control regions and structured gene for a protein having FMDH activity and their uses. US Patent 5389525 A. 1987.
Kada, G., Falk, H., Gruber, H.J., 1999a. Accurate measurement of avidin and streptavidin in crude biofluids with a new, optimized biotin-fluorescein conjugate. BBA–Gen. Subj. 1427, 33–43.
Kada, G., Kaiser, K., Falk, H., Gruber, H.J., 1999b. Rapid estimation of avidin and streptavidin by fluorescence quenching or fluorescence polarization. BBA–Gen. Subj. 1427, 44–48.
Ledeboer, A.M., Edens, L., Maat, J., Visser, C., Bos, J., Verrips, C.T., Janowicz, Z., Eckart, M., Roggenkamp, R., Hollenberg, C.P., 1985. Molecular cloning and characterization of a gene coding for methanol oxidase in *Hansenula polymorpha*. Nucleic Acids Res. 13, 3063–3082.
Mayer, A.F., Hellmuth, K., Schlieker, H., Lopez-Ulibarri, R., Oertel, S., Dahlems, U., Strasser, A.M.W., van Loon, A.P.G.M., 1999. An expression system matures: a highly efficient and cost-effective process for phytase production by recombinant strains of *Hansenula polymorpha*. Biotechnol. Bioeng. 63, 373–381.
H.M. Meade, J.L. Jeffrey, Production of streptavidin-like polypeptides. US Patent 5272254 A. 1984.
Miksch, G., Ryu, S., Risse, J.M., Flaschel, E., 2008. Factors that influence the extracellular expression of streptavidin in *Escherichia coli* using a bacteriocin release protein. Appl. Microbiol. Biotechnol. 81, 319–326.
Müller, J.M., Risse, J.M., Jussen, D., Flaschel, E., 2013. Development of fed-batch strategies for the production of streptavidin by *Streptomyces avidinii* based on power input and oxygen supply studies. J. Biotechnol. 163, 325–332.
Müller, J.M., Risse, J.M., Friehs, K., Flaschel, E., 2015. Model-based development of an assay for the rapid detection of biotin-blocked binding sites of streptavidin. Eng. Life Sci. 15, 627–639.
Müller, J.M., Wetzel, D., Flaschel, E., Friehs, K., Risse, J.M., 2016. Constitutive production and efficient secretion of soluble full-length streptavidin by an *Escherichia coli* 'leaky mutant'. J. Biotechnol. 221, 91–100.

Nogueira, E.S., Schleier, T., Dürrenberger, M., Ballmer-Hofer, K., Ward, T.R., Jaussi, R., 2014. High-level secretion of recombinant full-length streptavidin in *Pichia pastoris* and its application to enantioselective catalysis. Protein Expr. Purif. 93, 54–62.

Pähler, A., Hendrickson, W.A., Kolks, M.A., Argaraña, C.E., Cantor, C.R., 1987. Characterization and crystallization of core streptavidin. J. Biol. Chem. 262, 13933–13937.

Rösli, C., Rybak, J.N., Neri, D., Elia, G., 2008. Quantitative recovery of biotinylated proteins from streptavidin-based affinity chromatography resins. Methods Mol. Biol. 418, 89–100.

S.K. Rhee, E.S. Choi, C.H. Kim, J.H. Sohn, H.-A. Kang, H.-Y. Kim. 1999 Autonomously replicating sequences, GAPDH gene and promoter derived from Hansenula polymorpha, expression vectors containing same and method for the selection of transformant. US Patent US 5935789 A.

Sambrook, J., 1989. Molecular Cloning: A Laboratory Manual. Cold Spring Harbor Laboratory Press, New York.

Sano, T., Cantor, C.R., 1990. Expression of a cloned streptavidin gene in *Escherichia coli*. Proc. Natl. Acad. Sci. 87, 142–146.

Sano, T., Cantor, C.R., 1995. Intersubunit contacts made by tryptophan 120 with biotin are essential for both strong biotin binding and biotin-induced tighter subunit association of streptavidin. Proc. Natl. Acad. Sci. 92, 3180–3184.

Sano, T., Pandori, M.W., Chen, X., Smith, C.L., Cantor, C.R., 1995. Recombinant core streptavidins. J. Biol. Chem. 270, 28204–28209.

Skerra, A., Schmidt, T.G.M., 1990. Applications of a peptide ligand for streptavidin: the strep-tag. Biomol. Eng. 16, 79–86.

Sohn, J.H., Choi, E.S., Kim, C.H., Agaphonov, M.O., 1996. A novel autonomously replicating sequence (ARS) for multiple integration in the yeast *Hansenula polymorpha* DL-1. J. Bacteriol. 181, 1005–1013.

Song, H., Li, Y., Fang, W., Geng, Y., Wang, X., Wang, M., Qiu, B., 2003. Development of a set of expression vectors in *Hansenula polymorpha*. Biotechnol. Lett. 25, 1999–2006.

Suh, S.O., Zhou, J.J., 2010. Methylotrophic yeasts near Ogataea (Hansenula) polymorpha: a proposal of *Ogataea angusta* comb. nov.and *Candida parapolymorpha* sp. nov. FEMS Yeast Res. 10, 631–638.

Weis, R., Luiten, R., Skranc, W., Schwab, H., Wubbolts, M., Glieder, A., 2004. Reliable high-throughput screening with *Pichia pastoris* limiting yeast cell death phenomena. FEMS Yeast Res. 5, 179–189.

Weydemann, U., Keup, P., Piontek, M., Strasser, A.M.W., Schweden, J., Gellissen, G., Janowicz, Z.A., 1995. High-level secretion of hirudin by *Hansenula polymorpha*—authentic processing of three different preprohirudins. Appl. Microbiol. Biotechnol. 44, 377–385.

Wu, S.C., Qureshi, M.H., Wong, S.L., 2002. Secretory production and purification of functional full-length streptavidin from *Bacillus subtilis*. Protein Expr. Purif. 24, 348–356.

Yang, F., Milford, A.H., Sun, R., 2012. Value-added uses for crude glycerol—a byproduct of biodiesel production. Biotechnol. Biofuels 5, 13.

Journal of Biotechnology

Supplementary material to

Fed-batch production and secretion of streptavidin by *Hansenula polymorpha*: evaluation of genetic factors and bioprocess development

*David Wetzel [a,b], Jakob Michael Müller *[a,b], Erwin Flaschel [a], Karl Friehs [a], and Joe Max Risse [a]*

[a] Lehrstuhl für Fermentationstechnik, Technische Fakultät, Universität Bielefeld, PF 10 01 31, D-33501 Bielefeld, Germany

[b] equal contribution

[*] Corresponding author: Jakob Michael Müller
jmu@fermtech.techfak.uni-bielefeld.de

S1 - detailed description of the cloning strategy

The plasmid pAaZBgl (Ahamad et al. 2014) was used as backbone for the cloning work described here. For the purpose of recombinant protein production with *H. polymorpha* the *P. pastoris* derived promoter and 3` UTR of the AOX1 locus were substituted by *H. polymorpha*- derived sequences. Other functional parts of pAaZBgl like the *S. cerevisiae* *α*-MF signal sequence, the AOX1 transcription terminator, the Zeocin expression cassette, the Ampicillin resistance cassette and the pUC origin of replication were kept.

With primers 1 to 4 two fragments of pAaZBgl were amplified by PCR. One of them contained the *E. coli* – specific part including the pUC ori and the ampicillin resistance gene. The second fragment covered the yeast-specific elements i.e. the Zeocin resistance cassette, the MF-alpha secretion signal and the AOX1 transcription terminator. For heterologous gene expression in *H. polymorpha* the promoter sequences of both the FMD (formate dehydrogenase) and the MOX (methanol oxidase) gene were used. For recombination purpose the transcription terminator of the FMD gene was cloned. All three regulatory elements were amplified from the genome of the *H. polymorpha* strain ATCC 34438 by PCR using primers 5 to 10.

The two fragments of the pAaZBgl vector were assembled with the regions of the FMD or MOX promoter and the FMD terminator by Gibson Assembly.

Thereafter, different SAV coding genes were inserted into the newly designed expression vector for *H. polymorpha*. For this purpose, the vector was linearized using primers 11 and 12. The different SAV-coding genes were amplified using primers 13 to 16. For optimization of Kex2 cleavage during secretion of recombinant streptavidin in some constructs alanine and proline were chosen as the products` N-terminal amino acids i.e. AP-SAV and AP-coreSAV. Eilert et al. (2013) observed improved processing for this amino acid combination following the *S. cerevisiae* α-MF signal sequence. Accordingly, primers 17 and 18 were used to change genes coding for a coreSAV into AP-coreSAV.

During construction of the different plasmids the BglII site upstream of FMD or MOX promoter was deleted by PCR (primers 1 and 19). Using constructs with only one single BglII site led to improved transformation efficiencies after BglII digest compared to constructs with two BglII sites (data not shown).

Tab. S1 Primers combinations used for the construction of the final expression vectors.

Primer desig-nation	Sequence (orientation: 5`→3`)	remark
primer 1 (fwd)	ATGAGATTTCCTTCAATTTTTACTGC TGTTTTATTCGCAGCATCCTCCG	Amplification of the *E. coli* – specific part of pAaZBgl
primer 2 (rev)	ATGCGAGGATGCTGCTGGAGACGA TTCAA	
primer 3 (fwd)	AGATCTTCACTGACTCGCTGCGCTC GGTCG	Amplification of the yeast-specific part or pAaZBgl without promoter and 3` UTR of AOX1 locus
primer 4 (rev)	AGATCTGACGAAAGGGCCTCGTGAT ACGCCTA	
primer 5 (fwd)	GGCGTATCACGAGGCCCTTTCGTCA GATCTATCGCAGAAATGTATCTAAAC GCAAACTCC	Amplification of FMD promoter from *H. polymorpha* genome, introducing homologpus 3` extensions for introducing into pAaZBgl backbone
primer 6 (rev)	AAACAGCAGTAAAAATTGAAGGAAA TCTCATGATTTGATTGATGAAGGCA GAGAGCGCAAGGAGGC	
primer 7 (fwd)	GAATCGTCTCCAGCAGCATCCTCGC ATTGCGGTCTTGGAGGAGCTGATTG GATCTAG	Amplification of FMD terminator from *H. polymorpha* genome, introducing homologpus 3` extensions for introducing into pAaZBgl backbone
primer 8 (rev)	GACCGAGCGCAGCGAGTCAGTGAA GATCTCTTGACTTTCTGGGTGATGG TCTTGGAGG	

Tab. S1 (continued) Primers combinations used for the construction of the final expression vectors.

primer 9 (fwd)	AGGCGTATCACGAGGCCCTTTCGTC AGATCTGATGCACCAATTAATTGTTG CCGCATGCATCCTTGC	Amplification of MOX promoter from *H. polymorpha* genome, introducing homologpus 3` extensions for introducing into pAaZBgl backbone
primer 10 (rev)	TAAAACAGCAGTAAAAATTGAAGGA AATCTCATTTTGTTTTTGTACTTTAGA TTGATGTC	
primer 11 (fwd)	GCGGCCGCAAACGGTTTTAGCCTTA GAC	Linearization of the *H. polymorpha* specific expression vector for introduction of different SAV genes
primer 12 (rev)	TCTTTTCTCGAGAGATACCCCTTCTT CTTTAGCAGCAATGC	
primer 13 (fwd)	GAAGAAGGGGTATCTCTCGAGAAAA GAGCCGAGGCCGGCATCACCGGCA CCTG	Amplification of native *core*-SAV coding gene from *S. avidinii* genome and introducing homologous 3`-extensions for integration into *H. polymorpha* expression plasmid backbone
primer 14 (rev)	GTCTAAGGCTAAAACCGTTTGCGGC CGCTTATTAGGATGCCGCGGACGG CTTCAC	
primer 15 (fwd)	GAAGAAGGGGTATCTCTCGAGAAAA GAGCCCCCTCCAAGGACTCGAAGG CCCAGGTC	Amplification of full-length AP-SAV coding gene from *S. avidinii* genome and introducing homologous 3`-extensions for integration into *H. polymorpha* expression plasmid backbone
primer 16 (rev)	GTCTAAGGCTAAAACCGTTTGCGGC CGCTTATTACTGCTGAACGGCGTCG AGCGGGTTGC	
primer 17 (fwd)	CCCGCCGGCATCACCGGCACCTG	Linearization of coreSAV coding plasmids for introduction of alanine and proline as N-terminal amino acids (AP-coreSAV)
primer 18 (rev)	GGCTCTTTTCTCGAGAGATACCCCT TCTTC	
primer 1 (fwd, see above)	ATGAGATTTCCTTCAATTTTTACTGC TGTTTTATTCGCAGCATCCTCCG	Linearization of expression plasmids in order to delete BglII site upstream the expression cassette
primer 19 (rev)	GACGAAAGGGCCTCGTGATACGCC TATTTTTATAGGTTAATGTC	

6 Evaluation of alternative methods for the purification of SAV

In addition to studies on the optimization of the production of SAV, purification of the protein by a variety of methods was analyzed.

6.1 Motivation

Due to expensive materials and loss of product during the purification procedure, downstream processing (DSP) often causes the majority of cost associated to protein production. SAV is no exception to this rule: 2-iminobiotin agarose, which is used for affinity chromatography of SAV, is listed at a price of 307.50 € per 5 mL of gel material.[1] Moreover, the corresponding columns have to be replaced after few cycles of purification in the experience of the author, which is costly and unsustainable.

6.1.1 Goals of this study

Due to these aspects, cheaper and more ecological methods for the purification of the biotin-binding protein were in the focus of interest. For this project, several methods were evaluated using the supernatants of the homologous and heterologous producers studied in this thesis. The DSP procedures included diafiltration, fractional precipitation by ammonium sulfate and centrifugation, thermal inactivation of contaminants, and - targeting a novel method for the purification of SAV - aqueous two phase extraction (ATPE). All of these methods are based on inexpensive materials compared to purification by chromatography.

6.2 Host-dependent product purity

Generally, most supernatants analyzed in this study showed a low proportion of contaminating proteins. This was, however, not the case for supernatants of *E. coli* for the final process strategy described in Müller *et al.* (2016c), as qualitatively illustrated in Fig. 6.1.

[1] Sigma-Aldrich, retrieved 14^{th} of April, 2016

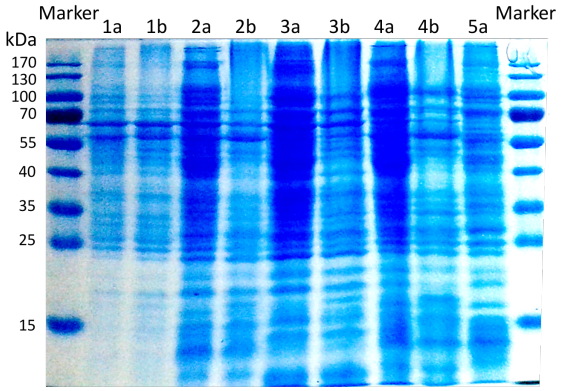

(a) Supernatants of *E. coli*, partially denatured.

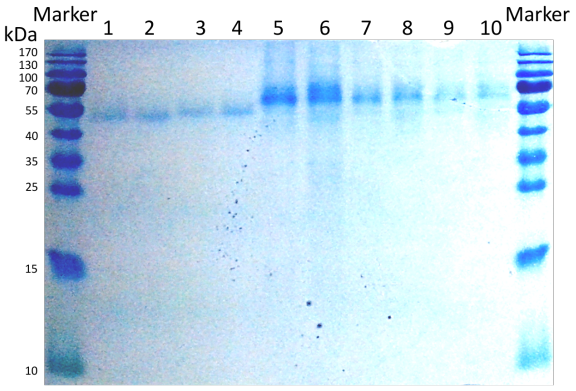

(b) Supernatants of *H. polymorpha*, partially denatured.

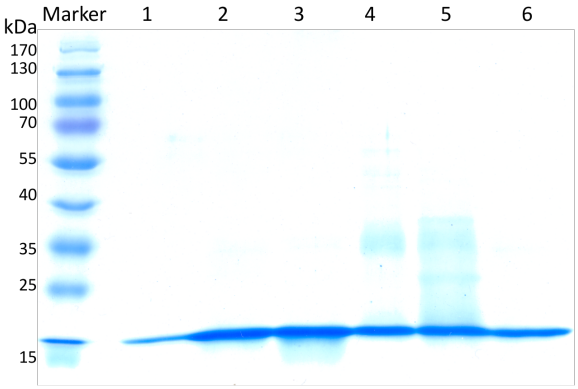

(c) Supernatants of *S. avidinii*, completely denatured.

Fig. 6.1: SDS-PAGE analysis of different supernatants used for DSP studies. Lane 1 in subfigure (c) shows a 1 μM solution of commercial SAV (Sigma), whereas all other lanes show supernatants of different cultivations of the optimized strains of all hosts, as described in the previous sections. Supernatants of *P. pastoris* resembled those of *H. polymorpha* (data not shown). The gel bands in subfigures (a) and (b) indicate that the samples were only partially denatured due to the presence of bands in the size of tetrameric SAV. SAV bands were identified by B4F-staining according to Humbert & Ward (2008) (data not shown). For the SDS-PAGE shown in subfigure (a), samples were applied to the gel without (sublabel a) and with (sublabel b) dilution.[2]

As a consequence of the load of macromolecular contaminants, most of the studies focused on supernatants of *E. coli*.

[2] The contrasts were adjusted using the image processing software GIMP (see Table 2.4, p. 24) to reduce background noise.

6.3 Summary of the results

The results of the corresponding studies are shown in the following sections. Detailed descriptions of the methods used for this section are shown in section 8.1.3 (p. 176*ff.*) in the supplementary material.

6.3.1 Aqueous two phase extraction

Aqueous two-phase extraction of SAV was tested in two different polymer-salt systems. First studies were performed in a PEG/citrate system, whereas PEG/phosphate systems were applied for all subsequent experiments due to the availability of detailed characteristics for the latter (Albertsson, 1986).

6.3.1.1 Preliminary studies in a PEG/citrate system

For preliminary studies, a PEG/citrate system was analyzed based on binodal curves of Kula & Vernau (1990). The supernatant used for the studies was derived from the cultivation of *S. avidinii* applying the optimized fed-batch process strategy developed in section 4 (p. 60*ff.*). Results are summarized in Fig. 6.2.

As can be concluded from the distribution of SAV in the screening, the majority of SAV was located in the PEG-rich phase for most of the conditions tested. This behavior was intensified by alkaline values of the pH. Generally, increased chain lengths of PEG caused a displacement of SAV from the PEG-rich top- to the citrate-rich bottom phase. A maximal proportion of SAV of 99% was located in the PEG-rich phase for all systems adjusted to pH 11, whereas the maximal proportion of 74.9 % of SAV in the citrate-rich phase was observed for the combination of two polymer chain lengths (PEG 1500 and PEG 3000). Based on these preliminary results, more detailed studies were performed using a PEG/phosphate system.

6.3.1.2 Detailed screening in a PEG/phosphate system

In a DoE-approach, the aqueous two-phase extraction of SAV in a polymer/salt-system consisting of PEG 4000 and potassium phosphate was analyzed. These experiments were based on supernatants of *E. coli* grown in twofold concentrated HSG medium in the presence of Triton™ and Pluronic®, as described in section 5.2 (p. 93*ff.*). The change of systems was performed due to the better characterization of PEG/phosphate-systems. This feature is demonstrated, e.g., by a broad availability of bionodal curves and compositions of top- and bottom-phases (Albertsson, 1986). This more detailed screening focused on one chain length of PEG, but contained systematic variations of the concentrations of salt and polymer, the pH, and the supplementation of sodium chloride. Like in the preliminary screening in the PEG/citrate system, SAV was successfully transferred to one specific phase by adjusting the

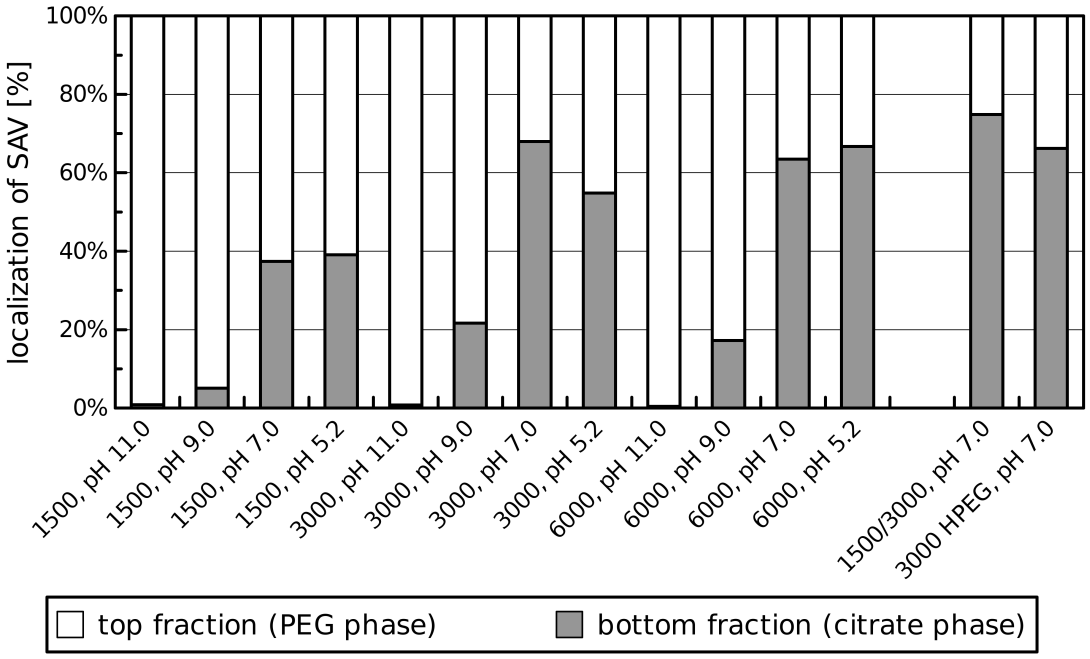

Fig. 6.2: Analysis of the absolute distribution of SAV in PEG/citrate systems. Proportions refer to the amount of SAV n_{SAV} in the whole system. Labels indicate the molecular weight of PEG used and the pH value to which it was adjusted. Phase ratios were typically balanced, with a slightly larger top phase. Exact phase volumes and system compositions are shown in Table 8.1 and 8.2 (p. 178 in the supplementary material). The HPEG-system corresponds to a PEG-rich system (phase ratio: 70 % top phase, 30 % bottom phase), whereas the 1500/3000-system contained both PEG 1500 and PEG 3000 in addition to citrate.

conditions. Table 6.1 sums up system compositions suitable for the extraction of SAV into either the top or the bottom phase.

As can be concluded from Table 6.1, the presence of high concentrations of potassium phosphate and either sour or alkaline pH values seemed to favor the transfer of SAV to the PEG-rich top phase of the system. A shift to the bottom phase was achieved by adjusting the pH to values in the range of the theoretical isoelectric point (pI) of the protein in a potassium phosphate-rich system with low concentrations of PEG. The former effect may be surprising regarding the charge of SAV, since the pI of SAV is relatively neutral,[3] causing a positive or negative net charge of the protein for strongly sour and alkaline pH values, respectively. Thus, contrary to the results, transfer to the salt-rich phase would be expected. However, the simple *in silico*-analysis of the pI does not reveal surface-related effects of

[3] Theoretical pI of 6.1 for full-length SAV according to the ProtParam-toolbox of the Swiss Institute of Bioinformatics, http://web.expasy.org/protparam/.

Tab. 6.1: Summary of ATPE compositions suitable for the aqueous two-phase extraction of SAV based on a supernatant of *E. coli*. All of the listed extractions resulted in a balanced ratio of top and bottom phase. The composition shown in the shaded row was analyzed in detail in subsequent studies (see Fig. 6.3). The major fraction of SAV for each extraction is printed in **bold face**.

$c_{PEG4000}$ [% (w/w)]	$c_{KH_2PO_4/K_2HPO_4}$ [% (w/w)]	c_{NaCl} [% (w/w)]	pH [-]	x_{top} [%] [a]	x_{bottom} [%] [a]
25.0	15.0	1.5	9.5	**85.5**	-
22.0	16.8	1.3	8.7	**90.9**	4.6
25.0	9.0	1.5	4.5	**100.7**	-
18.6	16.3	1.0	7.8	**83.1**	-
22.0	11.0	0.3	8.7	**96.9**	-
12.3	12.7	1.0	7.8	18.0	**94.9**
12.4	12.8	0.5	6.2	18.4	**100.4**
9.3	18.1	0.0	6.3	11.8	**109.2**
13.2	10.7	1.0	7.0	-	**98.0**

[a] Recovery of SAV in the top- and bottom phase of the extraction, respectively, **related to the initial quantity of SAV supplied to the system**. The overall percentage may exceed 100 % due to a varying activity of SAV in the phases.

the charge distribution, which may contribute to a different distribution of the protein in the system.

Unfortunately, for the majority of system compositions contaminating proteins distributed in the system in a manner comparable to SAV, resulting in poor improvements of product purity. The only promising candidate was the composition described in line 4 of Table 6.1 (shaded row). This system showed relatively suitable properties for the distribution of the total protein in each phase and in an SDS-PAGE analysis, as illustrated in Fig. 6.3. The corresponding extraction procedure removed at least a fraction of contaminating proteins by their extraction to the bottom phase of the two-phase system. SAV, on the other hand, was almost exclusively located in the top phase.

In addition to this moderate purification, the method may be useful for the concentration of SAV by using the conditions described and altering the ratio of the phases without modification of the relative composition of each phase.[4] Altered phase ratios could also improve purification by other system compositions according to Table 6.1. To a certain extent, this step also potentially allows removal of low molecular weight contaminants, which typically don't show a preference for one of the phases. However, this comes at the cost of new, extraction-derived contaminants (salts, polymer). Upcoming studies may furthermore combine the effect of chain-length dependent transfer of SAV to the salt-rich phase of the preliminary screening with the pH- and NaCl-based effects observed in the PEG/phosphate

[4] This can be achieved by using different working points, i.e., initial concentrations of salt and polymer, located on the same tie line in the binodal curve plot of the corresponding system, as shown in Fig. 2.10 in section 2.5.1 (p. 23).

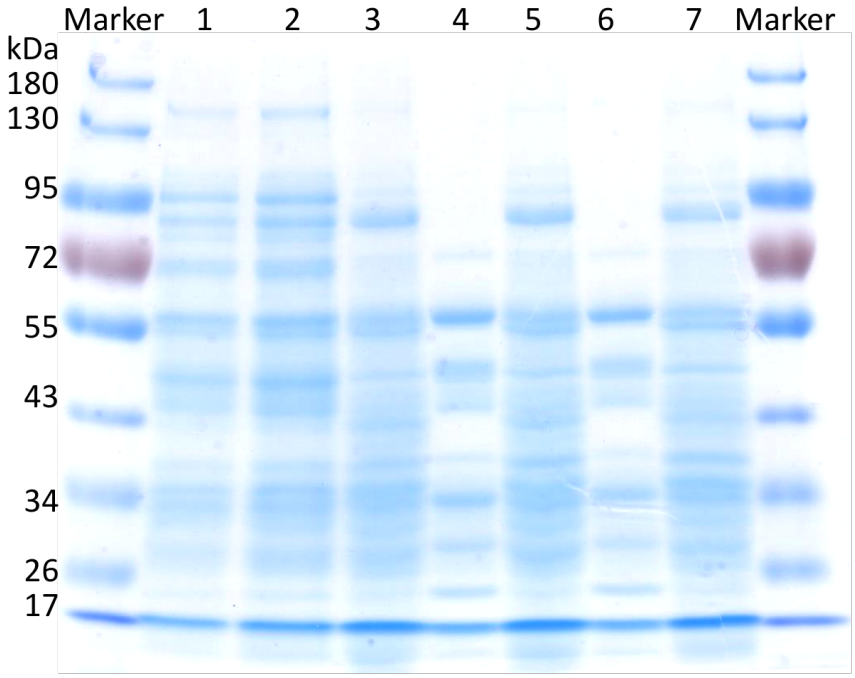

Fig. 6.3: SDS-PAGE analysis of the phases of an aqueous two-phase extraction applying a supernatant of *E. coli*. The overall composition of the system is described in line 4 of Table 6.1. The lanes show the supernatant used for the study in different dilutions (1:10 and 1:5, lanes 1 and 2) and composition of top (lanes 3, 5, 7) and bottom phases (lanes 4, 6), respectively, for three repetitions of the extraction. SAV bands were identified by the supplementation of B4F and UV imaging as described by Humbert & Ward (2008). The apparent molecular weight of SAV was in the range of 17 kDa.

system.

Furthermore, it may be interesting to analyze, whether affinity derivatives of PEG (like PEG-coupled HABA) would cause a more specific extraction of SAV in a system with one PEG-rich and one PEG-deprived phase and thus cause separation of SAV and contaminants. For this purpose, an analysis of the phase composition of each of the phases would be beneficial.

In respect to the following steps of purification, transfer of SAV to the phosphate-rich phase would be advantageous, as salts can easily be removed from the samples by dialysis, whereas separation of the product and PEG is more cumbersome. Alternatively, a two-step extraction could be performed in which SAV is first extracted to a PEG-rich top phase and afterwards extracted back to a phosphate-rich bottom phase.

6.3.2 Filtration

Diafiltration was successfully applied by hollow fibre modules in cross-flow operation to remove residual peptides and low molecular weight contaminants from the supernatant after cultivation. This procedure thus targeted the major contaminants of supernatants of *H. polymorpha*, *P. pastoris*, and *S. avidinii*. Depending on the molecular weight cut-off (MWCO) of the membrane, the method may also be used to selectively dispose of very small or very large contaminating proteins as well as chemical impurities like salts. Fig. 6.4 shows a potential flow chart for the combined removal of these compounds based on a tetrameric weight of SAV in the range of 50-66 kDa (see section 2.2, p. 5).

Generally, for the purpose of concentration of supernatants, ultra- instead of diafiltration would suffice.

Unfortunately, additional studies on the removal of biotin from biotin-blocked samples of SAV via diafiltration at elevated temperatures (60 and 70 °C) did not result in the recovery of blocked binding sites.

6.3.3 Ammonium sulfate precipitation

Based on the results of Suter *et al.* (1988), precipitation of SAV was studied by the addition of ammonium sulfate. The majority of SAV precipitated in the presence of 45-60 % of relative saturation, where 100 % saturation corresponds to a concentration of 767 g L^{-1} of the salt. The experiments thus brought about results comparable to the study of Nogueira (2013) (precipitation at 50 % saturation). However, the majority of contaminating proteins of the *E. coli*-supernatant precipitated in the same range of concentrations, preventing purification of the target protein. Therefore, the method is only suitable for alternative purposes like the concentration of SAV after fermentation.

6.3.4 Thermal inactivation of contaminating proteins

Based on the results of Gallizia *et al.* (1998) and the thermostability of SAV (González *et al.*, 1997), experiments on the thermal inactivation of contaminating proteins were performed. The experimental setup was based on incubation at 60, 75 and 80 °C for an appropriate period of time according to Fig. 3.3 (p. 56). Heat incubation was generally followed by centrifugation (4 °C, 10.000×g, 20 min) for the removal of resulting insoluble contaminants. An SDS-PAGE analysis based on central studies is depicted in Fig. 6.5.

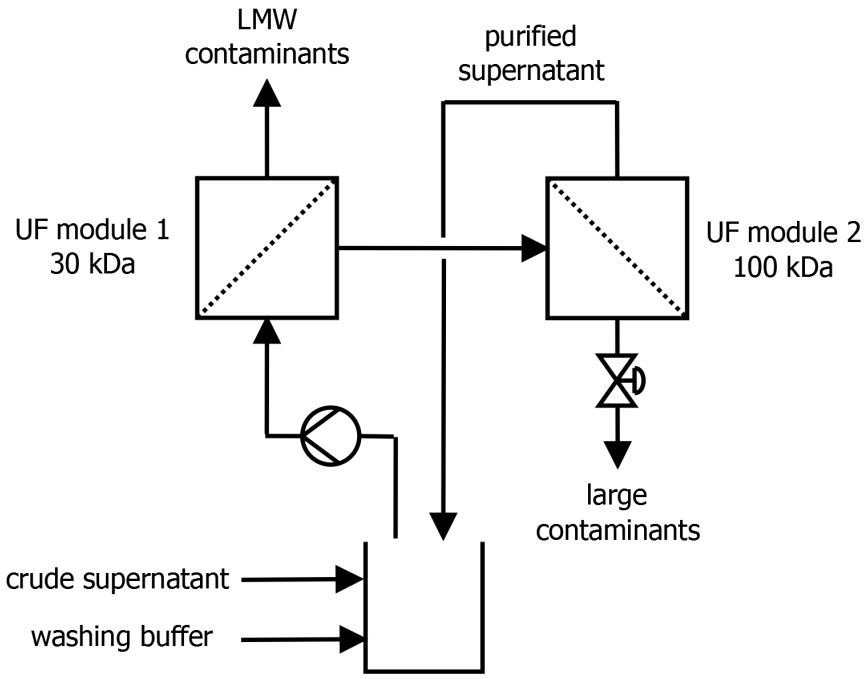

Fig. 6.4: Flow chart for a diafiltration process for the combined removal of low molecular weight (LMW) contaminants like salts, peptides, and small (30 kDa module) and large contaminating proteins (100 kDa module). The trans-membrane pressure (retentate pressure valve) for the second ultrafiltration (UF) module should be high enough to prevent loss of product.[5]

Densitometric evaluation of the gel revealed a relative decrease of the intensity of contaminating bands towards the SAV band by approximately 60 % for an incubation at 80 °C for 5 min. Based on the Bradford method (Bradford, 1976), the total protein in the supernatants was analyzed via the Roti®-Nanoquant system (Carl Roth GmbH + Co. KG, Karlsruhe, Germany). The evaluation indicated that the overall protein content did not decrease in a similar manner. This may indicate that contaminating proteins were degraded to peptides, which partially contribute to the signal in the Bradford measurement, but are not visible in gel-based analysis. These peptides could easily be removed by subsequent diafiltration.

For a preparative purification of SAV, incubation at lower temperatures for longer periods of time may be beneficial due to the time necessary for heat transfer during heating and cooling of the fluid prior to and after heat incubation, respectively. However, as visible from Fig. 6.5, the efficiency of purification seems to increase upon rising temperatures, posing a challenge due to contradictory demands. Thus, rapid heating and cooling for the thermal inactivation at high temperatures via efficient heat exchangers

[5] The chart was created using the flow chart software Dia (see Table 2.4, p. 24).

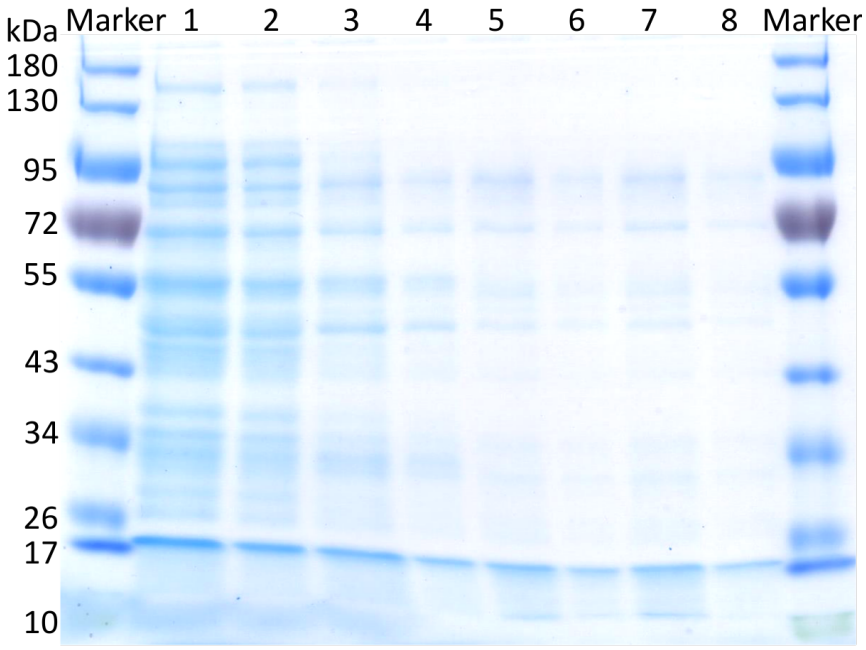

Fig. 6.5: SDS-PAGE analysis of the thermal inactivation of contaminating proteins in supernatants containing SAV. Lanes: supernatant of *E. coli*, diluted 1:5 and 1:10 (lanes 1, 2), supernatant after heat incubation at 60 °C for 30 min (1:5: lane 3, 1:10: lane 4), at 75 °C for 10 min (1:5: lane 5, 1:10: lane 6), and at 80 °C for 5 min (1:5: lane 7, 1:10: lane 8), respectively. SAV bands were identified by the supplementation of B4F and UV imaging as described by Humbert & Ward (2008). The apparent molecular weight of SAV was in the range of 17 kDa.

and large surface areas may be the method of choice. A flow chart for a corresponding process is shown in Fig. 6.6. This kind of purification process could, e.g., be combined with continuous cultivation of *S. avidinii*.

6.4 Suitability of different methods of purification

Fig. 6.7 sums up the suitability of the methods tested for different purposes in the DSP of SAV.

In addition to the use of these methods as the sole purification step, a variety of combined strategies may be suitable for improved results:

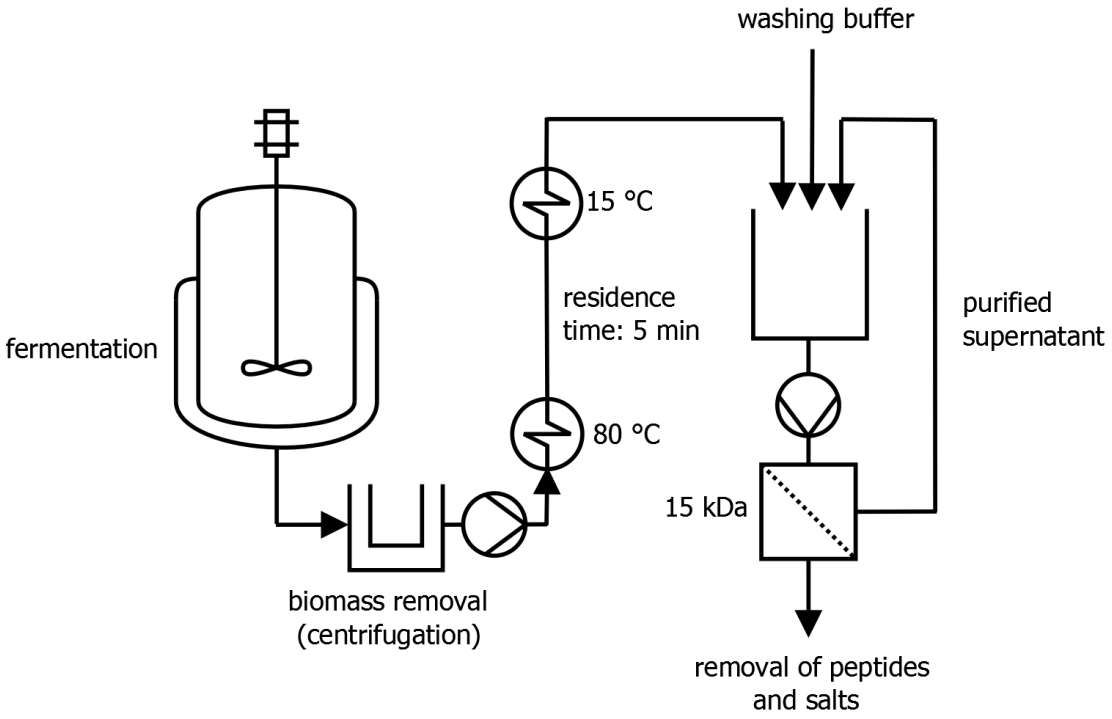

Fig. 6.6: Flow chart for an integrated process allowing the preparative removal of contaminants via thermal inactivation. The process consists of (a) fermentation, (b) biomass removal, (c) thermal inactivation at a suitable temperature (e.g., 80 °C) and residence time (e.g., 5 min), and (d) diafiltration for the removal of resulting peptides. The transfer from the bioreactor to the filtration device is performed once per batch or fed-batch fermentation fermentation or continuously for chemostat cultivation. Washing buffer is added several times for a step-wise dialysis of the sample.[6]

- Thermal inactivation may be integrated into diafiltration routines according to Fig. 6.4 to simultaneously denature and remove contaminating proteins, e.g., by tempering the feed vessel to 60 °C and applying a UF membrane permeable to peptides. Alternatively, when only less heat-stable filtration cassettes are available, heat-based inactivation could be performed batch-wise followed by separation via filtration at room temperature.

- Removal of residual peptides after thermal inactivation should also be possible by precipitation or by ATPE applying a suitable phase ratio.

- The use of proteases may primarily result in the degradation of contaminating proteins due to the stability of the core structure of SAV towards proteolysis (see section 2.2, p. 5). Thus, combined

[6] The chart was created using the flow chart software Dia (see Table 2.4, p. 24).

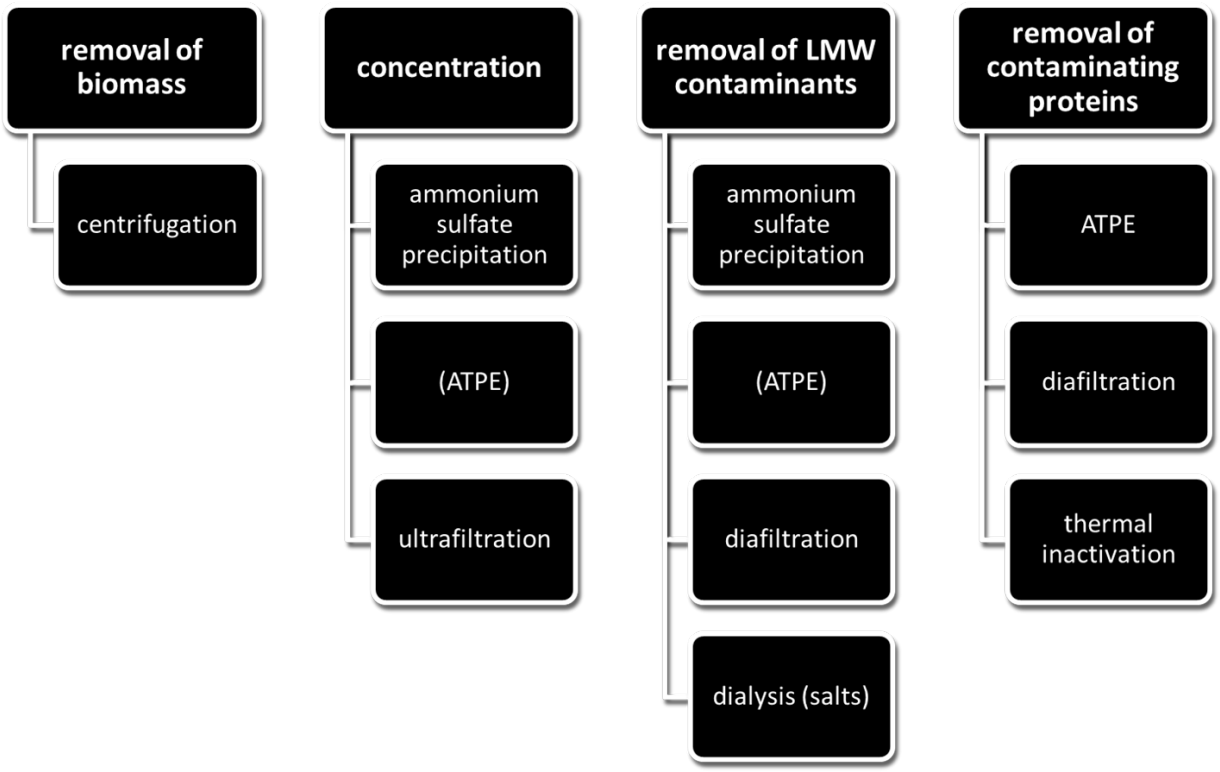

Fig. 6.7: Suitability of selected alternative methods of downstream processing for the purification of SAV. The ranking is alphabetical and does not reflect the suitability of the methods. Brackets indicate limited performance or high experimental effort for the corresponding method and the given purpose. Thermal inactivation is generally combined with centrifugation. Abbreviations: ATPE = aqueous two-phase extraction, LMW = low molecular weight.[7]

protease treatment, inactivation, e.g., by heat, and diafiltration via a membrane characterized by a low MWCO could improve product purity. The removal of proteases may also be achieved by ATPE.

- A two-step extraction may lead to increased purity, e.g. by extraction at pH 11 or pH 9 in a PEG 1500/citrate-system (Fig. 6.2) followed by the addition of PEG 3000 and acidification, or by combining suitable extractions from Table 6.1 for a PEG/phosphate system. Here, phase ratios altered in a suitable manner should improve the removal of contaminants.

- In respect to the continuous cultivation of *S. avidinii* (section 4.4.3, p. 86), different filtration modules would allow direct processing of the outflow volume by either the removal or the retention of biomass. Due to the large outflow volumes, both steps should be combined with

[7] Figure created in PowerPoint (see Table 2.4, p. 24).

ultrafiltration of the resulting supernatants to concentrate SAV. Operation in sterile conditions may furthermore allow the recycling of media for high dilution rates, which lead to high residual concentrations of substrate (see Fig. 4.9, p. 86).

In addition to these methods, precipitation by organic solvents like dimethyl ether as described by Nogueira (2013) remains an option for the rapid purification of SAV at low cost. However, corresponding steps would require explosionproof devices.

Generally, due to the high specificity of the interaction of SAV and biotin, the simple and inexpensive procedures shown in Fig. 6.7 may be sufficient for standard applications of SAV. For the supernatants of *S. avidinii*, *H. polymorpha*, and *P. pastoris*, methods like diafiltration, ammonium sulfate precipitation, and dialysis should already result in a relatively pure product by the removal of salts and residual peptides from complex media compounds. Remarkably, even aliquots of a crude supernatant of *S. avidinii* were successfully used for the quantitative detection of biotin and an immunological detection procedure in additional studies (data not shown). However, further investigations are necessary to analyze, whether the strategies described here are also sufficient for more complex applications, e.g., when the avoidance of cross-reactions is critical.

Concerning the general applicability of the results it has to be taken into account that for a large fraction of experiments the *E. coli* supernatant was used. This is not only relevant in respect to the chain length of SAV, which may, e.g., alter the properties of extraction via ATPE towards core SAV. As the impact of the media additives Triton™ and Pluronic® was not analyzed in a systematic manner, studies based on supernatants of other host organisms may bring about slightly different results. Potential effects of these compounds may, e.g., relate to phase separation behavior during ATPE and solubilization of proteins during precipitation. However, the preliminary screening for ATPE in a PEG/citrate system was based on a supernatant of *S. avidinii*. Nevertheless, the following studies in the PEG/phosphate system applying the *E. coli* supernatant brought about comparable overall tendencies for the distribution of SAV, suggesting a limited impact of the supplements. The same accounts for the results of ammonium sulfate precipitation, which led to findings resembling the data of Nogueira (2013).

7 Summary, concluding remarks and outlook

The challenges for the expression of the SAV gene by the hosts studied in this thesis were highly diverse. While optimization of culture conditions for the natural producer *S. avidinii* mainly focused on aspects of biochemical engineering and the complex morphology of the streptomycete, heterologous expression shed light on various facets of host toxicity of SAV and resulting complications of process design and strain maintenance. Moreover, the pH and temperature dependency of product accumulation and the supplementation of detergents were identified as critical parameters for heterologous production. A comparative analysis of SAV production by the various producers is given in this final chapter.

7.1 Comparative analysis of SAV production by four different hosts

All of the hosts studied throughout this thesis produced extracellular, bioactive SAV in optimized conditions. This may be supported by the absence of disulfide bonds and the relatively small size of the target protein. Apparently, the high GC-content of the native SAV gene (69.2 % for gene and secretion signal sequence) did not pose a major problem to expression. Table 7.1 and Fig. 7.1 sum up the results of central production processes for all hosts.

7.1.1 Comparison of the overall performance

The application of *S. avidinii* in a fed-batch process yielded an approximately twofold increased volumetric productivity towards the best-performing systems of *E. coli*, *P. pastoris* and *H. polymorpha*. Remarkably, the production of SAV by *S. avidinii* in a simple batch process in the bioreactor led to productivities in the range of optimized conditions for the heterologous producers. Moreover, the productivity by *S. avidinii* surpassed the accumulation of product in all heterologous hosts even in the early stage of cultivation (see Fig. 7.1a), when advantages of heterologous producers may apply. When referring, e.g., to literature values for the production of SAV by *E. coli*, product concentrations are typically low, but during the short cultivation period the productivity often leads to superior results

Tab. 7.1: Comparison of results for the different expression systems. Benchmark values for homologous and heterologous expression of the SAV gene, respectively, were highlighted by shading.

host/strain [a]	expression cassette [b]	P_{max} [μM] [c]	p_{max} [nM h^{-1}] [d]	$Q_{blocked}$ [%] [e]	$s_{P/X}$ [nmol g^{-1}] [f]	process [g]	remarks
STA CBS 730.72	native, fSAV	6.9±0.1	48.1	n.d. [h]	1026	B, com	[i]
STA CBS 730.72	native, fSAV	39.2	114	n.d. [h]	1600	FB, com	
ECO JW1667-5 [j]	P_{bla}, cst (crc), fSAV	1.6±0.1	43.6	8±4 % [k]	82	B, com	[l]
ECO JW1667-5 [j]	P_{bla}, cst (crc), fSAV	2.6±0.2	65.2	8±4 % [k]	159	FB, com	[l]
HPO ATCC 34438	P_{FMD}, ind (int), AP-fSAV	11.4±0.2	52.5	1±4 %	245	FB, syn	[m]
PPA X-33	P_{GAP}, cst (int), cSAV	2.0±0.1	27.1	11±2 %	62	FB, syn	
PPA X-33	P_{GAP}, cst (int), cSAV	4.2±0.1	57.8	0±2 %	140	FB, com	[n]

[a] host organism and strain used; STA = *S. avidinii*, ECO = *E. coli*, HPO = *H. polymorpha*, PPA = *P. pastoris*
[b] promoter: cst = constitutive, ind = inducible; type of vector: crc = circular, int = integration into genome; SAV gene: fSAV = full-length SAV (AA 1-159), AP-fSAV = full-length SAV with *N*-terminal alanine-proline modification, cSAV = core SAV (AA 13-139)
[c] maximal bioactive extracellular tetrameric concentration of SAV
[d] productivity to P_{max}
[e] proportion of biotin-blocked binding sites
[f] process selectivity: P_{max} / X_{max}, where X_{max} is the maximal concentration of DCW (see section 7.1.2)
[g] mode of operation: B = batch, FB = fed-batch; medium: com = complex, syn = synthetic
[h] not determined; nearly biotin-free according to the results from the development of the heat-based assay (see section 3.3, p. 30*ff.*)
[i] for a rotary frequency of the stirrer between 400 and 700 min^{-1}
[j] periplasmic 'leaky mutant'
[k] average value of 3 cultivations
[l] upon supplementation of the cultivation medium with a surfactant
[m] methanol-based induction
[n] continuous shift of temperature and pH throughout the process

towards other hosts due to rapid growth and strong induction (see Table 7.4, p. 167).

The natural producer brought about even more pronounced advantages regarding the final product concentration, which exceeded the product titers of all other systems by a factor of at least 3.4. As the cultivation of *S. avidinii* resulted in rather low concentrations of biomass (see Fig. 7.1), this brought about a drastically superior process selectivity for this host (factor $\geq$ 6.5).

Although at the cost of a methanol-based process, *H. polymorpha* ranks best among the heterologous hosts regarding product concentration, proportion of biotin-blocked binding sites and process selectivity, whereas the application of *E. coli* yielded the highest productivity.

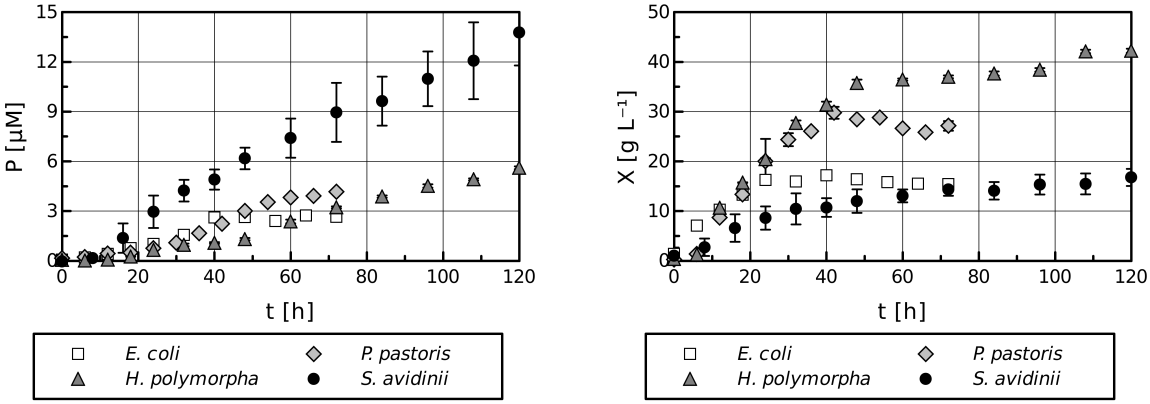

(a) Concentration of SAV P.

(b) Concentration of dry cell weight X.

Fig. 7.1: Graphical comparison of the final process strategies for the different hosts studied for this thesis. Only data for the first 120 h of the corresponding processes is shown for facilitated interpretation. The increase of the concentrations of product and biomass for *H. polymorpha* and *S. avidinii* remain nearly constant after this time. For *S. avidinii*, the courses refer to average values of three cultivations.

7.1.2 Discussion of the specific productivity

The optimized process strategies yielded maximal DCW concentrations of 24.5±1.0 g L^{-1} for *S. avidinii*, 17.2±0.3 g L^{-1} for *E. coli*, 29.8±1.2 g L^{-1} for *P. pastoris*, and 46.3±1.3 g L^{-1} for *H. polymorpha* (summarized in Table 7.2, p. 164). Related to these concentrations, the specific productivities p_{spec} lead to a different ranking of the organisms. These productivities were (ranked by performance) 4.65 nmol g^{-1} h^{-1} for *S. avidinii*, 3.79 nmol g^{-1} h^{-1} for *E. coli*, 1.94 nmol g^{-1} h^{-1} for *P. pastoris*, and 1.13 nmol g^{-1} h^{-1} for *H. polymorpha*.

This evaluation shows that the relatively high concentrations of product achieved for the yeast-based expression systems were partly due to a higher concentration of DCW compared to the competitors. Surprisingly, the increased concentration of biomass did not result in higher volumetric productivities than the system based on *E. coli*. Like observed for the productivity and maximal product concentration, the application of *S. avidinii* leads to the best performance regarding this parameter. In this context, two factors are noteworthy. Firstly, since the induction protocol for *H. polymorpha* was coupled to the dissolved oxygen signal as described in section 5.4 (p. 133*ff.*), the productivity can most likely be increased by providing a constant concentration of inducer and a constant oxygen saturation in the medium. This may relativize the differences to the other systems by a more efficient exploitation of the biomass. Secondly, the results for the continuous cultivation of *S. avidinii* (see section 4.4.3, p. 86) suggest that this host may be even more potent, reaching productivities of 221.3±32.0 nM h^{-1}

at a DCW concentration of only 4.0±0.5 g L^{-1} (D = 0.195 h^{-1}). This would correspond to an outstanding specific productivity of 55.6±10.6 nmol g^{-1} h^{-1}, by far surpassing the results of all other studies. Despite their preliminary nature and although values of p_{spec} in this order of magnitude are unlikely in other modes of operation, these parameters indicate that the organism offers an even higher potential than suggested by the optimized fed-batch process. Further fed-batch experiments will show to which extent these values can be reproduced during exponential feeding at a corresponding setpoint for μ. They may also elucidate at which point nutrients or other factors limit product formation for the long-term operation in other modes of cultivation.

7.1.3 Analysis of process robustness

The courses of the product concentration for the production of SAV by *E. coli* and *P. pastoris* were characterized either by defined maxima or by an asymptotic behavior (see Fig. 7.1, p. 158). Moreover, the properties depicted in Table 7.1 were only achieved by an elaborate optimization of process conditions, which in the case of *P. pastoris*[1] prolonged the period of SAV production. Therefore, at least for the conditions applied, the productive potential of these expression systems can be considered limited, which - among other factors - may be due to toxic effects on the host. Especially for *E. coli* this explanation seems plausible, since the dry cell weight concentration was very limited even for optimized conditions. *Vice versa*, high concentrations of DCW were only achieved for *P. pastoris* and *E. coli* when product concentrations were low.

As opposed to this, the accumulation of SAV by *H. polymorpha* and the natural producer *S. avidinii* remained constant in optimized conditions. Prolonged processes can therefore be expected to lead to higher concentrations of SAV. For *H. polymorpha*, constant product formation was achieved for a rather simple, unoptimized process based on the induction by methanol. SAV production by this host/promoter-combination thus seems to be an inherent, robust property. In contrast to this, process optimization was necessary for the production of high concentrations of SAV by *S. avidinii*. Optimization included the factors shear sensitivity, mycelial stability, and mode of feeding, suggesting that SAV production by the filamentous bacterium relies on a fine-tuned environment. This is supported by a high sensitivity towards shifts of the cultivation temperature observed in shake flask experiments, in which fluctuation to 33 instead of 30 °C led to marginal growth and product formation (data not shown). Furthermore, the morphology was a key factor in shake flasks, since pellet growth resulted in diminishing concentrations of SAV, whereas filamentous growth provided suitable properties for production. This sensitive behavior is typical for the production of antibiotics by streptomycetes, as observed e.g., for the production of thiostrepton by *S. laurentii* (Suzuki *et al.*, 1987). Finally, the cultivation of *S. avidinii* is prone to contaminations due to relatively low growth rates in the beginning

[1] Successive shift of temperature and pH throughout the cultivation.

of a cultivation and the absence of selective agents. In this context, Table 4.2 (p. 90) may provide the basis for a reduction of these effects by supplementing appropriate antibiotics. In conclusion, despite showing a favorable overall performance regarding product formation, production processes based on *S. avidinii* can be considered less robust.

7.1.4 Genetic stability of the SAV expression cassette

Expression of toxic genes commonly leads to a loss of plasmid or the expression cassette throughout fermentation, as described, e.g., for *E. coli* (Dumon-Seignovert *et al.*, 2004). However, problems of genetic instability of the expression cassette were only a minor factor during production studies for the constructs tested. The data of *S. avidinii* and *H. polymorpha* suggest sufficient stability in the range of weeks of cultivation. For *P. pastoris* and *E. coli* production was stable for several days. This indicates that the optimization of secretion efficiency and cultivation conditions for the GRAM-negative bacterium yielded sufficient plasmid stability, potentially by alleviating toxic effects. However, slight problems of stability emerged during the preparation of new glycerol stocks of the final producer strain of *E. coli* despite the addition of antibiotics (data not shown), which may be due to a relative instability of the population. Nevertheless, once a glycerol stock with producers was acquired, production was stable in expression studies. This is advantageous towards to the strategies of Sørensen *et al.* (2003b) and other researchers, which were based on fresh transformation of the producer strains prior to every study of induction.

Generally, production by the natural producer or by hosts based on integration of the expression cassette into the genome seems beneficial in respect to genetic stability. However, the results for *P. pastoris* (section 5.3.5.2, p. 131) suggest deficiencies of genetic stability upon multiple chromosomal integration of the SAV gene in the absence of antibiotics for yeast-based expression systems. This should be considered for further experiments.

7.1.5 Effect of the cultivation temperature

Interestingly, cultivation of the two heterologous hosts *E. coli* and *H. polymorpha* at 30 instead of 37 °C improved product formation. The lower temperature resembles the conditions usually applied for cultivation of the mesophile natural producer *S. avidinii*. Potential reasons for the increased product formation by the heterologous hosts at 30 °C include reduced proteolysis, facilitated folding, improved efficiency of secretion, and - closely related - decreased rates of protein synthesis, reducing the load of the secretory machinery. For *E. coli*, a temperature downshift from 37 to 23 or 15 °C resulted in improved production of a host-toxic TolAI-β-lactamase fusion construct (Mujacic *et al.*, 1999). For *P. pastoris*, lowering the cultivation temperature has been associated to reduced stress in the

endoplasmic reticulum, a lower impact of the unfolded protein response (Zhong *et al.*, 2014), higher concentrations of molecular chaperones, reduced flux in the TCA cycle, and reduced concentrations of proteins involved in the oxidative stress response (Dragosits *et al.*, 2009). These aspects were accompanied by higher concentrations of heterologous proteins.

Protein solubility is another important temperature-dependent aspect (Schein & Noteborn, 1988). Although this is improbable due to the relatively weak promoter used in the studies for *E. coli*, inclusion bodies may have been formed during cultivation at 37 °C, which would not have been detected in the fluorescence assay. This should be confirmed or disproved by additional experiments.

Generally, future experiments applying *E. coli* may focus on the application of inducible or temperature-sensitive promoters in two-stage processes, allowing unimpaired, rapid growth at 37 °C followed by induction at 30 °C or even lower temperatures. For the inducible construct based on *H. polymorpha* corresponding two-stage processes can directly be implemented.

7.1.6 Effect of the secretory potential of the host

As indicated by the combined results of all heterologous expression systems and by various findings in literature (Wang *et al.*, 2005; Miksch *et al.*, 2008), secretion seems to play an important role in the production of SAV. *P. pastoris* and *H. polymorpha* are known to have efficient secretory pathways (Romanos, 1995; Gellissen *et al.*, 1991), whereas the unfavorable surface structure of *E. coli* (see Fig. 2.8a, 19) prevents similar results for the *Gram*-negative bacterium (Nossal & Heppel, 1966). Therefore, it did not come as a surprise that secretion of SAV via the Sec pathway by *E. coli* targeting the unfolded transport to the periplasm did not yield comparable concentrations of SAV for *E. coli* than for the natural producer, who most likely uses the same secretory pathway.[2] This difference was still present upon comprehensive optimization of the genetic configuration and culture conditions.

However, expression of the SAV gene by the strain *E. coli* KRX - containing an intact outer membrane structure - resulted in a large proportion of SAV in the cyto- (22 %) and periplasm (43 %) without a impairing growth at low cell densities (see Fig. 1D in the corresponding research article; section 5.2.2, p. 93). It is therefore unclear, to which extent the limitation of the DCW concentration of *E. coli* JW1667-5 was due to the altered outer membrane rather than the production of SAV. Moreover, the course of the optical density of a plasmid-free clone of JW1667-5 resembled that of the transformed strain used for the expression of SAV (data not shown). In this context, the supplementation of large concentrations of SAV to the medium to strains with an intact outer membrane and to a 'leaky mutant' in the beginning of cultivation should lead to deeper insights. Furthermore, the use of stronger promoters may contribute to clarify the interdependency of dry cell weight, product concentration, and secretory efficiency. Corresponding studies seem worthwile, because - like mentioned in section 2.4.3

[2] Please refer to Fig. 8.1, p. 180 for an *in silico*-analysis of the native signal peptide.

(p. 15) - a negative correlation of the concentrations of DCW and SAV for *E. coli* BL21(DE3) can be deduced from the data of Miksch *et al.* (2008).

Regarding the results for *E. coli* KRX, soluble expression of SAV in the cytoplasm seems to be possible at high levels, unlike suggested by Sørensen *et al.* (2003b). Thus, the formation of inclusion bodies may be the result of inefficient secretion or excessive translational activity rather than problems of solubility of SAV.

Generally, vesicular transport by yeast seems to be more suitable for the secretion of SAV, allowing higher extracellular concentrations of the protein. Optimization of the secretion signal peptide in preliminary studies applying the methanol-inducible AOX1 promoter yielded only slight improvements (see section 5.3.5.1, p. 131). However, secretion efficiency may be increasingly important for the use of multi-copy integrants, suggesting detailed investigations on the application of optimized signal peptides (Xiong *et al.*, 2004; Lin-Cereghino *et al.*, 2013) for different levels of expression.

First estimates of the importance of secretory efficiency on SAV production by yeast may be achieved by the application of different concentrations of inducer for AOX1 promoter-based constructs. Accompanying experiments based on intracellular expression may also contribute to a better understanding of secretion-dependent host toxicity. In this context, the cellular localization of biotinylated proteins could be of importance, as discussed in section 2.4.3.3 (p. 18*ff.*).

7.1.7 Suitability of yeast-based expression systems for the production of SAV

The general potential of the yeast-based production of SAV is emphasized by previous reports on the successful expression of avidin genes by *P. pastoris* (Zocchi *et al.*, 2003; Jungo *et al.*, 2007a). In general, chromosomal integration of the expression cassette for the SAV gene may have contributed to a more stable expression towards episomal expression as performed using *E. coli*, which is discussed in section 7.1.4.

For *P. pastoris*, this thesis showed for the first time that the advantageous properties for expression of the SAV gene not only apply to methanol-based, but also to growth-coupled production processes using the biotin auxotrophic yeast. Toxic effects can partially be circumvented during induction-based processes by separation of growth and production. This is, however, not the case for constitutive production. Thus, the successful constitutive expression of the SAV gene is an indication for limited toxic effects.

Fortunately, glycosylation does not seem to be a problem for the activity of SAV derived from yeast-based expression. *N*-glycosylation is usually performed on asparagine residues as part of the consensus sequence Asn-Xaa-Ser/Thr, where Xaa is any AA except for proline (Marshall, 1972). A scan for

N-glycosylation sites in the SAV AA sequence based on the PROSITE pattern PS00001[3] resulted in no hits, supporting the beneficial features of the host for the expression of the SAV gene.

7.1.8 Analysis of product purity

Three of the four hosts studied in this thesis led to a relatively pure product based on SDS-PAGE analysis (see Fig. 6.1, p. 145). *E. coli* was the exception to this rule. The construct tested accumulated a large number of unspecific proteins in the supernatant. As the native secretory potential of the host is very limited (Nossal & Heppel, 1966), these contaminants are most likely the result of an uncontrolled release of proteins from the periplasm to the medium due to the instability of the outer membrane ('leaky mutant'), supported by the addition of surfactants. These properties suggest the use of a different host, if a high purity of SAV is required. Alternatively, the knockout of additional genes involved in the outer membrane formation may render the application of surfactants redundant. This could in turn lead to a more specific release of the target protein to the medium and thus reduce the load of contaminating proteins.

For *P. pastoris*, studies of cell viability accompanying bioreactor fermentations may contribute to a better understanding of the host toxicity of SAV. Moreover, they may result in an improved product purity by the optimization of culture conditions towards reduced cell lysis and improved protein secretion. Comparable studies have already been performed for methanol-based processes applying this yeast (Hohenblum *et al.*, 2003). As *H. polymorpha* was induced by methanol in this study, corresponding experiments may be beneficial for this host, too.

7.1.9 Ecological assessment

All previous sections focused on aspects of production. However, the ecological balance of the processes should also be considered. Since a complete life cycle assessment for all of the final processes would be too time-consuming, a more simple tool was employed for this purpose. A comparison of the production processes using the E(nvironmental) factor (Sheldon, 1992), originally applied for chemical reactions, allows a simple, qualitative assessment of the "greenness", i.e., ecological performance, of a given process. The dimensionless $E-factor$ is defined in equation 7.1.

$$E-factor=\frac{m_{waste}}{m_{product}} \tag{7.1}$$

where m_{waste} is the mass of waste generated during the process, i.e., all substrates except from water, and $m_{product}$ is the mass of product equivalents produced.

[3] Scan for common, non-mammalian N-glycosylation motifs, http://prosite.expasy.org/PDOC00001, version last updated May 1991, accessed 11^{th} of March, 2016.

Thus, lower values of the $E-factor$ correspond to beneficial ecological properties. As emphasized by Ni *et al.* (2014), the $E-factor$ does neither take into account water, nor the electricity necessary for the process. Moreover, it does not discriminate between toxic and harmless types of waste. However, its calculation is by far less time-consuming than more complex approaches. It may therefore serve as a compromise between significance and effort.

In addition to the $E-factor$-based evaluation, the ecological balance was analyzed in terms of the efficiency of biomass and product formation via the yield coefficients of biomass per substrate $Y_{X/S}$ and of product per substrate $Y_{X/P}$. Results of the assessment are shown in Table 7.2.

Tab. 7.2: Ecological assessment of the final processes. Positive and negative benchmark concentrations were labelled in green and red, respectively. All specifications of masses and yield coefficients were based on the assumption of volume constancy (sampling levels out feeding of substrates and corrective agents) for reasons of simplicity.

organism/process [a]	m_{waste} [b] [g]	m_{carbon} [c] [g]	P_{max} [d] [$g\,L^{-1}$]	X_{max} [e] [$g\,L^{-1}$]	$Y_{X/S}$ [f] [-]	$Y_{P/S}$ [g] [-]	$E-factor$ [h] [-]
STA B, com	45.6	27.6	0.44	7.0	0.25	0.016	103
STA FB, com	131.1	101.1	2.51	24.5	0.24	0.025	52
STA C, com [i]	28.0 [j]	10.0 [k]	0.16	5.5	0.55 [k]	0.016	179
STA C, com [l]	28.0 [j]	10.0 [k]	0.07	4.0	0.40 [k]	0.007	386
STA C, com [m]	28.0 [j]	10.0 [k]	0.03	2.8	0.28 [k]	0.003	931
ECO B, com	88.7	29.8	0.10	19.1	0.64 [n]	0.003	866
ECO FB, com	131.3	72.4	0.17	17.2	0.24 [n]	0.002	789
HPO FB, syn	445.0	416.5	0.75	46.3	0.11	0.002	593
PPA FB, syn	203.0	141.5	0.11	31.5	0.22	0.001	1911
PPA FB, com	220.0	176.6	0.22	29.8	0.17	0.001	987

[a] host organism, mode of operation and medium used for the process; organism: STA = *S. avidinii*, ECO = *E. coli*, HPO = *H. polymorpha*, PPA = *P. pastoris*; mode of operation: B = batch, FB = fed-batch, C = chemostat; type of medium: com = complex, syn = synthetic
[b] mass of waste generated (equation 7.1) per L of medium
[c] overall mass of carbon sources (methanol, glycerol, glucose) per L of medium
[d] maximal bioactive extracellular tetrameric concentration of SAV; conversion to mass concentrations according to the molecular weight specifications of Table 7.4
[e] maximal dry cell weight concentration
[f] yield coefficient of biomass per carbon source
[g] yield coefficient of product per carbon source
[h] environmental factor according to equation 7.1; mass of waste related to liters
[i] dilution rate $D = 0.058\,h^{-1}$
[j] waste calculated for one complete exchange of the volume
[k] The actual concentration of glucose was lower ($8.6\,g\,L^{-1}$) due to the co-sterilization of glucose and medium .(see 4.4.3, p. 86). The actual yield of biomass per substrate $Y_{X/S}$ may therefore be higher. Furthermore, the parameter estimation suggested a coefficient in the range of 0.71.
[l] dilution rate $D = 0.195\,h^{-1}$
[m] dilution rate $D = 0.320\,h^{-1}$
[n] These coefficients are influenced by insoluble aggregates caused by the addition of detergents and antifoam agent to the cultivation (see 5.2.2, p. 93*ff.*). The actual yield coefficients of biomass per substrate are likely to be lower.

As can be concluded from the results, batch and fed-batch processes applying *S. avidinii* are not

only superior to the heterologous production of SAV regarding product concentration and productivity, but also reduce process waste by a factor of up to 36.5. Surprisingly, even chemostat processes for the natural producer at dilution rates of up to $0.2\,h^{-1}$ yielded lower $E - factors$ than all heterologous processes despite drastically lower concentrations of product compared to the batch or fed-batch cultivation of *S. avidinii*. In regard to this parameter, the process for the cultivation of *P. pastoris* in a synthetic medium resulted in the worst outcome.

The yield coefficients $Y_{X/S}$ were relatively low for most of the processes, suggesting that optimization of the carbon-to-nitrogen ratio of the media may be worthwhile. Batch cultivation of *E. coli* resulted in the highest yield of 0.64, followed by chemostat cultivation of *S. avidinii* at low dilution rates. Due to diminishing growth on methanol, $Y_{X/S}$ for the cultivation of *H. polymorpha* reached a minimal value of 0.11. The yield coefficients for SAV $Y_{P/S}$ were even smaller and also show favorable properties for processes based on the natural producer (improvements of a factor of up to 25).

7.1.10 Summary of the qualitative host-specific properties

Table 7.3 sums up qualitative properties of the different hosts observed throughout the studies.

7.2 Comparison of the results to literature

Table 7.4 sums up reference values for the production of SAV reported in literature and benchmark results of this study.

The table indicates that the strategies used for the expression of the SAV gene in this study were successful, ranking well within the data reported in literature.

Productivities and product concentrations were lower than for methanol-based expression by *P. pastoris* (Casteluber *et al.*, 2012; Nogueira *et al.*, 2014), who reached concentrations in the range of 71 and 11 μM, respectively. However, the process of Nogueira and coworkers was based on a surprisingly high DCW concentration of $235\,g\,L^{-1}$ despite the application of unoptimized conditions.[4] This concentration decreases the process selectivity $s_{P/X}$. Moreover, concentrated oxygen had to be applied in the cultivation due to the high oxygen demand caused by the extraordinarily high DCW concentration.

The cultivation system of Casteluber *et al.* (2012), namely a spinner flask aerated through a porous stone at very high volumetric flow rates (4 vvm), is difficult to compare or scale up. This is due to insufficient characterization from an engineer's point of view and its unavailability in larger scales.

[4] The synthetic medium applied (BSM medium, Invitrogen/Life Technologies, 2002) typically leads to dry cell weight concentrations in the range of $100\,g\,L^{-1}$, reaching maximal values of up to $160\,g\,L^{-1}$ for highly optimized conditions (Jahic *et al.*, 2002).

Tab. 7.3: Challenges of the hosts studied in this thesis in regard to their potential to produce SAV. Effects of different aspects are compared qualitatively (+++ very strong, ++ strong, + weak) or quantitatively.

aspect	*S. avidinii*	*E. coli*	*P. pastoris*	*H. polymorpha*
requirements of bioprocess engineering	++	+	++	++
morphological effort	+++ [a]	+	+	+
robustness [b]	+	++	++	++
effort for genetic engineering	- [c]	+	+++	+++
product purity [d]	+++	+	+++	+++
duration of process setup [e]	24-48 h [f]	<24 h	<24 h	<24 h
process duration [g]	+++	+	++	+++
methanol-based [h]	no	no	no	yes [i]
no. of process stages [g]	2	2	2	3
genetic stability [j]	+++	+ [k]	++/+++ [l]	+++
GMO [m]	no	yes	yes	yes
secretory potential [n]	++ [o]	+	++	++
necessity of antibiotics	no	yes	yes/no [p]	yes/no [p]
ecological balance [q]	+++	+	+	++

[a] necessity of filamentous growth for suitable productive properties; issues of reproducibility for pellet growth
[b] summary process characteristics like risk of contamination and susceptibility towards shifting environmental conditions according to section 7.1.3
[c] not necessary, natural producer
[d] estimated from SDS-PAGE data
[e] preparation of fermenter and duration of pre-cultivation
[f] depends strongly on age of glycerol stock and inoculation density; for a fresh glycerol stock and a large inoculum size: approx. 24 h
[g] property of the final process strategies described in Table 7.1
[h] additional safety regulations and increased heat evolution and oxygen demand due to organic solvent; property of the final process strategy
[i] not necessary for production; constitutive promoters or derepression-based production may avoid this property
[j] considering the expression cassette: stability of product accumulation over time
[k] selection pressure necessary, risk of loss of plasmid
[l] stability may be lower for multi-copy integrants (see section 5.3.5.2, p. 131)
[m] genetically modified organism: potential additional regulations concerning treatment of leftover biomass and process safety
[n] general property of the host without optimization
[o] based on the literature survey for *S. lividans* given in section 2.4.3.3 (p. 18*ff.*)
[p] AB only necessary for selection, not for the actual bioprocess
[q] based on the $E-factor$-evaluation (Table 7.2)

Moreover, the system does not allow measurement or control of process parameters like pH and dissolved oxygen saturation, complicating cultivation in controlled conditions and interpretation of the results. Finally, the washing step performed by Casteluber *et al.* between growth and induction bears the risk of contamination. Therefore, a direct comparison to the bioreactor data of this study is difficult.

The novel expression system based on *H. polymorpha* seems to be one of the most efficient studied for the heterologous expression of a full-length SAV gene to date regarding the final product concentration.

Despite these properties, expression of SAV by *S. avidinii* was much more efficient than heterologous production rated by the final product concentration and productivity. Comparison to literature reveals

Tab. 7.4: Literature survey on the production of SAV by various hosts (actualized and modified version from Müller *et al.*, 2013) ranked by host and year of publication. Results from this thesis were labelled by shading of the corresponding rows.

organism	MW [kDa] [a]	P_{max} [mg L^{-1}] [b]	P_{max} [μM] [b]	p_{max} [nM h^{-1}] [c]	reference
S. avidinii	72	53	0.74	10.3	Aldwin *et al.* (1990)
S. avidinii	70	145	2.07	8.6	Cazin Jr. *et al.* (1988) and Suter *et al.* (1988)
S. avidinii	58 [d]	170	2.93	48.0	Kolomiets & Zdor (1998)
S. avidinii	52	160	3.1	18.3	Sumarningsih (2014)
S. avidinii	64	2509	39.2	114	this study
S. lavendulae	- [d]	201	n.sp.	n.sp. [e]	Zhang *et al.* (2007)
S. lividans	54 [d]	250	4.63	n.sp.	Meade & Jeffrey (1986)
S. lividans	66	56	0.9	6.4	Noda *et al.* (2015)
B. subtilis	68	50	0.74	61.3	Nagarajan *et al.* (1993)
B. subtilis	66 (88) [d]	50	0.79	37.0	Wu & Wong (2002)
B. subtilis	66 (88) [d]	94	1.42	109.2	Wu *et al.* (2002)
E. coli [f]	64	65	1.02	340.0	Sano & Cantor (1990b)
E. coli [f]	53	3	0.06	20 [g]	Thompson & Weber (1993)
E. coli	65.7	70	1.07	267.5	Gallizia *et al.* (1998)
E. coli	n.sp.	n.sp.	~0.26 [h]	36.4 [i]	Sørensen *et al.* (2003b)
E. coli	16.6 [j]	70	1.05	843.0 [j]	Wu & Wong (2006)
E. coli	60	96	1.6 [k]	200.0 [k]	Miksch *et al.* (2008)
E. coli	14 [l]	>50 [l]	0.89 [l]	44.5 [l]	Demonte *et al.* (2014)
E. coli [f]	61.2	370	6.1	378 [i]	Chen *et al.* (2014)
E. coli	64	167	2.6	65.2	this study
H. polymorpha	65.8 [m]	750	11.4	52.5	this study
P. pastoris	56	4000 [n]	71 [n]	n.sp.	Casteluber *et al.* (2012)
P. pastoris	63.5	650 [o]	11 [o]	67.9 [o]	Nogueira *et al.* (2014)
P. pastoris	53.1 [m]	221	4.16	57.8	this study
S. cerevisiae	- [d]	- [e]	0.001-0.01 [p]	- [e]	Hong Lim *et al.* (2012)

[a] molecular weight
[b] maximal tetrameric product concentration
[c] volumetric productivity to P_{max}
[d] MW not (clearly) given
[e] not specified
[f] insoluble expression as inclusion bodies; concentrations refer to bioactive SAV after refolding
[g] referring only to the cultivation time starting with induction (3 h); complete cultivation time not given
[h] cytoplasmic tetrameric SAV recalculated from the biotin-binding ability of an IF2-domain I-SAV fusion protein
[i] exact cultivation time not given; calculation based on an initial growth time of 4 h prior to induction
[j] monomeric SAV
[k] extracellular fraction
[l] expression of a maltose binding protein-monomeric SAV fusion protein; concentrations refer to tetrameric equivalents of the SAV-fraction
[m] theoretical MW (calculated)
[n] cultivation in an uncontrolled environment in spinner flasks (see text)
[o] based on a surprisingly high DCW concentration of 235 g L^{-1}
[p] estimated concentration of biotin equivalents; the concentration refers to a low OD_{600} of 4.0 of the culture

that - like discussed in the internal evaluation in section 7.1.1 and Fig. 7.1 - the productivity achieved for the filamentous bacterium surpasses the majority of productivities achieved by heterologous producers. Only a selection of systems based on *E. coli* (Sano & Cantor, 1990b; Gallizia *et al.*, 1998; Wu & Wong, 2006; Miksch *et al.*, 2008; Chen *et al.*, 2014) yielded higher productivities for a short period of time, but resulted in drastically lower maximal concentrations of SAV. The *E. coli*-based system studied in

this thesis also resulted in lower productivities than these reference constructs, which is potentially due to the relatively weak promoter.

New benchmark concentrations for the soluble production and secretion of SAV were achieved for *S. avidinii* and *E. coli*. The improvements were particularly strong for the natural producer, for which the product concentration was increased by a factor of 12.6 towards all reference studies using the same host.

7.3 Conclusions and outlook

The following conclusive sections may serve as a guideline for future experiments based on the results achieved in this thesis.

7.3.1 Conclusions

The host-vector-combinations and processes developed in this thesis may contribute to making SAV more accessible for further applications. From the perspective of handling, the systems constructed for *P. pastoris* and to a limited extent *E. coli*[5] should allow a simple production of SAV for laboratory purposes in shake flasks without deeper understanding of biochemical engineering or morphological aspects. However, regarding the overall productive potential of the hosts, the natural producer *S. avidinii* can be considered the most suitable of the constructs tested. The complex morphology of this organism can be compensated in shake flasks (section 4.4.1, p. 80), whereas in the bioreactor shearing of the mycelia quickly brought about filamentous growth without the addition of supplements or fine-tuning of conditions. The suitability of *S. avidinii* for the production of SAV is emphasized by extremely high process selectivities, which surpassed all selectivities of the further heterologous hosts tested by a factor of at least 6.5 in fed-batch operation (see Table 7.1).

However, the presumably most promising feature regarding the potential of *S. avidinii* for future studies may be the specific productivity achieved in chemostat cultivations (see section 4.4.3, p. 86 and section 7.1.2 in the final discussion). Along with the results from medium optimization (section 4.4.2, p. 85), they indicate that the findings presented here may just be one step towards more efficient production processes for the protein SAV by the filamentous bacterium.

Regarding simplified processes of purification, the preliminary results for the purification of SAV by the alternative methods analyzed in section 6 (p. 144*ff.*) suggest that for many purposes crude supernatants may be sufficient, if the hosts *S. avidinii*, *P. pastoris* or *H. polymorpha* are applied.

[5] Due to the potential genetic instability.

A crude supernatant of *S. avidinii* was successfully used for the detection of biotin and biotinylated compounds, whereas diafiltration was sufficient for advanced applications like the immobilization of SAV. In all of these cases, costly and time-consuming purification by iminobiotin columns may therefore be redundant. This is of particular importance regarding the laboratory-scale production of SAV for straightforward applications by research groups with limited biotechnological experience.

7.3.2 Outlook

The results of this thesis can be used for a more rational design of upcoming experiments. This final section is meant to facilitate the choice of relevant parameters for the purpose of further optimization.

7.3.2.1 Homologous expression of the SAV gene

In respect to the productive properties, product purity and ecological performance, *S. avidinii* seems to be the most promising host for upcoming studies. If the rather low biomass concentration can further be increased without harming the selectivity, optimized processes may yield even higher concentrations of product. For fed-batch processes, the results obtained during medium optimization (section 4.4.2, p. 85) are a useful starting point in this context. Their use can be combined with alternative feeding profiles like exponential feeding at suitable values of μ_{set}. However, effects on the viscosity of the culture broth can be expected here, which have to be carefully monitored (see section 2.4.1.1, p. 10). As can be concluded from the theoretical considerations (section 4.3.5, p. 74), increased concentrations of biomass potentially result in an only fractionally turbulent flow regime, which may reduce mass and energy transfer. For continuous cultivation, cell retention by membrane bioreactors or the use of immobilized biomass is of interest. These strategies may allow higher concentrations of biomass than in the previous studies even for high dilution rates (section 4.4.3, p. 86).

Further experiments may focus on genetic engineering of the natural producer (section 4.4.6, p. 88). Generally, the insertion of additional expression cassettes into the genome of *S. avidinii* may increase SAV production. Here, overexpression of signal peptidases is a potentially useful tool to avoid overloading of the secretory machinery of *S. avidinii* (Anné *et al.*, 2014). From the morphological perspective, enhanced productive properties in the shake flask could be achieved by overexpression of the *ssgA*-morphogene (Kraal *et al.*, 1999). This may lead to increased fragmentation and growth rates and thus improve the viscous properties of the culture broth. Genome sequencing of the strain would facilitate all of these experiments, which is currently in progress at the CeBiTec at Bielefeld University.

7.3.2.2 Heterologous expression of the SAV gene

Of the heterologous hosts tested, *H. polymorpha* and *P. pastoris* seem the most promising regarding the maximal product concentration. For both of these hosts, multiple insertion of the expression cassette into the genome may lead to improvements of the production of SAV. Yet, in this context, stabilization of the expression cassette could be a key factor, as indicated by the study based on *P. pastoris* (section 5.3.5.2, p. 131*f.*). The Zeocin™ resistance gene used for expression vectors of both hosts prevents stabilization of transformants by application of the antibiotic in production processes due to high cost. However, Lin-Cereghino *et al.* (2008) demonstrated that a modified resistance gene can be used for the selection of transformants of *P. pastoris* by kanamycin. This antibiotic is stable and cheap enough to allow supplementation of bioreactor cultures for the purpose of genetic stabilization. This strategy can be combined with optimization of the secretion signal sequence as performed by Lin-Cereghino *et al.* (2013) to alleviate potential effects of toxicity-induced problems of the genetic stability of the construct.

A detailed characterization of the properties of *H. polymorpha* in conditions of derepression rather than induction may be of interest targeting an improved process sustainability.

A recent study on the GAP-based expression of heterologous genes by *P. pastoris* (Güneș & Çalik, 2016) showed that optimization of the concentration of dissolved oxygen leads to an improvement of the production of a glucose isomerase by a factor of 2, when the setpoint for this process parameter is adjusted to 15 % of relative saturation rather than 20 %. In this project, only a lower boundary of the dissolved oxygen concentration of 20 % was applied without control mechanisms like a cascade for the stirrer for higher parameter values. Thus, fine tuning of the environmental conditions may lead to additional improvements for the production of SAV by this host.

Generally, the successful production of SAV by the yeasts *P. pastoris* and *H. polymorpha* suggests the use of non-conventional yeast strains like the dimorphic *Yarrowia lipolytica* or the methylotrophic *Candida boidinii* for upcoming projects, as both of them have already been used for the production of heterologous proteins with great success (Madzak *et al.*, 2004; Yurimoto & Sakai, 2009). Alternatively, less established species like *Arxula adeninivorans* could be employed for this purpose (Stöckmann *et al.*, 2009).

If - despite the results presented in this thesis - additional studies using *E. coli* JW1667-5 are performed, fine-tuning of the expression level seems worthwhile. This may be achieved either by exchange of the relatively weak promoter applied in this study or by modifying the plasmid copy number. Furthermore, genetic optimization of the host, e.g., by the knockout of protease genes or additional membrane-stabilizing structures could lead to reduced degradation of SAV and improved secretion,

respectively. However, the effect of corresponding modifications on growth should be analyzed carefully for the latter strategy.

Alternatively, the *lpp*-knockout of *E. coli* JW1667-5 could be tested for established producer strains. In the case of SAV, the 'Walker strains'[6] (Miroux & Walker, 1996), or other strains suited for the production of toxic proteins seem to be reasonable targets for this strategy. In general, the results for *E. coli* KRX (Fig. 1D in the research article) suggest that exchange of the strain may bring about higher concentrations of total SAV. Finally, for optimization of the coexpression of inhibitors (see section 5.2.5, p. 112*ff.*), fusion constructs of peptide ligands of SAV and destabilizing amino acids like PEST[7] regions (Rogers *et al.*, 1986) may facilitate the recovery of binding sites after the production process, if leakage of the inhibitor to the medium occurs.

7.3.2.3 Purification of SAV

Regarding alternative downstream processing approaches for the purification of SAV, improved results for the aqueous two-phase extraction of SAV may be achieved by incorporating additional parameters like the chain length of PEG and the incubation temperature into additional DoE-based experiments. These could be based on the systems showing a suitable distribution pattern in the PEG/phosphate studies (Table 6.1, p. 148). Additionally, modifications of the polymer, e.g. by affinity tags or hydrophobic groups, are an option (Diamond & Hsu, 1992). As suggested in section 6.4 (p. 152), a two-step extraction with a transfer of SAV to the polymer-phase followed by transfer to the salt-rich phase seems promising for improved performances of the strategy. Moreover, the application of ionic liquids for aqueous two-phase extraction would offer an even broader field of potentially useful parameters (Dreyer & Kragl, 2008). Alternatively, selective solubilization of SAV by inverse micelles could be applied (Goklen & Hatton, 1987).

For the purification of *E. coli*-derived SAV, fusion of the SAV gene to heat-responsive peptide tags like ELP (elastin-like polypeptides) seems promising. These peptides undergo phase transition upon heating, allowing the purification of tagged proteins by inverse transition cycling (Meyer & Chilkoti, 1999). In this procedure, the insolubility of the target protein upon heating is used for the removal of soluble contaminants, as illustrated in Fig. 8.6 (p. 185, supplementary material). The method is particularly interesting due to the heat stability of SAV (Fig. 3.3, p. 56) and the thermal inactivation of contaminating proteins (section 6.3.4, p. 150). It may therefore allow simultaneous inactivation of contaminants and purification of SAV by heat incubation and subsequent centrifugation at room temperature for the removal of insoluble contaminants, followed by the usual procedure of inverse

[6] The *E. coli* BL21(DE3)-derivatives C41(DE3) and C43(DE3).

[7] Sequences rich in the amino acids proline, glutamic acid, serine, and threonine, leading to increased degradation by the proteasome.

transition cycling. Facilitated procedures based on alternative peptide tags like 18A and ELK16 have been developed more recently (Xing *et al.*, 2011).

Generally, further studies on the use of SAV purified by the methods discussed in section 6 (p. 144*ff.*) should lead to clear conclusions on which product purity is necessary for different applications, facilitating the choice of the DSP strategy. In either case, the use of synthetic instead of complex production media may simplify purification in upcoming studies. Yet, in this context achieving filamentous growth is essential for the expression by *S. avidinii* due to the interdependency of medium composition and morphology (see section 4.4.1, p. 80).

7.3.2.4 Recovery of biotin-blocked binding sites

Finally, a comprehensive optimization of the methods for the removal of SAV-bound biotin (section 3.5, p. 55*ff.*) might result in a more efficient recovery of biotin-blocked binding sites of the protein. Many factors like incubation temperature, addition of urea, and adjustment of the pH value were only varied in "one factor at a time"-experiments. Thus, a design of experiments-approach may lead to synergistic effects and yield a more holistic view of biotin degradation. Moreover, the application of bandpass filters for the UV radiation-based treatment of SAV-bound biotin could partly protect the protein of damaging effects.

If these experiments are successful, this step may enable the recycling of SAV by recovering biotin-blocked binding sites after the application of SAV. Furthermore, it could contribute to the recovery of blocked sites on SAV columns used for the purification of Strep-tagged proteins (Schmidt *et al.*, 1996). And finally, it would facilitate heterologous production of SAV, by allowing the supplementation of larger concentrations of biotin to cultivation media without the necessity for methods of filtration- or dialysis-based de- and renaturing after cultivation.

8 Supplementary material

8.1 Additional methods

Additional methods are described in detail in the following sections.

8.1.1 Recovery of biotin-blocked binding sites

The recovery of biotin-blocked binding sites was tested by hydrogen peroxide treatment and UV radiation.

Supernatants containing SAV were acquired from the cultivation of *S. avidinii* as described in section 4 (p. 60*ff.*, final process strategy). The supernatants were mixed with an aqueous solution of biotin (100μM, Sigma-Aldrich Laborchemikalien GmbH, Seelze, Germany) to achieve full biotin-saturation of the binding sites. The supernatants were then either subjected one of two different methods of treatment or to a combination of both of them.

For the chemical degradation of biotin, the supernatant was mixed with varying concentrations of hydrogen peroxide (30 % (w/w) stock solution, Sigma-Aldrich). If not indicated otherwise, heat incubation was performed at 60 °C in 2 mL reaction tubes in standard laboratory heat blocks with water-filled wells. Samples of 150 μL were taken in intervalls of 10 min for 90 min. The activity of SAV was determined threefold by the standard fluorescence assay by Kada *et al.* (1999a,b) (free binding sites) and via heat-induced dissociation of biotin by the assay developed previously (overall binding sites; section 3, pp. 28; incubation at 70 °C for 10 min; $c_{SAV} \leq 300$ nM).

For UV treatment, samples were incubated on a transillumination device (TMW-20 Transilluminator, Model White/UV, UVP, San Gabriel, CA, U.S.A.) in 50 mL polypropylene tubes (Cellstar®, Greiner Bio-One GmbH, Frickenhausen, Germany) prior to fluorescence measurements according to the procedures described above.

8.1.2 Homologous production of SAV by *S. avidinii*

The following section contains additional methods for the cultivation of *S. avidinii* and analysis of the culture broth.

8.1.2.1 Viscosity measurements

The dynamic viscosity η was measured applying a falling ball viscometer of the type 001-1926 (Haake GmbH, Karlsruhe, Deutschland) and a ball characterized by a diameter of 3 mm. The density of the ball was calculated by weighing, whereas for the corresponding culture broths this parameter was determined by densitometry (DMA 48 density meter, chempro/PAAR, Graz, Austria).

Calculations were based on the force balance on the ball.[1] While falling, different forces level out after a short time, in which friction and buoyancy compensate the gravitational force, leading to a constant terminal velocity of the ball. The latter can be used for the calculation of the viscosity of Newtonian fluids. The geometry of the ball and this force balance result in the general equation 8.1 for the dynamic viscosity:

$$\eta = \frac{2}{9}\, g\, (\rho_{ball} - \rho_{medium})\, \frac{r^2 \cdot t}{s} \tag{8.1}$$

where g is the gravitational acceleration ($\approx 9.81\,\mathrm{m\,s^{-2}}$), ρ_{ball} and ρ_{medium} are the densities of ball and medium, respectively, r and t are the radius and falling time of the ball, respectively, and s is the falling distance covered in the viscometer (2 cm).

Values of η were calculated in mPa s.[2] The term

$$K = \frac{2}{9}\, \frac{r^2 \cdot g}{s} \tag{8.2}$$

represents the ball constant defined by the geometry of the system (ball diameter, diameter and length of cylinder). K was determined tenfold for the 3 mm ball and a reference fluid characterized by known properties (water at 30 °C; $\eta \approx 0.798$ mPa s; $\rho \approx 0.996\,\mathrm{g\,mL^{-1}}$) according to equation 8.3.

$$K = \frac{\eta_{ref}}{(\rho_{ball} - \rho_{ref})\, t} \tag{8.3}$$

where η_{ref} and ρ_{ref} are the dynamic viscosity and the density of the reference fluid, respectively.

The viscosity of a sample was then calculated by equation 8.4.

$$\eta = K\, (\rho_{ball} - \rho_{medium})\, t \tag{8.4}$$

[1] The theoretical considerations are roughly based on the online method "Measurement of viscosity in a vertical falling ball viscometer" (Ping Yuan & Ben-Yuan Lin, October 2008), http://www.americanlaboratory.com/913-Technical-Articles/778-Measurement-of-Viscosity-in-a-Vertical-Falling-Ball-Viscometer/, last checked 5th of April 2016.

[2] $1\,\mathrm{mPa\,s} = 10^{-3}\,\frac{\mathrm{N}}{\mathrm{m^2}}\,\mathrm{s} = 1\,\frac{\mathrm{g}}{\mathrm{s\,m}}$

To compensate for potential time-dependent effects (hysteresis of viscosity for small non-Newtonian effects, temperature dependency), the falling time was determined fivefold after reaching a constant value in a temperature-controlled environment (for the given purpose: the process temperature of 30 °C).

The values determined by this method should only be interpreted as an estimate of the rheological behavior of the broth due to the non-Newtonian behavior of highly concentrated filamentous culture broths (see 2.4.1.1, p. 10).

8.1.2.2 Pellet analysis by ImageJ

The area of pellets of *S. avidinii* was analyzed via a Digi Micro 1.3 USB microscope (1.3 MP, dnt, Dietzenbach, Germany). For this purpose, a culture volume of approximately 0.5 mL was adjusted to 10 mL in a petri dish by the addition of twofold demineralized water. The dish was placed on black cardboard. The sample was illuminated from above by soft, diffuse ambient light, which turned out to be optimal for maximal illumination of pellets and minimal background noise.

Properties of the pellets were evaluated by the image analysis software ImageJ. For this purpose, images were imported as image sequences and converted to 8-bit format. The threshold for the detection of pellet edges was manually adjusted to cover a region from 0 to 200. An additional image of a millimeter-scaled graph paper was used as a scale reference for the quantitative evaluation of the microscopic images by the software.

8.1.2.3 Microplate cultivation

Microplate cultivation was based on a modified version of the protocol by Sohoni *et al.* (2012). Cultivation was performed in squared 24 *well*-microplates (v-bottom, Axygen, Corning, USA). Glass beads (6 per well, diameter: 3 mm) were added to the wells prior to sterilization to avoid pellet formation. The plates were shaken at a frequency of 200 min^{-1} (shaking diameter: 20 mm) at 30 °C.

All experiments were performed in 5 replicates. Medium optimization was based on a DoE approach in the software MODDE. Randomized positions of the experiments in the wells were used for varying compositions of the medium. For the preparation of cultivation media, 18 mL of medium were mixed with 1 mL of 1 M MOPS-buffer (pH 7.0, sterile filtered). A volume of 200 μL of freshly thawed glycerol stock was used for inoculation of this mixture. Each of the wells was then filled with 3 mL of the resulting solution. After 48 and 96 h of cultivation, the loss of liquid volume was compensated by the addition of sterile water (approx. 500 and 800 μL per well, respectively, determined by differential weighing).

During cultivation, microplates were sealed by a gas-permeable membrane (Breathseal, Greiner bio-one, Frickenhausen, Germany).

8.1.2.4 Continuous cultivation

Continuous cultivation was performed in the MBR bioreactor used for Müller *et al.* (2013). M3 medium, composed as described in the same article, was prepared in a vessel with a filling volume of 260 L without adjustment of the pH value. All compounds of the medium were sterilized simultaneously for 45 min, resulting in a loss of glucose due to Maillard reactions (glucose supplemented: $10\,g\,L^{-1}$; glucose measured after sterilization: $8.6\,g\,L^{-1}$).

Flow in the MBR bioreactor was adjusted by a peristaltic pump. Outflow was based on a rising pipe and a second peristaltic pump adjusted to a higher setpoint, ensuring the removal of liquid exceeding the working volume of 3.16 L.

Cultivation parameters were a cultivation temperature of 30 °C, a setpoint for the pH of 7.0, a rotary frequency of the stirrer of $500\,min^{-1}$, and a total air flow rate of $6\,NL\,min^{-1}$. The composition of the inflow air was adjusted by the addition of oxygen from a medical oxygen concentrator (Topair 2, Kröber Medizintechnik GmbH, Dieblich, Germany) depending on the dissolved oxygen signal (ratio aeration). The relative dissolved oxygen concentration was kept constant at 80 % of a maximal saturation of 100 % gathered by calibration for a head pressure of 0.2 bar and aeration by regular air.

Cultivation at each dilution rate was performed until constant concentrations of SAV and DCW were achieved, but for at least 5 residence times.

8.1.3 Purification of SAV

Several methods used for the purification of SAV (section 6, p. 144*ff.* in the main document) are described in the following sections. As discussed in the main document, the methods were tested for a supernatant of *E. coli* if not stated otherwise.

Generally, total protein was determined via the Roti®-Nanoquant system (Carl Roth GmbH + Co. KG, Karlsruhe, Germany), whereas contaminating proteins were qualitatively analyzed via SDS-PAGE.

8.1.3.1 Thermal inactivation

Denaturing by thermal inactivation based on the results of Gallizia *et al.* (1998) was performed in volumes of 200 μL. Samples were incubated at 60, 75 or 80 °C. Three aliquots per temperature and incubation time were used for triplicate determination of the concentration of SAV after the procedure. Samples were incubated on ice directly after heat incubation. A reference sample was incubated at 4 °C for 60 min without heat incubation.

After thermal inactivation, all samples were subjected to centrifugation at $10.000\times g$ and 4 °C for 20 min for the removal of denatured and precipitated proteins. The supernatant was used for the determination of SAV according to the standard measurement procedure.

8.1.3.2 Ammonium sulfate precipitation

Precipitation of SAV by ammonium sulfate was performed based on the general procedure by Green & Hughes (1955) and the SAV-specific study of Suter *et al.* (1988). Precipitation was studied in 15 mL reaction tubes. A volume of 0.15 mL of supernatant and 2.85 mL of twofold demineralized water was incubated at 25 °C prior to the addition of solid ammonium sulfate. For precipitation, samples were incubated overnight at 4 °C after the addition of the salt. Subsequently, the samples were centrifuged at 40.000 $\times g$ and 0 °C for 30 min. Analysis of supernatant and precipitate was performed after separation, resuspension of the precipitate in water, and tempering to 25 °C.

The amount of ammonium sulfate necessary for the precipitation at a defined concentration was calculated according to Green & Hughes (1955).

8.1.3.3 Aqueous two-phase extraction

For the preliminary screening using a PEG/citrate system, PEG of three polymer chain lengths was used: PEG 1500 (Fluka, Buchs, Switzerland), PEG 3000 (Merck KGaA, Darmstadt, Germany), and PEG 6000 (Carl Roth GmbH + Co. KG, Karlsruhe, Germany). The composition of the system was based on Kula & Vernau (1990), yielding the initial system compositions shown in Table 8.1.

No phase separation was observed for the given concentrations at pH 5.2. Thus, the final amounts of both polymer and salt were increased to 2.5 and 1.6 g (PEG 1500 and citrate), 1.9 and 1.4 g (PEG 3000 and citrate), and 1.8 and 1.3 g (PEG 6000 and citrate), respectively, which resulted in an increase of the overall volume. The exact phase volumes for all systems used are shown in Table 8.2.

The systems were vortexed and incubated at RT for 20 min prior to the measurement of phase volumes and SAV.

More detailed experiments on the aqueous two-phase extraction of SAV were based on a PEG/ phosphate system and binodal curves from Albertsson (1986).

PEG 4000 (AppliChem GmbH, Darmstadt, Germany) and different potassium phosphate salts were used (K_2HPO_4 and KH_2PO_4, both also purchased from AppliChem). These compounds were prepared as aqueous stock solutions (20 % potassium phosphate buffer at pH 7, 60 and 20 % K_2HPO_4, 20 % KH_2PO_4, and 40 % PEG 4000; all concentrations referring to % (w/w)). The different potassium phosphate solutions were mixed in defined ratios to adjust the pH to the given setpoint by the Henderson-Hasselbalch equation as shown below. Additionally, NaCl was used as a supplement of the systems, which was added directly to the extraction volume in solid form.

$$pH = pK_A + log\frac{c_{base}}{c_{acid}} \tag{8.5}$$

Tab. 8.1: Composition of PEG/citrate systems used for the preliminary screening for the aqueous two-phase extraction of SAV. The amounts of PEG and citrate were mixed with 1 mL of a 720 nM (tetrameric) supernatant of SAV from *S. avidinii*, and adjusted to the target pH (5.2, 7.0, 9.0, 11.0) and a final volume of 10 mL.

MW PEG [Da] [a]	m_{PEG} [g]	$m_{citrate}$ [g]
1500	2.0	1.3
3000	1.5	1.1
6000	1.4	1.0
1500/3000 [b]	1.0/1.5 [b]	1.2
3000 HPEG [c]	3.0	0.5

[a] molecular weight of PEG used for the study
[b] mixture of PEG 1500 (first amount) and PEG 3000 (second amount)
[c] PEG-rich system, phase ratio not balanced (see Table 8.2)

where pK_A is the negative decadic logarithm of the dissociation constant of the acid K_A, and c_{base} and c_{acid} are the (molar) concentrations of the conjugated base (deprotonated acid) and the acid present in the solution, respectively, .

Extractions were prepared to reach an overall mass of 10 g. A volume of 350 μL of the corresponding SAV-containing supernatant was used for the extraction.

The extractions were mixed and incubated at 28 °C for 1 h. After determination of the phase volumes, the phases were separated and used for the measurement of SAV. Prior to the quantification of total protein according to Bradford (1976), PEG was removed by dichlormethane extraction followed by the removal of potassium phosphate via dialysis.

8.1.3.4 Dialysis

A 14 kDa cellulose bag (Visking type 8/32, Carl Roth GmbH + Co. KG, Karlsruhe, Germany) was used for dialysis, characterized by a width of 10 mm and a wall thickness of 0.05 mm. The average

Tab. 8.2: Phase volumes for the PEG/citrate-based extraction of SAV. Volumes of the PEG-rich top phase and the citrate-rich bottom phase are shown.

system [a]	V_{top} [mL]	V_{bottom} [mL]
1500, pH 11.0	5.5	4.5
1500, pH 9.0	5.6	4.4
1500, pH 7.0	5.6	4.4
1500, pH 5.2	6.5	4.5
3000, pH 11.0	5.6	4.4
3000, pH 9.0	5.6	4.4
3000, pH 7.0	5.5	4.5
3000, pH 5.2	6.5	4.5
6000, pH 11.0	5.6	4.4
6000, pH 9.0	5.5	4.5
6000, pH 7.0	5.6	4.4
6000, pH 5.2	6.5	4.5
1500/3000, pH 7.0 [b]	5.5	4.5
3000 HPEG, pH 7.0 [c]	7.0	3.0

[a] molecular weight of PEG and final pH value used for the study
[b] mixture of PEG 1500 and PEG 3000 according to Table 8.1
[c] PEG-rich system according to Table 8.1

length of the tubes used for dialysis was 10 cm. Filling volumes were in the range of 100 μL to 2 mL. Incubation was performed in a volume of 5 L of demineralized water stirred by a magnetic stirrer at 4 °C for 24 h.

8.2 Supporting results

A selection of supporting results is presented in the following section.

8.2.1 Results of the *in silico*-analysis of the native signal peptide of SAV from *S. avidinii*

The native secretion signal peptide of *S. avidinii* was analyzed *in silico*. Results are shown in Fig. 8.1.

Fig. 8.1: Results of the *in silico*-analysis of the native secretion signal peptide of SAV from *S. avidinii* by the prediction tool PRET-TAT described by Bagos *et al.* (2010). The cleavage site of the signal peptide (AA 1-24) was predicted accurately.

8.2.2 Recovery of biotin-blocked binding sites of SAV

Fig. 8.2, 8.3, and 8.4 show additional results for the recovery of biotin-blocked binding sites of SAV.

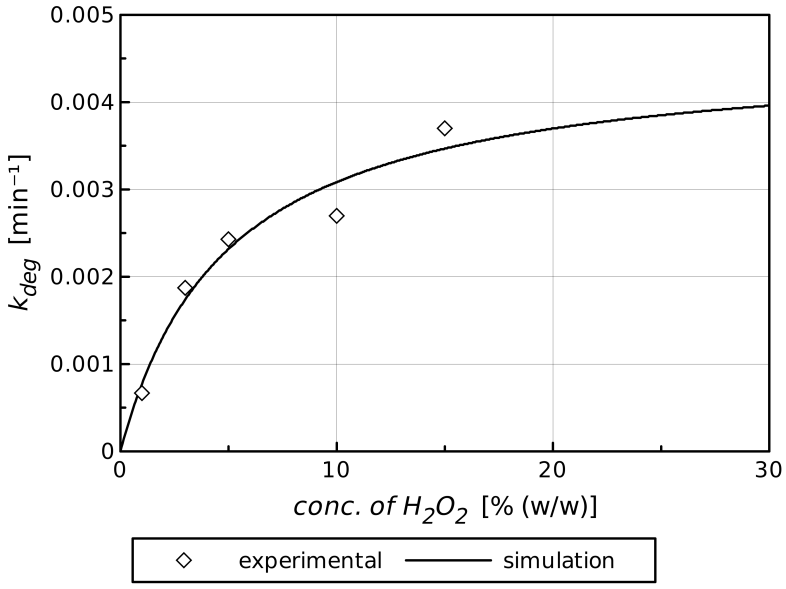

Fig. 8.2: Course of the degradation constant for a first-order degradation of biotin over the concentration of hydrogen peroxide at 60 °C derived from Fig. 3.4a (p. 58). The constants only apply in the initial phase of degradation and for high degrees of biotin saturation ($Q_{bl} \rightarrow 1$).

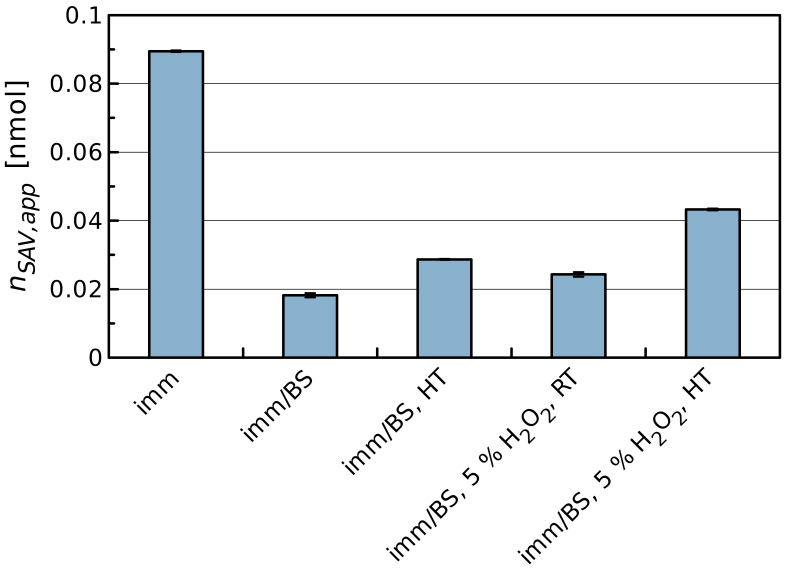

Fig. 8.3: Analysis of the recovery of biotin-blocked binding sites of immobilized SAV by hydrogen peroxide, displayed as the apparent amount of SAV detected in the fluorescence assay. Abbreviations: imm = immobilized SAV, BS = biotin-saturated sample, HT = sample incubated at 60 °C for 30 min. Furthermore, the concentration of H_2O_2 (in % (w/w)) during incubation is shown where it was supplemented to the samples.

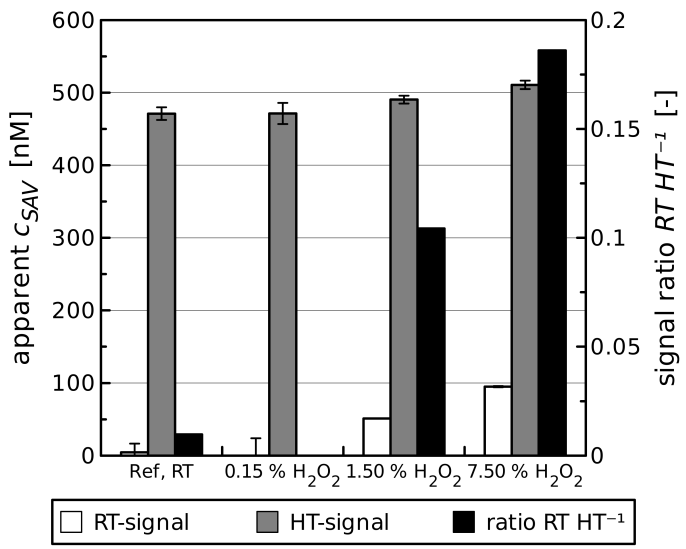

(a) Hydrogen peroxide treatment: qualitative study.

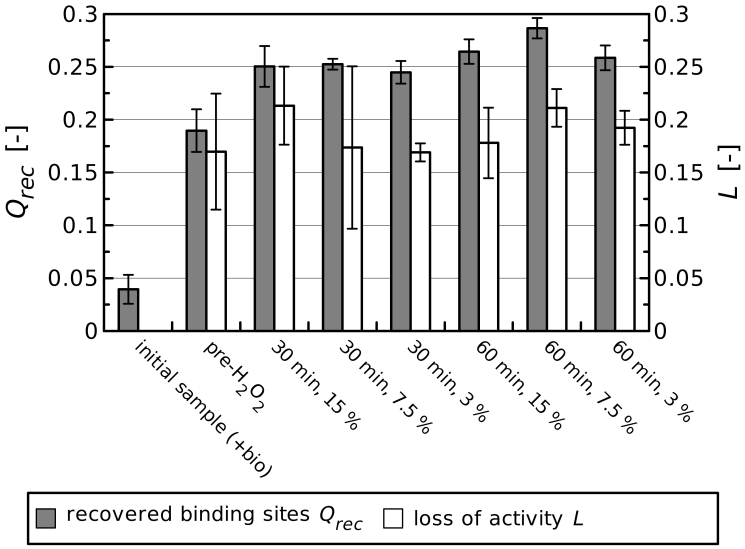

(b) Combined UV and hydrogen peroxide treatment: quantitative study.

Fig. 8.4: Results of studies for the non-denaturing degradation of SAV-bound biotin by UV radiation and hydrogen peroxide (concentrations in % (w/w)). (a) Qualitative study: Incubation of a biotin-saturated, SAV-containing supernatant at 60 °C for 60 min in the presence of varying concentrations of hydrogen peroxide. The apparent concentration of SAV c_{SAV} refers to a fluorescence measurement at room temperature. For the signal ratio $RTHT^{-1}$, the corresponding fluorescence was divided by the result of a measurement after 10 min of incubation at 70 °C (heat-based displacement of biotin) as a qualitative measure of the proportion of biotin-free binding sites (no dilution to $c_{SAV,HT} \leq 300\,\text{nM}$). (b) Quantitative study: normalized recovery Q_{rec} of blocked binding sites and inactivation L of overall binding sites in a supernatant containing 1.2 μM of SAV incubated on a transillumination device for 5 h, followed by treatment with varying concentrations of hydrogen peroxide at 60 °C for 30 or 60 min.

8.2.3 Course of the dynamic viscosity throughout a cultivation of *S. avidinii*

Determination of the dynamic viscosity during bioreactor fermentation of *S. avidinii* allowed conclusions on the state of growth of the culture, as depicted in the exemplary plot of Fig. 8.5.

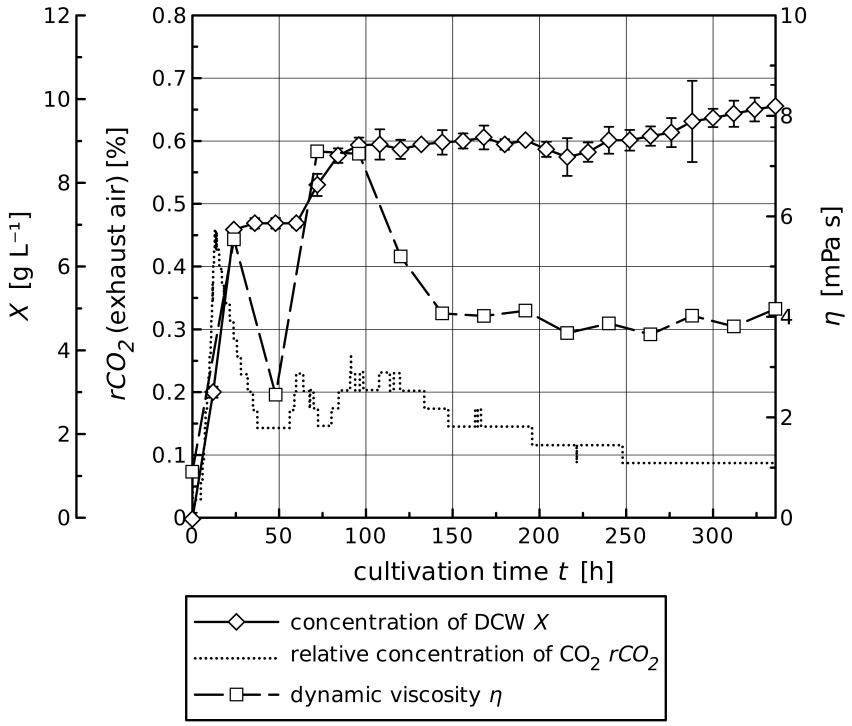

Fig. 8.5: Course of the dynamic viscosity η over the cultivation time for a bioreactor fermentation of *S. avidinii*. The course is compared to the courses of biomass and carbon dioxide in the exhaust air. The second increase of biomass (from 50-100 h of cultivation) was induced by the feeding of additional substrate.

8.2.4 Power input for the studies of *S. avidinii*

Table 8.3 shows the results of the calculations of Reynolds number and power input described in section 4.3.5 (p. 74).

Tab. 8.3: Theoretical power input for the given bioreactor.

	Reynolds number Re [-]			power input L [W]			corr. L [W] [a]			corr. L_{spec} [W L^{-1}]		
n [min^{-1}]	H_2O [b]	2N [c]	BS [d]	H_2O	2N	BS	H_2O	2N	BS	H_2O	2N	BS
200	20384	18573	2280	0.31	0.32	0.32	0.56	0.57	0.57	0.11	0.11	0.11
300	30576	27859	3421	1.05	1.08	1.07	1.88	1.94	1.93	0.38	0.39	0.39
350	35671	32502	3991	1.66	1.71	1.70	2.99	3.07	3.06	0.60	0.61	0.61
400	40767	37146	4561	2.48	2.55	2.54	4.46	4.59	4.57	0.89	0.92	0.91
500	50959	46432	5701	4.84	4.98	4.96	8.72	8.96	8.92	1.74	1.79	1.78
700	71343	65005	7981	13.29	13.66	13.60	23.92	24.58	24.48	4.78	4.92	4.90
900	91727	83578	10262	28.24	29.03	28.91	50.83	52.25	52.03	10.17	10.45	10.41
1100	112110	102150	12542	51.56	52.99	52.78	92.80	95.39	95.00	18.56	19.08	19.00
1300	132494	120723	14823	85.10	87.47	87.12	153.18	157.45	156.81	30.64	31.49	31.36
1500	152878	139296	17103	130.73	134.38	133.83	235.32	241.88	240.89	47.06	48.38	48.18

[a] corrected values of power input; lower Newton number due to the d/D-ratio (p. 72) and doubled L because of the number of stirrers (2).

[b] calculation for water (dynamic viscosity: 0.798 mPa s, density at 30 °C: 995.64 kg m^{-3})

[c] calculation for 2N medium (basic medium in the linear fed-batch processes in Müller *et al.* (2013); experimental dynamic viscosity: 0.9 mPa s, exp. density at 30 °C: 1023.4 kg m^{-3})

[d] calculation for a **b**iomass **s**uspension (BS); exp. dynamic viscosity: 7.3 mPa s, exp. density at 30 °C: 1019.2 kg m^{-3})

8.3 Additional figures

8.3.1 Inverse transition cycling for the purification of proteins

Fig. 8.6 visualizes the method of inverse transition cycling.

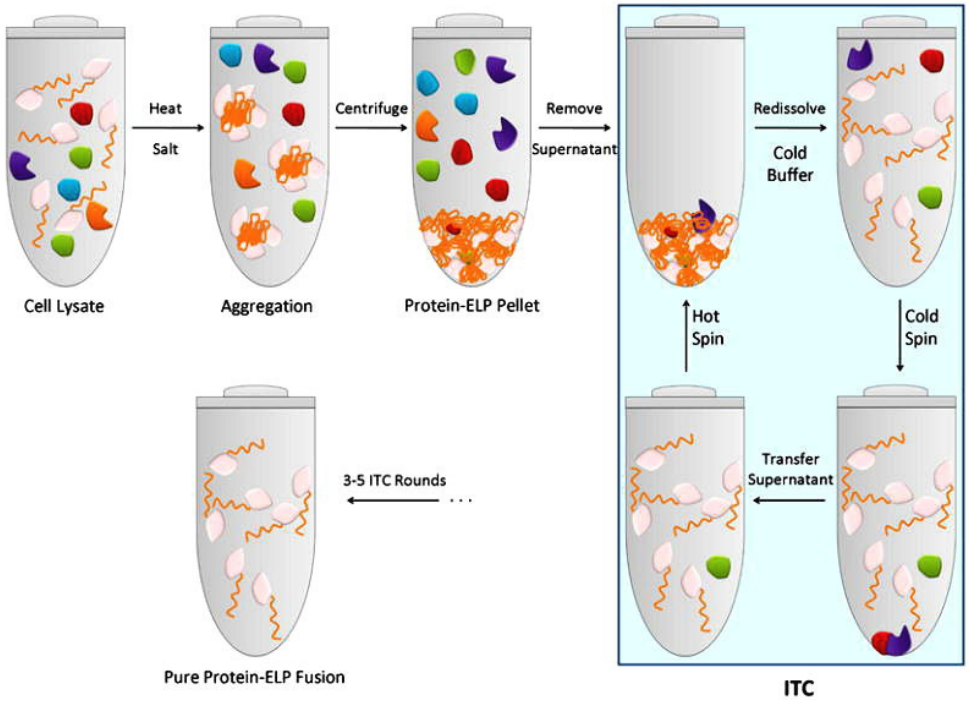

Fig. 8.6: Visualization of the purification of proteins by inverse transition cycling (ITC) according to Hassouneh *et al.* (2010). The target protein, which is fused to an elastin-like polypeptide (ELP), is precipitated by heating or the addition of salts. The supernatant is removed, the protein is redissolved in cold buffer, and again heated up for phase transition. These steps are repeated until sufficient purity is achieved.

Bibliography

Abelson J.N., Simon M.I. & Goeddel D.V. (Eds.), *Methods in Enzymology, Volume 185: Gene Expression Technology* (Academic Press, 1990), 1st Edn..

Albertsson P.A. (Ed.), *Partition of cell particles and macromolecules: separation and purification of biomolecules, cell organelles, membranes, and cells in aqueous polymer two-phase systems and their use in biochemical analysis and biotechnology* (Wiley, 1986), 3rd Edn..

Aldwin D.L., Toso R., Goodson R. & Hunter J. (1990): Improvement of production, assay and purification of streptavidin. *Journal of Industrial Microbiology* **5**(4), 239–246.

Anné J., Maldonado B., Van Impe J., Van Mellaert L. & Bernaerts K. (2012): Recombinant protein production and streptomycetes. *Journal of Biotechnology* **158**(4), 159–167.

Anné J., Vrancken K., Van Mellaert L., Van Impe J. & Bernaerts K. (2014): Protein secretion biotechnology in gram-positive bacteria with special emphasis on *Streptomyces lividans*. *Biochimica et Biophysica Acta (BBA) - Molecular Cell Research* **1843**(8), 1750–1761.

Aslan F.M., Yu Y., Mohr S.C. & Cantor C.R. (2005): Engineered single-chain dimeric streptavidins with an unexpected strong preference for biotin-4-fluorescein. *Proceedings of the National Academy of Sciences of the United States of America* **102**(24), 8507–8512.

Attwood P.V. & Wallace J.C. (2002): Chemical and catalytic mechanisms of carboxyl transfer reactions in biotin-dependent enzymes. *Accounts of Chemical Research* **35**(2), 113–120.

Bagos P.G., Nikolaou E.P., Liakopoulos T.D. & Tsirigos K.D. (2010): Combined prediction of Tat and Sec signal peptides with hidden Markov models. *Bioinformatics* **26**(22), 2811–2817.

Bailey J.E., *Biochemical Engineering Fundamentals* (McGraw-Hill, 1986), 2nd Edn..

Bandyopadhyay B., Humphrey A.E. & Taguchi H. (1967): Dynamic measurement of the volumetric oxygen transfer coefficient in fermentation systems. *Biotechnology and Bioengineering* **9**(4), 533–544.

Baneyx F. (1999): Recombinant protein expression in *Escherichia coli*. *Current Opinion in Biotechnology* **10**(5), 411–421.

Bayer E.A., Ben-Hur H., Hiller Y. & Wilchek M. (1989): Postsecretory modifications of streptavidin. *Biochemical Journal* **259**(2), 369–376.

Bayer E.A., Kulik T., Adar R. & Wilchek M. (1995): Close similarity among streptavidin-like, biotin-binding proteins from *Streptomyces*. *Biochimica et Biophysica Acta (BBA) - Gene Structure and Expression* **1263**(1), 60–66.

Blake M.R. & Weimer B.C. (1997): Immunomagnetic detection of *Bacillus stearothermophilus* spores in food and environmental samples. *Applied and Environmental Microbiology* **63**(5), 1643 –1646.

Boas M.A. (1924): An observation on the value of egg-white as the sole source of nitrogen for young growing rats. *Biochemical Journal* **18**(2), 422–424.

Bradford M.M. (1976): A rapid and sensitive method for the quantitation of microgram quantities of protein utilizing the principle of protein-dye binding. *Analytical Biochemistry* **72**, 248–254.

Braun S. & Vecht-Lifshitz S.E. (1991): Mycelial morphology and metabolite production. *Trends in Biotechnology* **9**(1), 63–68.

Bérdy J. (2012): Thoughts and facts about antibiotics: Where we are now and where we are heading. *The Journal of Antibiotics* **65**(8), 385–395.

Call D.R., Borucki M.K. & Loge F.J. (2003): Detection of bacterial pathogens in environmental samples using DNA microarrays. *Journal of Microbiological Methods* **53**(2), 235–243.

Casteluber M.C.F., Damasceno L.M., da Silveira W.B., Diniz R.H.S., Passos F.J.V. & Passos F.M.L. (2012): Cloning and expression of a functional core streptavidin in *Pichia pastoris*: strategies to increase yield. *Biotechnology Progress* **28**(6), 1419–1425.

Cazin Jr. J., Suter M. & Butler J. (1988): Production of streptavidin in a synthetic medium. *Journal of Immunological Methods* **113**(1), 75–81.

Cereghino G.P.L., Cereghino J.L., Ilgen C. & Cregg J.M. (2002): Production of recombinant proteins in fermenter cultures of the yeast *Pichia pastoris*. *Current Opinion in Biotechnology* **13**(4), 329–332.

Chaiet L. & Wolf F.J. (1964): The properties of streptavidin, a biotin-binding protein produced by *Streptomyces*. *Archives of Biochemistry and Biophysics* **106**, 1–5.

Chen B., Metera K. & Sleiman H.F. (2005): Biotin-terminated ruthenium bipyridine ring-opening metathesis polymerization copolymers: synthesis and self-assembly with streptavidin. *Macromolecules* **38**(4), 1084–1090.

Chen R. (2012): Bacterial expression systems for recombinant protein production: *E. coli* and beyond. *Biotechnology Advances* **30**(5), 1102–1107.

Chen X., Xu F., Peng F., Xu H., Luo W., Xu H. & Xiong Y. (2014): High-yield production of Streptavidin with native C-terminal in *Escherichia coli*. *African Journal of Biotechnology* **11**(33).

Chivers C.E., Crozat E., Chu C., Moy V.T., Sherratt D.J. & Howarth M. (2010): A streptavidin variant with slower biotin dissociation and increased mechanostability. *Nature Methods* **7**(5), 391–393.

Cos O., Ramón R., Montesinos J.L. & Valero F. (2006): Operational strategies, monitoring and control of heterologous protein production in the methylotrophic yeast *Pichia pastoris* under different promoters: A review. *Microbial Cell Factories* **5**(1), 17.

Cregg J.M., Cereghino J.L., Shi J. & Higgins D.R. (2000): Recombinant protein expression in *Pichia pastoris*. *Molecular Biotechnology* **16**(1), 23–52.

Cregg J.M., Vedvick T.S. & Raschke W.C. (1993): Recent advances in the expression of foreign genes in *Pichia pastoris*. *Bio/Technology (Nature Publishing Company)* **11**(8), 905–910.

Delic M., Valli M., Graf A.B., Pfeffer M., Mattanovich D. & Gasser B. (2013): The secretory pathway: exploring yeast diversity. *FEMS Microbiology Reviews* **37**(6), 872–914.

Demonte D., Dundas C.M. & Park S. (2014): Expression and purification of soluble monomeric streptavidin in *Escherichia coli*. *Applied Microbiology and Biotechnology* .

di Guan C., Li P., Riggs P.D. & Inouye H. (1988): Vectors that facilitate the expression and purification of foreign peptides in *Escherichia coli* by fusion to maltose-binding protein. *Gene* **67**(1), 21–30.

Diamond A.D. & Hsu J.T., *Aqueous two-phase systems for biomolecule separation*, Vol. 47 (Springer-Verlag, Berlin/Heidelberg, 1992).

Diaz-Moralli S., Tarrado-Castellarnau M., Alenda C., Castells A. & Cascante M. (2011): Transketolase-like 1 expression is modulated during colorectal cancer progression and metastasis formation. *PLOS One* **6**(9).

Dittmer J., Dittmer A., Della Bruna R. & Kasche V. (1989): A native, affinity-based protein blot for the analysis of streptavidin heterogeneity: consequences for the specificity of streptavidin mediated binding assays. *Electrophoresis* **10**(11), 762–765.

Doran P.M., *Bioprocess Engineering Principles* (Elsevier Science & Technology Books, 1995), 1st Edn..

Dragosits M., Stadlmann J., Albiol J., Baumann K., Maurer M., Gasser B., Sauer M., Altmann F., Ferrer P. & Mattanovich D. (2009): The effect of temperature on the proteome of recombinant *Pichia pastoris*. *Journal of Proteome Research* **8**(3), 1380–1392.

Dreyer S. & Kragl U. (2008): Ionic liquids for aqueous two-phase extraction and stabilization of enzymes. *Biotechnology and Bioengineering* **99**(6), 1416–1424.

Dumon-Seignovert L., Cariot G. & Vuillard L. (2004): The toxicity of recombinant proteins in *Escherichia coli*: a comparison of overexpression in BL21(DE3), C41(DE3), and C43(DE3). *Protein Expression and Purification* **37**(1), 203–206.

Dundas C.M., Demonte D. & Park S. (2013): Streptavidin-biotin technology: improvements and innovations in chemical and biological applications. *Applied Microbiology and Biotechnology* **97**(21), 9343–9353.

Ellis S.B., Brust P.F., Koutz P.J., Waters A.F., Harpold M.M. & Gingeras T.R. (1985): Isolation of alcohol oxidase and two other methanol regulatable genes from the yeast *Pichia pastoris*. *Molecular and Cellular Biology* **5**(5), 1111–1121.

Fall R.R., Alberts A.W. & Vagelos P.R. (1975): Analysis of bacterial biotin-proteins. *Biochimica et Biophysica Acta (BBA) - Protein Structure* **379**(2), 496–503.

Flowers T.H. & Williams S.T. (1977): Measurement of growth rates of streptomycetes: comparison of turbidimetric and gravimetric techniques. *Journal of General Microbiology* **98**(1), 285–289.

Flärdh K. & Buttner M.J. (2009): *Streptomyces* morphogenetics: dissecting differentiation in a filamentous bacterium. *Nature Reviews Microbiology* **7**(1), 36–49.

Fong R.B., Ding Z., Long C.J., Hoffman A.S. & Stayton P.S. (1999): Thermoprecipitation of streptavidin via oligonucleotide-mediated self-assembly with poly(N-isopropylacrylamide). *Bioconjugate Chemistry* **10**(5), 720–725.

Forster A.C., McInnes J.L., Skingle D.C. & Symons R.H. (1985): Non-radioactive hybridization probes prepared by the chemical labelling of DNA and RNA with a novel reagent, photobiotin. *Nucleic Acids Research* **13**(3), 745 –761.

Fudem-Goldin B. & Orr G.A. (1990): 2-Iminobiotin-containing reagent and affinity columns. *Methods in Enzymology* **184**, 167–173.

Funahashi A., Matsuoka Y., Jouraku A., Morohashi M., Kikuchi N. & Kitano H. (2008): CellDesigner 3.5: a versatile modeling tool for biochemical networks. *Proceedings of the IEEE* **96**(8), 1254–1265.

Furukawa H., Tanino T., Fukuda H. & Kondo A. (2006): Development of novel yeast cell surface display system for homo-oligomeric protein by coexpression of native and anchored subunits. *Biotechnology Progress* **22**(4), 994–997.

Gallizia A., de Lalla C., Nardone E., Santambrogio P., Brandazza A., Sidoli A. & Arosio P. (1998): Production of a soluble and functional recombinant streptavidin in *Escherichia coli*. *Protein Expression and Purification* **14**(2), 192–196.

Gamboa-Suasnavart R.A., Marín-Palacio L.D., Martínez-Sotelo J.A., Espitia C., Servín-González L., Valdez-Cruz N.A. & Trujillo-Roldán M.A. (2013): Scale-up from shake flasks to bioreactor, based on power input and *Streptomyces lividans* morphology, for the production of recombinant APA (45/47 kDa protein) from *Mycobacterium tuberculosis*. *World Journal of Microbiology and Biotechnology* **29**(8), 1421–1429.

Gasser B., Dragosits M. & Mattanovich D. (2010): Engineering of biotin-prototrophy in *Pichia pastoris* for robust production processes. *Metabolic Engineering* **12**(6), 573–580.

Gellissen G. (2000): Heterologous protein production in methylotrophic yeasts. *Applied Microbiology and Biotechnology* **54**(6), 741–750.

Gellissen G., Janowicz Z.A., Merckelbach A., Piontek M., Keup P., Weydemann U., Hollenberg C.P. & Strasser A.W. (1991): Heterologous gene expression in *Hansenula polymorpha*: efficient secretion of glucoamylase. *Biotechnology* **9**(3), 291–295.

Georgiou G. & Segatori L. (2005): Preparative expression of secreted proteins in bacteria: status report and future prospects. *Current Opinion in Biotechnology* **16**(5), 538–545.

Germeroth A.I., Hanna J.R., Karim R., Kundel F., Lowther J., Neate P.G.N., Blackburn E.A., Wear M.A., Campopiano D.J. & Hulme A.N. (2013): Triazole biotin: a tight-binding biotinidase-resistant conjugate. *Organic & Biomolecular Chemistry* **11**(44), 7700.

Goklen K.E. & Hatton T.A. (1987): Liquid-liquid extraction of low molecular-weight proteins by selective solubilization in reversed micelles. *Separation Science and Technology* **22**(2-3), 831–841.

González M., Argaraña C.E. & Fidelio G.D. (1999): Extremely high thermal stability of streptavidin and avidin upon biotin binding. *Biomolecular Engineering* **16**(1-4), 67–72.

González M., Bagatolli L.A., Echabe I., Arrondo J.L.R., Argaraña C.E., Cantor C.R. & Fidelio G.D. (1997): Interaction of biotin with streptavidin - thermostability and conformational changes upon binding. *Journal of Biological Chemistry* **272**(17), 11288–11294.

Graf A., Dragosits M., Gasser B. & Mattanovich D. (2009): Yeast systems biotechnology for the production of heterologous proteins. *FEMS Yeast Research* **9**(3), 335–348.

Green A.A. & Hughes W.L. (Eds.), *Protein fractionation on the basis of solubility in aqueous solutions of salts and organic solvents* (Academic Press, 1955).

Green N.M. (1970): Spectrophotometric determination of avidin and biotin. *Methods in Enzymology* (18A), 418–424.

Green N.M. (1990): Avidin and streptavidin. *Methods in Enzymology* **184**, 51–67.

Gretch D.R., Suter M. & Stinski M.F. (1987): The use of biotinylated monoclonal antibodies and streptavidin affinity chromatography to isolate herpesvirus hydrophobic proteins or glycoproteins. *Analytical Biochemistry* **163**(1), 270–277.

Grubmüller H., Heymann B. & Tavan P. (1996): Ligand Binding: Molecular Mechanics Calculation of the Streptavidin-Biotin Rupture Force. *Science* **271**(5251), 997–999.

Güneş H. & Çalik P. (2016): Oxygen transfer as a tool for fine-tuning recombinant protein production by *Pichia pastoris* under glyceraldehyde-3-phosphate dehydrogenase promoter. *Bioprocess and Biosystems Engineering* pp. 1–12.

GVC-Fachausschuss 'Mischvorgänge', *Mischen und Rühren* (Gesellschaft für Verfahrenstechnik und Chemieingenieurwesen, 1998), 1st Edn..

Hannig G. & Makrides S.C. (1998): Strategies for optimizing heterologous protein expression in *Escherichia coli*. *Trends in Biotechnology* **16**(2), 54–60.

Hassouneh W., Christensen T. & Chilkoti A. (2010): Elastin-like polypeptides as a purification tag for recombinant proteins. *Current Protocols in Protein Science* pp. Unit–6.11.

Helppolainen S.H., Määttä J.A.E., Halling K.K., Slotte J.P., Hytönen V.P., Jänis J., Vainiotalo P., Kulomaa M.S. & Nordlund H.R. (2008): Bradavidin II from *Bradyrhizobium japonicum*: a new avidin-like biotin-binding protein. *Biochimica et Biophysica Acta* **1784**(7-8), 1002–1010.

Helppolainen S.H., Nurminen K.P., Määttä J.A.E., Halling K.K., Slotte J.P., Huhtala T., Liimatainen T., Ylä-Herttuala S., Airenne K.J., Närvänen A., Jänis J., Vainiotalo P., Valjakka J., Kulomaa M.S. & Nordlund H.R. (2007): Rhizavidin from *Rhizobium etli*: the first natural dimer in the avidin protein family. *Biochemical Journal* **405**(3), 397–405.

Hertz R. & Sebrell W.H. (1942): Occurence of avidin in the oviduct and secretions of the genital tract of several species. *Science (New York, N.Y.)* **96**(2489), 257.

Hiller Y., Gershoni J.M., Bayer E.A. & Wilchek M. (1987): Biotin binding to avidin. Oligosaccharide side chain not required for ligand association. *Biochemical Journal* **248**(1), 167–171.

Hochuli E., Bannwarth W., Döbeli H., Gentz R. & Stüber D. (1988): Genetic approach to facilitate purification of recombinant proteins with a novel metal chelate adsorbent. *Nature Biotechnology* **6**(11), 1321–1325.

Hockenhull D. (1980): Inoculum development with particular reference to *Aspergillus* and *Penicillium*. *Fungal Biotechnology* (3), 1–24.

Hockney R.C. (1994): Recent developments in heterologous protein production in *Escherichia coli*. *Trends in Biotechnology* **12**(11), 456–463.

Hofmann K., Wood S.W., Brinton C.C., Montibeller J.A. & Finn F.M. (1980): Iminobiotin affinity columns and their application to retrieval of streptavidin. *Proceedings of the National Academy of Sciences of the United States of America* **77**(8), 4666–4668.

Hohenblum H., Borth N. & Mattanovich D. (2003): Assessing viability and cell-associated product of recombinant protein producing *Pichia pastoris* with flow cytometry. *Journal of Biotechnology* **102**(3), 281–290.

Hollenberg C.P. & Gellissen G. (1997): Production of recombinant proteins by methylotrophic yeasts. *Current Opinion in Biotechnology* **8**(5), 554–560.

Holmberg A., Blomstergren A., Nord O., Lukacs M., Lundeberg J. & Uhlén M. (2005): The biotin-streptavidin interaction can be reversibly broken using water at elevated temperatures. *Electrophoresis* **26**(3), 501–510.

Hong Lim K., Hwang I. & Park S. (2012): Biotin-assisted folding of streptavidin on the yeast surface. *Biotechnology Progress* **28**(1), 276–283.

Hoops S., Sahle S., Gauges R., Lee C., Pahle J., Simus N., Singhal M., Xu L., Mendes P. & Kummer U. (2006): COPASI - a COmplex PAthway SImulator. *Bioinformatics* **22**(24), 3067–3074.

Hortsch R. & Weuster-Botz D. (2010): Power consumption and maximum energy dissipation in a milliliter-scale bioreactor. *Biotechnology Progress* **26**(2), 595–599.

Hughmark G.A. (1980): Power requirements and interfacial area in gas-liquid turbine agitated systems. *Industrial & Engineering Chemistry Process Design and Development* **19**(4), 638–641.

Humbert N. & Ward T., Functionality screen of streptavidin mutants by non-denaturing SDS-PAGE using biotin-4-fluorescein. R. McMahon (Ed.), *Avidin-Biotin Interactions*, no. 418 in Methods In Molecular Biology, pp. 63–71 (Humana Press, 2008).

Hunter J.D. (2007): Matplotlib: A 2D graphics environment. *Computing In Science & Engineering* **9**(3), 90–95.

IBA Lifesciences (2009): Strep-tag FAQ. last downloaded 06/05/2015. URL http://www.iba-lifesciences.com/tl_files/uploads/bilder/produkte/streptag/Downloads/FAQ%20Strep%20tag.pdf.

Invitrogen/Life Technologies (2002): *Pichia* fermentation process guidelines, version B 053002. last downloaded 18/02/2016. URL https://tools.thermofisher.com/content/sfs/manuals/pichiaferm_prot.pdf.

Jahic M., Rotticci-Mulder J., Martinelle M., Hult K. & Enfors S.O. (2002): Modeling of growth and energy metabolism of *Pichia pastoris* producing a fusion protein. *Bioprocess and Biosystems Engineering* **24**(6), 385–393.

Jensen P.R. & Hammer K. (1998): The sequence of spacers between the consensus sequences modulates the strength of prokaryotic promoters. *Applied and Environmental Microbiology* **64**(1), 82–87.

Járai M., Gyory E. & Tombor J. (1969): Oxygen transfer in *Streptomyces* fermentation broths. *Biotechnology and Bioengineering* **11**(4), 605–622.

Jungo C., Schenk J., Pasquier M., Marison I.W. & von Stockar U. (2007a): A quantitative analysis of the benefits of mixed feeds of sorbitol and methanol for the production of recombinant avidin with *Pichia pastoris*. *Journal of Biotechnology* **131**(1), 57–66.

Jungo C., Urfer J., Zocchi A., Marison I. & von Stockar U. (2007b): Optimisation of culture conditions with respect to biotin requirement for the production of recombinant avidin in *Pichia pastoris*. *Journal of Biotechnology* **127**(4), 703–715.

Kada G., Falk H. & Gruber H.J. (1999a): Accurate measurement of avidin and streptavidin in crude biofluids with a new, optimized biotin-fluorescein conjugate. *Biochimica et Biophysica Acta (BBA) - General Subjects* **1427**(1), 33–43.

Kada G., Kaiser K., Falk H. & Gruber H.J. (1999b): Rapid estimation of avidin and streptavidin by fluorescence quenching or fluorescence polarization. *Biochimica et Biophysica Acta* **1427**(1), 44–48.

Kalofonos H.P., Rusckowski M., Siebecker D.A., Sivolapenko G.B., Snook D., Lavender J.P., Epenetos A.A. & Hnatowich D.J. (1990): Imaging of tumor in patients with indium-111-labeled biotin and streptavidin-conjugated antibodies: preliminary communication. *Journal of Nuclear Medicine: Official Publication, Society of Nuclear Medicine* **31**(11), 1791–1796.

Kaplan D.L., Mello C., Sano T., Cantor C. & Smith C. (1999): Streptavidin-based containment systems for genetically engineered microorganisms. *Biomolecular Engineering* **16**(14), 135–140.

Katz B.A. (1997): Binding of biotin to streptavidin stabilizes intersubunit salt bridges between Asp61 and His87 at low pH1. *Journal of Molecular Biology* **274**(5), 776–800.

Katz B.A., Liu B. & Cass R. (1996): Structure-based design tools: structural and thermodynamic comparison with biotin of a small molecule that binds to streptavidin with micromolar affinity. *Journal of the American Chemical Society* **118**(34), 7914–7920.

Kaul A., The Phase Diagram. R. Hatti-Kaul (Ed.), *Aqueous two-phase systems: methods and protocols*, no. 11 in Methods in Biotechnology, pp. 11–21 (Humana Press, 2000).

Kaup B.A., Ehrich K., Pescheck M. & Schrader J. (2008): Microparticle-enhanced cultivation of filamentous microorganisms: Increased chloroperoxidase formation by *Caldariomyces fumago* as an example. *Biotechnology and Bioengineering* **99**(3), 491–498.

Keefe A.D., Wilson D.S., Seelig B. & Szostak J.W. (2001): One-step purification of recombinant proteins using a nanomolar-affinity streptavidin-binding peptide, the SBP-tag. *Protein Expression and Purification* **23**(3), 440–446.

Khatri N.K. & Hoffmann F. (2006): Impact of methanol concentration on secreted protein production in oxygen-limited cultures of recombinant *Pichia pastoris*. *Biotechnology and Bioengineering* **93**(5), 871–879.

Kolomiets E.I. & Zdor N.A. (1998): A product of the strain *Streptomyces avidinii* VKM Ac1047: synthesis, purification and use in immunoassay technology. *Russian Biotechnology* **2**, 1–8.

Kraal B., M L.R.G. & van Wezel G.P. (1999): WO Patent 2000000613 A1, Reducing branching and enhancing fragmentation in culturing filamentous microorganisms.

Kula M. & Vernau J. (1990): European Patent No. EP0387760 A1, Verfahren zur Extraktion von Proteinen aus wässrigen Biomassesuspensionen.

Kurzban G.P., Bayer E.A., Wilchek M. & Horowitz P.M. (1991): The quaternary structure of streptavidin in urea. *The Journal of Biological Chemistry* **266**(22), 14470–14477.

Lamla T. & Erdmann V.A. (2004): The Nano-tag, a streptavidin-binding peptide for the purification and detection of recombinant proteins. *Protein Expression and Purification* **33**(1), 39–47.

Lee L.Y., Ong S.L., Hu J.Y., Ng W.J., Feng Y., Tan X. & Wong S.W. (2004): Use of semiconductor quantum dots for photostable immunofluorescence labeling of *Cryptosporidium parvum*. *Applied and Environmental Microbiology* **70**(10), 5732 –5736.

Lee S.Y. (1996): High cell-density culture of *Escherichia coli*. *Trends in Biotechnology* **14**(3), 98–105.

Lin-Cereghino G.P., Stark C.M., Kim D., Chang J., Shaheen N., Poerwanto H., Agari K., Moua P., Low L.K., Tran N., Huang A.D., Nattestad M., Oshiro K.T., Chang J.W., Chavan A., Tsai J.W. & Lin-Cereghino J. (2013): The effect of α-mating factor secretion signal mutations on recombinant protein expression in *Pichia pastoris*. *Gene* **519**(2), 311–317.

Lin-Cereghino J., Hashimoto M.D., Moy A., Castelo J., Orazem C.C., Kuo P., Xiong S., Gandhi V., Hatae C.T., Chan A. & Lin-Cereghino G.P. (2008): Direct selection of *Pichia pastoris* expression strains using new G418 resistance vectors. *Yeast* **25**(4), 293–299.

Livnah O., Bayer E.A., Wilchek M. & Sussman J.L. (1993): Three-dimensional structures of avidin and the avidin-biotin complex. *Proceedings of the National Academy of Sciences of the United States of America* **90**(11), 5076–5080.

Luedeking R. & Piret E.L. (1959): A kinetic study of the lactic acid fermentation. Batch process at controlled pH. *Journal of Biochemical and Microbiological Technology Engineering* I(4), 393–412.

Macauley-Patrick S., Fazenda M.L., McNeil B. & Harvey L.M. (2005): Heterologous protein production using the *Pichia pastoris* expression system. *Yeast* **22**(4), 249–270.

Madzak C., Gaillardin C. & Beckerich J.M. (2004): Heterologous protein expression and secretion in the non-conventional yeast *Yarrowia lipolytica*: a review. *Journal of Biotechnology* **109**(1-2), 63–81.

Makrides S.C. (1996): Strategies for achieving high-level expression of genes in *Escherichia coli*. *Microbiological Reviews* **60**(3), 512–538.

Malmstadt N., Hyre D.E., Ding Z., Hoffman A.S. & Stayton P.S. (2003): Affinity thermoprecipitation and recovery of biotinylated biomolecules via a mutant streptavidin-smart polymer conjugate. *Bioconjugate Chemistry* **14**(3), 575–580.

Marini P., Li S.J., Gardiol D., Cronan J.E. & Mendoza D.d. (1995): The genes encoding the biotin carboxyl carrier protein and biotin carboxylase subunits of *Bacillus subtilis* acetyl coenzyme A carboxylase, the first enzyme of fatty acid synthesis. *Journal of Bacteriology* **177**(23), 7003–7006.

Markwick N.P., Docherty L.C., Phung M.M., Lester M.T., Murray C., Yao J.L., Mitra D.S., Cohen D., Beuning L.L., Kutty-Amma S. & Christeller J.T. (2003): Transgenic tobacco and apple plants expressing biotin-binding proteins are resistant to two cosmopolitan insect pests, potato tuber moth and lightbrown apple moth, respectively. *Transgenic Research* **12**(6), 671–681.

Marshall R.D. (1972): Glycoproteins. *Annual Review of Biochemistry* **41**(1), 673–702.

Mayer A.F., Hellmuth K., Schlieker H., Lopez-Ulibarri R., Oertel S., Dahlems U., Strasser A.W.M. & van Loon A.P.G.M. (1999): An expression system matures: A highly efficient and cost-effective process for phytase production by recombinant strains of *Hansenula polymorpha*. *Biotechnology and Bioengineering* **63**(3), 373–381.

McCoy G.A., Litman T. & Douglass J.G. (1993): Energy-efficient electric motor selection handbook, revision 3 (DOE/CE - 0384). U.S. Department of Energy.

Meade H.M. & Jeffrey J.L. (1986): Production of streptavidin-like polypeptides (Biogen N.V., Patent WO 86/02077) .

Menkel F., *Einführung in die Technik von Bioreaktoren* (Oldenbourg R. Verlag, München, 1992).

Mergulhao F., Summers D. & Monteiro G. (2005): Recombinant protein secretion in *Escherichia coli*. *Biotechnology Advances* **23**(3), 177–202.

Metz B. & Kossen N.W.F. (1977): The growth of molds in the form of pellets - a literature review. *Biotechnology and Bioengineering* **19**(6), 781–799.

Metz B., Kossen N.W.F. & Suijdam J.C.v., The rheology of mould suspensions. *Advances in Biochemical Engineering, Volume 11*, no. 11 in Advances in Biochemical Engineering, pp. 103–156 (Springer Berlin Heidelberg, 1979).

Meyer D.E. & Chilkoti A. (1999): Purification of recombinant proteins by fusion with thermally-responsive polypeptides. *Nature Biotechnology* **17**(11), 1112–1115.

Miksch G., Ryu S., Risse J.M. & Flaschel E. (2008): Factors that influence the extracellular expression of streptavidin in *Escherichia coli* using a bacteriocin release protein. *Applied Microbiology and Biotechnology* **81**(2), 319–326.

Miroux B. & Walker J.E. (1996): Over-production of proteins in *Escherichia coli*: mutant hosts that allow synthesis of some membrane proteins and globular proteins at high levels. *Journal of Molecular Biology* **260**(3), 289–298.

Miyamoto S. & Kollman P.A. (1993): Absolute and relative binding free energy calculations of the interaction of biotin and its analogs with streptavidin using molecular dynamics/free energy perturbation approaches. *Proteins: Structure, Function, and Bioinformatics* **16**(3), 226–245.

Müller J.M., Bruhn S., Flaschel E., Friehs K. & Risse J.M. (2016a): GAP promoter-based fed-batch production of highly bioactive core streptavidin by *Pichia pastoris*. *Biotechnology Progress* **32**(4), 855–864.

Müller J.M., Risse J.M., Friehs K. & Flaschel E. (2015): Model-based development of an assay for the rapid detection of biotin-blocked binding sites of streptavidin. *Engineering in Life Sciences* **15**, 627–639.

Müller J.M., Risse J.M., Jussen D. & Flaschel E. (2013): Development of fed-batch strategies for the production of streptavidin by *Streptomyces avidinii* based on power input and oxygen supply studies. *Journal of Biotechnology* **163**(3), 325–332.

Müller J.M., Risse J.M., Jussen D. & Flaschel E. (2016b): Corrigendum to "Development of fed-batch strategies for the production of streptavidin by *Streptomyces avidinii* based on power input and oxygen supply studies" [J. Biotechnol. 163 (2013) 325-332]. *Journal of Biotechnology (article in press)* .

Müller J.M., Wetzel D., Flaschel E., Friehs K. & Risse J.M. (2016c): Constitutive production and efficient secretion of soluble full-length streptavidin by an *Escherichia coli* 'leaky mutant'. *Journal of Biotechnology* **221**, 91–100.

Morgan T.D., Oppert B., Czapla T.H. & Kramer K.J. (1993): Avidin and streptavidin as insecticidal and growth inhibiting dietary proteins. *Entomologia Experimentalis et Applicata* **69**(2), 97–108.

Morosoli R., Shareck F. & Kluepfel D. (1997): Protein secretion in streptomycetes. *FEMS Microbiology Letters* **146**(2), 167–174.

Määttä J.A., Helppolainen S.H., Hytönen V.P., Johnson M.S., Kulomaa M.S., Airenne T.T. & Nordlund H.R. (2009): Structural and functional characteristics of xenavidin, the first frog avidin from *Xenopus tropicalis*. *BMC Structural Biology* **9**, 63.

Mujacic M., Cooper K.W. & Baneyx F. (1999): Cold-inducible cloning vectors for low-temperature protein expression in *Escherichia coli*: application to the production of a toxic and proteolytically sensitive fusion protein. *Gene* **238**(2), 325–332.

Murray C., Sutherland P.W., Phung M.M., Lester M.T., Marshall R.K. & Christeller J.T. (2002): Expression of biotin-binding proteins, avidin and streptavidin, in plant tissues using plant vacuolar targeting sequences. *Transgenic Research* **11**(2), 199–214.

Muzykantov V.R., Christofidou-Solomidou M., Balyasnikova I., Harshaw D.W., Schultz L., Fisher A.B. & Albelda S.M. (1999): Streptavidin facilitates internalization and pulmonary targeting of an anti-endothelial cell antibody (platelet-endothelial cell adhesion molecule 1): a strategy for vascular immunotargeting of drugs. *Proceedings of the National Academy of Sciences* **96**(5), 2379–2384.

Nagarajan V., Ramaley R., Albertson H. & Chen M. (1993): Secretion of streptavidin from *Bacillus subtilis*. *Applied and Environmental Microbiology* **59**(11), 3894–3898.

Natale P., Brüser T. & Driessen A.J.M. (2008): Sec- and Tat-mediated protein secretion across the bacterial cytoplasmic membrane - distinct translocases and mechanisms. *Biochimica et Biophysica Acta (BBA) - Biomembranes* **1778**(9), 1735–1756.

Navakouski M.J., Vashkevich I.I. & Sviridov O.V. (2009): The effect of precipitation of the complexes of streptavidin with biotinylated proteins in agar gel. *Applied Biochemistry and Microbiology* **45**(1), 97–103.

Nett M., Ikeda H. & Moore B.S. (2009): Genomic basis for natural product biosynthetic diversity in the actinomycetes. *Natural Product Reports* **26**(11), 1362–1384.

Nguyen V.A.T., Huynh H.A., Hoang T.V., Ninh N.T., Pham A.T.H., Nguyen H.A., Phan T.N. & Cutting S.M. (2013): Killed *Bacillus subtilis* spores expressing streptavidin: a novel carrier of drugs to target cancer cells. *Journal of Drug Targeting* **21**(6), 528–541.

Ni Y. & Chen R. (2009): Extracellular recombinant protein production from *Escherichia coli*. *Biotechnology Letters* **31**(11), 1661–1670.

Ni Y., Holtmann D. & Hollmann F. (2014): How green is biocatalysis? To calculate is to know. *ChemCatChem* **6**(4), 930–943.

Nielsen J. (1996): Modelling the morphology of filamentous microorganisms. *Trends in Biotechnology* **14**(11), 438–443.

Niu H., Jost L., Pirlot N., Sassi H., Daukandt M., Rodriguez C. & Fickers P. (2013): A quantitative study of methanol/sorbitol co-feeding process of a *Pichia pastoris* Mut$^+$/pAOX1-*lacZ* strain. *Microbial Cell Factories* **12**, 33.

Noda S., Matsumoto T., Tanaka T. & Kondo A. (2015): Secretory production of tetrameric native full-length streptavidin with thermostability using *Streptomyces lividans* as a host. *Microbial Cell Factories* **14**(5).

Nogueira E.S., Schleier T., Dürrenberger M., Ballmer-Hofer K., Ward T.R. & Jaussi R. (2014): High-level secretion of recombinant full-length streptavidin in *Pichia pastoris* and its application to enantioselective catalysis. *Protein Expression and Purification* **93**, 54–62.

Nogueira E.S.P., *Dissertation - Novel approaches for the creation of artificial metalloenzymes* (Philosophisch-Naturwissenschaftliche Fakultät, Universität Basel, Switzerland, 2013).

Nordlund H.R., Hytönen V.P., Laitinen O.H. & Kulomaa M.S. (2005): Novel Avidin-like Protein from a Root Nodule Symbiotic Bacterium, *Bradyrhizobium japonicum*. *Journal of Biological Chemistry* **280**(14), 13250–13255.

Nossal N.G. & Heppel L.A. (1966): The release of enzymes by osmotic shock from *Escherichia coli* in exponential phase. *Journal of Biological Chemistry* **241**(13), 3055–3062.

Ochi K. (1989): Heterogeneity of ribosomal proteins among *Streptomyces* species and its application to identification. *Journal of General Microbiology* **135**(10), 2635–2642.

Olsvik E. & Kristiansen B. (1994): Rheology of filamentous fermentations. *Biotechnology Advances* **12**(1), 1–39.

Pähler A., Hendrickson W.A., Kolks M.A., Argaraña C.E. & Cantor C.R. (1987): Characterization and crystallization of core streptavidin. *The Journal of Biological Chemistry* **262**(29), 13933–13937.

Papagianni M., Mattey M. & Kristiansen B. (1999): The influence of glucose concentration on citric acid production and morphology of *Aspergillus niger* in batch and culture. *Enzyme and Microbial Technology* **25**(8-9), 710–717.

Papagianni M. & Moo-Young M. (2002): Protease secretion in glucoamylase producer *Aspergillus niger* cultures: fungal morphology and inoculum effects. *Process Biochemistry* **37**(11), 1271–1278.

Patzl M., *Dissertation - Development of a biotin-streptavidin-enzyme immunoassay for the determination of cortisol in blood and saliva of dogs* (Veterinärmedizinische Universität, Vienna, Austria, 1990).

Perbandt M., Bruns O., Vallazza M., Lamla T., Betzel C. & Erdmann V.A. (2007): High resolution structure of streptavidin in complex with a novel high affinity peptide tag mimicking the biotin binding motif. *Proteins* **67**(4), 1147–1153.

Pérez F. & Granger B.E. (2007): IPython: a system for interactive scientific computing. *Computing in Science and Engineering* **9**(3), 21–29.

Prakash O. & Eisenberg M.A. (1979): Biotinyl 5'-adenylate: corepressor role in the regulation of the biotin genes of Escherichia coli K-12. *Proceedings of the National Academy of Sciences* **76**(11), 5592–5595.

Pugsley A.P. (1993): The complete general secretory pathway in gram-negative bacteria. *Microbiological Reviews* **57**(1), 50–108.

Qureshi M.H., Yeung J.C., Wu S.C. & Wong S.L. (2001): Development and characterization of a series of soluble tetrameric and monomeric streptavidin muteins with differential biotin binding affinities. *Journal of Biological Chemistry* **276**(49), 46422–46428.

Reznik G.O., Vajda S., Sano T. & Cantor C.R. (1998): A streptavidin mutant with altered ligand-binding specificity. *Proceedings of the National Academy of Sciences* **95**(23), 13525–13530.

Rogers S., Wells R. & Rechsteiner M. (1986): Amino acid sequences common to rapidly degraded proteins: the PEST hypothesis. *Science* **234**(4774), 364–368.

Romanos M. (1995): Advances in the use of *Pichia pastoris* for high-level gene expression. *Current Opinion in Biotechnology* **6**(5), 527–533.

Rowland S.S., Zulty J.J., Sathyamoorthy M., Pogell B.M. & Speedie M.K. (1992): The effect of signal sequences on the efficiency of secretion of a heterologous phosphotriesterase by *Streptomyces lividans*. *Applied Microbiology and Biotechnology* **38**(1), 94–100.

Rucker R.B., Suttie J.W. & McCormick D.B., *Handbook of Vitamins* (CRC Press, 2007), 4th Edn..

Rybak J.N., Scheurer S.B., Neri D. & Elia G. (2004): Purification of biotinylated proteins on streptavidin resin: A protocol for quantitative elution. *Proteomics* **4**(8), 2296–2299.

Sano T. & Cantor C.R. (1990a): Cooperative biotin binding by streptavidin. Electrophoretic behavior and subunit association of streptavidin in the presence of 6 M urea. *Journal of Biological Chemistry* **265**(6), 3369–3373.

Sano T. & Cantor C.R. (1990b): Expression of a cloned streptavidin gene in *Escherichia coli*. *Proceedings of the National Academy of Sciences of the United States of America* **87**(1), 142–6.

Sano T. & Cantor C.R. (1995): Intersubunit contacts made by tryptophan 120 with biotin are essential for both strong biotin binding and biotin-induced tighter subunit association of streptavidin. *Proceedings of the National Academy of Sciences* **92**(8), 3180–3184.

Sano T., Pandori M.W., Chen X., Smith C.L. & Cantor C.R. (1995): Recombinant core streptavidins. A minimum-sized core streptavidin has enhanced structural stability and higher accessibility to biotinylated macromolecules. *The Journal of Biological Chemistry* **270**(47), 28204–28209.

Sano T., Vajda S., Reznik G.O., Smith C.L. & Cantor C.R. (1996): Molecular engineering of streptavidin. *Annals of the New York Academy of Sciences* **799**(1), 383–390.

Sano T., Vajda S., Smith C.L. & Cantor C.R. (1997): Engineering subunit association of multisubunit proteins: A dimeric streptavidin. *Proceedings of the National Academy of Sciences* **94**(12), 6153–6158.

Schaerlaekens K., Lammertyn E., Geukens N., De Keersmaeker S., Anné J. & Van Mellaert L. (2004): Comparison of the Sec and Tat secretion pathways for heterologous protein production by *Streptomyces lividans*. *Journal of Biotechnology* **112**(3), 279–288.

Schein C.H. & Noteborn M.H.M. (1988): Formation of soluble recombinant proteins in *Escherichia coli* is favored by lower growth temperature. *Nature Biotechnology* **6**(3), 291–294.

Schmidt T.G., Koepke J., Frank R. & Skerra A. (1996): Molecular interaction between the Strep-tag affinity peptide and its cognate target, streptavidin. *Journal of Molecular Biology* **255**(5), 753–766.

Schmidt T.G.M. & Skerra A. (1993): The random peptide library-assisted engineering of a C-terminal affinity peptide, useful for the detection and purification of a functional Ig Fv fragment. *Protein Engineering* **6**(1), 109–122.

Schmidt T.G.M. & Skerra A. (2007): The Strep-tag system for one-step purification and high-affinity detection or capturing of proteins. *Nature Protocols* **2**(6), 1528–1535.

Schneider C.A., Rasband W.S. & Eliceiri K.W. (2012): NIH Image to ImageJ: 25 years of image analysis. *Nature Methods* **9**(7), 671–675.

Schweizer E., Werkmeister K. & Jain M.K. (1978): Fatty acid biosynthesis in yeast. *Molecular and Cellular Biochemistry* **21**(2), 95–107.

Schwidop W.D., Klossek P., Müller R. & Claus R. (1990): Procedure for the purification of streptavidin by hydrophobic interaction chromatography. *Journal of Chromatography* **520**, 325–331.

Scilab Enterprises (2012): *Scilab: free and open source software for numerical computation*. Scilab Enterprises, Orsay, France. URL http://www.scilab.org.

Sheldon R.A. (1992): Organic synthesis - past, present and future. (Advantages of incorporating catalysis to organic synthesis). *Chemistry and Industry* **23**, 903–906.

Sohoni S., Bapat P. & Lantz A. (2012): Robust, small-scale cultivation platform for *Streptomyces coelicolor*. *Microbial Cell Factories* **11**(1), 9.

Sommer B., *Dissertation - Neue Strategien zur extrazellulären Produktion rekombinanter Proteine mit Escherichia coli* (Technische Fakultät, Universität Bielefeld, Germany, 2008).

Sørensen H.P. & Mortensen K.K. (2005): Advanced genetic strategies for recombinant protein expression in *Escherichia coli*. *Journal of Biotechnology* **115**(2), 113–128.

Sørensen H.P., Sperling-Petersen H.U. & Mortensen K.K. (2003a): Dialysis strategies for protein refolding: preparative streptavidin production. *Protein Expression and Purification* **31**(1), 149–154.

Sørensen H.P., Sperling-Petersen H.U. & Mortensen K.K. (2003b): A favorable solubility partner for the recombinant expression of streptavidin. *Protein Expression and Purification* **32**(2), 252–259.

Srisawat C. & Engelke D.R. (2001): Streptavidin aptamers: affinity tags for the study of RNAs and ribonucleoproteins. *RNA* **7**(4), 632–641.

Stanbury P.F., Whitaker A. & Hall S.J., *Principles of Fermentation Technology* (Pergamon, 1995), 2nd Edn..

Stapley E., Mata J., Miller I., Demmy T. & Woodruff H. (1963): Antibiotic MSD-235. I. Production by *Streptomyces avidinii* and *Streptomyces lavendulae*. *Antimicrobial Agents and Chemotherapy* **161**, 20–27.

Stöckmann C., Scheidle M., Dittrich B., Merckelbach A., Hehmann G., Melmer G., Klee D., Buchs J., Kang H.A. & Gellissen G. (2009): Process development in *Hansenula polymorpha* and *Arxula adeninivorans*, a re-assessment. *Microbial Cell Factories* **8**, 22.

Streit W.R. & Entcheva P. (2003): Biotin in microbes, the genes involved in its biosynthesis, its biochemical role and perspectives for biotechnological production. *Applied Microbiology and Biotechnology* **61**(1), 21–31.

Sumarningsih T.S. (2014): Production and purification of streptavidin with higher biotin-binding activity. *Indonesian Journal of Animal and Veterinary Sciences* **19**(3), 231–238.

Sunga A.J., Tolstorukov I. & Cregg J.M. (2008): Posttransformational vector amplification in the yeast *Pichia pastoris*. *FEMS Yeast Research* **8**(6), 870–876.

Suter M., Cazin Jr. J., Butler J. & Mock D. (1988): Isolation and characterization of highly purified streptavidin obtained in a two-step purification procedure from *Streptomyces avidinii* grown in a synthetic medium. *Journal of Immunological Methods* **113**(1), 83–91.

Suzuki T., Yamane T. & Shimizu S. (1987): Mass production of thiostrepton by fed-batch culture of *Streptomyces laurentii* with pH-stat modal feeding of multi-substrate. *Applied Microbiology and Biotechnology* **25**(6), 526–531.

Szafranski P., Mello C.M., Sano T., Smith C.L., Kaplan D.L. & Cantor C.R. (1997): A new approach for containment of microorganisms: Dual control of streptavidin expression by antisense RNA and the T7 transcriptional system. *Proceedings of the National Academy of Sciences* **94**(4), 1059 –1063.

Tahiri-Alaoui A. (2002): High affinity nucleic acid aptamers for streptavidin incorporated into bi-specific capture ligands. *Nucleic Acids Research* **30**(10), 45e.

Takakura Y., Sofuku K., Tsunashima M. & Kuwata S. (2016): Lentiavidins: Novel avidin-like proteins with low isoelectric points from shiitake mushroom (*Lentinula edodes*). *Journal of Bioscience and Bioengineering* **121**(4), 420–423.

Taskinen B., Zmurko J., Ojanen M., Kukkurainen S., Parthiban M., Määttä J.A.E., Leppiniemi J., Jänis J., Parikka M., Turpeinen H., Rämet M., Pesu M., Johnson M.S., Kulomaa M.S., Airenne T.T. & Hytönen V.P. (2013): Zebavidin - an avidin-like protein from zebrafish. *PLOS ONE* **8**(10), e77207.

Tausig F. & Wolf F.J. (1964): Streptavidin - a substance with avidin-like properties produced by microorganisms. *Biochemical and Biophysical Research Communications* **14**(3), 205–209.

Thompson L.D. & Weber P.C. (1993): Construction and expression of a synthetic streptavidin-encoding gene in *Escherichia coli*. *Gene* **136**(1-2), 243–246.

van't Riet K. (1983): Mass transfer in fermentation. *Trends in Biotechnology* **1**(4), 113–119.

van't Riet K. & Tramper J., *Basic Bioreactor Design* (CRC Press, 1991), 1st Edn..

Veiko V.P., Gul'ko L.B., Okorokova N.A., D'yakov N.A. & Debabov V.G. (1999): Cloning and expression of the streptavidin gene from *Streptomyces avidinii* in *Escherichia coli* and secretion of streptavidin by *E. coli* cells. *Bioorganicheskaya Khimiya* **25**(3), 184–188.

Walisko R., Krull R., Schrader J. & Wittmann C. (2012): Microparticle based morphology engineering of filamentous microorganisms for industrial bio-production. *Biotechnology Letters* **32**(11), 1975–1982.

Waner M.J., Navrotskaya I., Bain A., Oldham E.D. & Mascotti D.P. (2004): Thermal and sodium dodecylsulfate induced transitions of streptavidin. *Biophysical Journal* **87**(4), 2701–2713.

Wang C., Yang G., Luo Z. & Ding H. (2009): In vitro selection of high-affinity DNA aptamers for streptavidin. *Acta Biochimica et Biophysica Sinica* **41**(4), 335–340.

Wang W.W.S., Das D. & Suresh M.R. (2005): Biotin carboxyl carrier protein co-purifies as a contaminant in core-streptavidin preparations. *Molecular Biotechnology* **31**(1), 29–40.

Weber P.C., Ohlendorf D.H., Wendoloski J.J. & Salemme F.R. (1989): Structural origins of high-affinity biotin binding to streptavidin. *Science (New York, N.Y.)* **243**(4887), 85–88.

Weber P.C., Pantoliano M.W., Simons D.M. & Salemme F.R. (1994): Structure-based design of synthetic azobenzene ligands for streptavidin. *Journal of the American Chemical Society* **116**(7), 2717–2724.

Wetzel D., Müller J.M., Flaschel E., Friehs K. & Risse J.M. (2016): Fed-batch production and secretion of streptavidin by *Hansenula polymorpha*: Evaluation of genetic factors and bioprocess development. *Journal of Biotechnology* **225**, 3–9.

Wilson R. (2011): Preparation of single-stranded DNA from PCR products with streptavidin magnetic beads. *Nucleic Acid Therapeutics* **21**(6), 437–440.

Winkler M.A., *Chemical Engineering Problems in Biotechnology* (Springer Science & Business Media, 1990), 1st Edn..

Woese C. (1987): Bacterial evolution. *Microbiological reviews* **51**(2), 221–271.

Wongwicharn A., McNeil B. & Harvey L.M. (1999): Effect of oxygen enrichment on morphology, growth, and heterologous protein production in chemostat cultures of *Aspergillus niger* B1-D. *Biotechnology and Bioengineering* **65**(4), 416–424.

Wood G.S. & Warnke R. (1981): Suppression of endogenous avidin-binding activity in tissues and its relevance to biotin-avidin detection systems. *Journal of Histochemistry & Cytochemistry* **29**(10), 1196–1204.

Woolley D.W. & Longsworth L.G. (1942): Isolation of an antibiotic factor from egg white. *Journal of Biological Chemistry* **142**, 285–290.

Wu K., Analysis of protein-DNA binding by streptavidin-agarose pulldown. M. Bina (Ed.), *Gene Mapping, Discovery, and Expression*, no. 338 in Methods in Molecular Biology, pp. 281–290 (Humana Press, 2006). DOI: 10.1385/1-59745-097-9:281.

Wu S.C., Hassan Qureshi M. & Wong S.L. (2002): Secretory production and purification of functional full-length streptavidin from *Bacillus subtilis*. *Protein Expression and Purification* **24**(3), 348–356.

Wu S.C. & Wong S.L. (2002): Engineering of a *Bacillus subtilis* strain with adjustable levels of intracellular biotin for secretory production of functional streptavidin. *Applied and Environmental Microbiology* **68**(3), 1102–1108.

Wu S.C. & Wong S.L. (2006): Intracellular production of a soluble and functional monomeric streptavidin in *Escherichia coli* and its application for affinity purification of biotinylated proteins. *Protein Expression and Purification* **46**(2), 268–273.

Wucherpfennig T., Kiep K.A., Driouch H., Wittmann C. & Krull R., Chapter 4 - Morphology and rheology in filamentous cultivations. S.S.a.G.M.G. Allen I. Laskin (Ed.), *Advances in Applied Microbiology*, Vol. 72, pp. 89–136 (Academic Press, 2010).

Xing L., Wu W., Zhou B. & Lin Z. (2011): Streamlined protein expression and purification using cleavable self-aggregating tags. *Microbial Cell Factories* **10**, 42.

Xiong A.S., Yao Q.H., Peng R.H., Li X., Fan H.Q., Guo M.J. & Zhang S.L. (2004): Isolation, characterization, and molecular cloning of the cDNA encoding a novel phytase from *Aspergillus niger* 113 and high expression in *Pichia pastoris*. *Journal of Biochemistry and Molecular Biology* **37**(3), 282–291.

Yurimoto H. & Sakai Y. (2009): Methanol-inducible gene expression and heterologous protein production in the methylotrophic yeast *Candida boidinii*. *Biotechnology and Applied Biochemistry* **53**(2), 85–92.

Zeyaullah M., Kamli M.R., Islam B., Atif M., Benkhayal F.A., Nehal M., Rizvi M.A. & Arif Ali (2009): Metagenomics - an advanced approach for non-cultivable micro-organisms. *Biotechnology and Molecular Biology Reviews* **4**(3), 49–54.

Zhang A.L., Luo J.X., Zhang T.Y., Pan Y.W., Tan Y.H., Fu C.Y. & Tu F.z. (2009): Recent advances on the GAP promoter derived expression system of *Pichia pastoris*. *Molecular Biology Reports* **36**(6), 1611–1619.

Zhang L., Liu C., Gao Z.H., Cao Y. & Bai G. (2007): Research on the classification of *Streptomyces* strain ZG 0429 and purification of streptavidin. *Wei sheng wu xue bao (Acta Microbiologica Sinica)* **47**(1), 7–10.

Zhong Y., Yang L., Guo Y., Fang F., Wang D., Li R., Jiang M., Kang W., Ma J., Sun J. & Xiao W. (2014): High-temperature cultivation of recombinant *Pichia pastoris* increases endoplasmic reticulum stress and decreases production of human interleukin-10. *Microbial Cell Factories* **13**, 163.

Zlokarnik M., *Rührtechnik: Theorie und Praxis* (Springer DE, 1999), 1st Edn..

Zocchi A., Jobé A.M., Neuhaus J.M. & Ward T.R. (2003): Expression and purification of a recombinant avidin with a lowered isoelectric point in *Pichia pastoris*. *Protein Expression and Purification* **32**(2), 167–174.

Zurek C., Kubis E., Keup P., Hörlein D., Beunink J., Thömmes J., Kula M.R., Hollenberg C.P. & Gellissen G. (1996): Production of two aprotinin variants in *Hansenula polymorpha*. *Process Biochemistry* **31**(7), 679–689.

Danksagungen

Ganz allgemein gilt mein Dank zunächst dem fantastischen **Lehrstuhl für Fermentationstechnik**, der in den letzten fünf Jahren so etwas wie meine zweite Heimat war. Ich habe die großartige, kollegiale Atmosphäre sehr genossen!

Spezifischer möchte ich zuvorderst **Herrn Prof. Dr. Erwin Flaschel** danken, der traurigerweise nicht mehr unter uns ist. Er hat einen integralen Anteil an dieser Arbeit. Er nahm mich als Doktorand am Lehrstuhl für Fermentationstechnik der Universität Bielefeld auf und war in der Folge als ausnehmend wohlwollender und geduldiger Mentor jederzeit offen für Fragen aller Art. Ich bin ihm sehr dankbar für die zahlreichen *feedback*-Runden, die einerseits essenziell für die Fokussierung dieser Arbeit waren und andererseits in einem unvergleichlichen fachlichen Erkenntnisgewinn resultierten. Darüber hinaus bin ich ihm sehr verbunden für die Ermöglichung der Teilnahme an zahlreichen Konferenzen und Seminaren und darüber, als Dozent im Bachelor-Studiengang "Molekulare Biotechnologie" viel tiefer in die Abgründe der Verfahrenstechnik abtauchen zu können, als ich es je für möglich gehalten hätte. Ohne seine Faszination für Simulationen und Datenmodellierung wären diese Aspekte höchstwahrscheinlich kein Gegenstand dieser Arbeit.

Mein Dank gilt **Herrn Prof. Dr. Karl Friehs**, der die Arbeitsgruppe vorübergehend von Herrn Prof. Flaschel übernahm und seither zusammenhält, und der mir durch die Finanzierung dieser Arbeit in schwierigen Zeiten das Leben unter Brücken erspart hat. Ohne seine Mithilfe wäre die Arbeit aus gentechnischer Perspektive nicht in der heutigen Form. Auch für die mannigfaltige weitere Unterstützung bin ich ihm sehr dankbar.

Meinem Doktorvater **Dr. Joe Max Risse** danke ich für die tolle Betreuung. Er war mein erster Ansprechpartner und damit das *Alpha* und *Omega* bei Fragen jedweder Art in allen Phasen dieser Arbeit, beginnend mit der Bewerbung auf eine Promotionsförderung, einer unendlichen Zahl an experimentellen Problemstellungen und nicht zuletzt der Diskussion, Verschriftlichung und Präsentation der Ergebnisse. Seine sorfältigen, fundierten, geduldigen und stets äußerst scharfsinnigen Rückmeldungen war von unschätzbarem Wert für die Qualität der dieser Dissertation zugrunde liegenden Publikationen. Den enormen Freiraum, der mir für das Projekt eingeräumt wurde, habe ich zu jedem Zeitpunkt sehr geschätzt. Seine Arbeitsweise hat mich darüber hinaus viel über die kritische Auseinandersetzung mit der Fachliteratur gelehrt. Die Melange aus fachlichem *feedback* und einer allgegenwärtigen, feinen Prise Humor hat zu ebenso zahllosen wie ertragreichen und unterhaltsamen *meetings* geführt, welche leider auch gewaltige Mengen seiner wertvollen Zeit verschlungen haben. Tschuldigung! Vielen Dank, es hat viel Spaß gemacht mit Dir!

Herr Dipl.-Ing. Thomas Schäffer, der "Mann, der alles kann und deshalb auch alles machen muss" (O-Ton Prof. Flaschel), war der Schlüssel zum Erfolg der verfahrenstechnischen Aspekte dieser Arbeit. Seine sisyphos-esken Anstrengungen aus einem sturen, undichten und unberechenbaren Schrotthaufen namens Sixfors ein perfektes Fermentationssystem machen zu wollen, waren für den Verlauf der Arbeit unverzichtbar. Zahllose Arbeitsstunden und seine engelsgleiche Geduld brachten letztlich einen leidlich

funktionierenden "Fourfors" hervor, der die Grundlage für einen Großteil der Bioreaktor-Kultivierungen der hier präsentierten Studien war. Seine breiten Software-Kenntnisse waren integral für Fragestellungen der Prozessregelung und Netzwerk-Verwaltung. Ohne seine Ratschläge zu einem bunten Sammelsurium technischer Probleme wäre zudem eine derart reibungsfreie Analytik nicht möglich gewesen. Deshalb: Herzlichen Dank!

Dank meinen Mit-Doktoranden **Dominik Cholewa**,[3] **Philipp Grimm**, **Ram Shankar**, **Gabriele Kleiner**, **Jan Schwarzhans** und **Yingfei Shi** und dem mittlerweile pensionierten Dauer-Masteranden **Lars Wollenschläger** waren die Arbeitsstunden und gelegentlichen Wartezeiten im Verlauf des Projektes nicht trostlos und zermürbend, sondern oft höchst amüsant. Lustige Stunden zwischen Tür und Angel, Kaffeeraum und Labor, sowie Büro und Westend waren das viel zitierte Sahnehäubchen auf dieser Arbeit. *Merci beaucoup*, ich werde euch nicht vergessen!

David Wetzel, **Julia Hassa** und **Simon Bruhn** gilt mein Dank für die ebenso intelligente wie sorgfältige Bearbeitung wichtiger Facetten dieses Promotionsprojektes im Rahmen von Abschlussarbeiten, ohne die mehreren Teilbereichen viel Tiefgang abgehen würde.

Dem weiteren "Laborinventar", bestehend aus **Eberhard Wünsch**, **Galina Beck** und **Kirsten Leiwig**, danke ich herzlich für die mannigfaltige Unterstützung im Laboralltag.

Meinem Zweitgutachter **Prof. Dr. Jörn Kalinowski** und **Tetiana Gren** von der AG "Microbial Genomics and Biotechnology" am CeBiTec der Universität Bielefeld danke ich für die Kooperation zu genetischen und gentechnischen Aspekten der Streptavidin-Produktion mit *S. avidinii*, welche die Arbeit um eine wichtige Facette ergänzt haben und insbesondere im Blick auf künftige Studien von großem Interesse sein dürften. **Dr. Dirk Holtmann** und **Felicitas Vernen** vom DECHEMA-Forschungsinstitut (Arbeitsgruppe Bioverfahrenstechnik) bin ich für die fruchtbare Kooperation zur Morphologiekontrolle an diesem Stamm verbunden.

Weiterhin bedanke ich mich herzlich bei den Sponsoren dieses Promotionsprojektes: der **Deutschen Bundesstiftung Umwelt (DBU)** und insbesondere **Herrn Dr. Schaefer** gebührt Dank für die Förderung im Rahmen des Promotionsstipendienprogramms, welche nicht nur aus finanzieller Sicht die wichtigste Stütze des Projektes war, sondern mir durch die Stipendiatenseminare auch eine große persönliche Bereicherung war und meinen Horizont erweitert hat. Dem **Bielefelder Nachwuchsfonds** danke ich für die Abschlussförderung während der letzten Schritte dieses Promotionsprojektes, die die Grundlage für das sorgfältige Zusammenfassen der Ergebnisse in Form der Publikationen war. Letztlich gilt hier wie überall sonst: "Ohne Moos nix los."

Last but not least geht ein großer Dank an meine Freunde,[4] die für die nötige Auflockerung des Promotionsalltags gesorgt haben, und meine Eltern, die mir während des Projektes - und in all den Jahren zuvor - stets den Rücken gestärkt haben. **Herzlichen Dank!**

[3] Danke auch für die Korrektur dieser Arbeit, Doc!

[4] Übereinstimmungen mit dem Kollegenkreis können nicht ausgeschlossen werden.

Selbstständigkeitserklärung

Hiermit erkläre ich, die vorliegende Dissertation selbstständig und nur unter Benutzung der angegebenen Quellen angefertigt zu haben. Alle aus der Literatur wörtlich oder sinngemäß entnommenen Zitate und Abbildungen habe ich als solche kenntlich gemacht. Weiterhin erkläre ich, dass diese Arbeit weder vollständig noch teilweise einer anderen Prüfungsbehörde mit dem Ziel vorgelegt wurde, einen akademischen Titel zu erwerben.

Bielefeld, den 27.9.2016 Jakob Michael Müller